HEAT TRANSFER AND RESISTANCE IN THE LAMINAR FLOW OF LIQUIDS IN TUBES. VOLUME 1

B. S. Petukhov

Foreign Technology Division
Wright Patterson Air Force Base, Ohio

15 August 1969

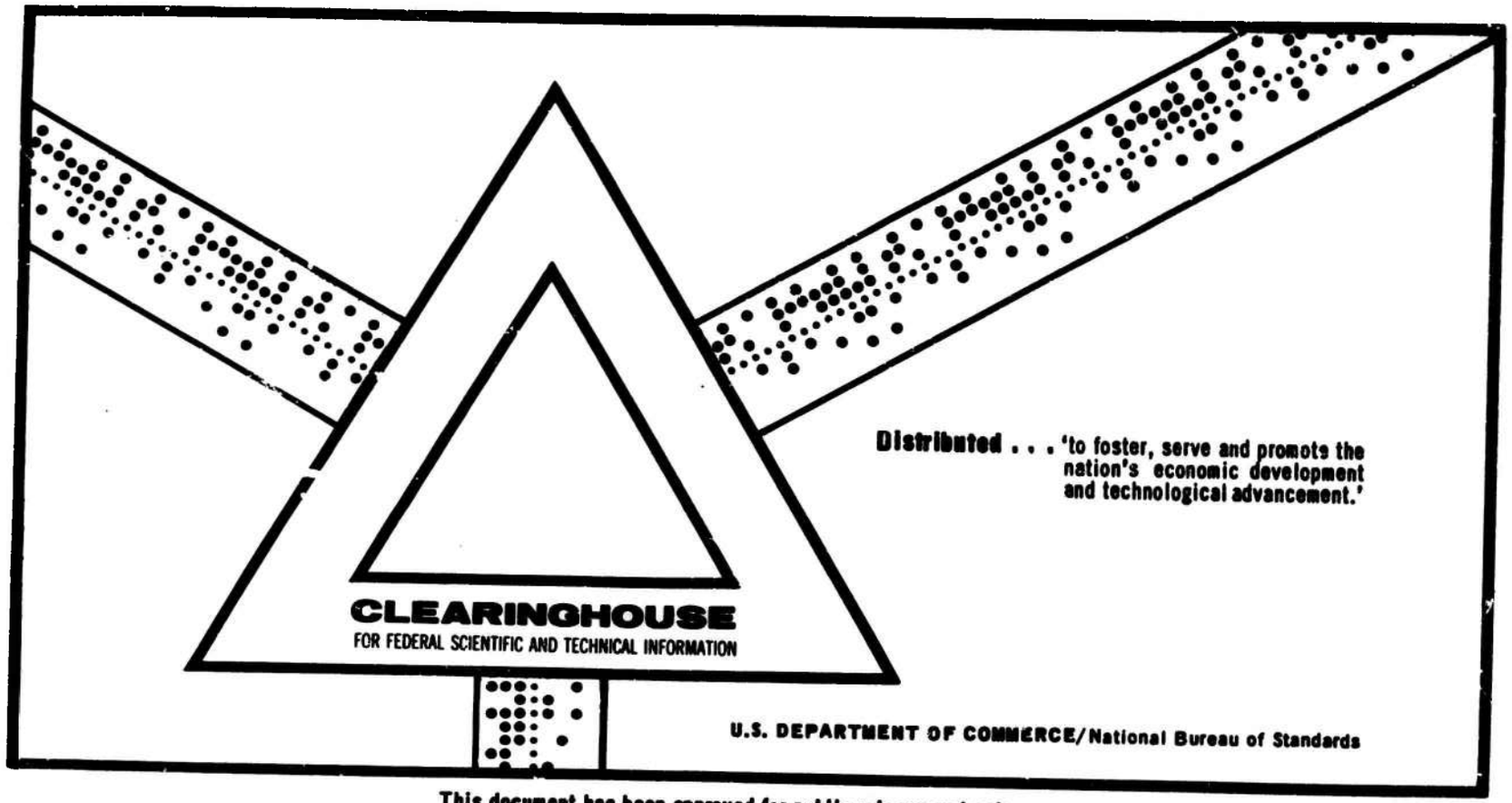

FTD-HT-23-757-68 Vol. I of II

FOREIGN TECHNOLOGY DIVISION

HEAT TRANSFER AND RESISTANCE IN THE LAMINAR FLOW OF LIQUIDS IN TUBES

By

B. S. Petukhov

FTD-HT- 23-757-68
Vol I of II

EDITED TRANSLATION

HEAT TRANSFER AND RESISTANCE IN THE LAMINAR FLOW OF LIQUIDS IN TUBES

By: B. S. Petukhov

English Pages: 1 - 243

Source: Teploobmen i Soprotivleniye Pri Laminarnom Techenii Zhidkosti V Trubakh (Heat Transfer and Resistance in the Laminar Flow of Liquids in Tubes). 1967, 1-411

Translated Under: F33657-68-D-0865-P002

PREPARED BY:

TRANSLATION DIVISION
FOREIGN TECHNOLOGY DIVISION
WP-AFB, OHIO.

FTD-HT- 23-757-68
Vol I of II

Date 15 Aug 19 69

DATA HANDLING PAGE

61-ACCESSION NO.	62-DOCUMENT LOC	30-TOPIC TAGS
TM9001145		heat theory, heat conductivity, heat convection, hydrodynamics, hydraulic resistance

60-TITLE HEAT TRANSFER AND RESISTANCE IN THE LAMINAR FLOW OF LIQUIDS IN TUBES

67-SUBJECT AREA

20, 13

12-AUTHOR/CO-AUTHORS

PETUKHOV, B. S.

10-DATE OF INFO

-----67

43-SOURCE

TEPLOOBMEN I SOPROTIVLENIYE PRI LAMINARNOM TECHENII ZHIDKOSTI V TRUBAKH, MOSCOW, IZD-VO ENERGIYA (RUSSIAN)

40-DOCUMENT NO.

FTD-HT-23-757-68

09-PROJECT NO.

72301-78

63-SECURITY AND DOWNGRADING INFORMATION	64-CONTROL MARKINGS	97-HEADER CLASN
UNCL, 0	NONE	UNCL

76-REEL FRAME NO.	77-SUPERSEDES	78-CHANGES	40-GEOGRAPHICAL AREA	NO OF PAGES
1889 1647			UR	521

CONTRACT NO.	X REF ACC. NO.	PUBLISHING DATE	TYPE PRODUCT	REVISION FREQ
F33657-68-D-0865-P002	65-AM7031120	94-	TRANSLATION	NONE

STEP NO.	ACCESSION NO.
02-UR/0000/67/000/000/0001/0411	

ABSTRACT

(U) This book is intended for scientific workers and engineers concerned with research work in the field of heat exchange. The book may also be useful to designers whose work is connected with the development of heat exchange systems. The book deals with theory and calculation of heat exchange and resistance in laminar flow of non-compressed liquid in a duct. Solutions of numerous problems are presented, as well as results of experimental investigations. Discussed are also problems of heat exchange in ducts of various geometric shapes under different boundary conditions in presence or absence in the flow of internal heat source and dissipation of energy under stationary and non-stationary conditions. Considerable attention is paid to problems of hydrodynamics and heat exchange under alternating physical properties of liquids and gases. All solutions are expressed by calculation formulas suitable for direct practical application. The book contains tables and graphs required for calculations. Each chapter is accompanied by Soviet and non-Soviet references.

DISCLAIMER NOTICE

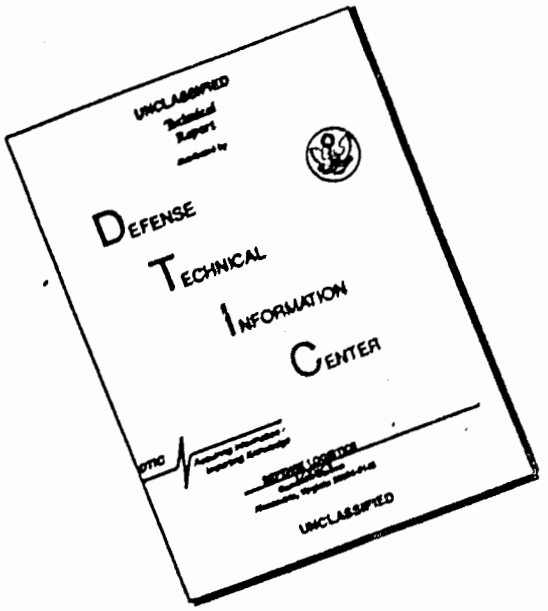

THIS DOCUMENT IS BEST QUALITY AVAILABLE. THE COPY FURNISHED TO DTIC CONTAINED A SIGNIFICANT NUMBER OF PAGES WHICH DO NOT REPRODUCE LEGIBLY.

TABLE OF CONTENTS

PREFACE

The problem of heat exchange during laminar flow of a liquid in a tube has recently received considerable development. While 10-15 years ago only isolated theoretical results were known, with few experimental data, questions of heat exchange and hydrodynamics in laminar tube flow have now moved to the point at which it is necessary to systematize all the available material, and to treat it from a unified viewpoint. Such a product is also useful since publications on heat exchange and hydrodynamics in laminar tube flow are scattered through numerous periodicals. Thus there is no doubt that the lack of generalizing studies hampers practical utilization of the results attained.

Interest in problems of heat exchange and hydrodynamics in laminar tube flow and intensive cultivation of such topics are a natural response to the rising demands of practice. There is ever more frequent need to design heat-exchange systems in which laminar motion of the fluid predominates. This is associated with the ever-wider utilization in technology of gases at high temperatures (i.e., increased viscosities) and viscous liquids, as well as with the development of compact heat-exchange systems. In addition to practical needs, the development of the theory of heat exchange in laminar tube flow of liquids has undoubtedly been facilitated by the application of new mathematical methods in this field, in particular the broadscale employment of computers.

This book represents a systematic treatment of theory and methods for determining heat exchange and resistance in laminar flow of incompressible fluids in tubes. The discussion is restricted to analysis of flow and heat exchange for Newtonian fluids in the absence of flow interaction with electric or magnetic fields. There are two reasons for this: monographs have recently been published on the mechanics of non-Newtonian fluids and magnetohydrodynamics; it is impossible to cover all aspects of the problem within the framework of a single book restricted in size.

The following organization has been adopted. After brief information on the basic equations of dynamics for a viscous fluid and the boundary and initial conditions (Chapter 1), we consider methods for determining the heat flow at a wall, the heat-transfer coefficient, and the hydraulic resistance (Chapter 2). Such data as is required for the subsequent analysis is given for the change in physical properties of liquids and gases as a function of temperature and pressure (Chapter 3). The examination of general questions terminates with an analysis of flow and heat exchange in tubes by the similarity method; this is used as a basis for classi-

fying possible cases of flow and heat exchange (Chapter 4).

The laws of isothermal fluid flow, which form the basis for the subsequent analysis of heat-exchange processes where the physical properties of the fluid are constant, are discussed in Chapter 5. Here results are given for determination of stationary and nonstationary flows in tubes differing in geometric shape, with fully developed velocity profile and in the hydrodynamic entrance section. This chapter has been condensed (most proofs are omitted) since it basically represents auxiliary (reference) material. When the physical properties of the fluid are variable, the motion problem is inseparable from the heat-exchange problem. Here the two problems are considered together.

The next nine chapters (Chapter 6-14) deal with problems of heat exchange and flow in tubes under stationary conditions when the flow has no internal heat sources or energy dissipation, and there is free convection. In these chapters, heat exchange is considered in round, flat, annular, prismatic, and cylindrical tubes, with wall boundary conditions of the first, second, and third kinds, for developed flow and in the hydrodynamic entrance section. In addition to heat exchange with constant physical properties, considerable attention is also devoted to heat exchange and friction when the liquid and gas properties vary (Chapters 7 and 9 and individual sections of other chapters). In particular, in Chapter 9 we consider heat exchange and friction in the supercritical region of state parameters for the material, and when there is equilibrium dissociation in a high-temperature gas flow.

In Chapter 15, we study stationary heat exchange when the flow contains internal heat sources and there is kinetic-energy dissipation, while in Chapter 16 we consider the joint action of forced and free convection both with and without heat sources in the flow.

The last chapter (17) contains a discussion of heat-exchange problems under nonstationary conditions. Here we consider the influence of nonstationarity produced by time-varying boundary conditions at the wall, by the variation in fluid velocity with time, and with simultaneous operation of both these factors.

Numerous studies by Soviet and foreign researchers, published in the periodical literature, are employed in the book. It also reflects work performed by the author together with his associates at the Moscow Power Institute. Chapters 7 and 9, as well as many sections of other chapters, are based almost completely on these studies.

Mathematical methods are widely employed in accordance with the nature of the topic, and in the interests of clear and convincing exposition. As a rule, after a problem is formulated, it is solved, and the results then analyzed. It is only in isolated cases requiring cumbersome computation that we have merely formulated the problem and given the computational results, completely or partially omitting intermediate calculations. In addition to the theoretical analysis, there are experimental data, particularly when the possibilities of theoretical analysis are restricted. Con-

siderable attention is giver to the physical interpretation of the results obtained. All solutions are carried through to computational relationships suitable for direct practical application. The tables and graphs required for calculation are given.

The author wishes to thank his colleagues of the engineering thermophysics department and the heat-exchange section of the Scientific Research Institute of High Temperatures [SRIHT](НИИВТ), who participated actively in discussion of the manuscript, and aided in selecting material, performing calculations, and preparing certain illustrations. The manuscript was read by K.D. Voskresenskiy, who made several useful comments. V.N. Popov did much work to edit and prepare the book. The author also wishes to extend his sincere thanks to them.

B. Petukhov

Chapter 1

BASIC EQUATIONS

1-1. Preliminary Remarks

A phenomenological method of investigation is usually employed in the theory of heat exchange and in hydrodynamics. Ignoring the microstructures of the material, we assume that the medium is continuous. The state of the continuous medium is characterized by macroscopic parameters. For a single-phase chemically homogeneous moving medium, such parameters are the temperature, pressure, and velocity. The physical properties of the medium (density, heat content, viscosity and thermal-conductivity coefficients), which in general depend on the temperature and pressure, are assumed to be known. By neglecting the microstructure of matter, we introduce certain restrictions on application of the phenomenological method. In the ensuing discussions, however, we shall only consider those problems in heat exchange and dynamics of a viscous fluid for which this method is fully applicable.

Thus the state of a liquid or gas flow will be specified if we know the fields for the velocity $\vec{w}$, pressure p, and temperature T, i.e., if we know the relationships

$$\left.\begin{aligned} \vec{w} &= \vec{w}(x, y, z, \tau); \\ p &= p(x, y, z, \tau); \\ T &= T(x, y, z, \tau), \end{aligned}\right\} \qquad (1\text{-}1)$$

where x, y, and z are the coordinates of the point and τ is the time.

Equations (1-1) refer to nonstationary velocity, pressure, and temperature fields. If $\vec{w}$, p, and T are stationary fields, then in place of (1-1) we have

$$\left.\begin{aligned} \vec{w} &= \vec{w}(x, y, z); \\ p &= p(x, y, z); \\ T &= T(x, y, z). \end{aligned}\right\} \qquad (1\text{-}2)$$

The theoretical study of heat exchange and fluid motion reduces primarily to determining (1-1) or (1-2). Knowing the $\vec{w}$, p, and T fields, as well as the way in which the physical properties depend on T and p, we can determine all quantities characterizing heat exchange and fluid motion (heat flows, hydraulic resistances, etc.).

To determine the five unknowns (the three components of the velocity vector $\vec{w}$, p, and T), we must have five equations. They are obtained from the basic conservation laws of physics (of mass, momentum, moment of momentum, and energy) in accordance with the generalized law of Newtonian viscous flow and the Fourier heat-conduction law. The equations thus found are called the equation of continuity, equations of motion, and energy equation. These equations, supplemented by relationships for the physical properties of the fluid as functions of temperature and pressure, form a closed equation system describing the process of convective heat exchange and fluid motion. Solution of this system in accordance with the boundary conditions permits us to determine (1-1) or (1-2).

In succeeding sections of this book, we shall give the equations of continuity, motion, and energy without derivation for single-phase chemically homogeneous and isotropic fluids in the absence of heat transfer by radiation. The derivations of these equations can be found in many courses in the mechanics of liquids and gases [1, 2, 3, 4].

As in hydrodynamics, we shall henceforth use the word "fluid" to mean both liquids and gases.

1-2. EQUATIONS OF CONTINUITY, MOTION, AND ENERGY

1. The equation of continuity, which expresses the law of conservation of mass for a moving fluid, has the following form in the general case:

$$\frac{\partial \rho}{\partial \tau}+\frac{\partial(\rho w_x)}{\partial x}+\frac{\partial(\rho w_y)}{\partial y}+\frac{\partial(\rho w_z)}{\partial z}=0, \qquad (1\text{-}3)$$

where w_x, w_y, and w_z are the projections of the velocity vector on the axis of a rectangular coordinate system; ρ is the fluid density, which depends on T and p.

For stationary flow, $\partial\rho/\partial\tau = 0$, and (1-3) takes the form

$$\frac{\partial(\rho w_x)}{\partial x}+\frac{\partial(\rho w_y)}{\partial y}+\frac{\partial(\rho w_z)}{\partial z}=0. \qquad (1\text{-}4)$$

If the fluid density is independent of pressure and temperature (ρ = const), we then have in place of (1-3)

$$\frac{\partial w_x}{\partial x}+\frac{\partial w_y}{\partial y}+\frac{\partial w_z}{\partial z}=0. \qquad (1\text{-}5)$$

2. The equation of motion for a viscous Newtonian fluid[1] with variable physical properties has the following form in rectangular coordinates:

[1] 1/14

$$\left.\begin{aligned}
\rho\frac{dw_x}{d\tau}&=\rho F_x-\frac{\partial p}{\partial x}+\frac{\partial}{\partial x}\left[\mu\left(2\frac{\partial w_x}{\partial x}-\frac{2}{3}\operatorname{div}\vec{w}\right)\right]+\\
&+\frac{\partial}{\partial y}\left[\mu\left(\frac{\partial w_x}{\partial y}+\frac{\partial w_y}{\partial x}\right)\right]+\frac{\partial}{\partial z}\left[\mu\left(\frac{\partial w_x}{\partial z}+\frac{\partial w_z}{\partial x}\right)\right];\\
\rho\frac{dw_y}{d\tau}&=\rho F_y-\frac{\partial p}{\partial y}+\frac{\partial}{\partial x}\left[\mu\left(\frac{\partial w_y}{\partial x}+\frac{\partial w_x}{\partial y}\right)\right]+\\
&+\frac{\partial}{\partial y}\left[\mu\left(2\frac{\partial w_y}{\partial y}-\frac{2}{3}\operatorname{div}\vec{w}\right)\right]+\frac{\partial}{\partial z}\left[\mu\left(\frac{\partial w_y}{\partial z}+\frac{\partial w_z}{\partial y}\right)\right];\\
\rho\frac{dw_z}{d\tau}&=\rho F_z-\frac{\partial p}{\partial z}+\frac{\partial}{\partial x}\left[\mu\left(\frac{\partial w_z}{\partial x}+\frac{\partial w_x}{\partial z}\right)\right]+\\
&+\frac{\partial}{\partial y}\left[\mu\left(\frac{\partial w_z}{\partial y}+\frac{\partial w_y}{\partial z}\right)\right]+\frac{\partial}{\partial z}\left[\mu\left(2\frac{\partial w_z}{\partial z}-\frac{2}{3}\operatorname{div}\vec{w}\right)\right].
\end{aligned}\right\}\qquad(1\text{-}6)$$

where

$$\frac{d}{d\tau}=\frac{\partial}{\partial\tau}+w_x\frac{\partial}{\partial x}+w_y\frac{\partial}{\partial y}+w_z\frac{\partial}{\partial z};\qquad(1\text{-}7)$$

F_x, F_y, and F_z are the projections of the mass-force stress vector on the coordinate axes; p is the pressure at the point under consideration; μ is the dynamic viscosity coefficient.

The density ρ and viscosity coefficient μ depend on temperature and pressure, so that they will vary in time and along the coordinates when there are temperature and pressure fields in the flow. Here (1-6) and (1-3) are insufficient to determine the six unknowns (w_x, w_y, w_z, p, ρ, and μ). To close the system we must bring in the energy equation, describing the temperature field, and the equations establishing the relationship between the physical properties and T and p.

If ρ and μ are constant, then (1-6) reduces to the form

$$\left.\begin{aligned}
\frac{\partial w_x}{\partial\tau}+\vec{w}\operatorname{grad}w_x&=F_x-\frac{1}{\rho}\cdot\frac{\partial p}{\partial x}+\nu\nabla^2 w_x;\\
\frac{\partial w_y}{\partial\tau}+\vec{w}\operatorname{grad}w_y&=F_y-\frac{1}{\rho}\cdot\frac{\partial p}{\partial y}+\nu\nabla^2 w_y;\\
\frac{\partial w_z}{\partial\tau}+\vec{w}\operatorname{grad}w_z&=F_z-\frac{1}{\rho}\cdot\frac{\partial p}{\partial z}+\nu\nabla^2 w_z,
\end{aligned}\right\}\qquad(1\text{-}8)$$

where $\nu = \mu/\rho$ is the kinematic viscosity coefficient.

We shall henceforth consider just one mass force, namely the gravitational force. Here $\vec{F}=\vec{g}$. The gravitational force exerts an influence on fluid motion only when there are free surfaces or a nonuniform density distribution in the flow. When there is confined flow (i.e., no free surfaces) and the density distribution is uniform, the gravitational force acting on a fluid element is balanced by the Archimedean displacement force. Thus the fluid moves as if it were weightless, which confirms the possibility of eliminating the gravitational force from the equations of motion, so that they can be written in the Helmholtz form. Here, consequently, the gravitational force can be neglected in determining the velocity field.[2]

With a nonuniform pressure distribution in a confined fluid flow, the action of the gravitational force is not balanced by the

[2]/14

Archimedean force. To introduce the resultant of these two forces, the lift, we transform the first two terms on the right sides of the equations. Since here $F=g$, we have in projection on the x axis:

$$\rho F_x - \frac{\partial p}{\partial x} = (\rho - \rho_0) g_x - \left(\frac{\partial p}{\partial x} - \rho_0 g_x\right).$$

where ρ_0 is the density at constant temperature T_0 for some fixed point in the flow.

Assuming the variations in ρ and T to be small as compared with the absolute values, we can let

$$\rho - \rho_0 = -\beta\rho (T - T_0),$$

where $\beta = -\frac{1}{\rho}\left(\frac{\partial \rho}{\partial T}\right)_p$ is the coefficient of volume expansion for the fluid.

The quantity $\rho_0 g_x$ can be represented as $\rho_0 g_x = \partial p_0/\partial x$ (and analogously for $\rho_0 g_y$ and $\rho_0 g_z$), where p_0 is the hydrostatic pressure, computed on the assumption that the fluid has density ρ_0 everywhere. Letting $p - p_0 = p_1$, we obtain

$$\left.\begin{aligned} \rho F_x - \frac{\partial p}{\partial x} &= -g_x \beta\rho (T - T_0) - \frac{\partial p_1}{\partial x}; \\ \rho F_y - \frac{\partial p}{\partial y} &= -g_y \beta\rho (T - T_0) - \frac{\partial p_1}{\partial y}; \\ \rho F_z - \frac{\partial p}{\partial z} &= -g_z \beta\rho (T - T_0) - \frac{\partial p_1}{\partial z}. \end{aligned}\right\} \qquad (1\text{-}9)$$

The first terms on the right side of (1-9) are the projections of the lift $-g\beta\rho(T-T_0)$ (referred to unit volume of a liquid particle)[3] on the axes of an arbitrarily oriented rectangular coordinate system. If the z axis is opposite in direction to $\vec{g}$, then the projections of the lift on the x and y axes will vanish, while the z-axis projection $g_z = -g$. Here, naturally, $\partial p_0/\partial z = -\rho_0 g$. We also note that in (1-9), it is convenient to replace $\beta\rho$ by $\beta_p \rho_0 = \beta\rho$ (see §3.2).

3. The energy equation for a single-phase chemically homogeneous isotropic fluid whose physical properties are arbitrary functions of temperature and pressure will have the following form when there is no heat transfer by radiation in the flow:

$$\rho \frac{dh}{d\tau} = \operatorname{div}(\lambda \operatorname{grad} T) + q_v + \frac{dp}{d\tau} + \Phi, \qquad (1\text{-}10)$$

or in different form,

$$\rho c_p \frac{dT}{d\tau} = \operatorname{div}(\lambda \operatorname{grad} T) + q_v - \frac{T}{\rho}\left(\frac{\partial \rho}{\partial T}\right)_p \frac{dp}{d\tau} + \Phi, \qquad (1\text{-}11)$$

where h is the enthalpy, referred to unit mass; T is the temperature; c_p is the isobaric heat capacity, referred to unit mass; λ is the

thermal-conductivity coefficient; q_v is the strength of the internal heat sources (amount of heat liberated by the sources per unit volume in unit time); Φ is the dissipation function:

$$\Phi=\mu\left\{2\left[\left(\frac{\partial w_x}{\partial x}\right)^2+\left(\frac{\partial w_y}{\partial y}\right)^2+\left(\frac{\partial w_z}{\partial z}\right)^2\right]+\left(\frac{\partial w_x}{\partial y}+\frac{\partial w_y}{\partial x}\right)^2+\right.$$
$$\left.+\left(\frac{\partial w_x}{\partial z}+\frac{\partial w_z}{\partial x}\right)^2+\left(\frac{\partial w_y}{\partial z}+\frac{\partial w_z}{\partial y}\right)^2-\frac{2}{3}(\operatorname{div}\vec{w})^2\right\}.$$

Expressions can be written on the basis of (1-7) for the total derivatives $dh/d\tau$, $dT/d\tau$ and $dp/d\tau$

We shall study heat exchange for flow of liquids and gases moving at velocities considerably below the speed of sound.

The quantity $-\frac{1}{\rho}\left(\frac{\partial\rho}{\partial T}\right)_p=\beta$ is usually very small for a liquid and, moreover, the pressure in the flow varies negligibly. Thus the third term on the right side of (1-11) is small as compared with the other terms and can be dropped. For an ideal gas $\beta = 1/T$ and the same term becomes equal to $dp/d\tau$. At gas velocities not exceeding ~0.3 the speed of sound, $dp/d\tau$ is small as compared with the other terms of the equation, and it can also be dropped.

Thus in either case, the flowing medium (liquid or gas moving at moderate speed) can be treated as if it were incompressible, i.e., we can assume that its density does not change substantially owing to a change in pressure. Since in either case the relative change in density produced by the dependence on T and p will not be large, div $\vec{w}$ will be small as compared with the other terms of the expression for the dissipation function, and it can be neglected. As a result, the energy equation takes the form

$$\rho c_p\frac{dT}{d\tau}=\operatorname{div}(\lambda\operatorname{grad}T)+q_v+\mu S, \qquad (1\text{-}12)$$

where μS is the value of Φ at $\operatorname{div}\vec{w}=0$.

If λ is constant, then (1-12) reduces to the form

$$\frac{dT}{d\tau}=a\nabla^2T+\frac{q_v}{\rho c_p}+\frac{\mu}{\rho c_p}S, \qquad (1\text{-}13)$$

where $a=\lambda/\rho c_p$ is the thermal-diffusivity coefficient for the fluid.

1-3. SYSTEM OF EQUATIONS DESCRIBING HEAT EXCHANGE IN A FLUID FLOW

The process of heat exchange in a flow of viscous incompressible fluid whose physical properties depend arbitrarily on the temperature[4] is described by the following equation system, which we write in rectangular coordinates:

4/14

$$
\left.
\begin{aligned}
&\rho c_p\left(\frac{\partial T}{\partial \tau}+w_x\frac{\partial T}{\partial x}+w_y\frac{\partial T}{\partial y}+w_z\frac{\partial T}{\partial z}\right)=\frac{\partial}{\partial x}\left(\lambda\frac{\partial T}{\partial x}\right)+\\
&\quad+\frac{\partial}{\partial y}\left(\lambda\frac{\partial T}{\partial y}\right)+\frac{\partial}{\partial z}\left(\lambda\frac{\partial T}{\partial z}\right)+q_v+\mu S;\\
&\rho\left(\frac{\partial w_x}{\partial \tau}+w_x\frac{\partial w_x}{\partial x}+w_y\frac{\partial w_x}{\partial y}+w_z\frac{\partial w_x}{\partial z}\right)=\rho g_x-\frac{\partial p}{\partial x}+\\
&+\frac{\partial}{\partial x}\left(2\mu\frac{\partial w_x}{\partial x}\right)+\frac{\partial}{\partial y}\left[\mu\left(\frac{\partial w_x}{\partial y}+\frac{\partial w_y}{\partial x}\right)\right]+\frac{\partial}{\partial z}\left[\mu\left(\frac{\partial w_x}{\partial z}+\frac{\partial w_z}{\partial x}\right)\right];\\
&\rho\left(\frac{\partial w_y}{\partial \tau}+w_x\frac{\partial w_y}{\partial x}+w_y\frac{\partial w_y}{\partial y}+w_z\frac{\partial w_y}{\partial z}\right)=\rho g_y-\frac{\partial p}{\partial y}+\\
&+\frac{\partial}{\partial x}\left[\mu\left(\frac{\partial w_y}{\partial x}+\frac{\partial w_x}{\partial y}\right)\right]+\frac{\partial}{\partial y}\left(2\mu\frac{\partial w_y}{\partial y}\right)+\frac{\partial}{\partial z}\left[\mu\left(\frac{\partial w_y}{\partial z}+\frac{\partial w_z}{\partial y}\right)\right];\\
&\rho\left(\frac{\partial w_z}{\partial \tau}+w_x\frac{\partial w_z}{\partial x}+w_y\frac{\partial w_z}{\partial y}+w_z\frac{\partial w_z}{\partial z}\right)=\rho g_z-\frac{\partial p}{\partial z}+\\
&+\frac{\partial}{\partial x}\left[\mu\left(\frac{\partial w_z}{\partial x}+\frac{\partial w_x}{\partial z}\right)\right]+\frac{\partial}{\partial y}\left[\mu\left(\frac{\partial w_z}{\partial y}+\frac{\partial w_y}{\partial z}\right)\right]+\frac{\partial}{\partial z}\left(2\mu\frac{\partial w_z}{\partial z}\right);\\
&\frac{\partial \rho}{\partial \tau}+\frac{\partial(\rho w_x)}{\partial x}+\frac{\partial(\rho w_y)}{\partial y}+\frac{\partial(\rho w_z)}{\partial z}=0;\\
&\rho=\rho(T);\ c_p=c_p(T);\ \lambda=\lambda(T);\ \mu=\mu(T).
\end{aligned}
\right\}
\qquad (1\text{-}14)
$$

The specific relationships for ρ, c_p, λ, and μ as functions of T is determined by the nature of the fluid (see Chapter 3).

Equations (1-14) contain nine dependent variables (T, w_x, w_y, w_z, p, ρ, c_p, λ and μ). We have nine equations to determine them. Thus the equation system describing convective heat transfer in the moving medium is closed.

System (1-14) is extremely complex, and very difficult to solve in general form. These difficulties are caused by the nonlinearity of the equations of motion and energy, introduced by the convective terms on the left sides, and the fact that the physical properties of the fluid depend on the temperature. Since μ and ρ depend on T, the velocity and temperature fields are interrelated. Thus the equations of motion and continuity cannot be solved in isolation from the energy equation.

The problem is simplified considerably if we assume that the viscosity and density are constant. Here the equations of motion remain independent of the energy equation, and the temperature field has no influence whatsoever on the velocity field. The latter fact can be shown by solving the equations of motion and continuity.

If the velocity distribution found is substituted into the energy equation, the nonlinearity of this equation, introduced by the convective terms on the left side, will vanish together with the dependence of ρ on T. The nonlinearity associated with the dependence of λ and c_p on T remains, however. The next step in simplification lies in the assumption that c_p and λ are also constant.

If all physical properties are constant, System (1-14) will take the form

$$\left.\begin{aligned}
&\frac{\partial t}{\partial \tau}+w_x\frac{\partial t}{\partial x}+w_y\frac{\partial t}{\partial y}+w_z\frac{\partial t}{\partial z}=a\left(\frac{\partial^2 t}{\partial x^2}+\frac{\partial^2 t}{\partial y^2}+\frac{\partial^2 t}{\partial z^2}\right)+\\
&\qquad+\frac{q_v}{\rho c_p}+\frac{\mu}{\rho c_p}S;\\
&\frac{\partial w_x}{\partial \tau}+w_x\frac{\partial w_x}{\partial x}+w_y\frac{\partial w_x}{\partial y}+w_z\frac{\partial w_x}{\partial z}=-\frac{1}{\rho}\frac{\partial p}{\partial x}+\\
&\qquad+\nu\left(\frac{\partial^2 w_x}{\partial x^2}+\frac{\partial^2 w_x}{\partial y^2}+\frac{\partial^2 w_x}{\partial z^2}\right);\\
&\frac{\partial w_y}{\partial \tau}+w_x\frac{\partial w_y}{\partial x}+w_y\frac{\partial w_y}{\partial y}+w_z\frac{\partial w_y}{\partial z}=-\frac{1}{\rho}\frac{\partial p}{\partial y}+\\
&\qquad+\nu\left(\frac{\partial^2 w_y}{\partial x^2}+\frac{\partial^2 w_y}{\partial y^2}+\frac{\partial^2 w_y}{\partial z^2}\right);\\
&\frac{\partial w_z}{\partial \tau}+w_x\frac{\partial w_z}{\partial x}+w_y\frac{\partial w_z}{\partial y}+w_z\frac{\partial w_z}{\partial z}=-\frac{1}{\rho}\frac{\partial p}{\partial z}+\\
&\qquad+\nu\left(\frac{\partial^2 w_z}{\partial x^2}+\frac{\partial^2 w_z}{\partial y^2}+\frac{\partial^2 w_z}{\partial z^2}\right);\\
&\frac{\partial w_x}{\partial x}+\frac{\partial w_y}{\partial y}+\frac{\partial w_z}{\partial z}=0.
\end{aligned}\right\}\qquad (1\text{-}15)^*$$

The assumption that the physical properties are constant substantially simplifies the equation system, so that it becomes possible to solve many problems in convective heat exchange. In addition, this assumption restricts the applicability of the results obtained to those real processes in which the physical properties of the fluid vary negligibly. Nonetheless, problems involving heat exchange under constant physical properties are of great interest, since they permit us to understand the basic laws characterizing various heat-exchange processes.

In the discussion to come, we shall require the energy, motion, and continuity equations in cylindrical coordinates. We let x, r, and φ represent the axial, radial, and azimuthal coordinates, respectively, and w_x, w_r, and w_φ the velocity components along these coordinates. Going from the rectangular system to the cylindrical, in place of (1-14) we obtain

$$\rho c_p\left(\frac{\partial T}{\partial \tau}+w_x\frac{\partial T}{\partial x}+w_r\frac{\partial T}{\partial r}+\frac{w_\varphi}{r}\cdot\frac{\partial T}{\partial \varphi}\right)=\frac{\partial}{\partial x}\left(\lambda\frac{\partial T}{\partial x}\right)+$$
$$+\frac{\partial}{\partial r}\left(\lambda\frac{\partial T}{\partial r}\right)+\frac{1}{r}\lambda\frac{\partial t}{\partial r}+\frac{1}{r^2}\cdot\frac{\partial}{\partial \varphi}\left(\lambda\frac{\partial T}{\partial \varphi}\right)+q_v+\mu S,$$

where

* /25

$$
\left.
\begin{aligned}
&S=2\left[\left(\frac{\partial w_x}{\partial x}\right)^2+\left(\frac{\partial w_r}{\partial r}\right)^2+\left(\frac{1}{r}\cdot\frac{\partial w_\varphi}{\partial \varphi}+\frac{w_r}{r}\right)^2\right]+\left(\frac{\partial w_x}{\partial r}+\frac{\partial w_r}{\partial x}\right)^2+\\
&\quad+\left(\frac{1}{r}\cdot\frac{\partial w_x}{\partial \varphi}+\frac{\partial w_\varphi}{\partial x}\right)^2+\left(\frac{1}{r}\cdot\frac{\partial w_r}{\partial \varphi}+\frac{\partial w_\varphi}{\partial r}-\frac{w_\varphi}{r}\right)^2;\\
&\rho\left(\frac{\partial w_x}{\partial \tau}+w_x\frac{\partial w_x}{\partial x}+w_r\frac{\partial w_x}{\partial r}+\frac{w_\varphi}{r}\cdot\frac{\partial w_x}{\partial \varphi}\right)=\rho g_x-\frac{\partial p}{\partial x}+\\
&+\frac{\partial}{\partial x}\left(2\mu\frac{\partial w_x}{\partial x}\right)+\frac{\partial}{\partial r}\left[\mu\left(\frac{\partial w_x}{\partial r}+\frac{\partial w_r}{\partial x}\right)\right]+\frac{1}{r}\mu\left(\frac{\partial w_x}{\partial r}+\frac{\partial w_r}{\partial x}\right)+\\
&\quad+\frac{1}{r}\cdot\frac{\partial}{\partial \varphi}\left[\mu\left(\frac{1}{r}\cdot\frac{\partial w_x}{\partial \varphi}+\frac{\partial w_\varphi}{\partial x}\right)\right];\\
&\rho\left(\frac{\partial w_r}{\partial \tau}+w_x\frac{\partial w_r}{\partial x}+w_r\frac{\partial w_r}{\partial r}+\frac{w_\varphi}{r}\frac{\partial w_r}{\partial \varphi}-\frac{w_\varphi^2}{r}\right)=\rho g_r-\frac{\partial p}{\partial r}+\\
&+\frac{\partial}{\partial x_i}\left[\mu\left(\frac{\partial w_r}{\partial x}+\frac{\partial w_x}{\partial r}\right)\right]+\frac{\partial}{\partial r}\left(2\mu\frac{\partial w_r}{\partial r}\right)+\frac{2}{r}\mu\left(\frac{\partial w_r}{\partial r}-\frac{w_r}{r}-\frac{1}{r}\cdot\frac{\partial w_\varphi}{\partial \varphi}\right)+\\
&\quad+\frac{1}{r}\cdot\frac{\partial}{\partial \varphi}\left[\mu\left(\frac{1}{r}\cdot\frac{\partial w_r}{\partial \varphi}+\frac{\partial w_\varphi}{\partial r}-\frac{w_\varphi}{r}\right)\right];\\
&\rho\left(\frac{\partial w_\varphi}{\partial \tau}+w_x\frac{\partial w_\varphi}{\partial x}+w_r\frac{\partial w_\varphi}{\partial r}+\frac{w_\varphi}{r}\cdot\frac{\partial w_\varphi}{\partial \varphi}+\frac{w_r w_\varphi}{r}\right)=\rho g_\varphi-\frac{1}{r}\cdot\frac{\partial p}{\partial \varphi}+\\
&+\frac{\partial}{\partial x}\left[\mu\left(\frac{\partial w_\varphi}{\partial x}+\frac{1}{r}\cdot\frac{\partial w_x}{\partial \varphi}\right)\right]+\frac{\partial}{\partial r}\left[\mu\left(\frac{\partial w_\varphi}{\partial r}+\frac{1}{r}\cdot\frac{\partial w_r}{\partial \varphi}-\frac{w_\varphi}{r}\right)\right]+\\
&+\frac{2}{r}\mu\left(\frac{\partial w_\varphi}{\partial r}+\frac{1}{r}\cdot\frac{\partial w_r}{\partial \varphi}-\frac{w_\varphi}{r}\right)+\frac{1}{r}\cdot\frac{\partial}{\partial \varphi}\left[2\mu\left(\frac{1}{r}\cdot\frac{\partial w_\varphi}{\partial \varphi}+\frac{w_r}{r}\right)\right];\\
&\frac{\partial \rho}{\partial \tau}+\frac{\partial(\rho w_x)}{\partial x}+\frac{\partial(\rho w_r)}{\partial r}+\frac{1}{r}\cdot\frac{\partial(\rho w_\varphi)}{\partial \varphi}+\rho\frac{w_r}{r}=0.
\end{aligned}
\right\}
\qquad (1\text{-}16)
$$

If all the physical properties of the fluid are constant, (1-16) takes the form

$$
\left.
\begin{aligned}
&\frac{\partial t}{\partial \tau}+w_x\frac{\partial t}{\partial x}+w_r\frac{\partial t}{\partial r}+\frac{w_\varphi}{r}\cdot\frac{\partial t}{\partial \varphi}=a\left(\frac{\partial^2 t}{\partial x^2}+\frac{\partial^2 t}{\partial r^2}+\frac{1}{r}\cdot\frac{\partial t}{\partial r}+\right.\\
&\quad\left.+\frac{1}{r^2}\cdot\frac{\partial^2 t}{\partial \varphi^2}\right)+\frac{q_v}{\rho c_p}+\frac{\mu}{\rho c_p}S;\\
&\frac{\partial w_x}{\partial \tau}+w_x\frac{\partial w_x}{\partial x}+w_r\frac{\partial w_x}{\partial r}+\frac{w_\varphi}{r}\cdot\frac{\partial w_x}{\partial \varphi}=-\frac{1}{\rho}\cdot\frac{\partial p}{\partial x}+\\
&+\nu\left(\frac{\partial^2 w_x}{\partial x^2}+\frac{\partial^2 w_x}{\partial r^2}+\frac{1}{r}\cdot\frac{\partial w_x}{\partial r}+\frac{1}{r^2}\cdot\frac{\partial^2 w_x}{\partial \varphi^2}\right);\\
&\frac{\partial w_r}{\partial \tau}+w_x\frac{\partial w_r}{\partial x}+w_r\frac{\partial w_r}{\partial r}+\frac{w_\varphi}{r}\frac{\partial w_r}{\partial \varphi}-\frac{w_\varphi^2}{r}=-\frac{1}{\rho}\cdot\frac{\partial p}{\partial r}+\\
&+\nu\left(\frac{\partial^2 w_r}{\partial x^2}+\frac{\partial^2 w_r}{\partial r^2}+\frac{1}{r}\cdot\frac{\partial w_r}{\partial r}-\frac{w_r}{r^2}+\frac{1}{r^2}\cdot\frac{\partial^2 w_r}{\partial \varphi^2}-\frac{2}{r^2}\cdot\frac{\partial w_\varphi}{\partial \varphi}\right);\\
&\frac{\partial w_\varphi}{\partial \tau}+w_x\frac{\partial w_\varphi}{\partial x}+w_r\frac{\partial w_\varphi}{\partial r}+\frac{w_\varphi}{r}\cdot\frac{\partial w_\varphi}{\partial \varphi}+\frac{w_r w_\varphi}{r}=-\frac{1}{r\rho}\cdot\frac{\partial p}{\partial \varphi}+\\
&+\nu\left(\frac{\partial^2 w_\varphi}{\partial x^2}+\frac{\partial^2 w_\varphi}{\partial r^2}+\frac{1}{r}\cdot\frac{\partial w_\varphi}{\partial r}-\frac{w_\varphi}{r^2}+\frac{1}{r^2}\cdot\frac{\partial^2 w_\varphi}{\partial \varphi^2}+\frac{2}{r^2}\cdot\frac{\partial w_r}{\partial \varphi}\right);\\
&\frac{\partial w_x}{\partial x}+\frac{\partial w_r}{\partial r}+\frac{1}{r}\cdot\frac{\partial w_\varphi}{\partial \varphi}+\frac{w_r}{r}=0.
\end{aligned}
\right\}
\qquad (1\text{-}17)
$$

1-4. INITIAL AND BOUNDARY CONDITIONS

To solve specific problems of fluid motion and heat exchange, we must add the so-called initial and boundary conditions to the basic equations.

The initial conditions consist in the specification of the velocity field, temperature field, and other dependent variables over the entire system volume[5] at the initial time (i.e., the time beginning at which we investigate the process occurring in the system). If fluid motion and heat exchange are stationary, there is no need to specify the initial conditions.

The boundary conditions reduce to specification of system geometry and the conditions for fluid motion and heat exchange at the system boundaries. The latter may be solid (surfaces of solids washed by a fluid) or fluid (for example, entrance section of a tube, outer boundary of a boundary layer, etc.).

A fluid flow in a tube is bounded by the inside surface of the walls, and by the entrance and exit sections. The boundary conditions must then be specified at these surfaces. We usually assume that the tube is a semibounded cylinder, i.e., that it extends to infinity in the direction of the flow. Here there is no need to specify the boundary conditions for the exit section.[6] The wall surfaces washed by the flow are ordinarily taken to be smooth.

The boundary conditions for the velocity at the surface of an impermeable wall are specified on the basis of the assumption that a viscous fluid will adhere to the wall surface. Accordingly, the normal and tangential components of the velocity vector with respect to the wall are assumed to be zero at the surface of a stationary impenetrable wall. The boundary conditions for the temperature at the wall are based on the assumption that the temperature field is continuous at the fluid-wall boundary.[7] Consequently, the fluid temperature at a given point on the wall surface must equal the temperature of the wall surface at this same point. This assumption is well confirmed by experiment for various fluids, other than rarefied gases. In the latter case, as we know, slipping occurs, and there is a temperature discontinuity between the gas and the wall surface. We shall not consider this case, however.

There are various ways of specifying the boundary conditions for the temperature field at the wall. Let us look at three very characteristic types of boundary conditions, which we may call boundary conditions of the first, second, and third types in accordance with the practice in heat-conduction theory.

Boundary conditions of the first kind are specified as the distribution of wall temperature (i.e., the temperature at the fluid-wall boundary) over the surface, and its time variation:

$$t_c = t_c(x_c, y_c, z_c, \tau), \qquad (1\text{-}18)$$

where x_s, y_s, and z_s are the coordinates of points on the wall surface.

Under stationary conditions, t_s will naturally be independent of the time. In the simplest case, t_s = const, i.e., it is constant over the surface and does not vary in time.

Boundary conditions of the second type involve specification of the distribution of heat-flow density at the wall over the surface, and its time variation. Since the fluid at the wall is stationary and, consequently, the Fourier law is applicable, specification of the heat-flow density q_s is equivalent to specification of the temperature gradient at the wall. We thus have

$$q_c = -\lambda\left(\frac{\partial t}{\partial n}\right)_{n=+0} = q_c(x_c, y_c, z_c, \tau), \qquad (1\text{-}19)$$

where λ is the thermal-conductivity coefficient for the fluid;

n is the normal to the wall surface, directed toward the fluid.

To determine the temperature field in this case, we must specify at least one value of the actual temperature at some point in the flow.

Boundary conditions of the third type are used when the fluid moving in the tube delivers heat to the ambient through the thin separating wall, but the wall temperature at the fluid boundary ($t_{n=0} = t_c$) is not specified; instead we have the ambient temperature t_{sr}. Here we can make the elementary assumption that the heat-flow density at the wall is proportional to the temperature difference $t_{n=0} - t_{cp}$. Assuming a thin wall and neglecting its heat capacity (for nonstationary heat exchange), we can write the boundary condition of the third kind as

$$-\lambda\left(\frac{\partial t}{\partial n}\right)_{n=+0} = K'(t_{cp} - t_{n=0}), \qquad (1\text{-}20)$$

where K' is a coefficient of proportionality, called the coefficient of heat transfer between the wall surface on the fluid side and the ambient. Here K' and t_{sr} can be specified either as functions of the distance along the tube axis and the time, or as constants in the simplest case. When $\frac{K'}{\lambda} \to \infty$ $t_{n=0} = t_c = t_{cp}$, i.e., the boundary conditions of the third kind reduce to boundary conditions of the first kind.

At the entrance section of the tube, the distributions of velocity and temperature over the section are specified as time functions. The transverse velocity components are ordinarily taken equal to zero, while the longitudinal velocity component and temperature are assumed to be uniform over the section.

It is not always possible to specify the thermal boundary conditions at the wall surface in the form of certain functions: $t_c(x_c, y_c, z_c, \tau)$ or $q_c(x_c, y_c, z_c, \tau)$. We encounter this situation, for example, when the width and physical properties (λ, ρ, c_p) of the wall material are commensurate with the tube radius and the correspond-

ing properties of the fluid. Here the temperature fields in the wall and the flow will differ substantially. Thus the temperature distribution on the fluid-wall boundary will not be known in advance and, consequently, cannot be specified beforehand.

Solution of such problems requires simultaneous consideration of the heat-exchange process in the fluid flow and the heat-conduction process in the wall. For this purpose, to the equation system describing the temperature field in the flow we must add the heat-conduction equation describing the temperature field in the wall, and at the fluid-wall boundary, we must specify the conditions for contact of these fields (such problems are thus often called contact problems). The contact conditions reduce to the following equations:

$$t_{n=+0} = t_c|_{n=-0};$$
$$\lambda\left(\frac{\partial t}{\partial n}\right)_{n=+0} = \lambda_c\left(\frac{\partial t_c}{\partial n}\right)_{n=-0},$$

where t is the fluid temperature; t_s is the wall temperature; λ and λ_s are the thermal-conductivity coefficients for fluid and wall.

The first equation follows from the assumption that the temperature field is continuous at the fluid-wall boundary, and the second from the law of conservation of energy.

Joint analysis of two or, even worse, three[8] contacting fields considerably complicates the problem. In practice, however, we most frequently have to do with fairly thin walls that are good heat conductors; in most cases (particularly under stationary conditions) this permits us to reduce the problem to consideration of the temperature field in the fluid flow alone.

Manuscript Page No.

Footnotes

5 [1]By a Newtonian fluid, we mean a fluid for which the relationship between the stresses (normal and tangential) and resulting strains for a liquid particle are described by the generalized Newton law.

6 [2]Naturally, in this case as well the pressure field will depend on the gravitational force.

7 [3]We note that this lift force introduced into the equation of motion is arbitrary, since it is represented on the assumption that the density of the fluid surrounding a fluid particle with density ρ is constant and equal to ρ_0.

8 [8]For an incompressible fluid, ρ is independent of the pres-

sure; the dependence of c_p, λ, and μ on p is in general negligible, and is disregarded in heat-exchange calculations, as a rule (see Chapter 3). The region near the saturation curve and the supercritical region represent exceptions.

9 *In writing the equations of motion we drop the term containing div $\vec{w}$, since it is small as compared with the other terms for an incompressible fluid.

10 *Here the symbol p represents the difference between the actual pressure at a given point in the flow and the hydrostatic pressure at the same point. In §1-2, this difference was represented by the symbol $p_1 = p - p_0$ (here grad $p_0 = \rho g$). Here and in the ensuing discussion, we drop the subscript 1.

We also note that here the temperature is represented by the symbol t, ordinarily employed when the temperature is measured in °C. If the temperature is measured in °K, however, we then generally employ the symbol T. It is convenient to measure temperature in °K, for example, for heat exchange when the moving gas has variable physical properties.

12 [5]That is, regions within which the process under study takes place.

12 [6]In applying the solution for a semibounded tube to tubes of finite length we naturally neglect singularities in flow and heat exchange near the exit section that are determined by the state of the flow beyond the exit section.

12 [7]In the sense that there are no discontinuities in the values of the temperature, rather than its derivatives.

14 [8]For example, the temperature fields in the flow within the tube, in the tube wall, and in the flow washing the wall from the outside.

Manuscript Page No.

Transliterated Symbols

12 c = s = stenka = wall

13 cp = sr = sreda = medium

Chapter 2

DETERMINING THE HEAT FLOW, HEAT-TRANSFER COEFFICIENT, AND HYDRAULIC RESISTANCE

2-1. HEAT FLOW AT FLUID-WALL BOUNDARY

Solving the equation system for convective heat exchange for performing measurements, we can find the temperature and velocity fields in the fluid flow. Assuming these fields to be known, let us consider methods for determining the amount of heat transferred from the wall to the fluid.

The fluid is stationary at the wall surface and, consequently, heat is transferred only by heat conduction. Thus according to the Fourier law, the heat-flow density at the wall is

$$q_c = -\lambda\left(\frac{\partial t}{\partial n}\right)_{n=0}, \qquad (2\text{-}1)$$

where n is the normal to the inside wall surface, directed toward the fluid; λ is the thermal-conductivity coefficient of the fluid.

In the general case, q_s varies along the surface and in time. Thus the heat flow at the wall, i.e., the amount of heat transferred in unit time from a wall with surface F to the fluid is

$$Q_c = \int_F q_c\, dF = -\int_F \lambda\left(\frac{\partial t}{\partial n}\right)_{n=0} dF. \qquad (2\text{-}2)$$

The amount of heat transferred from the wall to the fluid in time τ is

$$Q_{c\tau} = \int_0^\tau Q_c\, d\tau = \int_0^\tau d\tau \int_F q_c\, dF. \qquad (2\text{-}3)$$

As we can see from (2-1) and (2-2), to determine q_s, Q_s, and $Q_{s\tau}$ we need only know the temperature field in the flow and the thermal-conductivity coefficient for the liquid.

The heat flow at a wall can also be found from the energy-balance equation for a fluid element of length dx bounded by the tube walls and two sections normal to its axis. It is not difficult to obtain the energy-balance equation for such an element by inte-

grating the energy equation over the tube cross section. Let us do this for an incompressible fluid with variable physical properties, flowing in a round tube; for simplicity, we assume that the velocity and temperature fields are symmetric about the x axis of the tube.

Going from temperature to enthalpy in the left side of (1-12) and transforming it with the aid of the continuity equation, we obtain

$$\frac{\partial(\rho h)}{\partial\tau}+\frac{\partial(\rho w_x h)}{\partial x}+\frac{1}{r}\cdot\frac{\partial}{\partial r}(r\rho w_r h)=\frac{\partial}{\partial x}\left(\lambda\frac{\partial t}{\partial x}\right)+$$
$$+\frac{1}{r}\cdot\frac{\partial}{\partial r}\left(r\lambda\frac{\partial t}{\partial r}\right)+q_v+\mu S. \qquad (2\text{-}4)$$

We multiply this equation by $2\pi r\,dr$ and integrate it with respect to r from 0 to r_0 (where r_0 is the tube radius):

$$\int_0^{r_0}\frac{\partial(\rho h)}{\partial\tau}2\pi r\,dr+\int_0^{r_0}\frac{\partial(\rho w_x h)}{\partial x}2\pi r\,dr+2\pi\int_0^{r_0}d(r\rho w_r h)=$$
$$=\int_0^{r_0}\frac{\partial}{\partial x}\left(\lambda\frac{\partial t}{\partial x}\right)2\pi r\,dr+2\pi\int_0^{r_0}d\left(r\lambda\frac{\partial t}{\partial r}\right)+\int_0^{r_0}(q_v+\mu S)\,2\pi r\,dr. \qquad (2\text{-}5)$$

The third integral on the left side equals zero, since $w_r = 0$ when $r = r_0$. The second integral on the right side is

$$2\pi\int_0^{r_0}d\left(r\lambda\frac{\partial t}{\partial r}\right)=2\pi\left[r\lambda\frac{\partial t}{\partial r}\right]_{r=0}^{r=r_0}=\lambda\left(\frac{\partial t}{\partial r}\right)_{r=r_0}2\pi r_0=q_0 2\pi r_0.$$

If in (2-5) we change the sequence of differentiation with respect to τ or x and integration with respect to r, we obtain

$$\frac{\partial}{\partial\tau}\int_0^{r_0}\rho h\,2\pi r\,dr+\frac{\partial}{\partial x}\int_0^{r_0}\rho w_x h\,2\pi r\,dr=\frac{\partial}{\partial x}\int_0^{r_0}\lambda\frac{\partial t}{\partial x}2\pi r\,dr+$$
$$+q_0 2\pi r_0+\int_0^{r_0}(q_v+\mu S)\,2\pi r\,dr. \qquad (2\text{-}6)$$

We let f be the area of the tube cross section normal to the axis, and s the tube perimeter in this section. Then from (2-6) we find

$$q_0=\frac{1}{s}\left[\frac{\partial}{\partial\tau}\int_f\rho h\,df+\frac{\partial}{\partial x}\int_f\left(\rho w_x h-\lambda\frac{\partial t}{\partial x}\right)df-\right.$$
$$\left.-\int_f(q_v+\mu S)\,df\right]. \qquad (2\text{-}7)$$

It is not difficult to see that although Expression (2-7) for the density of the heat flow at the wall has been derived for a round tube, it is actually valid for a tube of any cross-sectional form that remains unchanged along the axis. If the heat-flow density at the wall varies along the perimeter, then

by q_s in (2-7) we should understand the heat-flow density in the given tube section averaged over the perimeter.

For stationary flow and heat exchange, (2-7) will take the form

$$q_c = \frac{1}{s}\left[\frac{d}{dx}\int_f \left(\rho w_x h - \lambda \frac{\partial t}{\partial x}\right) df - \int_f (q_v + pS)\, df\right]. \qquad (2\text{-}8)$$

The change in heat-flow density along the axis owing to heat conduction is usually small, and can be neglected in most cases (see §6-1). The same may be said of the heat liberated by dissipation. If, in addition, the flow has no internal sources ($q_v = 0$), then (2-8) is reduced to the form

$$q_c = \frac{1}{s}\frac{d}{dx}\int_f \rho w_x h\, df. \qquad (2\text{-}9)$$

For a tube section of length l, the heat flow from the wall to the liquid will evidently be

$$Q_c = \int_0^l q_c s\, dx. \qquad (2\text{-}10)$$

In the simplest case, where q_s is determined by (2-9), we have

$$Q_c = \left[\int_f \rho w_x h\, df\right]_{x=l} - \left[\int_f \rho w_x h\, df\right]_{x=0}. \qquad (2\text{-}11)$$

For computational simplicity, we introduce the mean mass enthalpy and mean mass temperature of the fluid. The mean mass enthalpy is defined as the ratio of the amount of heat passing through a given cross section in unit time owing to convective transfer to the fluid flow rate through this section:

$$\bar{h} = \frac{\int_f \rho w_x h\, df}{\int_f \rho w_x\, df}. \qquad (2\text{-}12)$$

By the mean mass temperature, we mean the temperature corresponding to the mean mass enthalpy. We represent it by $\bar{t}$ or $\bar{T}$, measured respectively in centigrade or absolute-temperature units.

If the heat capacity c_p is constant, then from (2-12) we obtain the following expression for the mean mass temperature of the fluid:

$$\bar{t} = \frac{\int_f \rho w_x t\, df}{\int_f \rho w_x\, df}. \qquad (2\text{-}13)$$

If ρ and c_p are constant, from (2-13) we have:

$$\bar{t} = \frac{\int w_x t \, df}{\int w_x \, df}. \qquad (2\text{-}14)$$

The physical meaning of $\bar{h}$ and $\bar{t}$ is easily understood if we imagine that the fluid in the given tube section is mixed in some way that its enthalpy and temperature have become identical over the section. This constant enthalpy and temperature will be the mean mass values. If w_x, ρ, and c_p are all constant over the section then, as we can see from (2-14), $\bar{t}$ will be the mean fluid temperature over the section.

Using the concept of the mean mass enthalpy, we can write (2-9) and (2-11) as

$$q_c = \frac{1}{s} G \frac{d\bar{h}}{dx}; \qquad (2\text{-}15)$$

$$Q_c = G(\bar{h}_l - \bar{h}_0), \qquad (2\text{-}16)$$

where $G = \int \rho w_x \, df$ is the mass fluid flowrate; $\bar{h}_l$ and $\bar{h}_0$ are the values of $\bar{h}$ at $x = l$ and $x = 0$.

If c_p is constant, then in place of (2-15) and (2-16) we have

$$q_c = \frac{1}{s} c_p G \frac{d\bar{t}}{dx}; \qquad (2\text{-}17)$$

$$Q_c = c_p G(\bar{t}_l - \bar{t}_0). \qquad (2\text{-}18)$$

2-2. LOCAL HEAT-TRANSFER COEFFICIENT

The heat-transfer coefficient is an important characteristic of the process of heat exchange between a wall and a fluid flow. The local heat-exchange coefficient is introduced by definition; it is the ratio of the heat-flow density at a given point on the wall surface to the difference between the wall temperature at this point and the fluid temperature.[1] Depending on how the fluid temperature is selected, there are two ways of defining the local heat-transfer coefficient:

$$\alpha = \frac{q_c}{t_c - \bar{t}}, \qquad (2\text{-}19)$$

$$\alpha = \frac{q_c}{t_c - t_0}, \qquad (2\text{-}20)$$

where q_s is the heat-flow density at the given point on the wall surface; t_s is the wall temperature at this same point; $\bar{t}$ is the mean mass temperature of the fluid at the considered section; t_0 is the temperature of the fluid at the entrance to the heated length of tube, and is constant over the section.

In the first case we say that α refers to the local temperature head, and in the second to the initial temperature head. The

[1] /27

particular method chosen to define α depends on the nature of the problem, and is based solely on considerations of convenience (we obviously should pick the method for which the relationship describing the variation in α will be simplest and most convenient for calculation).

Substituting q_s from (2-1) into (2-19), we obtain the following expression for the local heat-transfer coefficient:

$$\alpha = -\frac{\lambda}{t_c - \bar{t}}\left(\frac{\partial t}{\partial n}\right)_{n=0}. \qquad (2\text{-}21)$$

In the simplest case, where q_s can be represented in the form (2-17), we obtain

$$\alpha = \frac{c_p G}{s(t_c - \bar{t})}\cdot\frac{d\bar{t}}{dx}. \qquad (2\text{-}22)$$

Analogous equations can also be written when α refers to $t_s - t_0$.

In the general case, like q_s and t_s, the local heat-transfer coefficient may vary along the perimeter and length of the tube. If q_s and t_s are constant over the perimeter, α will vary only along the length. We can use (2-21) to determine the local heat-transfer coefficient at each point on the wall surface. We can also use (2-22) to compute just the mean heat-transfer coefficient over the perimeter in the given section. If the wall temperature varies along the perimeter, we then substitute the mean wall temperature over the perimeter into (2-22).

To conclude, we note that the numerical values of the heat-transfer coefficient and the way in which it changes along the length will depend not only on the flow and heat-exchange conditions, but also on the method used to define α, i.e., on whether we use (2-19) or (2-20).

2-3. VARIATION IN HEAT-FLOW DENSITY, FLUID TEMPERATURE, AND WALL TEMPERATURE ALONG TUBE LENGTH

In determining heat exchange in tubes, we ordinarily face two problems: determination of the variation in $\bar{t}$ and q_s along the tube length when we know $\alpha(x)$ and $t_s(x)$, and determination of the variation in $\bar{t}$ and t_s along the tube length when we know $q_s(x)$ and $\alpha(x)$. We consider both these problems for the elementary case in which the physical properties are constant, there are no internal heat sources, and the axial heat conduction and dissipation have negligible influence.

1. We begin with the first problem. Since we know the relationships $\alpha(x)$ and $t_s(x)$, to determine $\bar{t}(x)$ we can make use of (2-22). We write it as

$$\frac{d\bar{t}}{dx} + \frac{s\alpha}{Gc_p}\bar{t} = \frac{s\alpha}{Gc_p}t_c$$

or

$$\frac{d\bar{t}}{dx}+f(x)\bar{t}=g(x),$$

where

$$f(x)=\frac{s\alpha}{Gc_p};\ g(x)=\frac{s\alpha}{Gc_p}t_c.$$

Solving this equation under the boundary condition $\bar{t} = t_0$ at $x = 0$, we obtain

$$\bar{t}=e^{-\varphi(x)}\left[t_0+\int_0^x g(x)e^{\varphi(x)}dx\right], \qquad (2\text{-}23)$$

where

$$\varphi(x)=\int_0^x f(x)dx.$$

If the wall temperature is constant along the length (t_s = const), then

$$\bar{t}=e^{-\varphi}\left(t_0+t_c\int_0^x\varphi' e^{\varphi}dx\right)=e^{-\varphi}\left(t_0+t_c\int_0^{\varphi}e^{\varphi}d\varphi\right),$$

from which it follows that

$$\bar{t}=t_c+(t_0-t_c)e^{-\varphi}. \qquad (2\text{-}24)$$

If, in addition, α is constant along the length, then

$$\bar{t}=t_c+(t_0-t_c)e^{-\frac{s\alpha}{Gc_p}x}. \qquad (2\text{-}25)$$

The heat-flow density at the wall is found directly from (2-19):

$$q_c=\alpha(t_c-\bar{t}).$$

2. When we are given the distribution $q_s(x)$ and $\alpha(x)$, the variation in the mean mass temperature of the fluid along the length is found from (2-17). Integrating the latter with respect to x and using the boundary condition $\bar{t} = t_0$ at $x = 0$, we obtain

$$\bar{t}=t_0+\frac{s}{Gc_p}\int_0^x q_c(x)dx. \qquad (2\text{-}26)$$

Thus, for example, if q_s = const, then

$$\bar{t}=t_0+\frac{sq_c}{Gc_p}x,$$

i.e., $\bar{t}$ varies linearly as a function of x.

The wall temperature will evidently equal

$$t_c=\bar{t}+\frac{q_c(x)}{\alpha(x)}. \qquad (2\text{-}27)$$

With q_s = const and α = const, both t_s and $\bar{t}$ will vary linearly; here $t_s - \bar{t}$ = const.

2-4. MEAN HEAT-TRANSFER COEFFICIENT AND TEMPERATURE HEAD

The mean heat-transfer coefficient along the tube length, like the local coefficient, can be defined in different ways. Let us look at the principal methods.

Mean integral heat-transfer coefficient:

$$\bar{\alpha} = \frac{1}{l}\int_0^l \alpha\, dx. \qquad (2\text{-}28)$$

Heat-transfer coefficient referred to mean integral temperature difference:

$$\bar{\alpha} = \frac{Q_c}{F\overline{\Delta t}_n}, \text{ where } \overline{\Delta t}_n = \frac{1}{l}\int_0^l (t_c - \bar{t})\, dx. \qquad (2\text{-}29)$$

Heat-transfer coefficient referred to arithmetic mean temperature difference:

$$\bar{\alpha} = \frac{Q_c}{F\overline{\Delta t}_a}, \text{ where } \overline{\Delta t}_a = \bar{t}_c - \frac{1}{2}(t_0 + \bar{t}_l). \qquad (2\text{-}30)$$

The mean heat-transfer coefficient referred to the initial temperature difference:

$$\bar{\alpha} = \frac{Q_c}{F(\bar{t}_c - t_0)}. \qquad (2\text{-}31)$$

Here Q_s is the heat flow along the tube length from $x = 0$ to $x = l$: $F = sl$ is the inside surface of the tube segment of length l; α is the local or mean-perimeter heat-transfer coefficient a distance x from the entrance; t_s is the constant or mean-perimeter wall temperature a distance x from the entrance; $\bar{t}_s$ is the mean wall temperature over the surface for the tube segment of length l; t_0 and $\bar{t}_l$ are the mean mass fluid temperatures at $x = 0$ and $x = l$.

The choice of a particular method for defining $\bar{\alpha}$ is in general arbitrary. Nonetheless, for simplicity and clarity in representing the results of a theoretical or experimental investigation, and convenience in practical calculations, the method selected should agree with the nature of the problem under study.

Defining the mean integral heat-transfer coefficient in accordance with (2-28), we substitute the value of α from (2-22) into this expression:

$$\bar{\alpha} = \frac{1}{l}\int_0^l \alpha\, dx = \frac{1}{l}\cdot\frac{c_p G}{s}\int_0^l \frac{d\bar{t}}{t_c - \bar{t}}.$$

Integration is simple only if t_s = const. In such case, we have

$$\bar{\alpha} = \frac{c_p G}{Fl} \ln \frac{t_c - t_0}{t_c - \bar{t}_l}. \qquad (2\text{-}32)$$

Multiplying and dividing this equation by $\bar{t}_l - t_0$ and remembering that $c_p G(\bar{t}_l - t_0) = Q_0$, we can write it as

$$\bar{\alpha} = \frac{Q_0}{F\Delta\bar{t}_l}, \qquad (2\text{-}32a)$$

where

$$\Delta\bar{t}_l = \frac{\bar{t}_l - t_0}{\ln \frac{t_c - t_0}{t_c - \bar{t}_l}}. \qquad (2\text{-}33)$$

Thus if we use the mean integral heat-transfer coefficient when t_s = const for any type of variation in α along the length, and with the restrictions associated with the derivation of (2-22), we arrive at the concept of the mean logarithmic temperature difference $\Delta\bar{t}_l$. Here to determine $\bar{\alpha}$ we need not know the law governing the variation in α and $\bar{t}$ along the length.

For fluid moving in tubes, if the local heat-transfer coefficient is found in accordance with (2-19), it will usually vary along the length for the segment between $x = 0$ and $x = l_{n.t}$,[2] while for $x > l_{n.t}$, i.e., over the rest of the tube, it will remain constant. We let α_∞ represent this constant value of α.

At $x < l_{n.t}$, let $\alpha = f(x)$, and at $x \geq l_{n.t}$, let $\alpha = \alpha_\infty$ = const. Let us see how the mean heat-transfer coefficient will vary for values of $x >> l_{n.t}$. This question is significant when we process experimental data and compare the results of different experimental investigations.

The mean integral heat-transfer coefficient when $x > l_{n.t}$ can be represented as

$$\bar{\alpha} = \frac{1}{x}\int_0^x \alpha\, dx = \frac{1}{x}\left(\int_0^{l_{n.t}} \alpha\, dx + \int_{l_{n.t}}^x \alpha_\infty dx\right).$$

If we let

$$\bar{\alpha}_{n.t} = \frac{1}{l_{n.t}}\int_0^{l_{n.t}} \alpha\, dx,$$

represent the mean heat-transfer coefficient at the thermal initial segment, then the preceding equation can be written as

$$\frac{\bar{\alpha}}{\alpha_\infty} = \frac{l_{n.t}}{x}\left(\frac{\bar{\alpha}_{n.t}}{\alpha_\infty} - 1\right) + 1. \qquad (2\text{-}34)$$

[2] /28

from which it follows that when $x \to \infty$ (when $x >> l_{n.t}$, in practice), $\bar{\alpha} \to \alpha_\infty$. We note that this holds for various boundary conditions. For example, if $\bar{\alpha}_{n.t}/\alpha_\infty = 1{,}3$, then to within 3% $\bar{\alpha}$ will equal α_∞ when $x = 10 l_{n.t}$.

The heat-transfer coefficient, referred to the mean integral temperature difference at $x > l_{n.t}$ will equal, by definition,

$$\bar{\alpha} = \frac{Q_0}{F\overline{\Delta t}_x} = \frac{\int_0^{l_{n.t}} \alpha (t_0 - \bar{t})\, dx + \alpha_\infty \int_{l_{n.t}}^{x} (t_0 - \bar{t})\, dx}{\int_0^{l_{n.t}} (t_0 - \bar{t})\, dx + \int_{l_{n.t}}^{x} (t_0 - \bar{t})\, dx}. \qquad (2\text{-}35)$$

Using the relationships

$$\int_0^{l_{n.t}} (t_0 - \bar{t})\, dx = \overline{\Delta t}_{n.t} l_{n.t};$$

$$\int_0^{l_{n.t}} \alpha (t_0 - \bar{t})\, dx = \bar{\alpha}_{n.t} \overline{\Delta t}_{n.t} l_{n.t},$$

where $\Delta \bar{t}_{n.t}$ is the mean temperature difference at the thermal initial segment, we can reduce the expression for $\bar{\alpha}$ to the form

$$\frac{\bar{\alpha}}{\alpha_\infty} = \frac{\frac{\bar{\alpha}_{n.t}}{\alpha_\infty} + \varphi(x)}{1 + \varphi(x)},$$

where

$$\varphi(x) = \frac{1}{\overline{\Delta t}_{n.t} l_{n.t}} \int_{l_{n.t}}^{x} (t_0 - \bar{t})\, dx.$$

When t_s = const, we can use (2-25) to evaluate the last integral. We then obtain

$$\varphi(x) = -Ae^{-kx} + B,$$

where A, B, and k are constants.

Thus for constant wall temperature,

$$\frac{\bar{\alpha}}{\alpha_\infty} = \frac{\frac{\bar{\alpha}_{n.t}}{\alpha_\infty} - Ae^{-kx} + B}{1 - Ae^{-kx} + B},$$

from which we see that when $x \to \infty$,

$$\frac{\bar{\alpha}}{\alpha_\infty} = \frac{\frac{\bar{\alpha}_{n.t}}{\alpha_\infty} + B}{1 + B}.$$

Since in the general case $\bar{\alpha}_{n.т}/\alpha_\infty \neq 1$ for any values of x, $\bar{\alpha}$ will differ from α_∞. It is only in the special case for which $\bar{\alpha}_{n.т}/\alpha_\infty = 1$, that $\bar{\alpha} = \alpha_\infty$.

With constant heat-flow density at the wall (q_s = const), the numerator in (2-35) will equal $q_s x$, while the second integral in the denominator will equal $\frac{q_c}{\alpha_\infty}(x - l_{n.т})$. Thus the expression for $\bar{\alpha}$ can be written as:

$$\frac{\bar{\alpha}}{\alpha_\infty} = \frac{\frac{q_c}{\alpha_\infty}}{\Delta\bar{t}_{n.т}\frac{l_{n.т}}{x} + \frac{q_c}{\alpha_\infty}\left(1 - \frac{l_{n.т}}{x}\right)}.$$

It follows from this equation that when $x \to \infty$ $\bar{\alpha} = \alpha_\infty$.

In like manner, we can follow the lengthwise variation in the mean heat-transfer coefficients referred to the mean-arithmetic and initial temperature differences. When t_s = const, these heat-transfer coefficients approach zero when $x \to \infty$.

The mean heat-transfer coefficients, referred to the mean-logarithmic ($\bar{\alpha}_l$), mean-integral ($\bar{\alpha}_i$), mean-arithmetic ($\bar{\alpha}_a$), and initial ($\bar{\alpha}_n$) temperature differences are associated by the self-evident relationships

$$\bar{\alpha}_n \Delta t_n = \bar{\alpha}_a \Delta\bar{t}_a = \bar{\alpha}_i \Delta\bar{t}_i = \bar{\alpha}_l \Delta\bar{t}_l. \qquad (2\text{-}36)$$

With the aid of these expressions, it is not difficult to go from values of $\bar{\alpha}$ defined by one method to values defined by another.

2-5. HYDRAULIC RESISTANCE

In practice, we very often must determine the pressure drop when a fluid moves in a tube, i.e., the hydraulic resistance.

Assuming the velocity field and temperature field to be known, we find the pressure variation along the tube length. Let us do this for an incompressible fluid with variable physical properties flowing in a round tube; for simplicity, we assume that the velocity and temperature fields are symmetric about the x axis. Here the equation of motion for the longitudinal velocity component will have the form

$$\rho\left(\frac{\partial w_x}{\partial \tau} + w_x\frac{\partial w_x}{\partial x} + w_r\frac{\partial w_x}{\partial r}\right) = \rho g_x - \frac{\partial p}{\partial x} + \frac{\partial}{\partial x}\left(2\mu\frac{\partial w_x}{\partial x}\right) + \\ + \frac{1}{r}\cdot\frac{\partial}{\partial r}\left[r\mu\left(\frac{\partial w_x}{\partial r} + \frac{\partial w_r}{\partial x}\right)\right].$$

The order of magnitude of the term $\frac{\partial}{\partial x}\left(2\mu\frac{\partial w_x}{\partial x}\right)$ is small as compared with the last term on the right side of the equation, and

can be dropped. The left side of the equation can be transformed by using the equation of continuity. As a result we obtain

$$\frac{\partial(\rho w_x)}{\partial \tau}+\frac{\partial(\rho w_x^2)}{\partial x}+\frac{1}{r}\frac{\partial}{\partial r}(r\rho w_x w_r)=\rho g_x-\frac{\partial p}{\partial x}+$$
$$+\frac{1}{r}\frac{\partial}{\partial r}\left[r\mu\left(\frac{\partial w_x}{\partial r}+\frac{\partial w_r}{\partial x}\right)\right]. \qquad (2\text{-}37)$$

We apply (2-37) to a fluid element of length dx, bounded by the tube walls and by two sections normal to its axis. We multiply both sides of this equation by $2\pi r\,dr$, and integrate between 0 and r_0:

$$\int_0^{r_0}\frac{\partial(\rho w_x)}{\partial \tau}2\pi r\,dr+\int_0^{r_0}\frac{\partial(\rho w_x^2)}{\partial x}2\pi r\,dr+2\pi\int_0^{r_0}d(r\rho w_x w_r)=$$
$$=g_x\int_0^{r_0}\rho 2\pi r\,dr-\int_0^{r_0}\frac{\partial p}{\partial x}2\pi r\,dr+2\pi\int_0^{r_0}d\left[r\mu\left(\frac{\partial w_x}{\partial r}+\frac{\partial w_r}{\partial x}\right)\right]. \qquad (2\text{-}38)$$

The last integral on the left side equals zero. The integral on the right side is

$$2\pi\int_0^{r_0}d\left[r\mu\left(\frac{\partial w_x}{\partial r}+\frac{\partial w_r}{\partial x}\right)\right]=2\pi r_0\left(\mu\frac{\partial w_x}{\partial r}\right)_{r=r_0}=-2\pi r_0\sigma_0,$$

where

$$\sigma_0=\left(\mu\frac{\partial w_x}{\partial n}\right)_{n=0}=-\left(\mu\frac{\partial w_x}{\partial r}\right)_{r=r_0}$$

is the tangential stress at the wall; n is the normal to the inside surface of the wall.

In the appropriate terms of (2-38) we change the sequence of differentiation with respect to τ and x and integration with respect to r. As a result, the equation takes the form

$$\frac{\partial}{\partial \tau}\int_0^{r_0}\rho w_x 2\pi r\,dr+\frac{\partial}{\partial x}\int_0^{r_0}\rho w_x^2 2\pi r\,dr=g_x\int_0^{r_0}\rho 2\pi r\,dr-\frac{\partial}{\partial x}\int_0^{r_0}p 2\pi r\,dr-\sigma_0 2\pi r_0. \qquad (2\text{-}39)$$

We let

$$\bar{p}=\frac{1}{f}\int_f p\,df \quad\text{and}\quad \bar{\rho}=\frac{1}{f}\int_f \rho\,df$$

be the mean pressure and mean fluid density over a section; f, s are the tube cross-sectional area and perimeter; ψ is the angle between the x axis and the gravitational acceleration vector g. (We note that $g_x=g\cos\psi$).

Then from (2-39), we find

$$\frac{\partial \bar{p}}{\partial x} = -\frac{s}{f}\bar{\sigma}_0 - \frac{1}{f}\left[\frac{\partial}{\partial \tau}\int_f \rho w_x\, df + \frac{\partial}{\partial x}\int_f \rho w_x^2\, df\right] + \bar{\rho} g \cos\psi. \qquad (2\text{-}40)$$

Although Eq. (2-40) was derived for the example of a round tube, it actually is valid for a tube of any shape, provided the cross-section remains constant along the axis. In the general case, σ_s can vary over the tube perimeter. Thus we include in (2-40) the mean-perimeter value of tangential stress at the wall,

$$\bar{\sigma}_c = \frac{1}{s}\int_s \sigma_c\, ds = \frac{1}{s}\int_s \left(\mu \frac{\partial w_x}{\partial n}\right)_{n=0} ds. \qquad (2\text{-}41)$$

It is clear from (2-40) that the change in pressure along the tube length is produced by the expenditure of energy on friction between fluid and wall, by the change in velocity with time and in the flow kinetic energy along the tube length (owing to rearrangement of the velocity profile), and by the action of the gravitational force.

The quantity $\bar{\rho} g \cos\psi$ is the pressure gradient in the liquid at rest when there is the same distribution of $\bar{\rho}$ along the length as in the flow. We let $\bar{p}_0$ represent the pressure in the quiescent liquid, i.e., the hydrostatic pressure. Then

$$\frac{\partial \bar{p}_0}{\partial x} = \bar{\rho} g \cos\psi$$

and

$$\frac{\partial \bar{p}_1}{\partial x} = \frac{\partial (\bar{p} - p_0)}{\partial x} = \frac{\partial \bar{p}}{\partial x} - \bar{\rho} g \cos\psi, \qquad (2\text{-}42)$$

where $\bar{p}_1 = (\bar{p} - p_0)$ is the difference between the actual pressure in the moving fluid and the pressure in the fluid at rest.

As we can see from (2-40), the pressure $\bar{p}_1$ is independent of the gravitational force, so that it can be interpreted as the pressure in a flow of weightless fluid.

In our further study of fluid flow, we shall not consider the effect of the gravitational force (except for special cases, where particular stipulations will be made), and in place of the pressure $\bar{p}$, we shall consider $\bar{p}_1$. Where necessary, it is not difficult to go from the distribution of $\bar{p}_1(x, \tau)$ that has been found to the distribution of the actual pressure $\bar{p}(x, \tau)$. Integrating (2-42), we find

$$\bar{p}(x, \tau) = \bar{p}_1(x, \tau) + p_0(0, \tau) + g \cos\psi \int_0^x \bar{\rho}(x, \tau)\, dx. \qquad (2\text{-}43)$$

Henceforth, for brevity we shall write p rather than $\bar{p}_1$.

Using our notation ($p = \bar{p}_1 = \bar{p} - p_0$), we rewrite (2-40):

$$\frac{\partial p}{\partial x} = -\frac{s}{f}\bar{\sigma}_0 - \frac{1}{f}\left[\frac{\partial}{\partial \tau}\int_f \rho w_x\, df + \frac{\partial}{\partial x}\int_f \rho w_x^2\, df\right]. \qquad (2\text{-}44)$$

For stationary flow and heat exchange, (2-44) takes the form

$$\frac{dp}{dx}=-\frac{s}{f}\bar{\sigma}_0-\frac{1}{f}\frac{d}{dx}\int_f \rho w_x^2\,df. \qquad (2\text{-}45)$$

If ρ and w_x do not vary along the length, as occurs for an incompressible fluid with constant physical properties moving far from the tube entrance, the second term on the right side of (2-45) vanishes. In such case, the pressure gradient is determined completely by viscous friction, and does not vary along the length:

$$\frac{dp}{dx}=-\frac{s}{f}\bar{\sigma}_0=\text{const}. \qquad (2\text{-}46)$$

In other words, the pressure p decreases linearly along the length.

Integrating (2-45) between $x = 0$ and $x = l$, we find the pressure drop for the tube segment of length l:

$$\Delta p=p(0)-p(l)=\frac{s}{f}\int_0^l\bar{\sigma}_0\,dx+\frac{1}{f}\left[\left(\int_f \rho w_x^2\,df\right)_{x=l}-\left(\int_f \rho w_x^2\,df\right)_{x=0}\right]. \qquad (2\text{-}47)$$

If the fluid properties are constant and w_x does not vary along the length, then $\bar{\sigma}_s$ will also be constant along the length. In such case, integrating (2-46), we find

$$\Delta p=\frac{\bar{\sigma}_0 s l}{f}. \qquad (2\text{-}48)$$

From all of this it follows that to determine the hydraulic resistance by computation we must know the velocity field in the fluid flow and, in the general case, the temperature field (to determine the density field and the viscosity). We can then use (2-41) to determine $\bar{\sigma}_s$, and (2-47) to find the pressure drop. To determine Δp experimentally, we must measure the pressure fields at two low sections. Averaging these fields over the section and taking the difference of the mean values, we obtain Δp. In the elementary case where the pressure does not vary over the section, Δp is found by direct measurement of the pressure difference in two tube sections.

Manuscript Page No.

Footnotes

18 [1]According to the Newton-Rikhman law, the density of the heat flow at a wall is proportional to the difference between the wall temperature and the temperature of the fluid far from the wall. Here α is a coefficient of proportionality and, consequently, must not depend

$t_s - \bar{t}$. This holds provided the physicsl properties of the fluid do not depend on the temperature. By definition, we introduce α as the ratio of q_s to $t_s - \bar{t}$. In such case, no restrictions are imposed on the relationship between α and $t_s - \bar{t}$.

22 [2]This segment is called the thermal initial segment (see §6-1, etc.).

Manuscript Page No.	Transliterated Symbols
15	с = s = stenka = wall
21	а = a = arifmeticheskiy = arithmetic
21	и = i = integral'nyy = integral
22	л = l = logarifmicheskiy = logarithmic
22	н.т = n.t = [temperature head]
24	н = n = nachal'nyy = initial

Chapter 3

PROPERTIES OF LIQUIDS AND GASES ESSENTIAL TO HEAT-EXCHANGE CALCULATIONS

3-1. GENERAL INFORMATION

As we can see from Chapter 1, in determining convective heat exchange for a single-phase chemically homogeneous medium, the following physical properties of the medium, i.e., liquid or gas, are of importance: the density ρ, the specific heat capacity at constant pressure c_p, the dynamic viscosity coefficient μ, and the thermal-conductivity coefficient λ.

To characterize the relative variation in specific volume or density with a change in temperature, we use the volume expansion coefficient

$$\beta=\frac{1}{v}\left(\frac{\partial v}{\partial T}\right)_p=-\frac{1}{\rho}\left(\frac{\partial \rho}{\partial T}\right)_p,$$

where v is the specific volume and T the absolute temperature.

We also require composite quantities formed from these physical parameters:

the kinematic viscosity coefficient

$$\nu=\frac{\mu}{\rho},$$

the thermal diffusivity coefficient

$$a=\frac{\lambda}{c_p\rho}$$

and the Prandtl number

$$\mathrm{Pr}=\frac{\nu}{a}=\frac{\mu c_p}{\lambda}.$$

Thus if a temperature field and pressure field are present in the flow, the physical properties will vary from point to point, which may have a substantial influence on the nature of flow and heat exchange.

The physical properties of liquids (i.e., condensed media) will depend little on the pressure far from the critical point. Moreover the velocity of liquids will not be large in most cases,

so that the pressure variation in the flow will usually not exceed several atmospheres. With such a pressure variation, the physical properties of the liquid will vary negligibly. Thus we can always neglect the relationship between physical properties and pressure for liquids.

The physical properties of gases at fairly high temperatures and moderate pressures (more accurately, far from the saturation point and the near-critical region) will depend only slightly on the pressure, except for the density and kinematic viscosity. If the gas velocity is not large so that the pressure variation in the flow will be small as compared with the absolute pressure, then ρ can be assumed to be independent of the pressure; this is even truer of the other physical properties of the gas. In such case, like a liquid, the gas can be treated as an incompressible medium. When the gas moves at high velocity, the pressure variation in the flow can be quite considerable. Here the compressibility of the gas, i.e., the relationship between ρ (and thus ν) and p can be neglected. As for the other properties (c_p, μ, λ), they are usually assumed to be independent of p.

Thus the nonuniform distribution of physical properties in a flow of incompressible fluid is determined in the main by the way in which they depend on the temperature.

3-2. LIQUIDS

For liquids, the viscosity coefficwent varies particularly strongly with temperature; the density, specific heat content, and thermal-conductivity coefficient vary far less. This is clear from Table 3-1, which gives the ratios of the corresponding physical parameters at 10 and 100°C for certain liquids.

TABLE 3-1

Ratio of Physical Parameters at 10 and 100°C

1 Жидкость	$\frac{\rho_{10}}{\rho_{100}}$	$\frac{c_{p_{10}}}{c_{p_{100}}}$	$\frac{\lambda_{10}}{\lambda_{100}}$	$\frac{\mu_{10}}{\mu_{100}}$
2 Ртуть	1,02	1,02	1,13	1,25
3 Вода	1,04	1,0	0,84	4,6
4 Трансформаторное масло . .	1,09	0,88	1,1	15,3
5 Глицерин . . .	1,05	0,82	1,04	304

1) Liquid; 2) mercury; 3) water; 4) transformer oil; 5) glycerin.

For a theoretical determination of heat exchange, in most cases we can take ρ, c_p, and λ to be linear functions of temperature. Since ρ and λ decrease with temperature for most liquids,[1] while c_p increases, the interpolation equations have the form

$$\frac{\rho}{\rho_0} = 1 - \beta_\rho (t - t_0), \qquad (3\text{-}1)$$

$$\frac{c_p}{c_{p_0}} = 1 + \beta_c (t - t_0); \qquad (3\text{-}2)$$

$$\frac{\lambda}{\lambda_0} = 1 - \beta_\lambda (t - t_0), \qquad (3\text{-}3)$$

where ρ_0, c_{p_0}, and λ_0 are the values of the physical parameters at a fixed temperature t_0; β_ρ, β_c and β_λ are constants depending on the type of liquid and the temperature range (found from experimental data).

TABLE 3-2

Physical Properties of Water at Saturation Curve

t, °C	ρ, $кг/м^3$	$\beta \cdot 10^4$, $1/град$	c_p, $кДж/кг \cdot град$	h, $кДж/кг$	λ, $Вт/м \cdot град$	$a \cdot 10^8$, $м^2/сек$	$\mu \cdot 10^6$, $Н \cdot сек/м^2$	$\nu \cdot 10^6$, $м^2/сек$	Pr
	1	2	3	4	5	6	7	8	
0	999,8	—0,7	4,216	0	0,559	13,3	1788	1,788	13,5
10	999,6	0,95	4,191	42,04	0,579	13,8	1305	1,306	9,45
20	998,2	2,1	4,183	83,90	0,598	14,3	1004	1,006	7,02
30	995,6	3,0	4,178	125,69	0,613	14,7	801	0,805	5,46
40	992,2	3,9	4,178	167,51	0,627	15,1	653	0,658	4,35
50	988,0	4,6	4,183	209,30	0,639	15,5	549	0,556	3,60
60	983,2	5,3	4,183	251,12	0,650	15,8	470	0,478	3,02
70	977,7	5,8	4,191	292,99	0,661	16,1	406	0,415	2,57
80	971,8	6,3	4,195	334,94	0,669	16,4	355	0,365	2,22
90	965,3	7,0	4,204	376,98	0,677	16,7	315	0,326	1,95
100	958,3	7,5	4,216	419,10	0,683	16,9	282	0,295	1,74
120	943,1	8,5	4,245	503,7	0,686	17,1	237	0,252	1,47
140	926,1	9,7	4,287	589,1	0,685	17,2	201	0,217	1,26
160	907,4	10,8	4,342	675,3	0,680	17,3	174	0,191	1,11
180	886,9	12,1	4,409	763,2	0,671	17,2	153	0,172	1,00
200	864,7	13,5	4,497	852,4	0,657	16,9	136	0,158	0,935
220	840,3	15,2	4,614	943,7	0,640	16,5	124	0,148	0,897
240	813,6	17,2	4,769	1037,5	0,618	15,9	115	0,141	0,886
260	784,0	20,0	4,982	1135,0	0,592	15,2	106	0,135	0,891
280	750,7	23,8	4,588	1236,8	0,564	14,2	96	0,131	0,922
300	712,5	29,5	5,757	1344,8	0,532	13,0	91	0,128	0,987
320	667,1	38,0	6,57	1462,0	0,493	11,2	85	0,128	1,14
340	610,1	47,5	8,21	1594,8	0,447	8,93	78	0,127	1,42

1) kg/m^3; 2) deg; 3) c_p, kJ/kg·deg; 4) kJ/kg; 5) W/m·deg; 6) m^2/s; 7) $N \cdot s/m^2$; 8) m^2/s.

In isolated cases, the linear interpolation equations may prove inadequate to describe the way in which ρ, c_p, and λ actually depend on t. They then can be supplemented by terms containing higher powers of the temperature.

If we assume that ρ is a linear function of t, then the coefficient of volume expansion

$$\beta = -\frac{1}{\rho}\left(\frac{\partial \rho}{\partial T}\right)_p = \frac{\text{const}}{\rho}$$

will increase with temperature, while the coefficient

$$\beta_\rho = -\frac{1}{\rho_0}\left(\frac{\partial \rho}{\partial T}\right)_p = \text{const}$$

will remain constant. It is clear that $\beta\rho = \beta_\rho \rho_0$. Since ρ changes but slightly with temperature, the coefficient β is frequently assumed to be constant and equal to the mean value in the given temperature interval.

The coefficient of dynamic viscosity for liquids decreases with temperature, first rapidly and then more slowly. Its temperature dependence can be quite well approximated by the equation

TABLE 3-3

Physical Properties of Transformer Oil

t, °C	ρ, $\frac{kg}{m^3}$	$\beta \cdot 10^4$, $\frac{1}{deg}$	c_p, $\frac{kJ/kg}{kg \cdot deg}$	λ, $\frac{W}{m \cdot deg}$	$a \cdot 10^8$, $\frac{m^2}{sec}$	$\mu \cdot 10^4$, $\frac{N \cdot sec}{m^2}$	$\nu \cdot 10^6$, $\frac{m^2}{sec}$	Pr
1	2	3	4	5	6	7		
0	895,5	6,80	1,55	0,113	8,14	650	70,5	866
10	889,4	6,85	1,61	0,112	7,83	355	37,9	484
20	880,3	6,90	1,67	0,111	7,56	198	22,5	298
30	874,2	6,95	1,73	0,110	7,28	128	14,7	202
40	868,2	7,00	1,79	0,109	7,03	89	10,3	146
50	862,1	7,05	1,85	0,108	6,81	65,3	7,58	111
60	856,0	7,10	1,91	0,107	6,58	49,5	5,78	87,8
70	850,0	7,15	1,96	0,106	6,36	38,6	4,54	71,3
80	843,9	7,20	2,03	0,106	6,17	30,8	3,66	59,3
90	837,8	7,25	2,09	0,105	6,00	25,4	3,03	50,5
100	831,8	7,30	2,14	0,104	5,83	21,3	2,56	43,9
110	825,7	7,35	2,20	0,103	5,66	18,1	2,20	38,8
120	819,6	7,40	2,26	0,102	5,50	15,7	1,92	34,9

1) kg/m³; 2) deg; 3) kJ/kg·deg; 4) W/m·deg; 5) m²/s; 6) N·s/m²; 7) m²/s.

TABLE 3-4

Physical Properties of Sodium[1]

t, °C	ρ, $\frac{kg}{m^3}$	c_p, $\frac{kJ/kg}{kg \cdot deg}$	λ, $\frac{W}{m \cdot deg}$	$a \cdot 10^6$, $\frac{m^2}{sec}$	$\nu \cdot 10^6$, $\frac{m^2}{sec}$	Pr·10⁶
	1	2	3	4	5	
100	928	1,39	86,1	66,9	77,0	1,15
150	916	1,36	84,1	67,8	59,4	0,88
200	903	1,33	81,6	68,1	50,6	0,74
250	891	1,30	78,7	67,8	44,2	0,65
300	878	1,28	75,5	67,2	39,4	0,59
350	866	1,27	71,9	65,3	35,4	0,54
400	854	1,27	68,7	63,3	33,0	0,52
450	842	1,27	66,1	61,7	30,8	0,50
500	829	1,27	63,8	60,6	28,9	0,48
550	817	1,27	62,0	59,7	27,2	0,46
600	805	1,28	60,6	58,9	25,7	0,44
650	792	1,28	59,7	58,9	24,4	0,41
700	780	1,28	59,1	59,2	23,2	0,39

[1] $t_{пл} = 97,8°C$; $t_{кип} = 878°C$ (at atmospheric pressure).

1) kg/m³; 2) kJ/kg·deg; 3) W/m·deg; 4) m²/s; 5) m²/s.

$$\frac{\mu_0}{\mu} = 1 + \beta_{\mu 1}(t - t_0) + \beta_{\mu 2}(t - t_0)^2 + \ldots, \qquad (3\text{-}4)$$

where μ_0, $\beta_{\mu 1}$ and $\beta_{\mu 2}$ are constants determined experimentally. In the simplest case, we need only keep the first two terms of Series (3-4).

For the temperature dependence of the coefficient of viscosity, we also use interpolation equations of the form

$$\frac{\mu_0}{\mu} = \left(\frac{t}{t_0}\right)^b,$$
$$\frac{\mu}{\mu_0} = e^{-c(t - t_0)},$$

where μ_0, b, and c are constants.

The kinematic viscosity coefficient and Prandtl number for liquids decrease as the temperature goes up.

The way in which ν and Pr depend on t is determined, in the main, by the relationship between μ and t, since ρ, c_p and λ vary little with temperature.

3-3. GASES IN A STATE CLOSE TO THE IDEAL

In the region of state parameters far from the saturation curve and the near-critical region, i.e., at relatively low pressure and fairly high temperature, gas density is relatively low. Here the gas is in a state close to that of an ideal gas.[2] For such a gas, the Clapeyron-Mendeleyev equation holds; it establishes a simple relationship between gas density and temperature and pressure:

$$\frac{p}{\rho} = RT, \qquad (3\text{-}5)$$

where R is the gas constant.

If the pressure in the flow is constant (p = const), then

$$\frac{\rho}{\rho_0} = \frac{T_0}{T}, \qquad (3\text{-}6)$$

where ρ_0 is the density at T_0.

As we can see from (3-5), the coefficient of volume expansion for an ideal gas is

$$\beta = -\frac{1}{\rho}\left(\frac{\partial \rho}{\partial T}\right)_p = \frac{1}{T}.$$

The specific heat content at constant pressure for a monatomic gas in nearly ideal state is practically independent of temperature, while for biatomic, triatomic, and multiatomic gases it increases with temperature. Figure 3-1 gives an idea of the way in which c_p depends on T for biatomic and triatomic gases (air, carbon dioxide); it is clear from the figure that when the temperature changes, c_p varies far less than μ or λ. It is convenient to represent $c_p(T)$ as

a power function,

$$\frac{c_p}{c_{p_0}} = \left(\frac{T}{T_0}\right)^{n_c}, \qquad (3\text{-}7)$$

where n_c is a constant that depends on the type of gas and the temperature interval. Thus, for example, for air between 0 and 1500°C, n_c = 0.146; for carbon dioxide between 0 and 1000°C n_c=0,33.

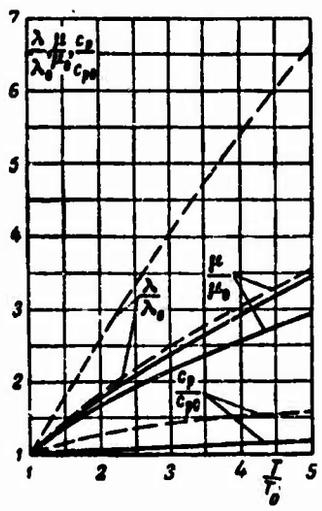

Fig. 3-1. Functions $\lambda(T)$, $\mu(T)$ and $c_p(T)$ for air (solid lines) and carbon dioxide (dashed lines). The values of λ_0, μ_0 and c_{p_0} correspond to T_0 = 273°K.

The ratio $k=c_p/c_v$ between gas heat content at constant pressure and constant volume decreases with temperature. For example, for air at 0°C k=1,40, while at 1000°C k=1,32.

The dynamic viscosity coefficient and coefficient of thermal conductivity for gases in the nearly ideal state increase with temperature. Figure 3-1 shows μ and λ as functions of T for biatomic and triatomic gases. For monatomic gases, the relationship is of approximately the same nature as for biatomic gases.

The change in the dynamic viscosity coefficient with temperature is described by the Saterland equation, which is derived in the kinetic theory of gases:

$$\frac{\mu}{\mu_0} = \left(\frac{T}{T_0}\right)^{3/2} \frac{T_0 + s}{T + s}, \qquad (3\text{-}8)$$

where s is a constant determined experimentally for the given gas; for example, between 0 and 1200°C s = 122°K for air, s = 102°K for nitrogen, s = 233°K for carbon dioxide.

TABLE 3-5

Values of Constants in Equations for Viscosity and Thermal Conductivity of Gases in the 0 to 1000°C Range

1 Газ	Химическая формула[2]	$\mu_0 \cdot 10^6$, $\frac{N \cdot сек}{м^2}$	n_μ	$\lambda_0 \cdot 10^3$, $\frac{вт}{м \cdot град}$	n_λ
5 Аргон	Ar	21,2	0,72	16,5	0,80
6 Гелий	He	18,4	0,68	143	0,73
7 Азот	N_2	16,7	0,68	24,2	0,80
8 Водород	H_2	8,36	0,678	172	0,78
9 Воздух	—	17,1	0,683	24,3	0,82
10 Кислород . . .	O_2	19,4	0,693	24,5	0,87
11 Водяной пар . .	H_2O	8,24	1,20	15,1	1,48
12 Двуокись углерода	CO_2	14,0	0,82	14,9	1,23
13 Аммиак	NH_3	0,936	1,06	21,0	1,53

The values of μ_0 and λ_0 correspond to $T_0 = 273°K$.

1) Gas; 2) chemical formula; 3) $N \cdot s/m^2$; 4) W/m·deg; 5) argon; 6) helium; 7) nitrogen; 8) hydrogen; 9) air; 10) oxygen; 11) water vapor; 12) carbon dioxide; 13) ammonia.

In many cases, in place of (3-8) it is more convenient to use an equation of the form

$$\frac{\mu}{\mu_0} = \left(\frac{T}{T_0}\right)^{n_\mu}. \qquad (3\text{-}9)$$

In general, the exponent n_μ depends on the temperature. At moderate temperatures it is close to unity; as the temperature increases it decreases, approaching a value of 0.5 according to (3-8). A constant value may be taken for n_μ for a given gas over a restricted, although fairly wide, temperature range. For example, for air between 90 and 300°K, $n_\mu = 8/9$. Table 3-5 gives values of μ_0 and n_μ for certain gases on the basis of published data [1].

The relationship between the thermal-conductivity coefficient and the temperature has the nature as $\mu(T)$, and can be represented by an equation of the same type:

$$\frac{\lambda}{\lambda_0} = \left(\frac{T}{T_0}\right)^{n_\lambda}. \qquad (3\text{-}10)$$

The exponent n_λ differs for different gases and moreover, is temperature-dependent. Like n_μ, however, n_λ may be taken to be constant over a restricted temperature range. Table 3-5 gives values of λ_0 and n_λ for certain gases. As the table shows, $n_\lambda > n_\mu$.

The difference between them is not great, however, for monatomic and biatomic gases.

For gases in a nearly ideal state, the Pr number depends principally on the number of atoms in the molecule. For monatomic gases, Pr equals 0.63 on the average; it is 0.72 for diatomic gases, and 0.75-0.9 for triatomic and multiatomic gases. Since λ increases somewhat more rapidly with the temperature than does μ, while c_p increases little with the temperature, the number $Pr = \mu c_p/\lambda$ changes slowly with temperature.

The information given here on the properties of a gas in nearly ideal state is valid provided the chemical composition of the gas (or gases forming the mixture) does not change under variations in temperature and pressure. This condition is fulfilled if the gas temperature at a given pressure does not exceed a specific value at which complex molecules begin to dissociate. For air, the temperature corresponding to inception of component dissociation (primarily O_2) is about 2000°C at atmospheric pressure.

TABLE 3-6

Physical Properties of Air at Atmospheric Pressure

t, °C	ρ, kg/m³	c_p, kJ/kg·deg	$\lambda \cdot 10^2$, W/m·deg	$a \cdot 10^6$, m²/sec	$\mu \cdot 10^6$, N·sec/m²	$\nu \cdot 10^6$, m²/sec	Pr
	1	2	3	4	5	6	
0	1,293	1,00	2,43	18,7	17,1	13,2	0,707
100	0,9460	1,01	3,19	33,3	21,9	23,2	0,696
200	0,7459	1,03	3,87	50,6	26,0	34,9	0,689
300	0,6157	1,05	4,45	69,5	29,7	48,2	0,695
400	0,5242	1,07	5,05	90,2	33,0	63,0	0,698
500	0,4564	1,09	5,62	113	36,2	79,3	0,704
600	0,4045	1,11	6,15	137	39,1	96,7	0,708
700	0,3628	1,13	6,66	162	41,7	115	0,710
800	0,3290	1,16	7,20	189	44,3	135	0,712
900	0,3009	1,18	7,61	215	46,6	155	0,721
1 000	0,2766	1,19	8,05	244	49,0	177	0,727
1 100	0,2570	1,21	8,48	273	51,2	199	0,731
1 200	0,2396	1,23	8,90	303	53,4	223	0,737
1 300	0,2244	1,24	—	—	55,5	247	—
1 400	0,2110	1,26	—	—	57,6	273	—
1 500	0,1991	1,28	—	—	59,6	299	—
1 600	0,1874	1,30	—	—	61,6	329	—
1 700	0,1789	1,33	—	—	63,6	356	—
1 800	0,1702	1,36	—	—	65,5	385	—

1) kg/m³; 2) kJ/kg·deg; 3) W/m·deg; 4) m²/s; 5) N·s/m²; 6) m²/s.

3-4. REAL GASES

Near the saturation curve and, particularly, in the supercritical region,[3] the properties of matter change substantially not only with temperature, but also with pressure. In this parameter region, the change in physical properties with temperature and pressure cannot be represented by relationships as simple as the one applying to a liquid or a gas in nearly ideal state.

It is convenient to characterize the deviation in specific volume or density of a real gas from the values corresponding to the equation of state of an ideal gas by the compressibility coefficient

$$z = \frac{pv}{RT} = \frac{p}{R\rho T}. \qquad (3\text{-}11)$$

For an ideal gas, $z = 1$. For real gases, z depends on temperature and pressure. If this relationship is represented as

$$z = f(\pi, \tau), \qquad (3\text{-}12)$$

where $\pi = p/p_{кр}$ and $\tau = T/T_{кр}$ are the reduced pressure and temperature, while p_{kr} and T_{kr} are the critical parameters; then by the law of corresponding states, this relationship will be roughly the same for different substances.

Figure 3-2 illustrates Relationship (3-12); the figure is taken from [9]. Using this graph, we can easily establish the region of values of p and T within which the equation of state of an ideal gas is valid. The real gas will obviously deviate more from an ideal gas the more z differs from unity. If we know the values of p_{kr} and T_{kr} for a given substance, we can then use Fig. 3-2 to determine the approximate value of ρ for the values of p and T.[4] Naturally, for exact calculations it is always preferable to use exact tables and diagrams compiled for the given substance.

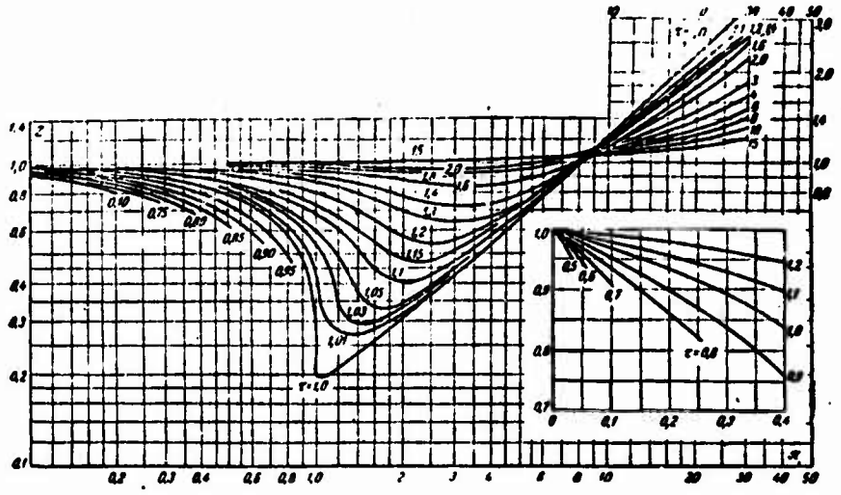

Fig. 3-2. Compressibility coefficient z of real gases as function of reduced pressure and temperature.

The coefficient of volume expansion $\beta = \frac{1}{v}\left(\frac{\partial v}{\partial T}\right)_p$ for a real gas depends essentially on temperature and pressure. In the supercritical region, when p = const the coefficient β first increases and then decreases with the temperature.[5] The value of β at the maximum point will be higher the closer the pressure p is to p_{kr}. At the critical point, $\beta = \infty$.

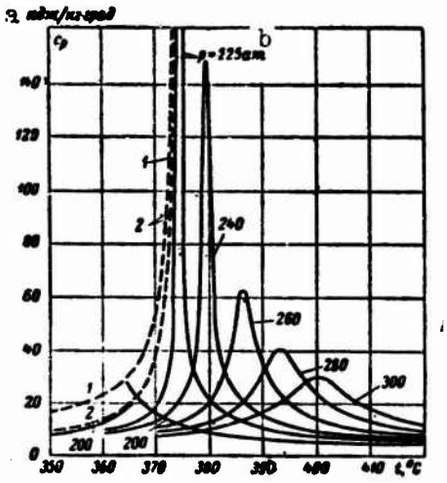

Fig. 3-3. Heat content of water and water vapor in near-critical region. 1) Saturation curve on vapor side; 2) saturation curve on water side. a) kJ/kg·deg; b) at.

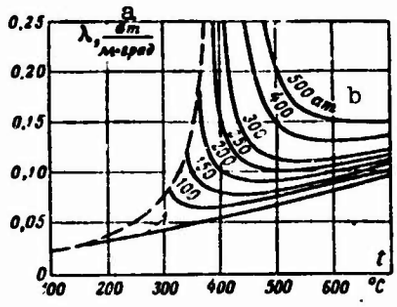

Fig. 3-4. Thermal-conductivity coefficient for water vapor. The dashed line shows the saturation curve. a) W/m·deg; b) at.

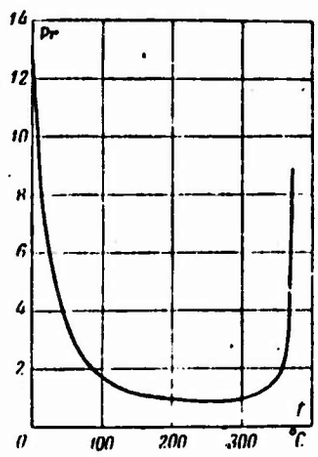

Fig. 3-5. Pr number for water at saturation curve.

The heat capacity c_p of a real gas varies sharply with temperature and pressure changes near the saturation curve and, in particular, in the supercritical region.

Figure 3-3 gives some idea of the way in which heat capacity varies with t and p; it gives data for water and water vapor. In the supercritical region, the heat capacity c_p passes through a maximum for certain temperature values, depending on the pressure. At the critical point,[6] $c_p=\infty$. At $p>p_{кр}$, the values of c_p at maximums will decrease as the pressure increases. Near the maximum points, the heat capacity may change by a factor of ten within a narrow range of temperature and pressure.

The coefficients of dynamic viscosity and thermal conductivity also experience substantial variations with temperature and pressure at high pressures. Figure 3-4 gives an idea of the relationships observed; it gives data on the thermal-conductivity coefficient of water vapor at pressures between 1 and 500 at and temperatures between 100 and 700°C (the qualitative variation in the viscosity is the same as that for the thermal conductivity).

The change in Pr near the saturation curve and in the supercritical region is associated chiefly with the change in c_p, since μ and λ vary less, and in almost the same way. Thus the curves for Pr will have roughly the same shape as the curves for c_p in Fig. 3-3. Figure 3-5 shows Pr for water at the saturation curve. For temperatures between 0 and 180°C, Pr drops rapidly with the temperature; this is associated with the reduction in μ and a certain increase in λ (here c_p varies negligibly). Between 180 and 310°C, Pr remains roughly constant, while above 310°C and up to the critical point, it rises rapidly in accordance with the rapid growth of c_p.

3-5. CLASSIFICATION OF HEAT-TRANSPORT MEDIA BY PRANDTL NUMBER

As we shall see later, the number $Pr=\mu c_p/\lambda$ is an essential characteristic of a heat-transport medium (liquid, gas) from the viewpoint of the features of the convective heat-exchange process. For different media, Pr will vary widely. Depending on the value of Pr, heat-transport media can be classified into three groups: media with $Pr \ll 1$, media with $Pr \approx 1$, and media with $Pr>1$.

The first group includes liquid-metal heat-transport media: sodium, lithium, sodium-calcium alloys, lead-bismuth alloys, mercury, etc. For the media of this group, Pr varies between about 0.005 and 0.05. This very low value of Pr for liquid metals is associated with their high thermal conductivity and relatively low heat capacity.

The second group of media includes gases at moderate pressures and liquids at high temperatures. For them, Pr varies within fairly narrow limits, roughly from 0.6 to 1.

The third group of heat-transport media consists of the nonmetallic liquids: water, various organic and inorganic liquids

[6] /40

(petroleum products, molten salts, etc.). For media in this group, Pr ordinarily ranges from 1 to 150-200. Certain liquids (glycerin and viscous oils, for example) have a Pr number at low temperatures that may reach several thousand or even tens of thousands. The high values of Pr for the third group is explained chiefly by their viscosity, in particular at low temperatures.

To conclude this chapter we note that the reference list includes several handbooks and monographs in which the reader can find data on the physical properties of liquids and gases that are required for heat-exchange calculation.

Manuscript Page No.

Footnotes

30 [1]For water, glycerin, and other strongly associated liquids, a different relationship is found between λ and t. Thus, for example, for water λ first increases with the temperature (at $t < 125°C$), and then decreases.

33 [2]The region of applicability of the ideal-gas model is more accurately determined in §3-4.

36 [3]The supercritical region is the region of parameters of state corresponding to $p \geq p_{kr}$.

37 [4]For helium, hydrogen, and nitrogen, better agreement with experiment is obtained if we add 8 to the values of p_{kr} and T_{kr}.

37 [5]In the supercritical region, the nature of the change in β is similar to the nature of the change in c_p (see below).

39 [6]For water, $p_{kr} = 225.65$ at and $t_{kr} = 374.15°C$.

Manuscript Page No.

Transliterated Symbols

32 пл = pl = plavleniye = melting

32 кип = kip = kipeniye = boiling

37 кр = kr = kriticheskiy = critical

Chapter 4

ANALYSIS OF FLOW AND HEAT EXCHANGE IN TUBES BY THE SIMILARITY METHOD

4-1. PRELIMINARY REMARKS

It is useful to begin the study of a given specific heat-exchange or fluid-motion problem with an analysis by the similarity method [1, 2, 3, 4]. Analysis of processes by the similarity method is based on reduction of the equations describing the investigated process and the corresponding initial and boundary conditions to dimensionless form. This reduction can be carried out either by a change of scales, or by the dimensionality method. The number of new dimensionless variables and constants occurring in the basic equations and initial and boundary conditions will be less than the number of dimensioned quantities essential to study of the process; this offers significant advantages. For an experimental investigation, utilization of the similarity method makes it possible to minize the number of quantities that must be varied during the experiments, and gives an efficient method for generalization of experimental data. The similarity method also proves useful for theoretical investigations; for example, it can sometimes be used to reduce the problem of finding a function of two variables to the problem of finding a function of one variable, or to finding a function to within a numerical constant. With the similarity method, it is convenient to analyze limiting cases and to generalize the results of numerical solutions.

In the succeeding sections of this chapter, application of the similarity method to problems of fluid motion and heat exchange in pipes will be illustrated.

4-2. ISOTHERMAL FLOW

In a tube with cross section that is arbitrary (but unchanged along the length) let an incompressible liquid filling the entire tube be at rest (Fig. 4-1). At the time taken as the initial instant ($\tau=0$), a constant pressure difference p_1-p_2 is instantaneously set up at the ends of the tube. At the next instant ($\tau>0$), a nonstationary fluid flow appears in the tube; later (as $\tau \to \infty$) it becomes stationary. Let the mean velocity of the stationary flow be given over the section; it equals $\bar{w}_\infty$.[1] The fluid enters the tube so that the velocity vector in the entrance section is directed along the axis, while the velocity is uniformly distributed over the section. The fluid temperature is the same everywhere, so that the physical properties of the fluid are constant. We analyze this

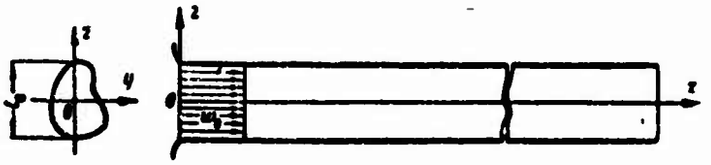

Fig. 4-1. Analysis of Problem of isothermal flow in tube.

problem by the similarity method. To do this, we set up its mathematical description.

Under the conditions considered, fluid motion is described by equation system (1-5), (1-8) in which we must set $F_x=F_y=F_z=0$:

$$\left.\begin{aligned}
&\frac{\partial w_x}{\partial \tau}+\vec{w}\,\mathrm{grad}\,w_x=-\frac{1}{\rho}\cdot\frac{\partial p}{\partial x}+\nu\nabla^2 w_x;\\
&\frac{\partial w_y}{\partial \tau}+\vec{w}\,\mathrm{grad}\,w_y=-\frac{1}{\rho}\cdot\frac{\partial p}{\partial y}+\nu\nabla^2 w_y;\\
&\frac{\partial w_z}{\partial \tau}+\vec{w}\,\mathrm{grad}\,w_z=-\frac{1}{\rho}\cdot\frac{\partial p}{\partial z}+\nu\nabla^2 w_z;\\
&\mathrm{div}\,\vec{w}=0,
\end{aligned}\right\} \qquad (4\text{-}1)$$

where p is the difference between the actual pressure in the flow and the hydrostatic pressure (see the footnote to page 10).

The initial conditions are:

for $\tau = 0$ $\qquad w_x=w_y=w_z=0.$ $\qquad (4\text{-}2)$

The boundary conditions are written as follows:

$$\left.\begin{aligned}
&\text{for } \tau>0,\ x=0,\ |y|<|y_c| \text{ and } |z|<|z_c|\ \ w_x=w_0(\tau),\ w_y=w_z=0;\\
&\text{for } \tau\to\infty,\ x=0,\ |y|<|y_c| \text{ and } |z|<|z_c\ \ w_x=w_0(\infty)=\bar{w}_\infty;\\
&\text{for } \tau>0,\ x>0,\ y=y_c \text{ and } z=z_c\ \ w_x=w_y=w_z=0,
\end{aligned}\right\} \qquad (4\text{-}3)$$

where y_s and z_s are the coordinates of points on the inside surface of the tube; w_0 is the velocity at the tube entrance; it is constant over the section but variable in time (for $\tau\to\infty, w_0\to\bar{w}_\infty$).

The equation specifying the form of the tube inside surface is

$$\varphi(y_c, z_c, l_0, l_1, \ldots, l_m)=0, \qquad (4\text{-}4)$$

where $l_0, l_1, \ldots, l_m$ are the characteristic dimensions of the tube cross-section.

We reduce Eqs. (4-1) and Conditions (4-2), (4-3), and (4-4) to dimensionless form, using the method of scale transformations

[3, 4]. Selecting l_0 and $\bar{w}_\infty$ as scale ratios, we introduce the dimensionless coordinates, linear dimensions, and velocities:

$$X=\frac{x}{l_0},\ Y=\frac{y}{l_0},\ Z=\frac{z}{l_0},\ L_1=\frac{l_1}{l_0},\ \ldots,\ L_m=\frac{l_m}{l_0};$$

$$W_x=\frac{w_x}{\bar{w}_\infty},\ W_y=\frac{w_y}{\bar{w}_\infty},\ W_z=\frac{w_z}{\bar{w}_\infty}\ \text{and}\ W_0=\frac{w_0}{\bar{w}_\infty}.$$

In (4-1)-(4-4), we replace the dimensioned variables $x, y, \ldots, w_0$ by the products of the dimensionless variables and the corresponding scale ratios, $Xl_0, Yl_0, \ldots, W_0\bar{w}_\infty$. In (4-1)-(4-4), we group the remaining dimensioned quantities and their scale ratios into dimensionless complexes; this yields a mathematical description of the process in dimensionless form:

$$\left.\begin{aligned}
&\frac{\partial W_x}{\partial \mathrm{Zh}}+(\vec{W}\,\mathrm{grad}\,W_x)\,\mathrm{Re}=-\frac{\partial}{\partial X}(\mathrm{Eu}\,\mathrm{Re})+\nabla^2 W_x;\\
&\frac{\partial W_y}{\partial \mathrm{Zh}}+(\vec{W}\,\mathrm{grad}\,W_y)\,\mathrm{Re}=-\frac{\partial}{\partial Y}(\mathrm{Eu}\,\mathrm{Re})+\nabla^2 W_y;\\
&\frac{\partial W_z}{\partial \mathrm{Zh}}+(\vec{W}\,\mathrm{grad}\,W_z)\,\mathrm{Re}=-\frac{\partial}{\partial Z}(\mathrm{Eu}\,\mathrm{Re})+\nabla^2 W_z;\\
&\mathrm{div}\,\vec{W}=0.
\end{aligned}\right\} \quad (4\text{-}5)$$

$$\text{for } \mathrm{Zh}=0\ W_x=W_y=W_z=0. \quad (4\text{-}6)$$

$$\left.\begin{aligned}
&\text{for } \mathrm{Zh}>0,\ X=0,\ |Y|<|Y_c|\ \text{and}\ |Z|<|Z_c|\ W_x=W_0(\mathrm{Zh}),\\
&W_y=W_z=0.\\
&\text{for } \mathrm{Zh}\to\infty,\ X=0,\ |Y|<|Y_c|\ \text{and}\ |Z|<|Z_c|\ W_x=W_0(\infty)=1.\\
&\text{for } \mathrm{Zh}>0,\ X\geqslant 0,\ Y=Y_c\ \text{and}\ Z=Z_c\ W_x=W_y=W_z=0.
\end{aligned}\right\} \quad (4\text{-}7)$$

$$\varphi(Y_c, Z_c, L_1, L_2, \ldots, L_m)=0. \quad (4\text{-}8)$$

In (4-5)-(4-8):

$\mathrm{Zh}=\frac{\nu\tau}{l_0^2}$ — Zhukovskiy number[2]:

$\mathrm{Eu}=\frac{p}{\rho\bar{w}_\infty^2}$ — Euler number;

$\mathrm{Re}=\frac{\bar{w}_\infty l_0}{\nu}$ — Reynolds number.

It follows from Eqs. (4-5), initial conditions (4-6), and boundary conditions (4-7) and (4-8) that the dimensionless dependent variables are functions of the following dimensionless independent variables and constant parameters:

$$W_x, W_y, W_z, \mathrm{Eu}=f_k(\mathrm{Zh}, X, Y, Z, \mathrm{Re}, L_1, L_2, \ldots, L_m). \quad (4\text{-}9)$$

where the f_k are unknown functions ($k=W_x, W_y, W_z, \mathrm{Eu}$), depending on the geometric shape of the tube cross section.

/56

For sufficiently large values of the Zhukovskiy number (Zh $\to \infty$) stationary flow will set in. In this case, in place of (4-9), we have

$$W_x, W_y, W_z, \mathrm{Eu} = F_h(X, Y, Z, \mathrm{Re}, L_1, L_2, \ldots, L_m). \qquad (4\text{-}10)$$

Let us now assume that sufficiently far from the tube entrance (at $X \to \infty$), the fluid velocity at each point in the flow will be parallel to the x axis.[3] Consequently, in this flow region $W_y = 0$, $W_z = 0$ and $\partial W_x/\partial X = 0$ (this last relation follows from the equation of continuity). Thus for the case under consideration the distribution of velocity W_x will be independent of X, and will be determined completely by the geometric shape of the tube cross section. Such a flow is said to be hydrodynamically stabilized.

For a stabilized flow, the second term on the left side of the first equation of (4-5) vanishes, while the second and third equations of (4-5) reduce to the following:

$$\frac{\partial \mathrm{Eu}}{\partial Y} = 0 \text{ and } \frac{\partial \mathrm{Eu}}{\partial Z} = 0.$$

Thus the number $\mathrm{Eu} = p/\rho\bar{w}^2$, or the dimensionless pressure, does not vary over the flow section,[4] so that in the case considered in place of System (4-5) we have the equation

$$-\frac{\partial W_x}{\partial \mathrm{Zh}} + \frac{\partial^2 W_x}{\partial Y^2} + \frac{\partial^2 W_x}{\partial Z^2} = \frac{\partial(\mathrm{Eu}\,\mathrm{Re})}{\partial X} = F(\mathrm{Zh}). \qquad (4\text{-}11)$$

The left side is independent of X, and the right side of Y and Z, so that both sides are functions of Zh alone.

From (4-11) and the corresponding initial and boundary conditions, we find that for stabilized flow

$$W_x = W_x(\mathrm{Zh}, Y, Z, L_1, L_2, \ldots, L_m), \qquad (4\text{-}12)$$

$$\frac{\partial \mathrm{Eu}}{\partial X} = \frac{1}{\mathrm{Re}}\Phi(\mathrm{Zh}, L_1, L_2, \ldots, L_m). \qquad (4\text{-}13)$$

If, in addition, the flow is stationary, then

$$W_x = W_x(Y, Z, L_1, L_2, \ldots, L_m), \qquad (4\text{-}12a)$$

$$\frac{d\,\overline{\mathrm{Eu}}}{dX} = \frac{1}{\mathrm{Re}}A(L_1, L_2, \ldots, L_m), \qquad (4\text{-}13a)$$

where A is a constant that depends on the geometry and relationship of dimensions of the tube cross section.

Let us now obtain dimensionless expressions for the hydraulic resistance. The latter is determined by the longitudinal gradient of the mean pressure over the section $\partial\bar{p}/\partial x$. The dimensionless mean-pressure gradient, taken with sign reversed, is called the local coefficient of hydraulic resistance:

$$\zeta = -\frac{\partial}{\partial X}\left(\frac{\bar{p}}{\frac{1}{2}\rho\bar{w}^2}\right) = -2\frac{\partial \overline{\mathrm{Eu}}}{\partial X}, \qquad (4\text{-}14)$$

where

$$\overline{Eu} = \frac{1}{f}\int_f Eu\, df = \frac{\bar{p}}{\frac{1}{2}\rho\bar{w}^2};$$

Here f is the area of the cross section normal to the tube axis.

For stationary flow of an incompressible liquid in a tube, we usually have $d\bar{p}/dx<0$ and, consequently, the coefficient ζ is positive.

The mean coefficient of hydraulic resistance for the tube segment between $x = 0$ and x will obviously equal

$$\bar{\zeta} = \frac{1}{x}\int_0^x \zeta\, dx = \frac{1}{X}\int_0^X \zeta\, dX = \frac{2}{X}(\overline{Eu}_0 - \overline{Eu}), \qquad (4\text{-}15)$$

where $\overline{Eu}_0$ is the value of $\overline{Eu}$ at $X = 0$.

If we substitute $\partial\bar{p}/\partial x$ from (2-44) into (4-14), we obtain

$$\zeta = \xi + \frac{2}{f}\left[\frac{\partial}{\partial Ho}\int_f W_x\, df + \frac{\partial}{\partial X}\int_f W_x^2\, df\right], \qquad (4\text{-}16)$$

while for a stationary flow,

$$\zeta = \xi + \frac{2}{f}\frac{d}{dX}\int_f W_x^2\, df, \qquad (4\text{-}16a)$$

where

$$\xi = \frac{2l_0 s}{f}\cdot\frac{\bar{\sigma}_s}{\rho\bar{w}^2} \qquad (4\text{-}17)$$

is the local coefficient of friction resistance; $Ho = Ho = \frac{\bar{w}\tau}{l_0}$ is the homochronicity number;[5] s is the perimeter of the tube cross section normal to the axis; $\bar{\sigma}_s$ is the tangential stress at the wall, averaged over the perimeter.

The first term in (4-16), i.e., the quantity ξ, allows for the energy expended in friction, while the second term allows for the change in velocity with time and in flow kinetic energy with length (owing to rearrangement of the velocity profile). On the basis of (4-9), (4-14), and the definition of $\overline{Eu}$ it is easy to see that ζ is a function of the following dimensionless quantities:

$$\zeta = \zeta(Zh, X, Re, L_1, L_2, \ldots, L_m). \qquad (4\text{-}18)$$

If the flow is stabilized over the entire tube length then, as we can see from (4-13), (4-14), and (4-15),

$$\zeta Re = \bar{\zeta} Re = \Phi_\zeta(Zh, L_1, L_2, \ldots, L_m). \qquad (4\text{-}19)$$

If, in addition, the flow is stationary, it then follows from (4-16) that $\zeta = \xi$, while

$$\xi \mathrm{Re} = A_\xi (L_1, L_2, \ldots, L_m). \qquad (4\text{-}20)$$

In other words, for a stationary stabilized flow, ξRe will be a constant depending solely on the geometry and dimensional relationships of the cross section.

The functions ζ, Φ_ζ, and the constant A_ξ are found theoretically or experimentally.

If the resistance coefficients are known, it is not difficult to determine the pressure variation along the length or the pressure drop across a certain segment of the tube. Thus, for example, for stationary flow we have from (4-14):

$$d\bar{p} = -\zeta \frac{\rho \bar{w}^2}{2} \frac{dx}{l_0}. \qquad (4\text{-}21)$$

Integrating this relationship over the length, we can find $p(x)$.

The pressure drop across the tube segment between $x = 0$ and x, which we represent as $\Delta p = \bar{p}_0 - \bar{p}$, is found from (4-15):

$$\Delta p = \bar{\zeta} \frac{\rho \bar{w}^2}{2} \frac{x}{l_0}. \qquad (4\text{-}22)$$

Relationship (4-22) is known in hydraulics as the Darcy-Weisbach law.

We have considered flow in a tube of arbitrary cross section that does not change along the axis. If the tube is round, then the only dimension determining the cross section is the tube diameter, and this can then be taken as the characteristic dimension, i.e., we let $l_0 = d$. Here the relative linear cross-sectional dimensions $L_1, L_2, \ldots, L_m$ are eliminated from the expressions found above.

4-3. HEAT EXCHANGE AND HYDRAULIC RESISTANCE IN FLOW OF LIQUID

Let us consider liquid flow and heat exchange in a smooth round pipe of diameter $d = 2r_0$.[6] At the tube entrance section, the velocity vector is directed along the axis, while the liquid velocity w_0 and temperature t_0 are constant over the section and invariant in time. At times preceding the initial instant ($\tau < 0$), the liquid temperature throughout the entire volume and the wall temperature are identical and equal to t_0; consequently, there is no heat exchange, and there is isothermal flow of the liquid in the tube. At the intial instant ($\tau = 0$), the wall temperature or density of the heat flow at the wall will change instantaneously, and take on values t_s or q_s that are constant in time and over the surface. During a certain time interval, a nonstationary transient will be observed in the tube; later (when $\tau \to \infty$) a stationary state

[6] /56

will set in. For generality, we shall assume that the physical properties of the liquid depend on the temperature.

Under these conditions, the liquid motion and the heat exchange are described by equation system (1-16). Assuming that there are no internal heat sources in the flow and neglecting the heat of friction, we drop the corresponding terms in the energy equation. We introduce the lift (see § 1-2) into the equation of motion, letting

$$\rho g_x - \frac{\partial p}{\partial x} = -g\beta_\rho \rho_0 (t - t_0)\cos\psi - \frac{\partial}{\partial x}(p - p_0), \qquad (4\text{-}23)$$

where p is the actual pressure in the liquid flow; p_0 is the hydrostatic pressure, computed on the assumption that the liquid has density ρ_0 everywhere; ψ is the angle between the x axis, which coincides with the tube axis, and the vector representing the gravitational force. We shall henceforth simply use p to represent the pressure difference $p - p_0$. We shall use Relationships (3-1)-(3-4) to allow for the way in which the physical properties of liquids depend on temperature. Thus our problem corresponds to the following equation system:[7]

$$\left.\begin{aligned}
\rho c_p\left(\frac{\partial t}{\partial \tau} + \vec{w}\,\mathrm{grad}\,t\right) &= \mathrm{div}\,(\lambda\,\mathrm{grad}\,t);\\
\rho\left(\frac{\partial w_x}{\partial \tau} + \vec{w}\,\mathrm{grad}\,w_x\right) &= -g\beta_\rho\rho_0(t - t_0)\cos\psi - \frac{\partial p}{\partial x} + \frac{\partial}{\partial x}\left(2\mu\frac{\partial w_x}{\partial x}\right) +\\
&+ \frac{1}{r}\cdot\frac{\partial}{\partial r}\left[r\mu\left(\frac{\partial w_x}{\partial r} + \frac{\partial w_r}{\partial x}\right)\right] + \frac{1}{r}\frac{\partial}{\partial \varphi}\left[\mu\left(\frac{1}{r}\cdot\frac{\partial w_x}{\partial \varphi} + \frac{\partial w_\varphi}{\partial x}\right)\right];\\
\frac{\partial \rho}{\partial \tau} + \mathrm{div}\,(\rho\vec{w}) &= 0;\\
\frac{\rho}{\rho_0} = 1 - \beta_\rho(t - t_0);\quad \frac{c_p}{c_{p_0}} &= 1 + \beta_c(t - t_0);\\
\frac{\lambda}{\lambda_0} = 1 - \beta_\lambda(t - t_0);\quad \frac{\mu_0}{\mu} &= 1 + \beta_\mu(t - t_0).
\end{aligned}\right\} \qquad (4\text{-}24)$$

where ρ_0, c_{p0}, λ_0 and μ_0 are the values of the liquid physical parameters at the entrance temperature t_0.

On the basis of the earlier analysis [see (4-10)], we can write the intial conditions as

$$\left.\begin{aligned}
&\text{for } \tau < 0,\ x \geqslant 0 \text{ and } 0 \leqslant r \leqslant r_0\ \frac{w_x}{w_0},\ \frac{w_r}{w_0} = F_k\left(\frac{x}{d},\ \frac{r}{d},\ \frac{w_0 d}{\nu_0}\right),\ (k = x, r);\\
&w_\varphi = 0;\ t = t_0.
\end{aligned}\right\} \qquad (4\text{-}25)$$

The boundary conditions have the form

$$\left.\begin{aligned}
&\text{for } \tau > 0,\ x = 0 \text{ and } 0 \leqslant r < r_0\ w_x = w_0,\ w_r = w_\varphi = 0,\ t = t_0;\\
&\text{for } \tau \geqslant 0,\ x \geqslant 0 \text{ and } r = r_0\ w_x = w_r = w_\varphi = 0,\ t = t_c \text{ or } \lambda\frac{\partial t}{\partial r} = q_c.
\end{aligned}\right\} \qquad (4\text{-}26)$$

1. Let us first analyze the problem of liquid motion and heat exchange for the case in which the wall temperature t_s is specified.

To transform Eqs. (4-24) and Conditions (4-25) and (4-26) to dimensionless form, we introduce the variable $\vartheta = t - t_0$, and select the following scales: d, w_0, $\vartheta_c = t_c - t_0$, ρ_0, c_{p_0}, λ_0 and μ_0. Using these scales, we introduce the dimensionless quantities

$$X = \frac{x}{d};\ R = \frac{r}{d};\ \vec{W} = \frac{\vec{w}}{w_0};\ \theta = \frac{\vartheta}{\vartheta_c} = \frac{t - t_0}{t_c - t_0};$$

$$P = \frac{\rho}{\rho_0};\ C_p = \frac{c_p}{c_{p_0}};\ A = \frac{\lambda}{\lambda_0} \text{ and } M = \frac{\mu}{\mu_0}.$$

After simple manipulations, we obtain a mathematical description of the process in dimensionless form:

$$\left.\begin{aligned}
PC_p\left[\frac{\partial\theta}{\partial \mathrm{Fo}} + \mathrm{Pe}(\vec{W}\,\mathrm{grad}\,\theta)\right] &= \mathrm{div}\,(A\,\mathrm{grad}\,\theta);\\
P\left[\frac{\partial W_x}{\partial \mathrm{Zh}} + \mathrm{Re}(\vec{W}\mathrm{grad})\vec{W}\right] &= -\frac{\mathrm{Gr}}{\mathrm{Re}}\theta\cos\psi - \frac{\partial}{\partial X}(\mathrm{Eu}\,\mathrm{Re}) + \frac{\partial}{\partial X}\left(2M\frac{\partial W_x}{\partial X}\right) +\\
&+ \frac{1}{R}\cdot\frac{\partial}{\partial R}\left[RM\left(\frac{\partial W_x}{\partial R} + \frac{\partial W_r}{\partial X}\right)\right] + \frac{1}{R}\cdot\frac{\partial}{\partial\varphi}\left[M\left(\frac{1}{R}\cdot\frac{\partial W_x}{\partial\varphi} + \frac{\partial W_\varphi}{\partial X}\right)\right];\\
\frac{\partial P}{\partial \mathrm{Ho}} + \mathrm{div}\,(P\vec{W}) &= 0;\\
P = 1 - \beta_\rho\vartheta_c\theta;\ C_p &= 1 + \beta_c\vartheta_c\theta;\\
A = 1 - \beta_\lambda\vartheta_c\theta;\ \frac{1}{M} &= 1 + \beta_\mu\vartheta_c\theta.
\end{aligned}\right\} \quad (4\text{-}27)$$

For $\mathrm{Fo} < 0$, $X \geq 0$ and $0 < R < \frac{1}{2}$

$$W_x,\ W_r = F_k(X,\ R,\ \mathrm{Re}),\ W_\varphi = 0,\ \theta = 0. \quad (4\text{-}28)$$

$$\left.\begin{aligned}
&\text{for } \mathrm{Fo} \geq 0,\ X = 0 \text{ and } 0 < R < \tfrac{1}{2}\\
&\quad W_x = 1,\ W_r = W_\varphi = 0,\ \theta = 0.\\
&\text{for } \mathrm{Fo} \geq 0,\ X \geq 0 \text{ and } R = \tfrac{1}{2}\\
&\quad W_x = W_r = W_\varphi = 0,\ \theta = 1.
\end{aligned}\right\} \quad (4\text{-}29)$$

In (4-27), (4-28), and (4-29), the symbols are as follows:

$\mathrm{Fo} = \frac{a_0\tau}{d^2}$ — Fourier numbers;

$a_0 = \frac{\lambda_0}{\rho_0 c_{p_0}}$ — Coefficient of thermal diffusivity;

$\mathrm{Zh} = \frac{\nu_0\tau}{d^2}$ — Zhukovskiy number;

$\mathrm{Ho} = \frac{w_0\tau}{d}$ — Homochronicity number;

$\mathrm{Eu} = \frac{p}{\rho_0 w_0^2}$ — Euler number;

$\mathrm{Pe} = \frac{w_0 d}{a_0}$ — Peclet number;

$\mathrm{Re} = \frac{w_0 d}{\nu_0}$ — Reynolds number;

$\mathrm{Gr} = \frac{g\beta_\rho\vartheta_c d_0^3}{\nu_0^2}$ — Grashof number.

The quantities $\beta_\rho\vartheta_c$, $\beta_c\vartheta_c$, $\beta_\lambda\vartheta_c$ and $\beta_\mu\vartheta_c$ can be represented in terms of the ratios of the corresponding physical parameters at temperatures t_s and t_0. Letting $\Theta = 1$ in the last four equations of System (4-27), we obtain

$$\left.\begin{aligned}\beta_\rho\vartheta_c &= 1-P_c,\ \beta_c\vartheta_c = C_{pc}-1,\\ \beta_\lambda\vartheta_c &= 1-\Lambda_c,\ \beta_\mu\vartheta_c = \frac{1}{M_c}-1,\end{aligned}\right\} \qquad (4\text{-}30)$$

where

$$P_c=\frac{\rho_r}{\rho_0},\quad C_{pc}=\frac{c_{pc}}{c_{p_0}},\quad \Lambda_c=\frac{\lambda_c}{\lambda_0}\ \text{and}\ M_c=\frac{\mu_c}{\mu_0}.$$

It follows from (4-27)—(4-30), that the dimensionless dependent variables are functions of the following dimensionless quantities:

$$\Theta,\ W_x,\ W_r,\ W_\varphi,\ Eu = f_k(Fo,\ Zh,\ Ho,\ X,\ R,\ \varphi,\ Pe,\ Re,\ Gr,\ \psi,\ P_c,\ C_{pc},\ \Lambda_c,\ M_c), \qquad (4\text{-}31)$$

where

$$k = \Theta,\ W_x,\ W_r,\ W_\varphi,\ Eu.$$

The Zh and Ho numbers appearing in (4-31) can be represented in terms of Fo, Re, and Pe:

$$Zh=\frac{Pe\,Fo}{Re};\quad Ho = Pe\,Fo.$$

Then (4-31) can be represented as

$$\Theta,\ W_x,\ W_r,\ W_\varphi,\ Eu = f_k(Fo,\ X,\ R,\ \varphi,\ Pe,\ Re,\ Gr,\ \psi,\ P_c,\ C_{pc},\ \Lambda_c,\ M_c). \qquad (4\text{-}32)$$

Naturally, in (4-32) we can introduce the ratio $\frac{Pe}{Re}=\frac{\nu_0}{a_0}=Pr$, i.e., the Prandtl number, in place of one of the controlling parameters Pe or Re.

We now obtain a system of dimensionless numbers for the heat transfer and hydraulic resistance.

We find the local heat-transfer coefficient; in accordance with (2-20),

$$\alpha=\frac{\lambda_0}{t_0-t_0}\left(\frac{\partial t}{\partial r}\right)_{r=r_0},$$

or in dimensionless form,

$$Nu=\Lambda_c\left(\frac{\partial\Theta}{\partial R}\right)_{R=\frac{1}{2}}, \qquad (4\text{-}33)$$

where $Nu=\frac{\alpha l}{\lambda_0}$ is the dimensionless heat-transfer coefficient, called the Nusselt number.

Substituting the values of Θ from (4-32) into (4-33), we see that Nu is a function of the following dimensionless quantities:

$$Nu = Nu(Fo, \ldots, \varphi, Pe, Re, Gr, \psi, P_c, C_{pc}, \Lambda_c, M_c). \quad (4\text{-}34)$$

In (4-33), the local heat-transfer coefficient pertains to the intial temperature head $t_s - t_0$. If we refer α to the local temperature head $t_s - \bar{t}$ (where $\bar{t}$ is the mean mass temperature of the liquid in the given section), then Nu will depend on the same dimensionless quantities, but the nature of the relationship will be different.

The local resistance coefficient ζ is determined from (4-14), in which

$$\overline{Eu} = \frac{4}{\pi}\int_0^{2\pi} d\varphi \int_0^{1/2} Eu R\, dR \quad (4\text{-}35)$$

when we consider a round tube.

Substituting the values of Eu from (4-32) into (4-35), from (4-14) we have

$$\zeta = \zeta(Fo, X, Pe, Re, Gr, \psi, P_c, C_{pc}, \Lambda_c, M_c). \quad (4\text{-}36)$$

Equations (4-32), (4-34) and (4-36) are valid both for a nonstationary transient and for the steady state. In the latter case, the temperature field does not depend on the time and, consequently, the Fo number on the right side of these equations must be dropped.

The number of dimensionless quantities on the right side of (4-32), (4-34) and (4-36) will be reduced significantly if we assume that the physical properties of the liquid do not depend on the temperature. In this case, the last four equations of System (4-27) drop out. In the remaining equations of this system, P, C_p, Λ, and M will equal unity. The term allowing for the influence of the gravitational force will vanish in the equation of motion (since $\beta_\rho = 0$, and thus Gr = 0), so that the velocity and temperature fields will be symmetric about the axis; the nonstationary term in the equation of motion will also vanish, since under the conditions considered the flow will be stationary when μ and ρ are constant.

Under such assumptions, the problem of fluid motion reduces to a special case of the problem considered in the preceding section. As for the heat-exchange problem, after the indicated simplifications are made in System (4-27), we find

$$\theta = \theta(Fo, X, R, Pe, Pr). \quad (4\text{-}37)$$

Substituting this expression into (4-33), we obtain

$$Nu = Nu(Fo, X, Pe, Pr). \quad (4\text{-}38)$$

For a stationary state, the Fo number will drop out of (4-37) and (4-38).

2. Let us now consider the same problem, but for the case in

which we are given the heat-flow density at the wall, q_s = const. Thus in place of the condition $t = t_s$ at $r = r_0$, we have the condition

$$\lambda_c\left(\frac{\partial t}{\partial r}\right)_{r=r_0} = q_0. \qquad (4\text{-}39)$$

In analyzing this problem we can use the same scales as in the preceding case (see paragraph 1) with the exception of the scale for the temperature. This scale must be selected as the difference $t_s - t_0$, since the wall temperature t_s is not known in this case. The scale for the temperature can be established from boundary condition (4-39); to do this, we write the condition in dimensionless form:

$$\frac{\lambda_c}{\lambda_0}\left[\frac{\partial}{\partial R}\left(\frac{t-t_0}{\frac{q_c d}{\lambda_0}}\right)\right]_{R=\frac{1}{2}} = 1. \qquad (4\text{-}40)$$

From this it is clear that the quantity

$$\vartheta_q = \frac{q_c d}{\lambda_0}$$

should be taken as the scale for the temperature; it has the dimensions of temperature.

If we introduce the dimensionless temperature

$$\theta = \frac{\vartheta}{\vartheta_q} = \frac{t-t_0}{\frac{q_c d}{\lambda_0}} \qquad (4\text{-}41)$$

and replace the scale ϑ_s by the scale ϑ_q, then the dimensionless mathematical description of the process (4-27), (4-28), and (4-29) also remain valid in the given case, with the exception of the last condition of (4-29), which should be replaced by Condition (4-40). Thus in the problem of fluid motion and heat exchange, for a specified heat-flow density at the wall, we have the following system of dimensionless numbers:

$$\theta, W_x, W_r, W_\varphi, \mathrm{Eu} = F_k(\mathrm{Fo}, X, R, \varphi, \mathrm{Pe}, \mathrm{Re}, \mathrm{Gr}, \psi, \beta_\rho\vartheta_q, \beta_c\vartheta_q, \beta_\lambda\vartheta_q, \beta_\mu\vartheta_q), \qquad (4\text{-}42)$$

where $k = \theta, W_x, W_r, W_\varphi, \mathrm{Eu}$;

$$\mathrm{Gr} = \frac{g\beta_\rho\vartheta_q d^4}{\nu_0^2} = \frac{g\beta_\rho q_c d^4}{\lambda_0\nu_0^2}.$$

All the remaining quantities have the same values as in §1.

The dimensionless temperature at the wall is the reciprocal of Nu, in which the heat-transfer coefficient α refers to the temperature difference $t_s - t_0$:

$$\theta_0 = \frac{t_s - t_0}{\frac{q_0 d}{\lambda_0}} = \frac{\lambda_0}{\alpha d} = \frac{1}{Nu},$$

where

$$\alpha = \frac{q_0}{t_0 - t_0}.$$

Letting $R = 1/2$ in the expression for θ (4-42), we obtain:

$$Nu = \frac{1}{\theta_0} = Nu(Fo, X, \varphi, Pe, Re, Gr, \psi, \beta_\rho \vartheta_q, \beta_c \vartheta_q, \beta_\lambda \vartheta_q, \beta_\mu \vartheta_q). \qquad (4\text{-}43)$$

The same system of dimensionless numbers is also obtained when α refers to the local temperature head $t_s - \bar{t}$.

From (4-14), (4-35) and (4-42) we find

$$\zeta = \zeta(Fo, X, Pe, Re, Gr, \psi, \beta_\rho \vartheta_q, \beta_c \vartheta_q, \beta_\lambda \vartheta_q, \beta_\mu \vartheta_q). \qquad (4\text{-}44)$$

If the physical properties of the fluid do not depend on the temperature, then the system of dimensionless numbers will be exactly the same when q_s and t_s are specified; here we need only allow for the fact that the dimensionless temperature θ will be determined differently in each of these cases.

4-4. HEAT EXCHANGE AND FRICTION RESISTANCE IN FLOW OF A GAS

The sole difference from the preceding problem (see §4-3) lies in the fact that it is not a liquid flowing through the tube, but a slowly[9] moving gas. Thus in the mathematical description of the process, the last four equations of System (4-24) must be replaced by relationships describing the change in the physical properties of the gas with temperature:

$$\frac{\rho}{\rho_0} = \frac{T_0}{T}, \quad \frac{c_p}{c_{p_0}} = \left(\frac{T}{T_0}\right)^{n_c}, \quad \frac{\lambda}{\lambda_0} = \left(\frac{T}{T_0}\right)^{n_\lambda}, \quad \frac{\mu}{\mu_0} = \left(\frac{T}{T_0}\right)^{n_\mu}, \qquad (4\text{-}45)$$

where ρ_0, c_{p_0}, λ_0 and μ_0 are the physical parameters of the gas at the entrance temperature T_0; n_c, n_λ and n_μ are constants that depend on the type of gas. Since the gas moves slowly, the relationship between the density and the pressure can be neglected (see §1-2, paragraph 3).

1. Let us first consider the case in which the constant wall temperature T_s = const is specified.

As we can see from (4-45), it is convenient to take T_0 as the scale for the temperature. Then the dimensionless temperature can be written in the form

$$\theta = \frac{T}{T_0}.$$

The previous scales are retained for the other quantities. After the equations and initial and boundary conditions have been transformed to dimensionless form, we obtain the same dimensionless numbers as before (see §4-3, paragraph 1), with certain ex-

[9] /57

ceptions. In place of the numbers $\beta_0\vartheta_0$, $\beta_0\vartheta_0$, etc., from the boundary condition at the wall ($\theta = \theta_s$ for $R = 1/2$), we obtain the number $\theta_0 = T_0/T_0$, and the numbers n_0, n_λ and n_μ from Relationship (4-45). To replace the Gr number in the dimensionless equation of motion, we introduce the number $\frac{g\beta_0 d^3 T_0}{\nu_0^2}$; multiplying it by $\theta_s - 1$, we obtain the previous number $Gr = \frac{g\beta_0 \vartheta_0 d^3}{\nu_0^2}$, where $\vartheta_0 = T_0 - T_0$. As a result, we arrive at the following system of dimensionless quantities:

$$\theta, W_x, W_r, W_\varphi, Eu = f_1(Fo, X, R, \varphi, Pe, Re, Gr, \psi, \theta_0, n_0, n_\lambda, n_\mu). \quad (4\text{-}46)$$

The number $\theta_0 = T_0/T_0$ is called the temperature factor.

Referring the local heat-transfer coefficient α to the temperature head ϑ_s, we obtain a relationship of the type (4-33) for Nu, but with $\theta_s - 1$ in the denominator. Substituting θ from (4-46) into this relationship, we obtain

$$Nu = Nu(Fo, X, \varphi, Pe, Re, Gr, \psi, \theta_0, n_0, n_\lambda, n_\mu). \quad (4\text{-}47)$$

On the basis of (4-14), (4-35), and the expression for Eu, from (4-46) we obtain

$$\zeta = \zeta(Fo, X, Pe, Re, Gr, \psi, \theta_0, n_0, n_\lambda, n_\mu). \quad (4\text{-}48)$$

When the temperature heads are not very great, the relationship between c_p and T can be neglected, and we can take $n_s = 0$. Moreover, in most cases we can let $n \approx n_\mu \approx n$.

2. If we are given the constant heat-flow density at the wall, $q_s = \text{const}$, then determining the dimensionless temperature in the form $\theta = T/T_0$, we obtain the same system of dimensionless numbers as with (4-46), (4-47) and (4-48), with the sole difference that from the boundary condition, in this system we replace θ_s by the dimensionless number

$$\theta_q = \frac{q_0 d}{\lambda_0 T_0}.$$

The dimensionless wall temperature $\theta_0 = T_0/T_0$, which in our case is the dependent variable, will be a function of the following quantities:

$$\theta_0 = \theta_0(Fo, X, \varphi, Pe, Re, Gr, \psi, \theta_q, n_0, n_\lambda, n_\mu). \quad (4\text{-}49)$$

Naturally, the number

$$Nu = \frac{q_0 d}{\lambda_0 (T_0 - T_0)} = \frac{\theta_q}{\theta_0 - 1}$$

also depends on these quantities.

Finally, if it proves convenient, we can treat $\bar{\theta}_c(X, \varphi)$ as an independent variable,[10] and Nu or θ_q as dependent variables. In such case, we arrive at the system of dimensionless quantities (4-47). It is natural that the functions will in general differ in form for T_s = const and q_s = const.

Comparing the systems of dimensionless quantities for a gas and a liquid, we see that the scle difference lies in the dimensionless quantities allowing for the way in which the physical properties of the gas and liquid depend on the temperature. If the physical properties of the gas and liquid are constant, then their dimensionless systems and the relationships among the dimensionless quantities will be identical.

4-5. LIMITING CASES OF FLOW AND HEAT EXCHANGE

To keep the ensuing discussion simple, we shall assume that all physical properties of the liquid (gas) are constant, with the exception of the density. We consider the dependence of ρ on t only since this is associated with the appearance of lift forces. In all other respects, we shall also assume that the density is constant. Then for the fluid-motion and heat-exchange problem considered in the last two sections, we obtain the following system of dimensionless equations:[11]

$$\left.\begin{aligned} &\frac{\partial\theta}{\partial Fo}+\mathrm{Pe}(\vec{W}\,\mathrm{grad}\,\theta)=\nabla^2\theta;\\ &\frac{\partial W_z}{\partial Fo}+\mathrm{Re}(\vec{W}\,\mathrm{grad})\vec{W}=-\frac{\mathrm{Gr}}{\mathrm{Re}}\theta\cos\psi-\frac{\partial}{\partial X}(\mathrm{Eu}\,\mathrm{Re})+\nabla^2 W_z;\\ &\mathrm{div}\,\vec{W}=0. \end{aligned}\right\} \quad (4\text{-}50)$$

To this system, we must add the initial and boundary conditions, which have the same form as before [see (4-28), (4-29), and (4-40)].

We have the following relationships for the local values of the Nusselt number and hydraulic-resistance coefficient, according to (4-33), (4-14), and (4-35):

$$\mathrm{Nu}=\left(\frac{\partial\theta}{\partial R}\right)_{R=\frac{1}{2}}; \quad (4\text{-}51)$$

$$\zeta=-\frac{8}{\pi}\frac{\partial}{\partial X}\int_0^{2\pi}d\varphi\int_0^{1/2}\mathrm{Eu}\,R\,dR. \quad (4\text{-}52)$$

In the general case, the viscosity, inertial, and gravitational forces will be commensurate in the fluid flow. Thus we say that such a flow is viscous-inertial-gravitational. In analyzing it, we must take into account all terms of the equation of motion. Here we find from (4-50), the initial and boundary conditions, (4-51), nd (4-52) that Nu and ϑ depend on the following quantities:

$$Nu = Nu(Fo, X, \varphi, Pe, Re, Gr, \psi); \quad (4-53)$$

$$\zeta = \zeta(Fo, X, Pe, Re, Gr, \psi). \quad (4-54)$$

Let us now consider certain limiting cases for flow and heat exchange.

a) A viscous-inertial flow corresponds to negligibly small influence of gravitational forces (lift forces) as compared with the viscosity and inertial forces. If we drop the first term on the right side of the equation of motion and recall that in the absence of lift forces Eu, W_x, and W_r will not depend on θ, i.e., the flow will become stationary[12] and symmetric about the axis, we obtain the following system of dimensionless numbers for this case:

$$Nu = Nu(Fo, X, Pe, Re); \quad (4-55)$$

$$\zeta = \zeta(X, Re). \quad (4-56)$$

b) Viscous-gravitational flow corresponds to negligible influence of inertial forces as compared with the viscosity and gravitational forces. Dropping the left side in the equation of motion, we find

$$Nu = Nu(Fo, X, \varphi, Pe, Gr \cdot Pr, \psi); \quad (4-57)$$

$$\zeta Re = f_\zeta(Fo, X, Pe, Gr \cdot Pr, \psi). \quad (4-58)$$

Thus Gr and Pr enter into (4-57) and (4-58) as a product, while the resistance coefficient $\zeta \sim 1/Re$.

c) A viscous flow corresponds to negligible influence of inertial and gravitational forces as compared with the viscosity forces.

Looking at the facts noted in paragraph "a," we find it obvious that the inertial forces are unimportant as compared with the viscosity forces when $W_r = 0$ and, consequently, $\partial W_x/\partial X = 0$, i.e., when hydrodynamic stabilization sets in. Dropping the corresponding terms in the equation of motion, we obtain

$$Nu = Nu(Fo, X, Pe); \quad (4-59)$$

$$\zeta = \xi = \frac{const}{Re}. \quad (4-60)$$

If we also assume that the variation in heat-flow density owing to heat conduction along the axis is small as compared with the variation along the radius, i.e., $\frac{\partial^2\Theta}{\partial X^2} \ll \frac{\partial^2\Theta}{\partial R^2}$, then in place of (4-59) we obtain

$$Nu = Nu\left(Fo, \frac{X}{Pe}\right). \quad (4-61)$$

After the stationary state has commenced, the Fo number vanishes from all of the equations given here.

Viscous and viscous-gravitational flow can only occur in laminar flow of the liquid, i.e., for Reynolds numbers below the critical value. But viscous-inertial and viscous-inertial-gravitational flows are observed with both laminar and turbulent flow regimes. Although the system of dimensionless numbers (4-53)-(4-56) was obtained by analyzing the basic equations for laminar flow, they also are valid in turbulent flow. The reason is that transfer of momentum and heat by turbulent exchange (i.e., by velocity and temperature pulsations) depends on the same Re and Pe numbers that already occur in Systems (4-53)-(4-56).

The influence of free convection on forced flow is reflected in Gr (or Gr·Pr). If it is small, the flow will be viscous or viscous-inertial. For sufficiently large values of Gr, we observe a transition to viscous-gravitational or viscous-inertial-gravitational flow.

To conclude we note that the results given in this chapter were obtained solely with the aid of an analysis of the mathematical description of the process by the similarity method.

Manuscript Page No.

Footnotes

41 [1]We note that specifying $\bar{w}_\infty$ is equivalent to specifying $p_1 - p_2$. We shall henceforth assume that $\bar{w}_\infty$ has been specified, since this is more convenient for analysis.

43 [2]The number w/l_0^2, expressing the dimensionless time in problems on nonstationary flow of a viscous fluid, is called the Zhukovskiy number, and represented by the symbol Zh in honor of the outstanding Russian mechanics Scholar Nikolay Yegorovich Zhukovskiy (1847-1921), whose contributions to the development of hydrodynamics and aerodynamics are generally recognized.

44 [3]This assumption finds good confirmation, as we shall see later.

44 [4]Here and in the ensuing discussion, we shall use $\bar{w}$ rather than $\bar{w}_\infty$ to represent the mean velocity over a section in stationary flow.

45 [5]We note that the Ho and Zh numbers are associated by the relationship Ho=ReZh, so that it is easy to go from one to the other in the equations.

46 [6]The tube is assumed to be round only for purposes of simplification. The results of the subsequent analysis are just as valid for tubes of arbitrary cross section, provided the system of dimensionl ss numbers is supple-

mented by the relative linear dimensions characterizing the cross section.

47 [7]The equations for the projections of the velocity w_r w_φ are omitted to reduce the bookkeeping.

[8] The term $\partial w_z/\partial \tau$ is retained in the equation of motion, since owing to the dependence of ρ and μ on the temperature, the flow during a transient will be nonstationary, even though by hypothesis w_0 does not change in time.

52 [9]That is, the gas velocity is small as compared with the speed of sound.

54 [10]Here θ_s should be specified by a function of the coordinates X and φ at the tube wall.

54 [11] The equations are obtained directly from (4-27) if we use the assumptions made. Here the equations for the velocity projections w_r and w are also omitted.

55 [12] We recall that in this problem (see §4-3), nonstationarity results solely from the time variation of the thermal boundary conditions. If the physical properties of the fluid are constant, this will not result in disturbance of the stationary nature of the flow.

Manuscript Page No.

Transliterated Symbols

42 c = s = stenka = wall

Chapter 5

ISOTHERMAL FLOW

5-1. GENERAL INFORMATION ON STATIONARY STABILIZED FLOW

In this chapter we shall consider isothermal flow of an incompressible fluid, i.e., a flow such that the temperature field in the stream is uniform and consequently, the physical properties of the fluid are constant.

As theory and experiment have shown, the nature of fluid flow near the entrance section of a tube depends essentially on the entrance conditions. At a sufficient distance from the entrance section, however, this relationship vanishes. Far from the entrance the fluid moves so that the velocity vector at each point in the flow is parallel to the tube axis.[1] As we have already noted in §4-2, we say that such a flow is hydrodynamically stabilized. If the tube is sufficiently long, then, beginning at a certain distance from the entrance, the flow can always be assumed to be stabilized. For fairly short tubes, it is necessary to allow for the features of flow in the initial segment (see §5-4).

Let there be a stationary stabilized flow of fluid in a tube of arbitrary cross section, whose axis coincides with the x axis of a rectangular coordinate system. In this case $\partial w_x/\partial\tau=0$, $w_y=w_z=0$ and, consequently, $\frac{\partial p}{\partial y}=\frac{\partial p}{\partial z}=0$ and $\frac{\partial w_x}{\partial x}=0$ (here p is the difference between the real pressure in the flow and the hydrostatic pressure). Thus in stabilized flow, the pressure is constant over a section and varies only with the length, while the velocity w_x changes only over a section and is constant with length. Taking this into account, we write the equation of motion as

$$\mu\left(\frac{\partial^2 w_x}{\partial y^2}+\frac{\partial^2 w_x}{\partial z^2}\right)=\frac{dp}{dx}=\text{const}.$$

Since w_x is a function of y and z alone, while p is a function of x, the right and left sides of this equation equal the same constant. In particular, this implies that p varies linearly along the tube. We let

$$-\frac{dp}{dx}=\frac{\Delta p}{l}=\text{const},$$

where Δp is the pressure across the tube segment of length l. Then the preceding equation can be rewritten as

$$\frac{\partial^2 w_x}{\partial y^2}+\frac{\partial^2 w_x}{\partial z^2}=-\frac{\Delta p}{\mu l}. \qquad (5\text{-}1)$$

To find the distribution of velocity w_x, we must solve (5-1) under a boundary condition at the wall that requires the velocity w_x to equal zero.

Equation (5-1) is a Poisson equation, which can be solved by various mathematical methods. Exact solutions can be obtained, for example, with the aid of functions of a complex variable. The approximate methods used include the method of finite differences, as well as variational methods that make it possible to obtain an approximate solution in analytic form. From the mathematical viewpoint, the problem considered is equivalent to the problem of torsion in a long beam. Thus with certain modifications, the solutions known in elasticity theory for problems involving torsion in beams of various shapes can be used to determine velocity profiles in tubes with the same cross-sectional form. There are many studies containing solutions of Eq. (5-1) for tubes of various shapes [1-7]. Some of them will be given in subsequent sections.

After the velocity distribution has been found, it is not difficult to calculate the tangential stress at the wall. The local stress is

$$\sigma_0=\mu\left(\frac{\partial w_x}{\partial n}\right)_{n=0},$$

where n is the normal to the inside surface of the wall. The mean tangential stress over the perimeter is

$$\bar{\sigma}_0=\frac{1}{s}\int_s \mu\left(\frac{\partial w_x}{\partial n}\right)_{n=0} ds,$$

where s is the tube perimeter.

It is convenient to use the hydraulic-resistance coefficient ζ to determine the pressure drop; in the present case, it coincides with the friction-resistance coefficient ξ (see §4-2). By definition, ξ equals the dimensionless pressure gradient, taken with reverse sign:

$$\xi=-\frac{2l_0}{\rho\bar{w}^2}\cdot\frac{dp}{dx}=\frac{2l_0}{\rho\bar{w}^2}\cdot\frac{\Delta p}{l}, \qquad (5\text{-}2)$$

where l_0 is one of the cross-sectional dimensions, selected as a scale ratio; $\bar{w}$ is the mean fluid velocity over the section.

The quantity ξ is associated with $\bar{\sigma}_s$ by Relationship (4-17):

$$\xi=\frac{2l_0 s}{f}\frac{\bar{\sigma}_c}{\rho\bar{w}^2},$$

where f is the cross-sectional area of the tube.

The choice of scale l_0 is arbitrary, and is still not fixed. Thus we can take any quantity as a scale that has the dimensions of length, being guided by considerations of convenience. Let us take $l_0 = 4f/s$. This is called the equivalent diameter of the tube. Thus we take as the scale

$$d_e = \frac{4f}{s}.$$

Utilization of this scale offers the following advantages: a) it simplifies (4-17); b) the scale is determined uniquely for tubes of different geometric form; c) for a round tube (the most common case), d_e simply equals the tube diameter d. The choice of d_e as the scale may prove desirable for other reasons as well; more of this later.

After we introduce d_e, (5-2) and (4-17) will take the form

$$\xi = \frac{2d_e}{\rho\bar{w}^2} \cdot \frac{\Delta p}{l}, \qquad (5\text{-}2a)$$

$$\xi = \frac{8\bar{\sigma}_c}{\rho\bar{w}^2}. \qquad (5\text{-}3)$$

Substituting the expression for $\bar{\sigma}_s$ into (5-3), we find

$$\xi \mathrm{Re} = \frac{8}{s} \int_s \left(\frac{\partial W_x}{\partial N}\right)_{N=0} ds, \qquad (5\text{-}4)$$

where

$$W_x = \frac{w_x}{\bar{w}}, \quad \mathrm{Re} = \frac{\bar{w}d_e}{\nu}, \quad N = \frac{n}{d_e}.$$

If the change in velocity from zero at the wall to the value at the flow core were to take place in a thin layer at the wall (far thinner than the cross-sectional dimensions), then the flow conditions at the wall, i.e., $(\partial W_x/\partial N)_{N=0}$ would be the same at different points on the perimeter even for tubes of different shapes. Then, as (5-4) shows, owing to the utilization of d_e, we would obtain the same value of ξRe for tubes differing in shape. In actuality, however, in laminar flow W_x varies over the entire section, and the velocity profile depends essentially on the cross-sectional geometry. Thus despite the utilization of d_e, the value of ξRe will also depend on the shape and relationship of cross-sectional dimensions.[2]

If we know the velocity distribution in a tube of specified geometry, we can use (5-4) to calculate its resistance coefficient ξ (see §§5-2 and 5-3). Using the value found for ξ and (5-2a), we can easily find the pressure drop across a tube segment of length l:

$$\Delta p = \xi \frac{\rho\bar{w}^2}{2} \frac{l}{d_e}. \qquad (5\text{-}5)$$

5-2. STABILIZED FLOW IN CYLINDRICAL AND PRISMATIC TUBES

1. For flow in a *round tube*, Eq. (5-1) is conveniently written in cylindrical coordinates. Since the flow is symmetric about the x axis, the equation takes the form

$$\frac{1}{r}\cdot\frac{d}{dr}\left(r\frac{dw_x}{dr}\right)=-\frac{\Delta p}{\mu l}$$

where r is the running radius.

Integrating twice, we find the general solution:

$$w_x=-\frac{\Delta p}{4\mu l}r^2+c_1\ln r+c_2. \qquad (5\text{-}6)$$

The boundary conditions have the form

$$\text{for } r=0 \quad \frac{dw_x}{dr}=0;$$

$$\text{for } r=r_0 \quad w_x=0,$$

where r_0 is the inside radius of the tube.

Using these conditions, we find the constants:

$$c_1=0,\ c_2=\frac{\Delta p r_0^2}{4\mu l}.$$

Substituting in (5-6), we obtain the equation for the velocity distribution:

$$w_x=\frac{\Delta p}{4\mu l}(r_0^2-r^2). \qquad (5\text{-}7)$$

The mean fluid velocity over a section is

$$\bar{w}=\frac{1}{\pi r_0^2}\int_0^{r_0} w_x 2\pi r\,dr=\frac{\Delta p}{2r_0^2\mu l}\int_0^{r_0}(r_0^2-r^2)\,r\,dr=\frac{\Delta p r_0^2}{8\mu l}.$$

The maximum velocity is

$$w_{\text{макс}}=\frac{\Delta p r_0^2}{4\mu l}=2\bar{w}.$$

Equation (5-7) can be written as

$$w_x=2\bar{w}\left(1-\frac{r^2}{r_0^2}\right). \qquad (5\text{-}8)$$

or as

$$w_x=2\bar{w}\left[2\frac{r_0-r}{r_0}-\frac{(r_0-r)^2}{r_0^2}\right], \qquad (5\text{-}8a)$$

where $r_0 - r$ is the distance from the wall to the point considered.

Thus the fluid velocity for motion in a round tube is distributed parabolically (Fig. 5-1).

The volume flowrate of the fluid is

$$V = \pi r_0^2 \bar{w} = \frac{\pi r_0^4 \Delta p}{8\mu l}. \qquad (5\text{-}9)$$

This equation represents the Poiseuille law.

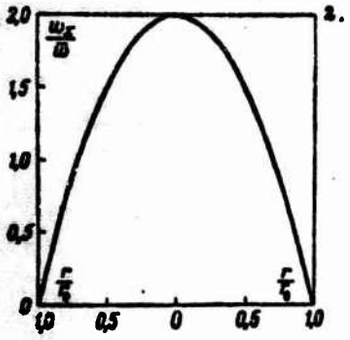

Fig. 5-1. Velocity profile in round tube with stabilized flow.

We use (5-4) and (5-8) to determine the friction-resistance coefficient:

$$\xi \mathrm{Re} = 64, \qquad (5\text{-}10)$$

where $\mathrm{Re} = \bar{w}d/\nu$.

The velocity distribution (5-8) and resistance law (5-10) have received good experimental confirmation.

The distribution of velocity in a *flat tube* (i.e., between parallel plates) of width $2r_0 = h$ can be found by solving (5-1) (without the second term on the left side) under appropriate boundary conditions. As a result we obtain

$$w_x = \frac{3}{2}\bar{w}\left(1 - \frac{y^2}{\ldots}\right) = 6\bar{w}\left[\frac{r_0 - y}{h} - \frac{(r_0 - y)^2}{h^2}\right], \qquad (5\text{-}11)$$

where y is the distance along the normal from the tube axis to the point under consideration.

Itis clear from (5-11) that the velocity on the axis of the flat tube is $w_{\text{макс}} = \frac{3}{2}\bar{w}$.

Using (5-4) and (5-11), we find that for a flat tube

$$\xi \mathrm{Re} = 96, \qquad (5\text{-}12)$$

where $\mathrm{Re} = \bar{w}d_э/\nu$, $d_э = 2h$.

3. For the velocity distribution in a *round annular tube* (i.e., in the region between two coaxial cylinders), the general solution of (5-6) is valid. Determining the constants of integration from the boundary conditions ($w_x = 0$ when $w = r_1$ and $r = r_2$), we obtain the velocity-distribution law:

$$w_x = -\frac{\Delta p}{4\mu l}\left[(r_2^2 - r_1^2)\frac{\ln\frac{r}{r_1}}{\ln\frac{r_2}{r_1}} - (r^2 - r_1^2)\right],$$

where r_1 and r_2 are the radii of the inner and outer cylinders.

From the last equation we find the radius corresponding to the maximum value of velocity:

$$r_0 = \sqrt{\frac{r_2^2 - r_1^2}{2\ln\frac{r_2}{r_1}}}.$$

The mean velocity over a section is

$$\bar{w} = \frac{\Delta p}{8\mu l}\left(r_2^2 + r_1^2 - \frac{r_2^2 - r_1^2}{\ln\frac{r_2}{r_1}}\right).$$

Thus the velocity distribution in an annular tube can also be represented as:

$$w_x = 2\bar{w}\,\frac{(r_2^2 - r^2)\ln\frac{r_1}{r_0} - (r_2^2 - r_1^2)\ln\frac{r}{r_0}}{r_2^2 - r_1^2 + (r_2^2 + r_1^2)\ln\frac{r_1}{r_0}}. \qquad (5\text{-}13)$$

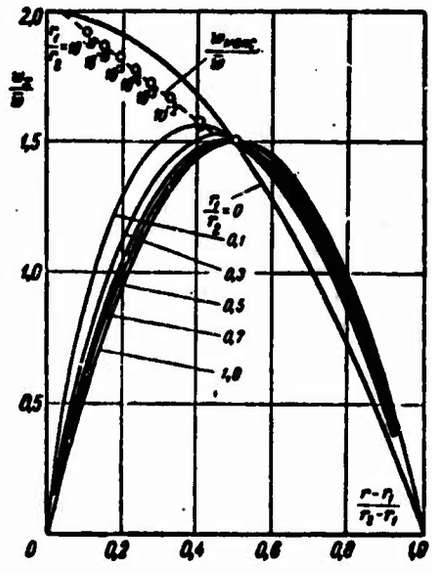

Fig. 5-2. Velocity profiles in annular tube with stabilized flow.

Figure 5-2 represents the dimensionless velocity $w_x/\bar{w}$ as a function of the dimensionless distance from the wall $r - r_1/r_2 - r_1$ for various values of r_1/r_2. As r_1/r_2 decreases, the velocity maximum shifts toward the inside wall of the tube. For values $0{,}1 < \frac{r_1}{r_2} < 1$ this shift is relatively slight. In Fig. 5-2, the dashed line shows the positions of the velocity maximums.

TABLE 5-1

Values of ξRe for Tubes of Annular, Elliptical, and Rectangular Cross Section

a Круглая кольцевая труба. r_1 и r_2 — радиусы внутреннего и наружного цилиндров	$\frac{r_1}{r_2}$	0,001	0,01	0,05	0,1	0,2	0,4	0,6	0,8	1,0	
	ξ Re	74,08	80,11	86,27	89,37	92,36	94,71	95,55	95,92	96,00	
b Эллиптическая труба. b_1 и b_2 — полуоси эллипса	$\frac{b_2}{b_1}$	0,1	0,2	0,3	0,4	0,5	0,6	0,7	0,8	0,9	1,0
	ξ Re	77,25	74,43	71,55	69,18	67,26	65,92	64,96	64,38	64,13	64,00
c Прямоугольная труба. b и h — длины сторон прямоугольника	$\frac{b}{h}$	1	1,25	1,5	2	2,28	3	4	5	10	∞
	ξ Re	56,90	57,47	58,82	62,14	64,00	65,35	72,90	76,29	84,61	96,00

a) Round annular tube, r_1 and r_2 are the radii of the inner and outer cylinders; b) elliptical tube, b_1 and b_2 are the semiaxes of the ellipse; c) rectangular, b and h are the lengths of the rectangle sides.

When r_1 drops to zero, corresponding to flow in a round tube, (5-13) reduces to (5-8). In the other limiting case in which $r_2 - r_1 \ll r$ (flow in a flat tube), (5-13) reduces to (5-11).

The friction-resistance coefficient for an annular tube is found from the relationship

$$\xi \mathrm{Re} = \frac{64\left(1-\frac{r_1}{r_2}\right)^2}{1+\left(\frac{r_1}{r_2}\right)^2+\frac{1-\left(\frac{r_1}{r_2}\right)^2}{\ln\frac{r_1}{r_2}}}, \qquad (5\text{-}14)$$

where $\mathrm{Re} = \bar{w} d_h/\nu$; $d_h = 2(r_2 - r_1)$.

Table 5-1 gives values of ξRe for an annular tube as a function of r_1/r_2.

4. The velocity distribution in a tube of *elliptical cross section* is described by the equation

$$w_x = 2\bar{w}\left(1-\frac{y^2}{b_1^2}-\frac{z^2}{b_2^2}\right), \qquad (5\text{-}15)$$

where b_1 and b_2 are the semimajor and semiminor axes of the ellipse.

TABLE 5-2

Equations for Velocity Profiles in Prismatic Tubes

1 Форма поперечного сечения	2 Уравнение для w_x
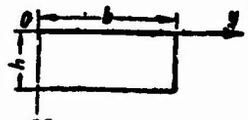 3 Прямоугольник	$w_x = \frac{16\Delta p}{\pi^4 l\mu} \sum_{m=1,3,5\ldots}^{\infty} \sum_{n=1,3,5\ldots}^{\infty} \frac{\sin\frac{m\pi y}{b} \sin\frac{n\pi z}{h}}{mn\left(\frac{m^2}{b^2}+\frac{n^2}{h^2}\right)}$ (5-16)
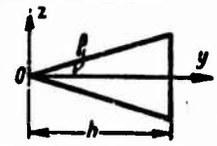 4 Равнобедренный треугольник	$w_x = 3\bar{w}\frac{(B+2)(z^2-y^2\operatorname{tg}^2\beta)}{h^2(B-2)\operatorname{tg}^2\beta}\left[\left(\frac{y}{h}\right)^{B-2}-1\right]$, (5-17) где $B=\sqrt{4+\frac{5}{2}\left(\frac{1}{\operatorname{tg}^2\beta}-1\right)}$
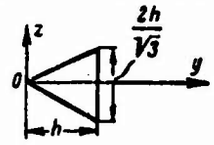 5 Равносторонний треугольник	$w_x = 45\bar{w}\left\{\left(\frac{y}{h}-1\right)\left[\left(\frac{z}{h}\right)^2-\frac{1}{3}\left(\frac{y}{h}\right)^2\right]\right\}$ (5-17a)
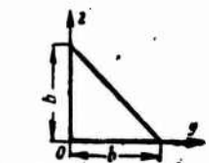 6 Прямоугольный равнобедренный треугольник	$w_x = \frac{16\Delta p b^2}{\pi^4 l\mu}\left[\sum_{m=1,3,5\ldots}^{\infty}\sum_{n=2,4,6\ldots}^{\infty}\frac{n\sin\frac{m\pi y}{b}\sin\frac{n\pi z}{b}}{m(n^2-m^2)(m^2+n^2)}+\right.$ $\left.+\sum_{m=2,4,6\ldots}^{\infty}\sum_{n=1,3,5\ldots}^{\infty}\frac{m\sin\frac{m\pi y}{b}\sin\frac{n\pi z}{b}}{n(m^2-n^2)(m^2+n^2)}\right]$ (5-18)
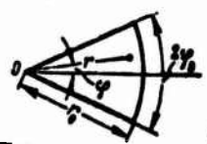 7 Сектор круга	$w_x = -\frac{\Delta p}{4l\mu}\left\{r^2\left(1-\frac{\cos 2\varphi}{\cos 2\varphi_0}\right)-\frac{16r_0^2(2\varphi_0)^2}{\pi^4}\times\right.$ $\left.\times\sum_{n=1,3,5\ldots}^{\infty}(-1)^{\frac{n+1}{2}}\left(\frac{r}{r_0}\right)^{\frac{n\pi}{2\varphi_0}}\frac{\cos\frac{n\pi}{2\varphi_0}\varphi}{n\left[n^2-\left(\frac{4\varphi_0}{\pi}\right)^2\right]}\right\}$ (5-19)

1) Cross-sectional shape; 2) equation for w_x; 3) rectangle; 4) isosceles triangle; 5) equilateral triangle; 6) isosceles right triangle; 7) sector of circle.

The velocity reaches its maximum on the tube axis (i.e., for $y = 0$ and $z = 0$); as for a round tube, this maximum is 2 times the mean velocity.

The friction-resistance coefficient is found from the relationship

$$\xi \mathrm{Re} = 8\left(\frac{d_e}{b_2}\right)^2\left[1+\left(\frac{b_2}{b_1}\right)^2\right].$$

Table 5-1 gives the values of ξRe as a function of the b_2/b_1.

5. Table 5-2 gives equations for the velocity profiles in *prismatic tubes* with cross section in the shape of a rectangle, triangle, and sector of a circle. As an example, Fig. 5-3 shows velocity profiles in a sector tube for various sector flare angles. As we might expect, as the angle decreases, the velocity maximum shifts toward the cylindrical wall.[3]

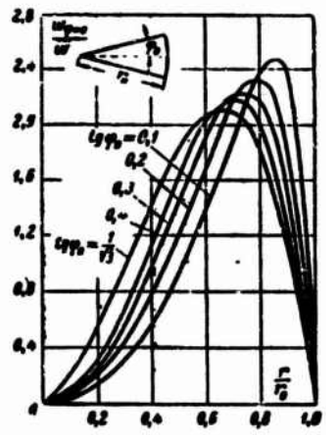

Fig. 5-3. Velocity profiles along central line of sector tube for various sector flare angles (stabilized flow).

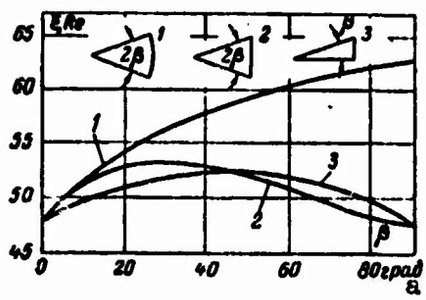

Fig. 5-4. Values of ξRe for tubes with cross section in form of sector of circle, isosceles triangle, and right triangle. a) deg.

Table 5-1 gives values of ξRe for tubes of rectangular cross section, calculated in terms of the equivalent diameter. For tubes with cross section in the form of isosceles triangles [9]

$$\xi \mathrm{Re} = \frac{48(1-\mathrm{tg}^2\beta)(B+2)}{(B-2)(\mathrm{tg}\beta+\sqrt{1+\mathrm{tg}^2\beta})^4}, \qquad (5\text{-}20)$$

where β is half the vertex angle of the isosceles triangle, and B is the perimeter, found from the equation given in Table 5-2.

For example, for $\beta = 30°$ (equilateral triangle), $\xi Re = 53.33$. For $\beta = 45°$ (isosceles right triangle), Eq. (5-20) gives an indefinite result; expanding it, we see that here $\xi Re = 52.71$.

Figure 5-4 shows ξRe as a function of flare angle for tubes with cross sections in the form of a sector of a circle, isosceles triangle, or right triangle.

It is noteworthy that for tubes of various profiles ξRe varies within fairly narrow limits: roughly from 48 to 96 or from 0.75 to 1.5 times the value of ξRe for round tubes.

5-3. STABILIZED FLOW IN BANK OF ROUND CYLINDERS IN LONGITUDINAL FLOW

Flow along a bank of circular cylinders (tubes or bars) is encountered in many heat-exchange systems. The cylinders are ordinarily positioned in the bank at the corners of equilateral triangles or at the corners of a square (Fig. 5-5). If we assume that the bank consists of many cylinders, while the cylinder diameters and positions are identical, we need only consider the flow in an element *ABCD* of this system.

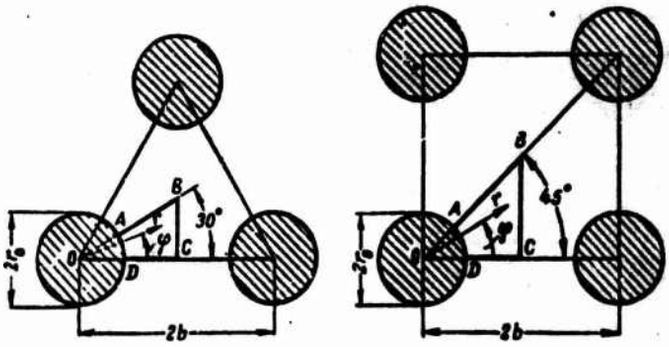

Fig. 5-5. The problem of longitudinal flow past a bank of circular cylinders. a) Cylinders located at corners of equilateral triangle; b) cylinders located at corners of square.

The two-dimensional velocity field in the systems shown in Fig. 5-5 is described by the equation

$$\frac{\partial^2 w_x}{\partial r^2} + \frac{1}{r}\cdot\frac{\partial w_x}{\partial r} + \frac{1}{r^2}\cdot\frac{\partial^2 w_x}{\partial \varphi^2} = -\frac{\Delta p}{\mu l}.$$

The boundary conditions have the following form:

$w_x = 0$ for $r = r_0$; $\frac{\partial w_x}{\partial \varphi} = 0$ for $\varphi = 0$ and $\varphi = 30°$ (Fig. 5-5,a) or $\varphi = 45°$ (Fig. 5-5,b); $\frac{\partial w_x}{\partial n} = 0$ for $r = \frac{b}{\cos\varphi}$ (n is the normal to plane BC).

An approximate solution of this problem has been obtained by Sparrow and Loeffler [10]. The velocity distribution is described by the following equations:

TABLE 5-3

Values of Constants δ_j and ε_j in Equation for Velocity Profiles with Longitudinal Flow Past Banks of Circular Cylinders[1]

1 Цилиндры расположены по углам равностороннего треугольника

$\frac{b}{r_0}$	δ_1	δ_2	δ_3	δ_4	δ_5	δ_6
1,0	—0,0305	0,0053	—0,0003	—0,0002	0,0000	→
1,01	—0,0319	0,0052	—0,0001	—0,0002	0,0000	→
1,02	—0,0332	0,0051	0,0000	—0,0001	0,0000	→
1,03	—0,0345	0,0049	0,0002	—0,0001	0,0000	→
1,04	—0,0357	0,0046	0,0002	—0,0001	0 0000	→
1,05	—0,0368	0,0043	0,0003	—0,0001	0,0000	→
1,10	—0,0416	0,0028	0,0004	0,0000	→	→
1,20	—0,0469	0,0007	0,0002	0,0000	→	→
1,50	—0,0502	—0,0007	0,0000	→	→	→
2,00	—0,0505	—0,0008	0,0000	→	→	→
4,00	—0,0505	—0,0008	0,0000	→	→	→

2 Цилиндры расположены по углам квадрата

$\frac{b}{r_0}$	ε_1	ε_2	ε_3	ε_4	ε_5	ε_6
1,05	—0,0904	0,0073	0,0032	0,0002	—0,0001	0,0000
1,10	—0,0987	0,0036	0,0029	0,0005	0,0000	→
1,20	—0,1104	—0,0024	—0,0015	0,0003	0,0001	0,0000
1,50	—0,1225	—0,0091	—0,0002	0,0000	→	→
2,00	—0,1250	—0,0105	—0,0006	0,0000	→	→
4,00	—0,1253	—0,0106	—0,0006	0,0000	→	→

[1]The arrows in the table indicate that zeros follow everywhere.

1) Cylinders located at corners of equilateral triangle; 2) cylinders located at corners of square.

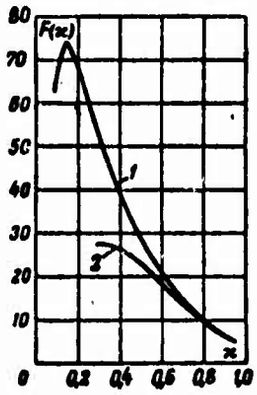

Fig. 5-6. Function $F(\kappa)$ for bank of cylinders in longitudinal flow. 1) Cylinders located at angles of equilateral triangle; 2) cylinders located at corners of square.

for cylinders located at the corners of an equilateral triangle,

$$w_z=\frac{\Delta p b^2}{l\mu}\left\{\frac{\sqrt{3}}{\pi}\ln\frac{r}{r_0}-\frac{1}{4}\left[\left(\frac{r}{b}\right)^2-\left(\frac{r_0}{b}\right)^2\right]+\right.$$
$$\left.+\sum_{j=1}^{m}\frac{\delta_j}{6j}\left(\frac{r}{b}\right)^{6j}\left[1-\left(\frac{r_0}{r}\right)^{12j}\right]\cos 6j\varphi\right\}; \qquad (5\text{-}21)$$

for cylinders located at the corners of a square,

$$w_z=\frac{\Delta p b^2}{l\mu}\left\{\frac{2}{\pi}\ln\frac{r}{r_0}-\frac{1}{4}\left[\left(\frac{r}{b}\right)^2-\left(\frac{r_0}{b}\right)^2\right]+\right.$$
$$\left.+\sum_{j=1}^{m}\frac{\varepsilon_j}{4j}\left(\frac{r}{b}\right)^{4j}\left[1-\left(\frac{r_0}{r}\right)^{8j}\right]\cos 4j\varphi\right\}. \qquad (5\text{-}22)$$

In these equations, δ_j and ε_j are constants depending on b/r_0. Their values are given in Table 5-3.

The friction-resistance coefficient ξ is found from the relationship

$$\xi\mathrm{Re}\frac{1-\varkappa}{4\varkappa}=\frac{1}{4}\xi\mathrm{Re}_d=F\left(\frac{b}{r_0}\right). \qquad (5\text{-}23)$$

In (5-23) we have: $\mathrm{Re}=\frac{\bar{w}d_e}{\nu}$; $\mathrm{Re}_d=\frac{\bar{w}d}{\nu}$; d_e is the equivalent diameter, calculated from the wetted perimeter of the bank flow section; $d = 2r_0$ is the cylinder diameter; $\varkappa$ is the ratio of the bank flow-section area to the area of the entire bank (i.e., the ratio of the area of quadrangle *ABCD* to the area of triangle *OBC*);

$$\varkappa=1-\frac{\varphi_0}{\left(\frac{b}{r_0}\right)^2\operatorname{tg}\varphi_0}.$$

With cylinders located at the corners of a triangle $\varphi_0=\pi/6$, while with cylinders at corners of a square, $\varphi_0=\pi/4$.

Figure 5-6 shows F as a function of b/r_0 or, what is the same thing, as a function of $\varkappa$, for the two types of cylinder configuration considered. For a bank of specified geometry we first find $\varkappa$ and then use Fig. 5-6 to find $F(\varkappa)$; we finally calculate ξ from (5-23).

Figure 5-7 shows the distribution of the tangential stress at the cylinder surface as a function of the angle for various values of b/r_0. For b/r_0 close to unity, the tangential-stress distribution is extremely nonuniform. At $b/r_0 \geq 1.5$ for cylinders at the corners of a triangle, however, and for $b/r_0 \geq 2$ for cylinders at the corners of a square, the tangential stress is nearly uniformly distributed over the circumference. Thus for sufficiently wide banks (b/r_0 greater than the values indicated), the velocity can be assumed to be a function of the radius alone.

An approximate determination of the flow in such banks can be made by the method first proposed by Leybenson [11]. If we replace triangle *OBC* (see Fig. 5-5a, b) by a sector of a circle with radius r_0 so that the sector and triangle are of equal area, we can use the general solution (5-6) for a round annular tube. Determining the constants c_1 and c_2 from the boundary conditions $w_z|_{r=r_0}=0$ and $\frac{dw_z}{dr}\Big|_{r=r_0}=0$, we obtain the equations for the velocity profiles. These equations have the same form as (5-21) and (5-22), but without the last terms containing the series. We obtain the following expression for the resistance coefficient:

$$\xi \mathrm{Re}=\frac{64\left[\left(\frac{r_\phi}{r_0}\right)^2-1\right]^2}{4\left(\frac{r_\phi}{r_0}\right)^4\ln\frac{r_\phi}{r_0}-3\left(\frac{r_\phi}{r_0}\right)^4+4\left(\frac{r_\phi}{r_0}\right)^2-1}. \qquad (5\text{-}24)$$

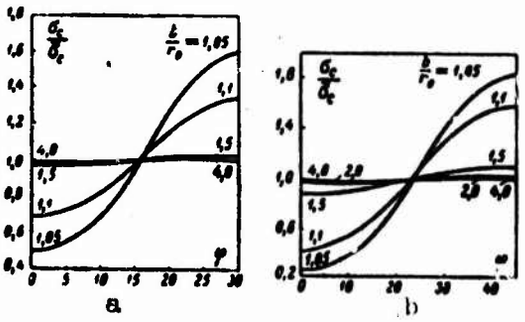

Fig. 5-7. Distribution of tangential stress at wall over cylinder circumference with cylinders located at angles of equilateral triangle (a) and at corners of square (b).

With the cylinders located at the corners of an equilateral triangle

$$r_\phi=\left(\frac{2\sqrt{3}}{\pi}\right)^{1/2}b;$$

$$d_0=2r_0\left[\frac{6}{\sqrt{3}\pi}\left(\frac{b}{r_0}\right)^2-1\right].$$

With the cylinders located at the corners of a square[4] with sides $2b_1$ and $2b_2$,

$$r_\phi=2\sqrt{\frac{b_1b_2}{\pi}},$$

$$d_0=2r_0\left(\frac{4}{\pi}\frac{b_1b_2}{r_0^2}-1\right).$$

5-4. HYDRODYNAMIC INITIAL SEGMENT

If a certain arbitrary velocity distribution is specified at the entrance section of a tube, then as we move away from the entrance, under the action of the viscosity forces, the velocity profile will tend to take on a shape corresponding to stabilized flow. Thus the latter can be treated as a limiting state to which the flow changes in the initial segment at a sufficient distance from the entrance. As is proven in the dynamics of a viscous fluid, a flow with steady velocity profile corresponds to minimum energy losses to friction.

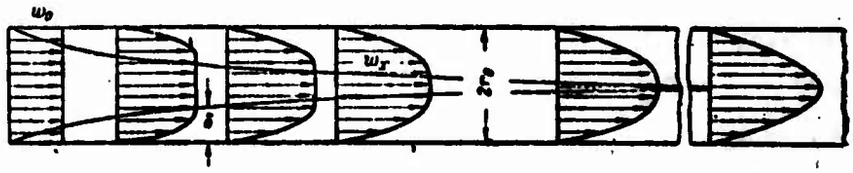

Fig. 5-8. Development of velocity profile in initial segment of round tube.

If the fluid is delivered to the tube from a sufficiently large reservoir, and the tube edges are well rounded, then the velocity distribution in the entrance section will be uniform (Fig. 5-8). Owing to the action of friction forces and adhesion of the fluid to the wall, a layer of retarded fluid will appear in the flow near the wall; this is called the dynamic boundary layer. For sufficiently large Reynolds numbers, near the entrance this layer will be thin as compared with the tube radius. In the direction of the normal to the wall, the fluid velocity in the boundary layer will vary from zero at the wall to the velocity at the flow core. Since the core does not experience the retarding effect of the friction forces, the velocity distribution will remain uniform here. As we move away from the entrance, the boundary layer becomes thicker, the flow-core section contracts, and the core velocity increases (since the flowrate through any tube section is constant). This process continues until the boundary layer developing at the walls fills the entire tube cross section, at a sufficient distance from the entrance. In the section where this occurs, formation of the velocity profile is finished, and the profile will no longer vary with length as we move away from the entrance (for isothermal flow of an incompressible fluid).

The separation of the flow into two regions, the dynamic boundary layer within which the action of the friction forces is concentrated, and the flow core where the friction forces are negligibly small, permits us to construct an approximate method for determining the flow in the initial segment. There are other methods for solving this problem that do not require introduction of the boundary-layer concept.

Let us consider flow in the initial segment of a *round tube* with a uniform velocity distribution at the entrance. Such flow has been determined on the basis of the boundary-layer

notion by Shiller [12], with later improvements by other investigators [13, 14]. We let $\delta(x)$ represent the thickness of the boundary layer and, following [12], we assume that the fluid velocity in the core is constant over the section:

$$w_x = w_1(x),$$

while the velocity in the boundary layer is distributed parabolically:

$$\frac{w_x}{w_1} = 2\frac{y}{\delta} - \frac{y^2}{\delta^2} = 2\left(\frac{r_0 - r}{\delta}\right) - \left(\frac{r_0 - r}{\delta}\right)^2.$$

As a consequence, for $\delta = r_0$, the velocity profile in the initial segment will go over to the velocity profile for stabilized flow.

We write these equations in dimensionless form:

$$\left.\begin{aligned} W_x &= W_1(X) \text{ (for } 0 \leqslant R \leqslant 1-\tilde{\delta}); \\ W_x &= W_1\left[2\left(\frac{1-R}{\tilde{\delta}}\right) - \left(\frac{1-R}{\tilde{\delta}}\right)^2\right] \text{ (for } 1-\tilde{\delta} \leqslant R \leqslant 1), \end{aligned}\right\} \qquad (5\text{-}25)$$

where $W_x = \frac{w_x}{w_0}$, $W_1 = \frac{w_1}{w_0}$, $R = \frac{r}{r_0}$, $\tilde{\delta} = \frac{\delta}{r_0}$, w_0 is the constant velocity of the fluid at the entrance.

The relationship between W_1 and $\tilde{\delta}$ can be established from the condition requiring that the flowrate be constant:

$$2\pi \int_0^{r_0-\delta} w_1 r\, dr + 2\pi \int_{r_0-\delta}^{r_0} w_x r\, dr = w_0 \pi r_0^2.$$

Substituting the expression for w_x into this equation and integrating, we find

$$W_1 = \frac{6}{6 - 4\tilde{\delta} + \tilde{\delta}^2}. \qquad (5\text{-}26)$$

To find the way in which δ and the mean pressure p over the section depend on x, we require two more equations. One of them can be the conservation of momentum equation (2-45). For the case under consideration, it is written as

$$\rho \frac{d}{dx} \int_0^{r_0} w_x^2 r\, dr + \frac{r_0^2}{2} \cdot \frac{dp}{dx} + r_0 \sigma_0 = 0,$$

where

$$\sigma_0 = -\mu \left(\frac{\partial w_x}{\partial r}\right)_{r=r_0} = 2\frac{\mu w_1}{\delta},$$

or, in dimensionless form

$$\frac{d}{dX} \int_0^1 W_x^2 R\, dR - \frac{1}{4} \cdot \frac{d}{dX}\left(\frac{p_0 - p}{\frac{1}{2}\rho w_0^2}\right) + 8\frac{W_1}{\tilde{\delta}} = 0, \qquad (5\text{-}27)$$

where

$$X=\frac{1}{\mathrm{Re}}\cdot\frac{x}{d},\quad \mathrm{Re}=\frac{w_0 d}{\nu},\quad d=2r_0;$$

here p_0 is the pressure at the tube entrance section; the quantity X is called the reduced distance to the entrance.

As the second equation, Shiller used the Bernoulli equation, written for the flow core; he simultaneously assumed that the pressure in the given core section equals the mean pressure in the same section of the tube. This assumption is quite justified for small x, but becomes less and less accurate as x increases, owing to the increased thickness of the boundary layer, i.e., the region of viscous dissociation. As a result, the Shiller solution becomes inaccurate when we move far enough away from the entrance. Thus, following [14], in place of the Bernoulli equation we shall use the approximate equation for the mechanical energy balance of the entire flow, also taking into account the energy loss caused by viscous dissipation. We write this equation for the flow segment from the entrance section to a certain section located a distance x from the entrance. On the assumption that $w^2_x \gg w^2_r$, and that all derivatives of the velocity can be neglected except for $\partial w_x/\partial r$, we obtain

$$\frac{1}{2}\rho\int_0^{r_0} w_x^3\, 2\pi r\,dr-\frac{1}{2}\rho w_0^3\pi r_0^2+(p-p_0)w_0\pi r_0^2+$$

$$+\mu\int_0^x dx\int_0^{r_0}\left(\frac{\partial w_x}{\partial r}\right)^2 2\pi r\,dr=0,$$

or in dimensionless form

$$\int_0^1 W_x^3 R\,dR-\frac{1}{2}-\frac{1}{2}\left(\frac{p_0-p}{\frac{1}{2}\rho w_0^2}\right)+8\int_0^X dX\int_0^1\left(\frac{\partial W_x}{\partial R}\right)^2 R\,dR=0. \qquad (5\text{-}28)$$

Solving (5-25)-(5-28) simultaneously, we can find the way in which $\tilde{\delta}$ depends on X and $\frac{p_0-p}{\frac{1}{2}\rho w_0^2}$ depends on $\tilde{\delta}$. Omitting the intermediate manipulations, we give the final result:

$$\left[336\tilde{\delta}-26\ln(1-\tilde{\delta})+318\ln(2-\tilde{\delta})+148\ln K(\tilde{\delta})+\frac{27(52\tilde{\delta}+3)}{K(\tilde{\delta})}-\right.$$

$$\left.-\frac{2064}{\sqrt{2}}\operatorname{arctg}\left(\frac{\tilde{\delta}-2}{\sqrt{2}}\right)\right]_0^{\tilde{\delta}}=1680X, \qquad (5\text{-}29)$$

where $K(\tilde{\delta})=6-4\tilde{\delta}+\tilde{\delta}^2$,

$$\frac{p_0-p}{\frac{1}{2}\rho w_0^2}=\frac{1}{420}\left[3816\ln(2-\tilde{\delta})-416\ln(1-\tilde{\delta})-1700\ln K(\tilde{\delta})-\right.$$

$$-\frac{3(\tilde{\delta}+382)}{K(\tilde{\delta})}+\frac{324(108-\tilde{\delta})}{K^2(\tilde{\delta})}+\frac{1979}{\sqrt{2}}\operatorname{arctg}\left(\frac{2-\tilde{\delta}}{\sqrt{2}}\right)\Bigg]_0^{\tilde{\delta}}+\frac{24(15-14\tilde{\delta}+4\tilde{\delta}^2)}{5K^2(\tilde{\delta})}-2 \quad (5\text{-}30)$$

Using (5-29) to find the way in which $\tilde{\delta}$ depends on X (this relationship is shown in Fig. 5-9), it is not difficult for us to determine the remaining flow characteristics in the initial segment. From (5-25) and (5-26), we find the velocity distribution $W_x=W_x(R, X)$, while (5-30) yields the variation in pressure $\frac{p_0-p}{\frac{1}{2}\rho w_0^2}$ as a function of X. For sufficiently large X, the solution found goes over asymptotically to the solution for stabilized flow. The computational results are in good agreement with experiment.[5]

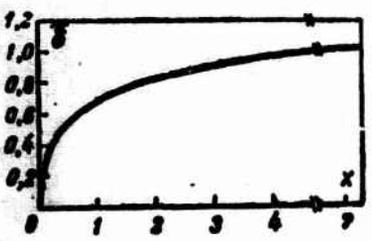

Fig. 5-9. Boundary-layer thickness as function of X.

Numerous investigators have solved the problem of fluid motion in the initial segment of a round tube by direct integration of the equation of motion, under various simplifications introduced for the purpose of linearization. It was precisely in this way that the problem was first solved by Bussinesk, whose results, refined by Atkinson and Gol'dshteyn [15], are in good agreement with experiment at a sufficient distance from the entrance but are inaccurate near the entrance section. This problem has also been considered by Targ [16], Langhaar [17], and others [18, 19]. Their results more properly describe the variation in velocity with tube length.

TABLE 5-4

Values of Constants β_n in (5-31)

n	1	2	3	4	5	6
β_n	5,136	8,417	11,62	14,80	17,96	21,12
n	7	8	9	10	11	12
β_n	24,27	27,42	30,57	33,72	36,86	40,01

Targ obtained the following equation for the distribution of the longitudinal velocity component and the pressure drop in the initial segment for a uniform velocity distribution at the entrance:

$$W_x=2(1-R^2)-4\sum_{n=1}^{\infty}\frac{1}{\beta_n^2}\left[1-\frac{J_0(\beta_n R)}{J_0(\beta_n)}\right]\exp(-4\beta_n^2 X), \quad (5\text{-}31)$$

TABLE 5-5

Values of Φ as a function of X for Initial Segment of Round Tube

$X=\frac{1}{Re}\cdot\frac{x}{d}$	$\Phi(X)$
0,000205	20,0
0,00083	11,0
0,001805	8,0
0,003575	6,0
0,00535	5,0
0,00838	4,0
0,0137	3,0
0,0179	2,5
0,0237	2,0
0,0341	1,4
0,0449	1,0
0,0620	0,6
0,0760	0,4

$$\frac{p_0-p}{\frac{1}{2}\rho w_0^2}=64X+\frac{2}{3}-8\sum_{n=1}^{\infty}\frac{1}{\beta_n^2}\exp(-4\beta_n^2X), \quad (5\text{-}32)$$

where J_0 is a Bessel function of order zero; $\beta_n (n=1, 2, 3...)$ are the successive roots of a Bessel function of second order, J_2. Their values are given in Table 5-4.

The Langhaar equation for the velocity profile under the same conditions has the form

$$W_x=\frac{I_0[\Phi(X)]-I_0[R\Phi(X)]}{I_0[\Phi(X)]}. \quad (5\text{-}33)$$

where I_0 and I_2 are modified Bessel functions; Φ is a certain function of X whose values are given in Table 5-5. The pressure variation can be computed by substituting (5-33) into (5-28).

Figure 5-10 shows the velocity distribution over the tube section for various values of X, while Fig. 5-11 gives the variation in axial velocity with length.[6] As we can see, the uniform velocity profile at the entrance becomes parabolic as we move toward greater X.

The distance from the tube entrance at which the influence of the initial velocity distribution ceases to influence fluid motion is called the length of the hydrodynamic initial segment, $l_{n.g}$. For isothermal flow, the reduced length of the hydrodynamic initial segment can be found as the value of $X=\frac{1}{Re}\frac{l_{n.r}}{d}=B$ for which the axial velocity differs by no more than 1% from the axial velocity for stabilized flow. Thus the relative length of the hydrodynamic initial segment is

$$\frac{l_{n.r}}{d}=B\,Re, \quad (5\text{-}34)$$

where B is a constant.

Calculations carried out with (5-31) give a value $B = 0.04$; (5-33) yields $B = 0.0575$. The value closest to the actual figure is apparently $B = 0.065$, calculated on the basis of the Bussinesk solution, which is in good agreement with experiment for large reduced lengths. It follows from (5-34) that the length of the dynamic initial segment may be considerable; for example, when $Re = 2000$, $l_{n.g} = 130d$.

Table 5-6 shows the results of a determination of the pressure variation in the initial segment of a tube. For $X \leq 0.0075$, the Shiller method was used, while for $X \geq 0.0075$, the Bussinesk method was used (at $X = 0.0075$, there is roughly a 2% difference between the results computed by these two methods). It is conven-

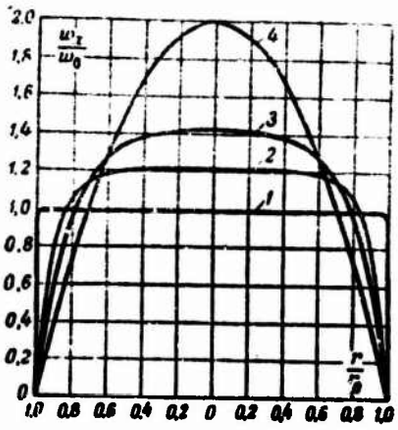

Fig. 5-10. Velocity distribution in initial segment of round tube for various values of X. 1) $X = 0$ (entrance section); 2) $X = 0.00083$; 3) $X = 0.00357$; 4) $X \to \infty$ (parabolic profile).

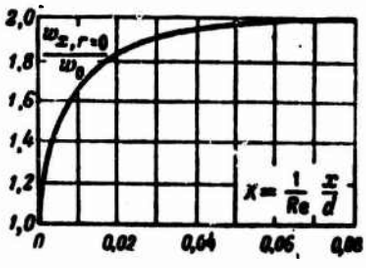

Fig. 5-11. Variation of axial velocity in initial segment of round tube.

TABLE 5-6

Values of $\frac{p_0 - p}{\frac{1}{2}\rho w_0^2}$ in Initial Segment of Round Tube

$X = \frac{1}{Re}\cdot\frac{x}{d}$	$\frac{p_0-p}{\frac{1}{2}\rho w_0^2}$	$X = \frac{1}{Re}\cdot\frac{x}{d}$	$\frac{p_0-p}{\frac{1}{2}\rho w_0^2}$
0	0	0,0075	1,36
0,0005	0,32	0,0100	1,63
0,0010	0,46	0,0125	1,88
0,0015	0,56	0,0150	2,10
0,0020	0,65	0,0200	2,51
0,0025	0,73	0,0250	2,88
0,0035	0,87	0,0300	3,24
0,0045	1,00	0,0350	3,59
0,0055	1,11	0,0400	3,93
0,0065	1,22	0,0450	4,26
0,0075	1,33	0,0500	4,59
		0,0550	4,92

ient to represent the pressure variation in the initial segment in terms of the local and mean resistance coefficients:

$$dp = -\zeta \frac{\rho \bar{w}^2}{2} \cdot \frac{dx}{d},$$

$$p_0 - p = \bar{\zeta} \frac{\rho \bar{w}^2}{2} \cdot \frac{x}{d}, \qquad (5\text{-}35)$$

where $\bar{w} = w_0$ in the case under consideration.

Using (5-32), for example, we find:

$$\zeta \mathrm{Re} = 64 + 32 \sum_{n=1}^{\infty} \exp(-4\beta_n^2 X). \qquad (5\text{-}36)$$

Computational results with good experimental confirmation have shown [13] that at values $X \leq 0.001$, the following simple relationships are valid:

$$\left.\begin{aligned} \zeta \mathrm{Re} &= 6{,}87 \left(\frac{1}{\mathrm{Re}} \cdot \frac{x}{d}\right)^{-1/2}, \\ \bar{\zeta} \mathrm{Re} &= 13{,}74 \left(\frac{1}{\mathrm{Re}} \cdot \frac{x}{d}\right)^{-1/2}. \end{aligned}\right\} \qquad (5\text{-}37)$$

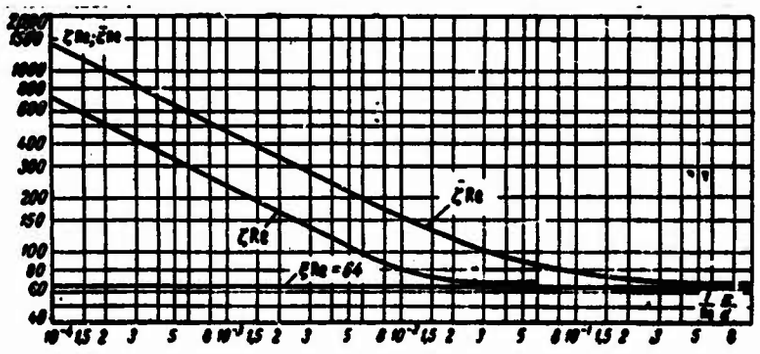

Fig. 5-12. Local and mean resistance coefficients in initial segment of round tube.

Figure 5-12 shows $\bar{\zeta}\mathrm{Re}$ and $\zeta\mathrm{Re}$ as functions of X. When $X \to 0$, $\zeta\mathrm{Re}$ and $\bar{\zeta}\mathrm{Re}$ approach a constant value corresponding to stabilized flow. To within 1%, ζ takes on a constant value at a distance $x = l_{n.g}$ from the entrance, while $\bar{\zeta}$ takes on a constant value at a far greater distance equaling $\sim 40 l_{n.g}$.

For $x \geq l_{n.r}$, it is convenient to write (5-35) as

$$\frac{p_0 - p}{\frac{1}{2}\rho \bar{w}^2} = \bar{\zeta}_{x = l_{n.r}} \frac{l_{n.r}}{d} + \zeta \frac{x - l_{n.r}}{d},$$

where $\zeta = 64/\mathrm{Re}$ is the friction-resistance coefficient, constant over the length, for $x > l_{n.g}$. Since

$$\overline{\zeta}_{x=l_{n.r}}\mathrm{Re} = \mathrm{const} \text{ and } \frac{1}{\mathrm{Re}}\cdot\frac{l_{n.r}}{d} = \mathrm{const},$$

then

$$p_0 - p = \left(\xi\frac{x}{d} + k\right)\frac{\rho\bar{w}^2}{2}, \qquad (5\text{-}38)$$

where k is a constant. According to the data of various authors, k ranges from 1.040 to 1.159. A value $k = 1.12$ is apparently closest to the true figure.

We note that in the general case (for $x < l_{n.g}$), the local friction-resistance coefficient ξ will also vary with the length. Here $\xi < \zeta$, and only at $x = 0$ and $x > l_{n.g}$ will these coefficients coincide.

2. The flow in the initial segment of a *flat tube* (i.e., between parallel plates) has been studied by Leybenzon [22], and later by Schlichting [15], Targ [16], and others [23]. Targ obtained the following equations for the velocity distribution and pressure drop in the initial segment for a uniform velocity distribution at the entrance:

$$W_x = \frac{3}{2}(1 - Y^2) - 2\sum_{n=1}^{\infty}\frac{1}{\gamma_n}\left[1 - \frac{\cos(\gamma_n Y)}{\cos\gamma_n}\right]\exp(-16\gamma_n^2 X), \qquad (5\text{-}39)$$

$$\frac{p_0 - p}{\frac{1}{2}\rho w_0^2} = 96X + \frac{2}{5} - 4\sum_{n=1}^{\infty}\frac{1}{\gamma_n^2}\exp(-16\gamma_n^2 X), \qquad (5\text{-}40)$$

where

$$W_x = \frac{w_x}{w_0},\quad Y = \frac{y}{r_0},\quad X = \frac{1}{\mathrm{Re}}\cdot\frac{x}{d_e},$$

and $\mathrm{Re} = \frac{w_0 d_e}{\nu}$; $d_e = 2h$ is the equivalent diameter; $h = 2r_0$ is the tube width; γ_n are the successive roots of the equation $\tan x = x$.

The relative length of initial segment for a flat tube, calculated with the aid of (5-39), equals

$$\frac{l_{n.r}}{d_e} = 0{,}0113\,\mathrm{Re}. \qquad (5\text{-}41)$$

The value of the constant in (5-41) is very close to the value obtained by Schlichting (0.01). For a flat tube, if we use d_e, the value of k in (5-38) lies in the 0.601–0.626 range.

3. The flow in the initial segment of an *annular tube* has been considered elsewhere [24, 25, 26] for a uniform velocity distribution at the entrance. According to the data of [25], the reduced length of the initial segment will have the following values, depending on r_1/r_2:

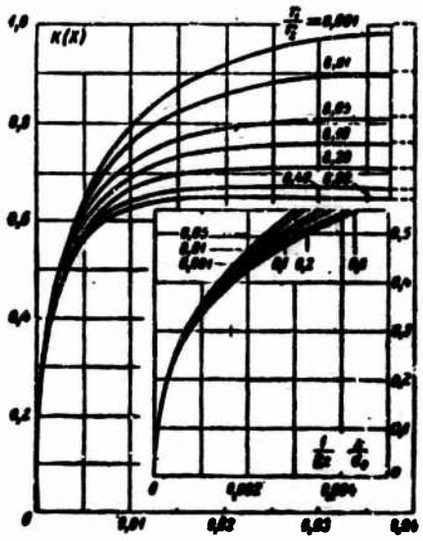

Fig. 5-13. Curves for $K(X)$ at various values of r_1/r_2. The dashed lines on the right represent $K(\infty)=k$.

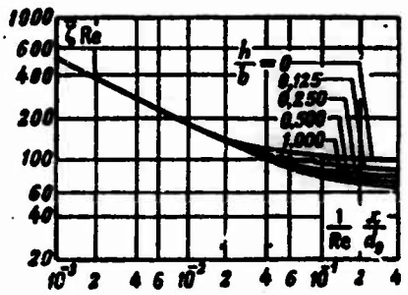

Fig. 5-14. Resistance coefficient ζ for tubes of rectangular cross section.

r_1/r_2	0,02	0,05	0,10	0,25	0,50	1,0
$\frac{1}{Re}\cdot\frac{l_{in.r}}{d_g}$	0,0205	0,0174	0,0145	0,0117	0,0105	0,0100

Here $Re=w_0d_g/\nu$, $d_g=2(r_2-r_1)$.

The pressure drop in the initial segment of an annular tube can be calculated from the equation proposed by Sparrow and Lin [26]:

$$\frac{p_0-p}{\frac{1}{2}\rho w_0^2}=\xi\frac{x}{d_g}+K(X), \qquad (5\text{-}42)$$

where ξ is the friction-resistance coefficient for stabilized flow (see Table 5-1); $K(X)$ is a function allowing for the change

in flow kinetic energy and for the additional energy expended on friction in the initial segment as compared with a stabilized flow. Figure 5-13 shows values of $K(X)$. When $X = 0$, $K(X) = 0$, while when $X \to \infty$ (for $x > l_{n.g}$ in practice), $K(X)$ approaches a constant value that depends solely on r_1/r_2. In the latter case, $K(\infty) = k$, and (5-42) reduces to (5-38).

4. The flow in the initial segment of a *rectangular tube* has been investigated by Frankl' and Baklanov [27], as well as by Han [28]. The reduced lengths of the initial segment are shown for tubes with various ratios of sides in Table 5-7 [28]. These lengths are determined, as usual, from the condition requiring that the velocity on the tube axis at $x = l_{n.g}$ differ by no more than 1% from the velocity on the axis for the fully developed flow.

TABLE 5-7

Reduced Length of Initial Segment and Value of Constant k for Tubes of Rectangular Cross Section

$\frac{a}{b}$	$\frac{1}{Re}\frac{l_{n.r}}{d_h}$	k
1.0	0.0752	2.0
0.75	0.0735	2.00
0.50	0.0660	1.80
0.25	0.0427	1.36
0.125	0.0227	1.10
0	0.0099	0.85

The pressure drop in the initial segment of a tube of rectangular cross section can be calculated from (5-35), and for $x > l_{n.g}$ from (5-38) (if we replace d by d_e in the equations). Figure 5-14 shows the resistance coefficient $\bar{\zeta}$ in (5-35) for tubes of rectangular cross section, while the constant k in (5-38) is given in Table 5-7. The Reynolds number in Table 5-7 and Fig. 5-14 was calculated on the basis of the equivalent diameter.

5-5. CRITICAL REYNOLDS NUMBER. INFLUENCE OF ROUGHNESS

1. As we know, there are two basic forms of motion for a viscous fluid, laminar and turbulent. Laminar flow becomes turbulent at a certain value of the Reynolds number, called the critical value.

$$Re_{кр} = \left(\frac{\bar{w}d_e}{\nu}\right)_{кр}.$$

If for a given flow of fluid in a tube the Reynolds number $Re < Re_{kr}$, the flow will be laminar; if $Re > Re_{kr}$, it will be turbulent. The critical Reynolds number depends essentially on the tube entrance conditions and the conditions in the fluid flow ahead of the entrance. The smaller the disturbances in the fluid flow entering the tube and in the entrance section (for example, owing to flow separation from the walls when flowing past sharp edges, the higher the critical Reynolds number. Thus special measures aimed at reducing disturbances have made it possible to obtain laminar flow in a tube for Reynolds numbers of up to 40,000. It is apparently possible to obtain still higher values of critical Reynolds number by carefully eliminating disturbances. In practice, however, it is more important to know the lower bound for the critical Reynolds number than the upper bound. The existence of such a bound has been established in numerous experimental studies. Hence-

forth, when we speak of the critical Reynolds number Re_{kr}, we shall mean the lower bound. If $Re < Re_{kr}$, then any strong disturbance at the tube entrance will be damped at a sufficient distance from the entrance, and the flow will remain laminar. If $Re > Re_{kr}$, however, then under ordinary conditions (i.e., for the disturbances observed in practice), the flow will become turbulent.

Leaving aside the question of laminar-flow stability and the processes involved in the transition to turbulent flow, we shall only give certain data on the critical Reynolds numbers. Numerous experimental investigations have shown that for isothermal flow in round tubes, $Re_{kr} \approx 2300$. For tubes whose cross section is not round, the value of Re_{kr} calculated on the basis of the equivalent diameter will have roughly the same value as for round tubes. Thus for annular tubes, $Re_{kr} = 2000\text{-}2800$; according to data in certain older studies, Re_{kr} depends on r_1/r_2, increasing as the ratio decreases [12]. For rectangular tubes, including flat ducts, $Re_{kr} \approx 2000\text{-}2300$. For tubes of triangular cross section, if the angles are not too acute (about 45° or more), $Re_{kr} \approx 2000$.

Fig. 5-15. Laminar- and turbulent-flow regions in triangular tube with acute angle. 1) Turbulent region; 2) laminar region.

In tubes whose cross section includes narrow corner zones, both laminar and turbulent flows may exist simultaneously. This is quite clear from Fig. 5-15, which shows the results of visual observations on flow in a triangular tube with a vertex angle of 11.5° for the isosceles-triangle section [29]. It turned out that when a smoke probe was moved along the centerline from the vertex to the base, the stream of smoke was first completely quiescent, i.e., the flow was laminar. Next stability was lost (waves traveled along the smoke stream; their amplitude increased with distance from the vertex); turbulent flow finally set in (the smoke stream became blurred a short distance from the probe). The curve of Fig. 5-15 was obtained by such observations at various Reynolds numbers and fixed values of x/h (points on the graph) at which

stability loss first occurred. Below this curve there is a region of laminar flow; above there is a region of transition and developed turbulent flow. The Reynolds number at which the flow remains laminar over the entire cross section turns out to be considerably below the critical Reynolds number for round tubes. As Re increases, the laminar region contracts, but even at quite high Re, it does not vanish completely; the flow near the angle remains laminar

The critical Reynolds numbers given here are precisely the values such that a sufficient distance from the tube entrance a deviation from laminar-flow laws takes place owing to the first appearance of turbulence. If the entrance does not produce flow separation (the flow enters, for example, through a nozzle with smooth outline), near the tube entrance section the flow may remain laminar even for values $Re >> Re_{kr}$. The segment over which laminar flow is preserved decreases as Re increases. Beyond the laminar-flow section there is a region of transition from laminar to turbulent flow, and beyond this a region of developed turbulent flow.

Under heat-exchange conditions, fluid flow may be significantly nonisothermal. Owing to the relationship between the physical properties of the fluid and the temperature, the velocity distribution may differ from that accompanying isothermal flow. Here, the critical Reynolds numbers may also have values differing from those indicated above (see, for example, §16-1).

Data on critical Reynolds numbers for flows in bent tubes and for nonstationary flows in tubes are given in §5-6 and 5-7.

2. Theoretical calculations for laminar flows are carried out on the assumption that the tube is smooth. Real tubes are rough, however. We thus must face the question of the degree to which computational results for smooth tubes can apply to actual, i.e., rough, tubes. This question has been answered by the well-known experiments of Nikuradze, in which a study was made of the hydraulic resistance of tubes with artificial roughness (sand). The relative roughness of tubes (ratio of projection height to tube radius) varies widely from 1/15 to 1/507. Experiments have shown that in laminar flow, all rough tubes possess the same hydraulic resistance as smooth tubes. It also turns out that the critical Reynolds number does not depend on the roughness. These experimental facts can be explained as follows. The fluid in the depressions is practically stationary, while under the conditions considered, the fluid flows past the projections without separation and, consequently, without the formation of vortices. The reason is that the Reynolds number for the projections (calculated from the projection height and the velocity of the flow incident on the projections) proves below the value at which flow separation occurs. Since with unseparated flow at the projections, the pressure resistance is very low or even zero, the resistance of rough tubes is the same as that of smooth tubes. Since no vortices appear, the critical Reynolds numbers also prove identical.

Naturally, as the relative roughness grows, a value will be reached, called the critical value, at which the foregoing conditions cease to be satisfied. On the assumption that vortex formation begins at a Reynolds number of 50 for a projection, Shiller obtained the following expression for the critical value of relative roughness:

$$\left(\frac{e}{r_0}\right)_{кр} \approx \frac{5}{\sqrt{Re}}.$$

Thus if the relative tube roughness is less than the critical value, the results obtained for smooth tubes can be used for rough-tube flow calculations.

5-6. FLOW IN BENT TUBES

Everything that has been said above is valid only for fluids flowing in straight tubes. In practice, we often use tubes bent along a spiral (coils). Several turns of such a coil are shown in Fig. 5-16a. A centrifugal force acts on each particle of a fluid moving in a curved tube. This force will be greater the greater the velocity of the particle. Thus greater centrifugal forces will act on fluid particles located at the center of the tube than on particles near the wall where the flow velocity is small. The centrifugal forces cause the fluid particles at the center of the tube to move away from the center of curvature of the tube, while the particles at the wall, forced out by the particles, coming from the center of the tube, move toward the center of curvature. As a consequence, a transverse circulation appears in the tube (Fig. 5-16b, c); the particles participating in the circulation also move along the curved axis of the tube. Thus the resultant motion can be imagined to take place along two flattened spirals with different directions of rotation, filling the tube cross section. The velocity profile will not be axisymmetric for such a flow; the maximum of the longitudinal velocity component will be shifted away from the center of curvature. Figure 5-16d shows velocity profiles in the cross section of a coil for $D/d = 40$ and $Re = 4000$;[7] the measurements were reported in [30]. The profile has well-defined asymmetry in the AB plane (Fig. 5-16b); in the CD plane, the velocity in the core is nearly constant, while it drops rapidly near the walls.

As theoretical and experimental investigations have shown, the factor determining the influence of curvature in laminar flow is the parameter $K = Re\sqrt{\frac{d}{D}}$, introduced by Dean. Here $Re = \bar{w}d/\nu$, $D = 2R$, d is the tube diameter, R is the coil radius of curvature.

For values $K < 13.5$, the tube curvature still has no influence on the nature of fluid flow. In this case, the streams of fluid move parallel to the curved tube axis; there is no transverse circulation in the flow, and the velocity distribution and resistance law in bent tubes turn out to be the same as in straight tubes. The limiting Re number at which such flow is still maintained will evidently equal

$$Re_{кр} = 13{,}5\sqrt{\frac{D}{d}}.$$

[7] 7/94

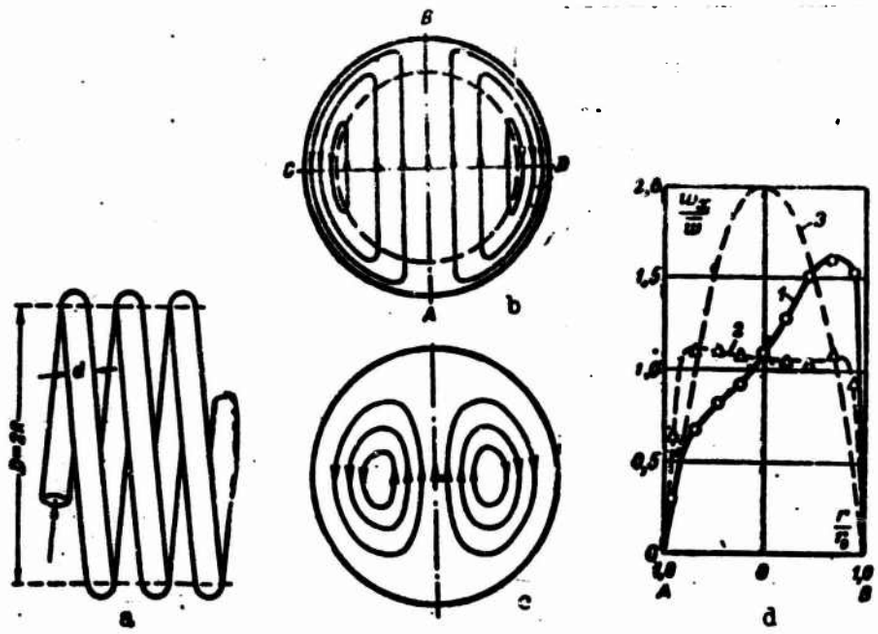

Fig. 5-16. Flow in bent tube. a) Coil diagram; b) transverse circulation for large values of K; c) the same, for small K; d) velocity profiles in AB plane (1) and CD plane (2), and Poiseuille profile (3).

For values $K > 13.5$, although the flow will still be laminar, transverse circulation will appear. Thus the velocity distribution and resistance law will change.

Dean has made a theoretical study of fully developed flow in round bent tubes (coils) [31]. His results, however, obtained by a perturbation method, are valid only for small K ($K < 36$). Figure 5-16c shows the pattern of secondary flows for this case. This problem has been studied by other authors for large K. A very complete analysis was recently given by Mori and Nakayama [30]. As in certain earlier studies, in [30] it is assumed that the flow in the tube consists of a core within which viscosity forces can be neglected, and a thin boundary layer. The solutions for the velocity field in each of these regions are joined by the boundary conditions. The calculations are carried out by successive approximations. Figure 5-16b shows the pattern of secondary flows for large values of K. In second approximation, the following equation is obtained for the resistance coefficient in a bent tube:

$$\frac{\xi}{\xi_{np}} = \frac{0,1080K^{1/2}}{1-3,253K^{-1/2}}. \qquad (5-43)$$

Here $\xi = -\frac{\partial p}{\partial x}\frac{d}{\frac{1}{2}\rho\bar{w}^2}$; p is the pressure at a given point in the flow;[6] x is the longitudinal coordinate, coinciding with the curved axis of the tube (the calculations are carried out on the assumption that $\frac{\partial p}{\partial x} = \frac{\partial p}{R\partial\varphi}$, where φ is the longitudinal angular coordinate);

[6]/94

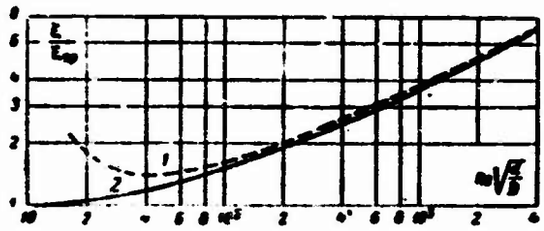

Fig. 5-17. Relative resistance coefficient for coils of round tubing on basis of data from theoretical calculation (1) and experiment (2).

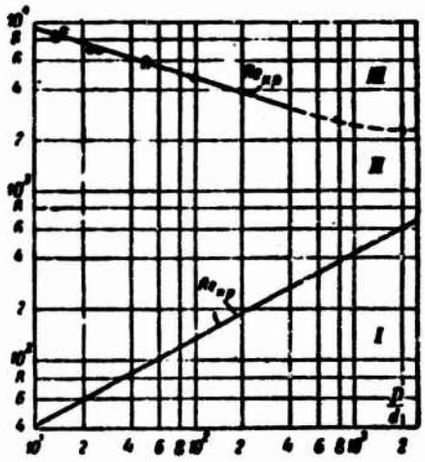

Fig. 5-18. Re_{kr} and Re_{pr} as functions of D/d for coils.

ξ_{pr} is the resistance coefficient for a straight tube at the same Re value as in the bent tube.

The results of experimental investigations into hydraulic resistance of coils of round tubing in the $13.5 \leq K \leq 5000$ range are well described by the empirical equation proposed by Ito:

$$\frac{\xi}{\xi_{pr}} = \frac{21.5K}{(1.56 + \log K)^{5.75}}. \qquad (5\text{-}44)$$

Figure 5-17 shows the ratio ξ/ξ_{pr} as a function of the parameter K (curve 2). When $K \leq 13.5$, the ratio $\xi/\xi_{pr} = 1$, while with a further increase in K, the ratio rises continuously. Thus ξ is larger the smaller the radius of curvature of the tube. The relationship between ξ and Re will be different than for a straight tube: while $\xi_{pr} \sim Re^{-1}$, $\xi \sim Re^{-n}$, where $n < 1$. The theoretical equation (5-43) (curve 1) is in good agreement with experimental data for $K > 100$; for smaller values of K, it gives incorrect results. Naturally, Eqs. (5-43) and (5-44) are valie only for values of $Re < Re_{cr}$.

The critical Reynolds number for coils depends on the coil radius of curvature, with the number increasing as the radius decreases. Figure 5-18 shows experimental data on $Re_{kr} = f(D/d)$. They show that in bent tubes when D/d is not large, Re_{kr} will be significantly greater than for straight tubes. This is apparently connected with the stabilizing influence of the centrifugal force and the transverse circulation that it excites for the flow at the wall.

The experimental data shown in Fig. 5-18 can be represented by the empirical equation [32]

$$Re_{kp} = 1500\left(\frac{R}{d}\right)^{-0.3}, \qquad (5\text{-}45)$$

which is suitable for values $3 \leqslant \frac{R}{d} \leqslant 200$, where $R = \frac{1}{2}D$.

Figure 5-18 also shows Re_{pr} as a function of D/d. The curves for Re_{pr} and Re_{kr} divide the entire flow region into three characteristics zones: the first (I) corresponds to laminar flow without transverse circulation, the second (II) to laminar flow with transverse circulation, and the third (III) to turbulent flow. We also note that the transition from laminar to turbulent flow is accompanied by a monotonic decrease in the resistance coefficient for bent tubes.

5-7. NONSTATIONARY STABILIZED FLOW IN TUBES

In this section, we confine the discussion to stabilized nonstationary flows, which are realized in practice in long tubes.

Let there be confined flow of a fluid in a long cylindrical or prismatic tube. Neglecting the entrance and exit effects, we assume that at any point in the flow and at any time, the vector representing the fluid velocity will be directed along the x axis of the tube. Consequently, $w_y = w_z = 0$ and $\partial w_x/\partial x = 0$.

Then the first equation of System (4-1) takes the form

$$\frac{\partial w_x}{\partial \tau} - \nu \nabla^2 w_x = -\frac{1}{\rho}\frac{\partial p}{\partial x}, \qquad (5\text{-}46)$$

while the other two equations yield $\frac{\partial p}{\partial y} = \frac{\partial p}{\partial z} = 0$.

Since $w_x = w_x(y, z, \tau)$ while $p = p(x, \tau)$, it then follows from (5-46) that the pressure gradient is independent of the coordinates, and can just be a specified function of the time: $-\frac{\partial p}{\partial x} = f(\tau)$.

Thus the equation of motion for nonstationary stabilized flow will have the form

$$\frac{\partial w_x}{\partial \tau} = \nu \nabla^2 w_x + \frac{1}{\rho} f(\tau). \qquad (5\text{-}47)$$

Integration of this equation requires that the following be

a) the initial condition in the form of a function specifying the velocity distribution at the initial time, $w_x = \bar{w}_0(y, z)$ for $\tau = 0$;

b) boundary conditions, in a form requiring that the velocity w_x equal zero at the inside surface of the tube, and symmetry conditions for the types of flows to be considered later;

c) the law governing the change in pressure gradient with time, i.e., the function $f(\tau)$ for $\tau \geq 0$;

The problem of nonstationary fluid motion in a round cylindrical tube was solved in 1882 in a fairly general formulation (for any initial conditions and a specified law governing the variation in pressure gradient with time) by the well-known Russian mechanics scholar I.S. Gromek [33]. This problem was later studied with application to various specific conditions by numerous authors [34-40].

Equation (5-47) has the same form as the heat-conduction equation for a nonstationary temperature field in a solid with internal heat sources whose strengths vary in time. If the geometric form of the flow in the tube and the geometric shape of the body are identical, if the laws governing the time variation of the pressure gradient and of the internal-source strength of the body coincide, and if the initial and boundary conditions are identical for both problems, then the solution to the heat-conduction problem can also be treated as the solution to the corresponding problem of fluid motion in a tube. Since solutions are known for several appropriate problems in heat-conduction theory [41], these solutions can be used directly or after some modification (for example, if the initial conditions do not match) to determine nonstationary flows in tubes.

Here we give solutions for certain problems of nonstationary fluid flow in long tubes, since they subsequently will be used in analyzing nonstationary heat-exchange processes.

1. *Flow in a flat tube with step variation in pressure gradient.* In a flat tube of width $2r_0$, let there be stationary stabilized flow of a fluid with a mean velocity over a section of $\bar{w}_1 = -\frac{r_0^2}{3\mu}\left(\frac{\partial p}{\partial x}\right)_1$, where $-\left(\frac{\partial p}{\partial x}\right)_1$ is the pressure gradient, which is constant in time. At a certain time taken as the origin ($\tau = 0$), the pressure gradient changes instantaneously (i.e., in a step) and takes on another constant value $-\left(\frac{\partial p}{\partial x}\right)_2$. After a certain time has elapsed (when $\tau \to \infty$), a new stationary regime is established in the tube; it is characterized by a mean velocity $\bar{w}_2 = -\frac{r_0^2}{3\mu}\times\left(\frac{\partial p}{\partial x}\right)_2$.

Under these conditions, the nonstationary velocity distribution during the transient is represented by the following equation [36, 37]:

$$\frac{w_x}{\bar{w}_2} = \frac{3}{2}(1 - Y^2) - 6\left(1 - \frac{\bar{w}_1}{\bar{w}_2}\right)\sum_{i=0}^{\infty}\frac{(-1)^i}{E_i^3}\cos(E_i Y)\exp(-E_i^2 Zh), \qquad (5\text{-}48)$$

where $Y = y/r_0$ is the dimensionless coordinate of the point, measured from the tube axis; $E_i=(i+1/2)\pi$; $Zh=\nu t/r_0^2$ is the Zhukovskiy [Joukowsky] number.

Equation (5-48) holds for all cases of step variation in the pressure gradient, except for the cases $\bar{\omega}_1 = 0$ (i.e., the initial pressure gradient equals zero and the fluid is initially stationary) and $\bar{\omega}_2 = 0$ (the pressure gradient drops to zero). In the latter case, if we multiply (5-48) by $\bar{\omega}_2/\bar{\omega}_1$ and let $\bar{\omega}_2 = 0$, the equation reduces to the form

$$\frac{\bar{w}_2}{\bar{w}_1}=6\sum_{i=0}^{\infty}\frac{(-1)^i}{E_i^2}\cos(E_iY)\exp(-E_i^2Zh). \qquad (5\text{-}48a)$$

Figure 5-19 shows velocity profiles for various values of the Zh number, computed with the aid of (5-48a).

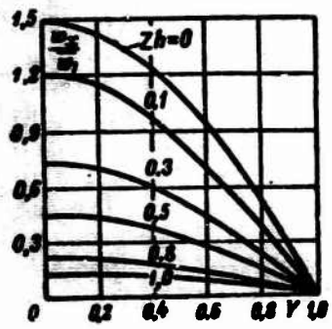

Fig. 5-19. Velocity profile for deceleration of flow in flat tube.

We find the mean velocity over the section by integrating (5-48) with respect to Y between 0 and 1:

$$\frac{\bar{w}}{\bar{w}_2}=1+6\left(\frac{\bar{w}_1}{\bar{w}_2}-1\right)\sum_{i=0}^{\infty}\frac{1}{E_i^4}\exp(-E_i^2Zh), \qquad (5\text{-}49)$$

or in more convenient form,

$$\frac{\bar{w}-\bar{w}_2}{\bar{w}_1-\bar{w}_2}=6\sum_{i=0}^{\infty}\frac{1}{E_i^4}\exp(-E_i^2Zh). \qquad (5\text{-}49a)$$

Using (5-49a), we can evaluate the time τ_s required to establish a new stationary state after a step variation in the pressure gradient. If we determine τ_s fromthe condition requiring that the change in mean velocity $\bar{\omega}_1 - \bar{w}$ be 95% of the total change $\bar{\omega}_1 - \bar{\omega}_2$, i.e., if we let

$$\frac{\bar{w}-\bar{w}_2}{\bar{w}_1-\bar{w}_2}=0{,}05=6\sum_{i=0}^{\infty}\frac{1}{E_i^4}\exp(-E_i^2Zh_s),$$

and find Zh_s from this, we then obtain $Zh_s=\frac{\nu\tau_s}{r_0^2}=1{,}21$. For example, for water at room temperature, in a tube 6.36 mm wide, it takes $\tau_s \approx 12$ s to reach the stationary state. For air under the same conditions, τ_s is less by a factor of nearly 15, since the kinematic viscosity coefficient for air is so much greater than for water.

It is interesting to see how the tangential stress at the wall changes for an unsteady flow (σ_s) as compared with a steady flow

($\sigma_{s.s}$) for exactly the same mean velocity. For this purpose, we compute the ratio

$$\frac{\sigma_c}{\sigma_{cs}} = \frac{\sigma_c r_0}{3\mu\bar{w}},$$

where $\sigma_c = -\mu\left(\frac{\partial w_x}{\partial y}\right)_{y=r_0}$; $\sigma_{cs} = 3\frac{\mu\bar{w}}{r_0}$; $\bar{w}$ is the instantaneous value of mean velocity.

Using (5-48), we find

$$\frac{\sigma_c}{\sigma_{cs}} = \frac{1 - 2\left(1 - \frac{\bar{w}_1}{\bar{w}_2}\right)\sum_{l=0}^{\infty}\frac{1}{E_l^2}\exp(-E_l^2 Zh)}{1 - 6\left(1 - \frac{\bar{w}_1}{\bar{w}_2}\right)\sum_{l=0}^{\infty}\frac{1}{E_l^4}\exp(-E_l^2 Zh)}. \qquad (5\text{-}50)$$

Figure 5-20 shows the way in which $\sigma_s/\sigma_{s.s}$ depends on Zh for various pressure-gradient ratios $\left(\frac{\Delta p}{\Delta x}\right)_2 / \left(\frac{\Delta p}{\Delta x}\right)_1$, or what is the same thing, for various $\bar{w}_2/\bar{w}_1$.

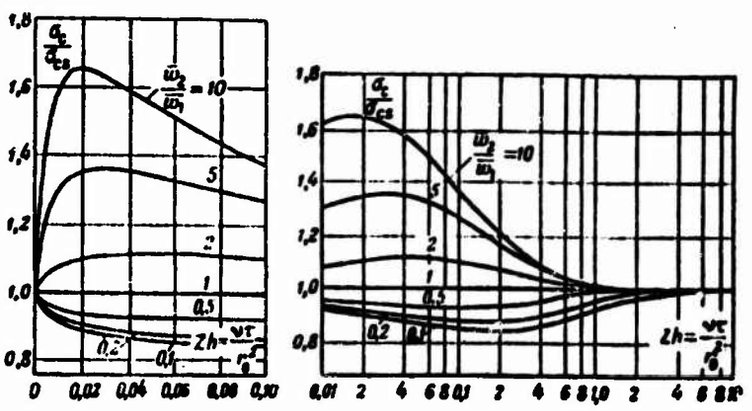

Fig. 20. Ratio $\sigma_s/\sigma_{s.s}$ as a function of time for unsteady flow in a flat tube.

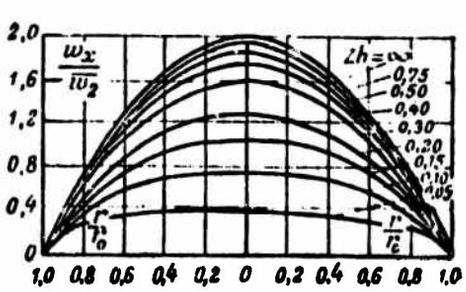

Fig. 5-21. Velocity profiles for acceleration of a flow in a round tube from $\bar{w}_1 = 0$ to $\bar{w}_2$.

For flows with acceleration ($\bar{w}_2 > \bar{w}_1$), the ratio σ_c/σ_{c0} first rises rapidly as Zh increases, passes through a maximum, and then drops to the initial constant value of unity. For decelerated flows ($\bar{w}_2 < \bar{w}_1$), we find the reverse pattern, although it is not as pronounced. This behavior of σ_c/σ_{c0} is explained by the fact that at low Zh, the velocity gradient at the wall changes more rapidly than the mean flow velocity, while the opposite situation prevails for high values of the number.

2. ***Flow in a round tube under step variation in pressure gradient.*** Stationary stabilized flow in a round tube with mean velocity $\bar{w}_1 = -\frac{r_0^2}{8\mu}\left(\frac{\partial p}{\partial x}\right)_1$ is disturbed owing to a step change in pressure gradient from $(\partial p/\partial x)_1$ to the value $(\partial p/\partial x)_2$. After a certain time, a new stationary regime is established in the tube; it is characterized by a mean velocity

$$\bar{w}_2 = -\frac{r_0^2}{8\mu}\left(\frac{\partial p}{\partial x}\right)_2.$$

The solution obtained for this problem by Gromek [33] leads to the following expression for the velocity distribution during the transient:

$$\frac{w_x}{\bar{w}_2} = 2(1-R^2) - 16\left(1 - \frac{\bar{w}_1}{\bar{w}_2}\right)\sum_{i=1}^{\infty}\frac{J_0(\lambda_i R)}{\lambda_i^3 J_1(\lambda_i)}\exp(-\lambda_i^2 \mathrm{Zh}), \qquad (5\text{-}51)$$

where the λ_i are the roots of a zero-order Bessel function J_0; $R = r/r_0$; $\mathrm{Zh} = \nu\tau/r_0^2$; r_0 is the tube radius; J_1 is a first-order Bessel function.

Equation (5-51) is valid both for flow acceleration and deceleration, including the cases $\bar{w}_1 = 0$ and $\bar{w}_2 = 0$. It can also be written in a form resembling (5-48a).

Figure 5-21 shows velocity profiles at different times; they are found from Eq. (5-51) for the case in which the fluid is stationary at the initial instant ($\bar{w}_1 = 0$), and then accelerates under the action of an abruptly appearing pressure gradient $(\partial p/\partial x)_2$. It is characteristic that during the initial period of acceleration, the velocity has identical values over almost the entire tube cross section, and the influence of friction becomes noticeable only near the wall. It is only after a certain time has elapsed that the influence of friction extends all the way to the center of the tube. As the time increases, the velocity profile goes over asymptocally to a parabolic Poiseuille profile.

Multiplying (5-51) by $2RdR$ and integrating between 0 and 1, we obtain an expression for themean velocity over the section:

$$\frac{\bar{w}}{\bar{w}_2} = 1 + 32\left(\frac{\bar{w}_1}{\bar{w}_2} - 1\right)\sum_{i=1}^{\infty}\frac{1}{\lambda_i^4}\exp(-\lambda_i^2 \mathrm{Zh}). \qquad (5\text{-}52)$$

The tangential stress at the wall is

$$\sigma_c = -\mu\left(\frac{\partial w_x}{\partial r}\right)_{r=r_0} = \frac{4\mu\bar{\bar{w}}_2}{r_0}\left[1-4\left(1-\frac{\bar{\bar{w}}_1}{\bar{\bar{w}}_2}\right)\sum_{i=1}^{\infty}\frac{1}{\lambda_i^2}\exp(-\lambda_i^2 Zh)\right]. \quad (5\text{-}53)$$

3. *Pulsating flow of fluid in flat tube.* Let there be pulsating flow of a fluid in a flat tube owing to sinusoidal oscillations superposed on the stationary pressure gradient. Thus the instantaneous pressure gradient will be the following periodic time function:

$$\frac{\partial p}{\partial x} = \left(\frac{dp}{dx}\right)_*\left(1+\frac{\gamma}{2}\cos\omega\tau\right), \quad (5\text{-}54)$$

where $\left(\frac{dp}{dx}\right)_* = -3\,\frac{\mu\bar{\bar{w}}}{r_0^2}$ is the stationary component of the pressure gradient; $\bar{\bar{w}}$ is the flow velocity averaged over time and over the section; $2r_0$ is the tube width; $\gamma/2$ is the dimensionless amplitude of pressure oscillations; ω is the oscillation frequency. The oscillation period will obviously equal $\tau_0 = 2\pi/\omega$.

As before, the flow is assumed to be stabilized, i.e., the velocity w_x is independent of the coordinate x.

Solution of this problem [40] leads to the following equation for the velocity distribution over the section and over time:

$$\frac{w_x}{\bar{\bar{w}}} = \frac{3}{2}[(1-Y^2)+\gamma U]. \quad (5\text{-}55)$$

The first term on the right side, $\left[\frac{3}{2}(1-Y^2)\right]$, is the stationary component of the velocity; the second, $\left(\frac{3}{2}\gamma U\right)$, is the nonstationary, i.e., pulsating component. We obtain the following expression for U:

$$U = \frac{\sin\omega\tau}{2M^2} + \frac{1}{2M^2(A^2+B^2)}[(A\cos MY\,\mathrm{ch}\,MY - B\sin MY\,\mathrm{sh}\,MY)\cos\omega\tau -$$
$$-(B\cos MY\,\mathrm{ch}\,MY + A\sin MY\,\mathrm{sh}\,MY)\sin\omega\tau], \quad (5\text{-}56)$$

where $A = \sin M\cdot\mathrm{sh}\,M$; $B = \cos M\cdot\mathrm{ch}\,M$; $M = \left(\frac{\omega r_0^2}{2\nu}\right)^{1/2}$; $Y = \frac{r}{r_0}$.

The independent variable $\omega\tau$ can be represented in terms of the Zhukovskiy number: $\omega\tau = 2M^2Zh$, where $Zh = \nu\tau/r_0^2$.

Figure 5-22a, b, c, d show the distribution of velocity U over the tube section for various values of $\omega\tau$ and M. The value of U varies periodically as $\omega\tau$ varies from 0 to 360°. The graphs show curves just for $\omega\tau < 180°$, since by symmetry $U(\omega\tau+\pi) = -U(\omega\tau)$. For $M = 0.1$, the frequency is so small that the profiles of the pulsating velocity component are quasistationary, i.e., for each value of $\omega\tau$ the velocity profiles will be the same as for stationary flow with the same instantaneous value of pressure gradient. As M increases, the profiles of the pulsating velocity component become ever less parabolic, while the amplitude of the velocity oscillations decreases. Thus for $M = 5$, the amplitude is less than 1/20 of the amplitude at $M = 0.1$.

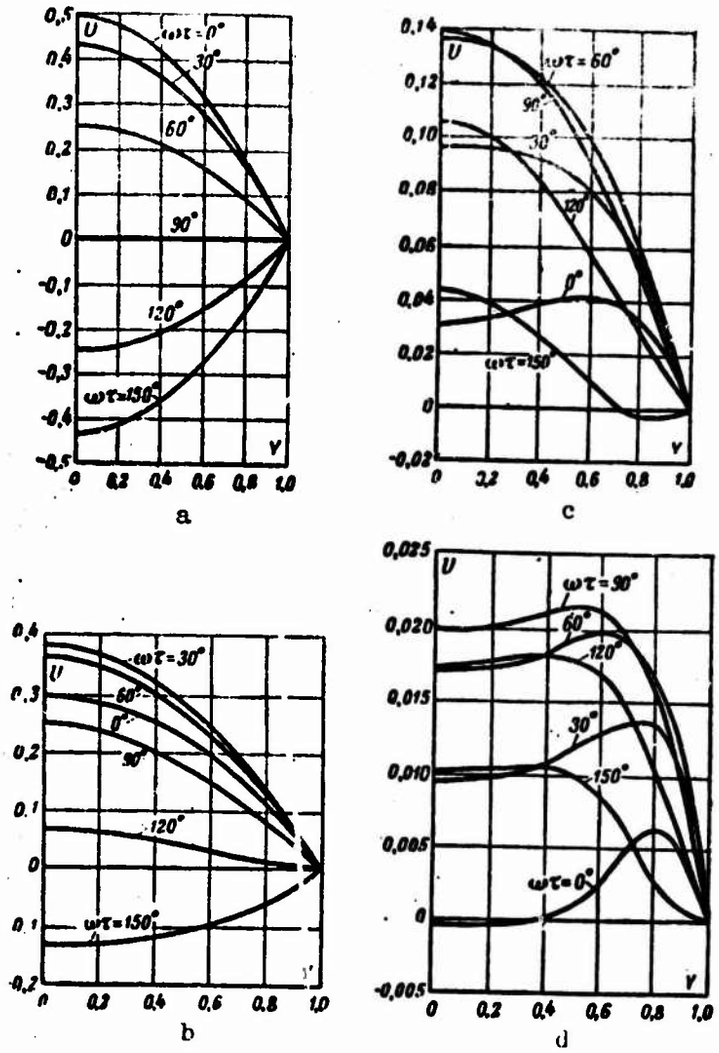

Fig. 5-52. Distribution of pulsating velocity component over tube section for various values of ωτ. a) $M = 0.1$; b) $M = 1$; c) $M = 2$; d) $M = 5$.

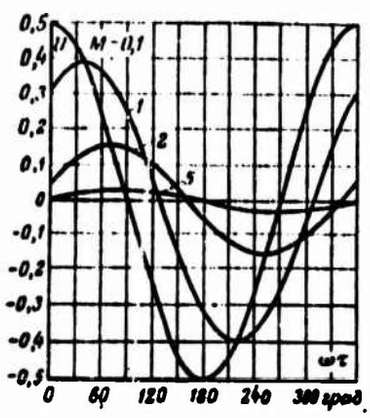

Fig. 5-23. Pulsating velocity component averaged over section for various values of M. 1) deg.

We find the mean flow velocity over the section by integrating (5-55) with respect to Y between 0 and 1:

$$\frac{\bar{w}}{\bar{w}} = 1 + \gamma \bar{U}, \tag{5-57}$$

where

$$\bar{U} = \frac{3 \sin \omega\tau}{4M^2} + \frac{3}{16M^2(A^2+B^2)}[(\mathrm{sh}\,2M - \sin 2M)\cos\omega\tau - (\mathrm{sh}\,2M + \sin 2M)\sin\omega\tau]. \tag{5-58}$$

Figure 5-23 shows $\bar{U}$ as a function of $\omega\tau$ for various values of M. When $M = 0.1$, the mean pulsating velocity over the section will follow the pressure gradient. As M increases, the maximum of $\bar{U}$ will shift more and more with respect to the pressure-gradient peak, and at the same time the amplitude of the velocity oscillations will decrease.

The critical Reynolds number for pulsating flow, calculated from the velocity $\bar{w}$ averaged over time and over the section will be less than for stationary flow. Thus, for example, measurement results [42] yield the following values of critical Reynolds number for pulsating flow in a round tube:

ω, Hz	0	5	10	15	20
$Re_{кр} = \frac{\bar{w}d}{\nu}$	2310	1730	1610	1550	1510

These results are understandable if we remember that at certain times, when the instantaneous value of mean velocity $\bar{w}$ passes through a maximum, the number $\frac{\bar{w}d}{\nu} > \frac{\bar{w}d}{\nu}$, so that in actuality the transition to turbulent flow occurs at a higher Reynolds number, equaling $\bar{w}d/\nu$. During the rest of the cycle (until the new $\bar{w}$ peak), the turbulence appearing evidently cannot be damped.

Manuscript Page No.

Footnotes

58 [1]This is true only for isothermal flow in straight tubes with arbitrary cross section that does not change along the tube axis.

60 [2]For turbulent flow at large values of Re, the change in velocity basically occurs within a thin layer at the wall. Thus if we use d_e as the characteristic dimension, the resistance law will be roughly the same for tubes differing in shape. A large difference in resistance laws is often observed, however, for individual geometric forms with turbulent flow.

66 [3]It is sometimes stated that for laminar flow in prismatic tubes, as in turbulent flow, there is transverse circulation in the corners. Actually, there is no circulation for laminar flow. This has been shown experimentally for a triangular tube [8].

70 [4]Equation (5-24) can be used not only for cylinders located at the corners of triangles and squares, but also at the corners of rectangles.

74 [5]Velocity profiles in the initial segment of a round tube have been measured by Nikuradze [20] and Reshotko [21].

75 [6]The curves of Figs. 5-10 and 5-11 were plotted from Eq. (5-33). Other equations for W_x yield similar results.

83 [7]At this value of Re, flow in a coil with $D/d = 40$ is still laminar (see below).

84 [8]Since the flow is stabilized, $\partial p/\partial x = \text{const}$. However, $\partial p/\partial r \neq 0$ owing to the presence of secondary flows.

86 [9]Existence of such a flow can be demonstrated by qualitative investigation of theproperties of the generalized solution to the nonlinear Navier-Stokes equation. Such a solution has been constructed and certain of its properties investigated [43].

Manuscript Page No.	Transliterated Symbols
59	с = s = stenka = wall
60	э = e = ekvivalentnyy = equivalent
61	макс = maks = maksimal'nyy = maximum
75	н.г = n.g = gidrodinamicheskiy nachal'nyy = hydrodynamic initial
80	кр = kr = kriticheskiy = critical
83	пр = pr = predel'nyy = limiting
84	пр = pr = pryamoy = straight

Chapter 6

HEAT EXCHANGE IN ROUND AND FLAT TUBES WITH CONSTANT PHYSICAL PROPERTIES OF THE FLUID AND BOUNDARY CONDITIONS OF THE FIRST KIND

6-1. HEAT EXCHANGE IN A ROUND TUBE WITH CONSTANT WALL TEMPERATURE

Let us look at heat exchange with viscous flow of a fluid in a round tube for the case of constant wall temperature. We make the following assumptions:

1) the confined fluid flow and the heat-exchange process are stationary;

2) the fluid is incompressible; its physical properties are constant (i.e., do not depend on temperature or pressure);

3) the fluid flow is stabilized, i.e., the velocity profile does not vary along the length (the heat-exchange segment precedes the isothermal damping segment over which the velocity profile is formed); the fluid flowrate is specified or, what is the same, we know the mean fluid velocity over a section;

4) the fluid temperature at the entrance section to the heat-exchange segment is constant over the section and equal to t_0;

5) for the heat-exchange segment, the temperature of the inside wall surface of the tube is constant and equal to t_s $t_s \neq t_0$;

6) there are no internal heat sources in the flow, and the amount of heat liberated owing to energy dissipation is negligible;[1]

7) the changein heat flow along the tube axis owing to heat conduction is small as compared with the heat-flow change along the axis caused by convection.

This problem was first solved by Graetz (1885)[1]. It was again solved independently by Nusselt (1910) [2]. A somewhat different solution was obtained by Shumilov and Yablonskiy [3]. We shall consider the Graetz-Nusselt solution, using values of the constants later refined by several investigators [4, 5, 6].

We write the energy equation for an incompressible fluid with constant physical properties when the flow has no internal heat sources and there is no energy dissipation. In cylindrical coordinates, this equation has the form

$$w_x \frac{\partial t}{\partial x} + w_r \frac{\partial t}{\partial r} + \frac{w_\varphi}{r} \cdot \frac{\partial t}{\partial \varphi} = a\left(\frac{\partial^2 t}{\partial x^2} + \frac{1}{r} \cdot \frac{\partial t}{\partial r} + \frac{\partial^2 t}{\partial r^2} + \frac{1}{r^2} \cdot \frac{\partial^2 t}{\partial \varphi^2}\right). \qquad (6\text{-}1)$$

When the fluid has constant physical properties, the heat-exchange process has no influence on fluid flow. In this case, the fluid moves as if the flow were isothermal. For laminar stabilized flow in a round tube, the velocity component along the axis is

$$w_x = 2\bar{w}\left(1 - \frac{r^2}{r_0^2}\right),$$

while the radial and circumferential components are

$$w_r = w_\varphi = 0.$$

Here $\bar{w}$ is the mean fluid velocity over the section; r_0 is the tube radius.

In virtue of the axial symmetry of the temperature field,

$$\frac{\partial t}{\partial \varphi} = \frac{\partial t^2}{\partial \varphi^2} = 0.$$

According to Assumption 7,

$$\frac{\partial}{\partial x}(\rho c_p w_x t) \gg \frac{\partial}{\partial x}\left(\lambda \frac{\partial t}{\partial x}\right),$$

or

$$w_x \frac{\partial t}{\partial x} \gg a \frac{\partial^2 t}{\partial x^2}.$$

since w_x is independent of x. Thus the first term on the right side of (6-1) can be dropped.

To understand the conditions under which Assumption 7 is satisfied, let us make an approximate estimate of the quantities in this last inequality:

$$w_x \approx \bar{w};\ \frac{\partial t}{\partial x} \approx \frac{t - t_0}{x};\ \frac{\partial^2 t}{\partial x^2} \approx \frac{t - t_0}{x^2}.$$

Consequently, this inequality can be rewritten as

$$\frac{\bar{w}x}{a} \gg 1,$$

or

$$\frac{x}{d} \gg \frac{1}{\mathrm{Pe}},$$

where $\mathrm{Pe} = \bar{w}d/a$; d is the tube diameter.

Thus if Pe $\geq$ 100, Assumption 7 is satisfied for almost the entire tube length (for $x/d \geq 1$ in any case). For gases (Pr $\approx$ 1) and nonmetallic liquids (Pr $\approx$ 1–1000), this condition will almost

always be satisfied. For liquid metals (Pr≈0,005–0,05) it may or may not be satisfied. In this last case, the term d^2t/dx^2 must be retained in Eq. (6-1); it allows for the change in heat flow owing to heat conduction along the axis (see Chapter 10).

Taking all of this into account and introducing a new variable for the temperature, $\vartheta = t - t_c$ (t_c is the wall temperature), we can write the energy equation corresponding to our problem in the form

$$\frac{\partial^2\vartheta}{\partial r^2} + \frac{1}{r}\cdot\frac{\partial\vartheta}{\partial r} = \frac{2\bar{\omega}}{a}\left[1-\left(\frac{r}{r_0}\right)^2\right]\frac{\partial\vartheta}{\partial x}.$$

The boundary conditions have the form

$$\text{for } x=0 \text{ and } 0\leqslant r<r_0 \quad \vartheta=\vartheta_0,$$
$$\text{for } x\geqslant 0 \text{ and } r=0 \quad \frac{\partial\vartheta}{\partial r}=0,$$
$$\text{for } x\geqslant 0 \text{ and } r=r_0 \quad \vartheta=0,$$

where $\vartheta_0 = t_0 - t_c$.

For convenience in the subsequent computations, we reduce the equation and boundary conditions to dimensionless form. To do this, we introduce the dimensionless variables

$$\Theta=\frac{\vartheta}{\vartheta_0}=\frac{t-t_c}{t_0-t_c} \text{ and } R=\frac{r}{r_0}.$$

After elementary manipulations we obtain

$$\frac{\partial^2\Theta}{\partial R^2}+\frac{1}{R}\cdot\frac{\partial\Theta}{\partial R}=(1-R^2)\frac{\partial\Theta}{\partial X}. \tag{6-2}$$

$$\text{for } X=0 \text{ and } 0\leqslant R<1 \quad \Theta=1; \tag{6-3}$$

$$\left.\begin{aligned}&\text{for } X\geqslant 0 \text{ and } R=0 \quad \frac{\partial\Theta}{\partial R}=0;\\ &\text{for } X\geqslant 0 \text{ and } R=1 \quad \Theta=0,\end{aligned}\right\} \tag{6-4}$$

where

$$X=\frac{a}{2\bar{\omega}r_0}\cdot\frac{x}{r_0}=\frac{2}{\mathrm{Pe}}\cdot\frac{x}{d}.$$

The dimensionless coordinate X or, more accurately, the quantity $\frac{1}{\mathrm{Pe}}\frac{x}{d}$, is called the reduced length of the tube.

Let us attempt to solve differential equation (6-2) by separating the variables. To do this, we represent the dimensionless temperature $\Theta(X, R)$ as the product of two functions, one of which depends solely on X and the other solely on R:

$$\Theta(X, R) = \varphi(X)\psi(R). \tag{6-5}$$

Substituting (6-5) into Eq. (6-2), we obtain

$$\varphi\psi'' + \frac{1}{R}\varphi\psi' = (1-R^2)\psi\varphi'.$$

To separate the variables, we divide both sides of the equation by $\varphi\psi(1-R^2)$. Then the equation takes the form

$$\frac{\varphi'}{\varphi}=\frac{\psi''+\frac{1}{R}\psi'}{\psi(1-R^2)}=-\varepsilon^2.$$

Since the left side of this equation depends on X alone and the right side on R alone, they can be equal only if the left and right sides of the equation equal the constant $-\varepsilon^2$. We note that this constant must be negative, since if this were not the case it would turn out that as X increases the temperature Θ increases without limit, and this contradicts the formulation of the problem with t_s = const. We thus have two ordinary differential equations:

$$\frac{d\varphi}{dX}=-\varepsilon^2\varphi; \tag{6-6}$$

$$\frac{d^2\psi}{dR^2}+\frac{1}{R}\cdot\frac{d\psi}{dR}+\varepsilon^2(1-R^2)\psi=0. \tag{6-7}$$

A solution of the first equation is

$$\varphi=Ae^{-\varepsilon^2X}, \tag{6-8}$$

where A is a constant of integration.

We rewrite the second equation as

$$\frac{d^2\psi}{d(\varepsilon R)^2}+\frac{1}{\varepsilon R}\cdot\frac{\partial\psi}{d(\varepsilon R)}+\left[1-\frac{(\varepsilon R)^2}{\varepsilon^2}\right]\psi=0. \tag{6-9}$$

The solution of (6-9) must satisfy the following boundary conditions:

$$\left.\begin{aligned}&\text{for } R=0\ \frac{d\psi}{dR}=0;\\&\text{for } R=1\ \psi=0.\end{aligned}\right\} \tag{6-4a}$$

This problem is known in mathematical physics as the eigenfunction problem, or the Sturm-Liouville problem.

A solution of linear differential equation (6-9) cannot be obtained in closed form. Nusselt suggested that it be sought as a power series,

$$\psi=\sum_{n=0}^{\infty}b_n\xi^n,$$

where $\xi = \varepsilon R$.

Substituting this expression for ψ into (6-9) and requiring that (6-9) be satisfied for any ξ, we obtain relationships for the coefficients b_n. Substituting this expression into (6-9), we have

$$\sum_{n=0}^{\infty}n(n-1)b_n\xi^{n-2}+\sum_{n=0}^{\infty}nb_n\xi^{n-2}+\left(1-\frac{\xi^2}{\varepsilon^2}\right)\sum_{n=0}^{\infty}b_n\xi^n=0,$$

or

$$\sum_{n=0}^{\infty} n^2 b_n \xi^{n-2} + \sum_{n=0}^{\infty} b_n \xi^n - \sum_{n=0}^{\infty} \frac{b_n}{\varepsilon^2} \xi^{n+2} = 0.$$

We renumber in the last equation; in particular, we reduce the exponent for ξ to the same value in all terms. To do this, we let $k = n - 2$ in the first term, $k = n$ in the second, and $k = n + 2$ in the third. As a result we obtain

$$\sum_{k=-2}^{\infty} (k+2)^2 b_{k+2} \xi^k + \sum_{k=0}^{\infty} b_k \xi^k - \sum_{k=2}^{\infty} \frac{b_{k-2}}{\varepsilon^2} \xi^k = 0.$$

Taking some of the terms to the left of the first and second summation signs, we rewrite the equation as

$$b_1 \xi^{-1} + (4b_2 + b_0) + (9b_3 + b_1)\xi + \sum_{k=2}^{\infty} \left[(k+2)^2 b_{k+2} + b_k - \frac{b_{k-2}}{\varepsilon^2} \right] \xi^k = 0.$$

This equation must be satisfied for any ξ, the coefficients on terms containing different powers of ξ must equal zero, i.e.,

$$b_1 = 0;$$

$$b_3 = -\frac{b_0}{4};$$

$$b_2 = -\frac{b_1}{9} = 0;$$

$$b_{k+2} = \frac{1}{(k+2)^2} \left(\frac{b_{k-2}}{\varepsilon^2} - b_k \right) \text{(for } k \geq 2).$$

Thus the coefficients on even terms are represented by the two preceding even coefficients, and those on the odd terms by the corresponding two odd coefficients. Since $b_1 = 0$ and $b_3 = 0$, the coefficients on the series terms containing odd powers of ξ will equal zero. Thus the solution for $\psi(R)$ can be represented as a series containing εR in even powers alone, i.e.,

$$\psi(\varepsilon R) = \sum_{n=0}^{\infty} b_{2n} (\varepsilon R)^{2n}, \qquad (6\text{-}10)$$

where

$$b_0 = 1^2 \qquad (n = 0);$$

$$b_2 = \frac{b_0}{4} = -\frac{1}{4} \qquad (n = 1);$$

$$b_{2n} = \frac{1}{(2n)^2} \left(\frac{1}{\varepsilon^2} b_{2n-4} - b_{2n-2} \right) \qquad (n \geq 2).$$

In expanded form, (6-10) is written as

$$\psi(R) = 1 - \frac{1}{4}(\varepsilon R)^2 + \frac{1}{16}\left(\frac{1}{\varepsilon^2} + \frac{1}{4} \right)(\varepsilon R)^4 + \ldots \qquad (6\text{-}10a)$$

This series converges for any εR and ε.

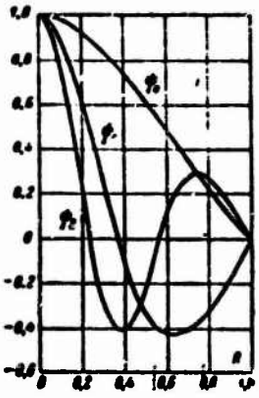

Fig. 6-1. The function $\psi_n(R)$ for heat exchange in a round tube with t_s = const.

The constant ε is found with the aid of the second boundary condition of (6-4a). Applying this condition to (6-10a), we obtain

$$1-\frac{1}{4}\varepsilon^2+\frac{1}{16}\left(\frac{1}{\varepsilon^2}+\frac{1}{4}\right)\varepsilon^4+\ldots=0. \qquad (6\text{-}11)$$

Equation (6-11) has an infinite set of roots, called the eigenvalues of Problem (6-9) and (6-4a). According to Nusselt's calculations, the first three eigenvalues equal: $\varepsilon_0=2{,}705$; $\varepsilon_1=6{,}66$; $\varepsilon_2=10{,}3$. To each eigenvalue there corresponds the eigenfunction

$$\psi(\varepsilon_n R, \varepsilon_n)=\psi_n(R).$$

The first three functions $\psi_n(R)$ are shown in Fig. 6-1 for n = 0, 1, and 2.

Thus a particular solution of differential equation (6-2) satisfying the boundary condition at the wall can be written as

$$\theta_n=A_n e^{-\varepsilon_n^2 X}\psi_n(R).$$

This solution is only valid for the special case in which the temperature distribution at the entrance has the form $\theta_0=A_n\psi_n(R)$ however. Solution of the problem in the general case, where an arbitrary temperature distribution $\theta_0(R)$ is specified at the entrance must be sought as the sum of all special solutions:

$$\theta=\sum_{n=0}^{\infty}A_n e^{-\varepsilon_n^2 X}\psi_n(R). \qquad (6\text{-}12)$$

Only the coefficients A_n are unknown in (6-12). They are found from the boundary condition at the entrance. Let the temperature distribution at the entrance, i.e., at X = 0, be described

by the function $\theta_0(R)$ [in our case, $\theta_0(R) = 1$]. We can then write

$$\theta_0(R)=\sum_{n=0}^{\infty} A_n\psi_n(R). \tag{6-13}$$

The coefficients A_n are determined from (6-13) with allowance for the orthogonality property of the eigenfunctions. Let us prove this property.

Since the function ψ_n and ψ_m $(m\neq n)$ are solutions of (6-7), we can write

$$\left.\begin{aligned}\frac{d}{dR}\left(R\frac{d\psi_n}{dR}\right)+\varepsilon_n^2 R(1-R^2)\psi_n=0,\\ \frac{d}{dR}\left(R\frac{d\psi_m}{dR}\right)+\varepsilon_m^2 R(1-R^2)\psi_m=0.\end{aligned}\right\} \tag{6-14}$$

Multiplying the first equation by ψ_m and the second by ψ_n, and subtracting the first equation from the second, we obtain

$$\psi_n\frac{d}{dR}\left(R\frac{d\psi_m}{dR}\right)-\psi_m\frac{d}{dR}\left(R\frac{d\psi_n}{dR}\right)=(\varepsilon_n^2-\varepsilon_m^2)R(1-R^2)\psi_n\psi_m.$$

The left side of this equation can be represented as

$$\frac{d}{dR}\left[R\left(\psi_n\frac{d\psi_m}{dR}-\psi_m\frac{d\psi_n}{dR}\right)\right].$$

Integrating this last equation with respect to R between 0 and 1, we obtain

$$(\varepsilon_n^2-\varepsilon_m^2)\int_0^1\psi_n\psi_m R(1-R^2)\,dR=R\left(\psi_n\frac{d\psi_m}{dR}-\psi_m\frac{d\psi_n}{dR}\right)\Bigg|_0^1. \tag{6-15}$$

The right side of (6-15) vanishes when $R = 0$ and $R = 1$ [since $\psi_n(1)=\psi_m(1)=0$]. Since $\varepsilon_n\neq\varepsilon_m$, we obtain the orthogonality property for the eigenfunctions:

$$\int_0^1\psi_n\psi_m R(1-R^2)\,dR=0 \text{ for } m\neq n.$$

On the basis of this relationship, we can calculate the coefficients A_n of the series in (6-12). To do this we multiply both sides of (6-13) by $\psi_n R(1-R^2)\,dR$ and integrate between $R = 0$ and 1. Making allowance for the orthogonality property, we obtain

$$A_n=\frac{\int_0^1\theta_0(R)\psi_n(R)R(1-R^2)\,dR}{\int_0^1\psi_n^2(R)R(1-R^2)\,dR}. \tag{6-16}$$

We evaluate the integral in the numerator of (6-16) for our

case, i.e., for $\Theta_0 = 1$. To do this, we rewrite the first equation of (6-14) as

$$\psi_n R(1-R^2)\,dR = -\frac{1}{\varepsilon_n^2} d\left(R\frac{d\psi_n}{dR}\right).$$

Integrating this expression between 0 and 1, we find

$$\int_0^1 \psi_n(R) R(1-R^2)\,dR = -\frac{1}{\varepsilon_n^2}\left(\frac{d\psi_n}{dR}\right)_{R=1}. \qquad (6\text{-}17)$$

The integral in the denominator of (6-16),

$$N_n = \int_0^1 \psi_n^2(R) R(1-R^2)\,dR$$

can be evaluated on the basis of (6-15). We drop the subscript m on the quantity ε_m in (6-15), and treat ε as a continuously varying quantity that approaches ε_n in the limit. Then N_n will be the limit of the integral, which in virtue of (6-15) can be represented as follows:

$$N_n = \lim_{\varepsilon\to\varepsilon_n}\int_0^1 \psi_n\psi R(1-R^2)\,dR = \lim_{\varepsilon\to\varepsilon_n}\frac{R\left(\psi_n\frac{d\psi}{dR}-\psi\frac{d\psi_n}{dR}\right)\Big|_0^1}{\varepsilon_n^2-\varepsilon^2}.$$

When $\varepsilon \to \varepsilon_n$, this fraction exhibits an indeterminacy of the 0/0 type. Removing this indeterminacy, i.e., differentiating numerator and denominator with respect to ε, letting $R = 1$ and $R = 0$, and recalling that $\psi(1)=\psi_n(1)=0$, we obtain

$$N_n = \lim_{\varepsilon\to\varepsilon_n}\frac{R\left[\psi_n\frac{\partial}{\partial\varepsilon}\left(\frac{d\psi}{dR}\right)-\frac{d\psi_n}{dR}\cdot\frac{\partial\psi}{\partial\varepsilon}\right]\Big|_0^1}{-2\varepsilon} = \lim_{\varepsilon\to\varepsilon_n}\frac{\left(\frac{d\psi_n}{dR}\cdot\frac{\partial\psi}{\partial\varepsilon}\right)_{R=1}}{2\varepsilon}$$

and, finally,

$$N_n = \int_0^1 \psi_n^2 R(1-R^2)\,dR = \frac{1}{2\varepsilon_n}\left[\frac{d\psi_n}{dR}\left(\frac{\partial\psi}{\partial\varepsilon}\right)_{\varepsilon=\varepsilon_n}\right]_{R=1}. \qquad (6\text{-}18)$$

Substituting (6-17) and (6-18) into (6-16), we obtain the final expression for the coefficients A_n where $\Theta_0 = 1$:

$$A_n = -\frac{2}{\varepsilon_n\left(\frac{\partial\psi}{\partial\varepsilon}\right)_{\substack{\varepsilon=\varepsilon_n\\ R=1}}}. \qquad (6\text{-}19)$$

The derivative $\left(\frac{\partial\psi}{\partial\varepsilon}\right)_{\substack{\varepsilon=\varepsilon_n\\ R=1}}$ is found from (6-10a).

The calculations yield the following values for the first three coefficients: $A_0 = 1.477$; $A_1 = -0.810$; $A_2 = 0.385$.

TABLE 6-1

Eigenfunctions in Problem of Heat Exchange in a Round Tube for t_s = const

R	ψ_0	ψ_1	ψ_2	ψ_3	ψ_4	ψ_5
0.00	1.000000	1.000000	1.000000	1.000000	1.000000	1.000000
0.05	[illegible]	[illegible]	[illegible]	[illegible]	[illegible]	[illegible]
0.10	0.981845	[illegible]	[illegible]	[illegible]	[illegible]	[illegible]
0.15	0.959508	[illegible]	[illegible]	[illegible]	[illegible]	[illegible]
0.20	0.928893	[illegible]	[illegible]	[illegible]	[illegible]	[illegible]
0.25	[illegible]	[illegible]	[illegible]	[illegible]	[illegible]	[illegible]
0.30	0.845468	0.233452	[illegible]	[illegible]	[illegible]	[illegible]
0.35	0.794305	[illegible]	[illegible]	[illegible]	[illegible]	[illegible]
0.40	[illegible]	−0.109593	[illegible]	[illegible]	[illegible]	[illegible]
0.45	[illegible]	−0.243018	[illegible]	[illegible]	[illegible]	[illegible]
0.50	[illegible]	−0.342141	[illegible]	[illegible]	[illegible]	[illegible]
0.55	[illegible]	[illegible]	[illegible]	[illegible]	[illegible]	[illegible]
0.60	[illegible]	[illegible]	[illegible]	[illegible]	[illegible]	[illegible]
0.65	0.416713	[illegible]	[illegible]	[illegible]	[illegible]	[illegible]
0.70	0.351010	[illegible]	[illegible]	[illegible]	[illegible]	[illegible]
0.75	[illegible]	[illegible]	[illegible]	[illegible]	[illegible]	[illegible]
0.80	0.224264	[illegible]	[illegible]	[illegible]	[illegible]	[illegible]
0.85	[illegible]	[illegible]	[illegible]	[illegible]	[illegible]	[illegible]
0.90	[illegible]	[illegible]	[illegible]	[illegible]	[illegible]	[illegible]
0.95	0.052019	[illegible]	[illegible]	[illegible]	[illegible]	[illegible]
1.00	0.000000	0.000000	0.000000	0.000000	0.000000	0.000000

TABLE

Eigenvalues and Constants in Problem of Heat Exchange in Round Tube for t_s = const

n	ε_n	ε_n^2	A_n	B_n*
0	2.7043644	7.3135868	+1.4764354	0.7487450
1	[illegible]	[illegible]	[illegible]	[illegible]
2	[illegible]	[illegible]	[illegible]	[illegible]
3	14.671078	[illegible]	[illegible]	[illegible]
4	[illegible]	[illegible]	[illegible]	[illegible]
5	[illegible]	[illegible]	[illegible]	[illegible]
6	[illegible]	[illegible]	[illegible]	[illegible]
7	[illegible]	[illegible]	[illegible]	[illegible]
8	[illegible]	[illegible]	[illegible]	[illegible]
9	[illegible]	[illegible]	[illegible]	[illegible]
10	[illegible]	[illegible]	[illegible]	[illegible]

*This constant will be required later.

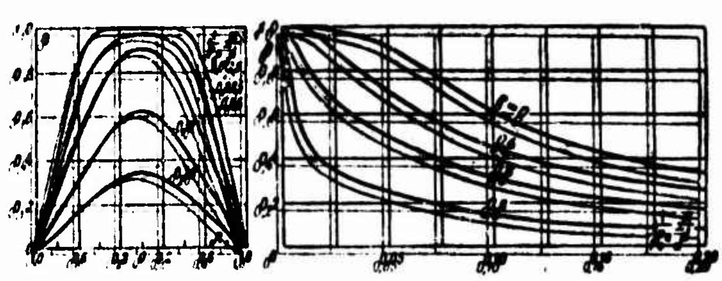

Fig. 6-2. Temperature distribution in fluid flow along tube radius and length with constant wall temperature.

Thus by these calculations we have determined the constants ε_n and A_n needed to determine the temperature distribution with Eq. (6-12). We again write this equation in somewhat different form:

$$\frac{t-t_c}{t_0-t_c}=\sum_{n=0}^{\infty}A_n\psi_n\left(\frac{r}{r_0}\right)\exp\left(-2\varepsilon_n^2\frac{1}{\mathrm{Pe}}\cdot\frac{x}{d}\right). \qquad (6\text{-}12a)$$

The values of the eigenfunctions, eigenvalues ε_n, and the constant A_n in (6-12) or (6-12a) are determined from (6-10), (6-11), and (6-19), respectively. Their values, computed by Nusselt, are given below. More exact values for $\psi_n(R)$, ε_n and A_n are given in Tables 6-1 and 6-2 [6].

It is difficult to use this method to determine the eigenvalues and eigenfunctions for large values of n. In this connection, Sellers, Tribus, and Klein [7] have constructed an asymptotic solution of Eq. (6-7), letting $\varepsilon_n \to \infty$. The following expressions were obtained for the eigenvalues, eigenfunctions, and constants:

$$\varepsilon_n=4n+\frac{8}{3}; \qquad (6\text{-}20)$$

$$A_n=(-1)^n\,2{,}84606\varepsilon_n^{-2/3}; \qquad (6\text{-}21)$$

for small R (near the tube axis)

$$\psi_n(R)=J_0(\varepsilon_n R); \qquad (6\text{-}22)$$

for moderate values of R

$$\psi_n(R)=\sqrt{\frac{2}{\pi\varepsilon_n R}}\cdot\frac{\cos\left[\frac{\varepsilon_n}{2}R\sqrt{1-R^2}+\frac{\varepsilon_n}{2}\arcsin R-\frac{\pi}{4}\right]}{(1-R^2)^{1/4}}; \qquad (6\text{-}22a)$$

for R close to unity (near the wall),

$$\psi_n(R)=\sqrt{\frac{2}{3}(1-R)}\,(-1)^n J_{1/3}\left[\frac{\varepsilon_n\sqrt{8}}{3}(1-R)^{3/2}\right]; \qquad (6\text{-}22b)$$

$$B_n=-\frac{1}{2}A_n\left(\frac{d\psi_n}{dR}\right)_{R=1}=1{,}01276\varepsilon_n^{-1/3}, \qquad (6\text{-}23)$$

where $J_{1/3}$ is a Bessel function of order 1/3.

The asymptotic solution also proves valid for finite values of ε_n. A comparison of results for this computation and the exact solution (Tables 6-1 and 6-2) shows good agreement at both large and small n. In any case, the approximate values of the constants and functions can be used for values $n \geq 3$.

Figure 6-2 shows the temperature distribution in the fluid flow, calculated from (6-12a). For small values of the reduced length $\left(\frac{1}{\mathrm{Pe}}\frac{x}{d}<0{,}05\right)$, the fluid temperature near the axis will vary

little along the tube radius and length. It is only near the wall that large changes in temperature both along R and X will be observed.

The region of small reduced-length values is characteristic in that it is here that growth takes place in the thermal boundary layer within which the temperature varies. The temperature distribution in the flow core, whose cross section contracts with increasing X, remains almost uniform (the temperature is approximately equal to the entrance temperature).

Sufficiently far from the entrance, the thermal boundary layers join, and heat exchange encompasses the entire tube cross section. Beginning at a certain value of the reduced length, the temperature profiles become similar, i.e., the temperatures in different sections differ only in absolute value, while the law governing the temperature variation over the radius remains the same. The solution (6-12a) reflects this nature of the temperature field. For small reduced lengths, the temperature distribution is described by a series. As X increases, the influence of the last terms of the series rapidly decreases as compared with that of the earlier terms. Finally, when the reduced length is sufficiently large, all terms of the series, except the first, can be neglected. Here

$$\frac{t-t_c}{t_0-t_c}=A_0\psi_0\left(\frac{r}{r_0}\right)\exp\left(-2a_0^2\frac{1}{\mathrm{Pe}}\frac{1}{x}\right). \qquad (6\text{-}24)$$

From this it is clear that the temperature variation along a radius is described for any x is described by exactly the same function $\psi_0(r/r_0)$ (see Fig. 6-1), while for all values of r, the variation with length is exponential.

Let us determine the mean mass temperature of the fluid in an arbitrary tube section. According to Eq. (2-14),

$$\bar{t}=\frac{1}{w_m\pi r_0^2}\int_0^{r_0} t w_x 2\pi r\,dr,$$

or in dimensionless form

$$\bar{\theta}=\frac{\bar{t}-t_c}{t_0-t_c}=2\int_0^1 \theta W_x R\,dR.$$

In our case, $W_x=\frac{w_x}{w}=2(1-R^2)$ and, consequently,

$$\bar{\theta}=4\int_0^1 \theta(1-R^2)R\,dR.$$

Substituting the value of θ from (6-12) into this expression, we find

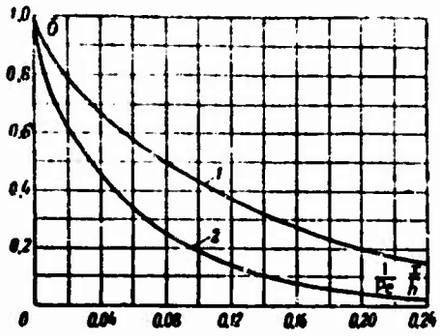

Fig. 6-3. Variation in $\bar{\theta}$ over tube length. 1) Flat tube; 2) round tube (in the latter case, h corresponds to d).

$$\bar{\theta}=4\sum_{n=0}^{\infty}A_n\exp\left(-2\varepsilon_n^2\frac{1}{\mathrm{Pe}}\frac{x}{d}\right)\int_0^1\psi_n(R)R(1-R^2)dR.$$

Taking (6-17) into account, we finally obtain

$$\frac{\bar{t}-t_c}{t_0-t_c}=8\sum_{n=0}^{\infty}\frac{B_n}{\varepsilon_n^2}\exp\left(-2\varepsilon_n^2\frac{1}{\mathrm{Pe}}\cdot\frac{x}{d}\right), \qquad (6\text{-}25)$$

where

$$B_n=-\frac{1}{2}A_n\left(\frac{d\psi_n}{dR}\right)_{R=1}.$$

Figure 6-3 illustrates the function (6-25). When $X=0, \bar{\theta}=\theta_0=1$. As the reduced length increases, $\bar{\theta}$ decreases; beginning at a certain value, it decreases exponentially. For $X\to\infty, \bar{\theta}\to 0$.

Let us now determine the local heat-transfer coefficient, referring it to the difference between the mean mass temperature of the fluid and the wall temperature:

$$\alpha=\frac{q_c}{t_c-\bar{t}}=\frac{\lambda\left(\frac{\partial t}{\partial r}\right)_{r=r_0}}{\bar{t}-t_c}.$$

Here q_s is the density of the heat flow at the wall, λ is the thermal-conductivity coefficient of the fluid or, in dimensionless form,

$$\mathrm{Nu}=\frac{\alpha d}{\lambda}=-\frac{2}{\bar{\theta}}\left(\frac{\partial\theta}{\partial R}\right)_{R=1}=-2\left[\frac{\partial}{2\partial}\left(\frac{t-t_c}{\bar{t}-t_c}\right)\right]_{R=1}.$$

Substituting the derivative found from (6-12) and the value of $\bar{\theta}$ from (6-25) into the above equation, we obtain an expression for the local Nusselt number:

$$\mathrm{Nu} = \frac{\sum_{n=0}^{\infty} B_n \exp\left(-2\varepsilon_n^2 \frac{1}{\mathrm{Pe}} \cdot \frac{x}{d}\right)}{2\sum_{n=0}^{\infty} \frac{B_n}{\varepsilon_n^2} \exp\left(-2\varepsilon_n^2 \frac{1}{\mathrm{Pe}} \cdot \frac{x}{d}\right)}. \qquad (6\text{-}26)$$

Figure 6-4 shows Nu as a function of X. When $X \to 0$, i.e., at the entrance to the heated segment, $\mathrm{Nu} \to \infty$. The reason is that the derivative of the temperature at the wall, $(\partial t/\partial r)_{r=r_0}$, becomes infinite at the entrance section, while the temperature head $\bar{t} - t_s$ is finite. The infinite value of $(\partial t/\partial r)_{r=r_0}$ results from the computational scheme adopted for the process, according to which when $X = 0$ the fluid temperature is uniformly distributed over the radius, and equal to t_0, but when $r = r_0$, it changes abruptly from t_0 to t_s. In fact, owing to heat transfer in the wall and the fluid by heat conduction, in the axial direction the derivative $(\partial t/\partial r)_{r=r_0}$ and, consequently, Nu will have large, but finite values at $X = 0$.

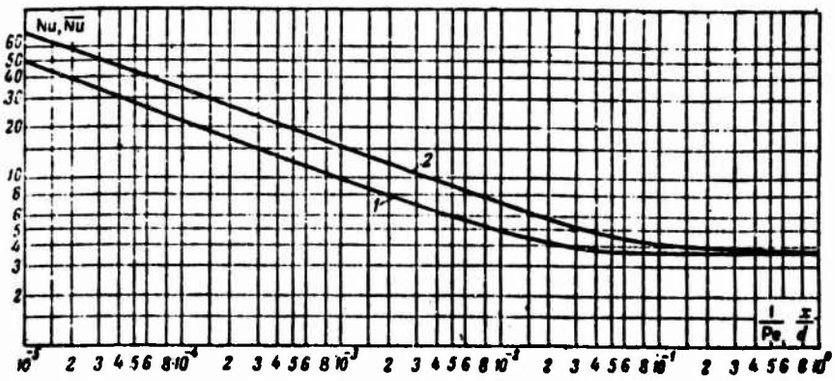

Fig. 6-4. Variation in local (1) and mean (2) Nusselt numbers over length of round tube with t_s = const.

As X increases, Nu decreases, asymptotically approaching a constant value. This occurs since beginning at a certain value of X the temperature profiles in different sections become similar, and the temperature field is described by just the first term of the series in Eq. (6-12a), i.e., Eq. (6-24). Here the dimensionless excess temperature, represented as the ratio $\frac{t-t_0}{t-t_c}$, will cease to vary with the length. Since Nu is uniquely determined by $\frac{t-t_0}{t-t_c}$ it will also take on a constant value. In other words, the field of the dimensionless excess temperature $\frac{t-t_c}{\bar{t}-t_c}$ and the Nusselt number will become selfsimilar with respect to the coordinate X. As we shall see later, the property of temperature-field selfsimilarity at large values of X is characteristic of many heat-exchange problems for fluid flow in tubes.

This constant value of the Nusselt number is called the limiting value, and represented by Nu_∞. Letting X go to infinity in (6-26) and considering only the first terms of the series in the numerator and denominator, we have

$$Nu_\infty = \frac{\varepsilon_0^2}{2} = 3{,}657 \approx 3{,}66. \qquad (6\text{-}27)$$

From this it follows that the limiting heat-transfer coefficient is

$$\alpha_\infty = 3{,}66 \frac{\lambda}{d}.$$

Thus α_∞ depends only on the thermal-conductivity coefficient of the fluid and the tube diameter.

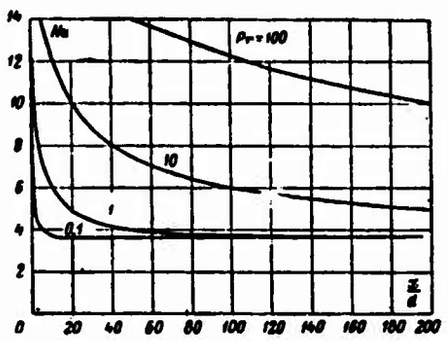

Fig. 6-5. Variation in Nu over length of round tube with Re = = 2000 and various values of Pr.

It is clear from what we have said that the entire length of the heated (cooled) tube can be divided into two segments. The temperature profile is formed in the first segment, i.e., the law describing the radial temperature distribution changes with length from the initial form (at $X = 0$) to some limiting form $\psi_0(R)$, while Nu decreases with the length. In the second segment, the radial temperature distribution does not vary with length (although the absolute temperature values do change), and Nu remains constant. The first segment is called the thermal initial segment, and the second the stabilized heat-exchange segment. While the temperature field and heat exchange in the thermal initial segment depend substantially on the temperature distribution at the entrance, there is no such influence in the stabilized heat-exchange segment.

The length of the thermal initial segment $l_{n.t}$ can arbitrarily be defined as the distance from the entrance section at which Nu takes on a constant (limiting) value, to within a specified accuracy. Taking 1% accuracy, on the basis of (6-26), we find that the reduced length of the thermal initial segment is $\frac{1}{Pe}\frac{l_{n.t}}{d} = 0{,}055$,

while the relative length is

$$\frac{l_{n.t}}{d} = 0.055\ \mathrm{Pe}. \qquad (6\text{-}28)$$

For a specified Reynolds number, the length of the thermal initial segment is determined by the Prandtl number (Fig. 6-5). Thus for liquid-metal heat-transport media, having values of Pr from roughly 0.005 to 0.05, $l_{n.t}$ will not exceed several diameters; for gases with Pr ≈ 1, $l_{n.t}$ reaches ~100d; for nonmetallic liquids (water, mineral oils, and other viscous liquids) with Pr from 1 to 100 or more, $l_{n.t}$ may vary from several hundred to several thousand or even tens of thousands of diameters. In particular, this shows that in tubes of heat exchangers used for heating or cooling fluids with Pr > 1, heat exchange in viscous flow takes place over the entire tube length in the region of the thermal initial segment.

Direct utilization of (6-26) is extremely inconvenient in practical determination of heat transfer near the tube entrance, since here it is necessary to compute many terms of the series. For small reduced lengths, however, the solution (6-26) can be simplified by substitution of the asymptotic values of ε_n and B_n from (6-20) and (6-23), and substitution of an integral for the sum. Using this method, Lipkis [5, 7] has shown that for $\frac{1}{\mathrm{Pe}}\frac{x}{d} < 10^{-4}$ (6-26) takes the form

$$\mathrm{Nu} = 1{,}077\left(\frac{1}{\mathrm{Pe}}\cdot\frac{x}{d}\right)^{-1/3} - 1{,}7. \qquad (6\text{-}26a)$$

For $\frac{1}{\mathrm{Pe}}\cdot\frac{x}{d} \geqslant 10^{-3}$, we can use the interpolation equation [8a]

$$\mathrm{Nu} = 3{,}655 + \frac{0{,}2355}{\left(\frac{1}{\mathrm{Pe}}\frac{x}{d}\right)^{0.488}\exp\left(57{,}2\frac{1}{\mathrm{Pe}}\frac{x}{d}\right)}, \qquad (6\text{-}26b)$$

which describes the results of a computation performed with high accuracy by a numerical method, with no more than 0.5% deviation.

The mean heat-transfer coefficient and, accordingly, the mean Nusselt number for a tube segment of length l (from $x = 0$ to $x = l$) can be determined in different ways (see §2-4). We first find an expression for the mean integral heat-transfer coefficient:

$$\bar{\alpha} = \frac{1}{l}\int_0^l \alpha\, dx.$$

From the heat-balance equation for an element of length dx

$$\alpha\bar{\vartheta}2\pi r_0\, dx = -\pi r_0^2\,\bar{w}\rho c_p\, d\bar{\vartheta},$$

where $\bar{\vartheta} = \bar{t} - t_c$, we find

$$\alpha\, dx = -\frac{\bar{w}d\rho c_p}{4}\cdot\frac{d\bar{\vartheta}}{\bar{\vartheta}}.$$

Consequently,

$$\bar{\alpha} = -\frac{\bar{w} d \rho c_p}{4l} \int_{\bar{\vartheta}_0}^{\bar{\vartheta}_{x=l}} \frac{d\bar{\vartheta}}{\bar{\vartheta}} = -\frac{\bar{w} d \rho c_p}{4l} \ln \frac{\bar{\vartheta}_{x=l}}{\vartheta_0}$$

and

$$\overline{\mathrm{Nu}} = \frac{\bar{\alpha} d}{\lambda} = -\frac{1}{4} \mathrm{Pe} \frac{d}{l} \ln \bar{\vartheta}_{x=l}.$$

Substituting in $\bar{\vartheta}_{x=l}$ from (6-25), we finally obtain

$$\overline{\mathrm{Nu}} = -\frac{1}{4} \mathrm{Pe} \frac{d}{l} \ln \left[8 \sum_{n=0}^{\infty} \frac{B_n}{\varepsilon_n^2} \exp\left(-2\varepsilon_n^2 \frac{1}{\mathrm{Pe}} \cdot \frac{l}{d} \right) \right]. \qquad (6\text{-}29)$$

At the entrance to a heated segment, $\overline{\mathrm{Nu}}$, like Nu, approaches infinity; far from the entrance, i.e., for $\frac{1}{\mathrm{Pe}} \cdot \frac{l}{d} \to \infty$, $\overline{\mathrm{Nu}}$ takes on a constant value equaling $\mathrm{Nu}_\infty = 3.66$ (see Fig. 6-4). The distance from the entrance at which $\overline{\mathrm{Nu}}$ becomes constant, to within 1%, will be substantially greater than for the local Nu number, however. This distance is called the length of the thermal initial segment or the mean heat transfer, $\bar{l}_{\text{n.t}}$. Calculations show that

$$\frac{\bar{l}_{\text{n.t}}}{d} = 1{,}365 \mathrm{Pe}, \qquad (6\text{-}30)$$

i.e.,

$$\bar{l}_{\text{n.t}} \approx 25 l_{\text{n.t}}.$$

For approximate calculations, we can replace (6-29) by the interpolation equation [8b]

$$\overline{\mathrm{Nu}} = 3{,}66 + \frac{0{,}0668 \mathrm{Pe} \frac{d}{l}}{1 + 0{,}04 \left(\mathrm{Pe} \frac{d}{l} \right)^{2/3}}. \qquad (6\text{-}31)$$

For $\mathrm{Pe} \frac{l}{d} < 250$, this equation yields a deviation of no more than +4% from the exact solution.

The mean heat-transfer coefficient $\bar{\alpha}$ calculated here should be referred to the mean logarithmic temperature head. This is shown by the expression given above for $\bar{\alpha}$, from which it is easy to obtain the following equation for the amount of heat transferred from the wall to the fluid:

$$Q_c = \frac{\pi d^2}{4} \bar{w} \rho c_p (\bar{\vartheta}_{x=l} - \vartheta_0) = \bar{\alpha} \Delta \bar{t}_{\text{л}} \pi d l,$$

where

$$\Delta \bar{t}_{\text{л}} = \frac{\vartheta_{x=l} - \vartheta_0}{\ln \frac{\vartheta_0}{\vartheta_{x=l}}} = \frac{(t_c - t_0) - (t_c - \bar{t}_{x=l})}{\ln \frac{t_c - t_0}{t_c - \bar{t}_{x=l}}}.$$

It is not difficult to write equations for $\bar{\alpha}$ and $\overline{Nu}$, referred to other temperature heads (see §2-4). Naturally, they will differ from (6-29).

Thus, for example, referring the heat-transfer coefficient to the mean arithmetic temperature difference, i.e., letting

$$\bar{\alpha} = \frac{Q_c}{F\Delta\bar{t}_a},$$

where

$$Q_c = \frac{\pi d^2}{4}\bar{w}\rho c_p(\bar{\vartheta}_{x=l} - \vartheta_0); \qquad F = \pi dl \text{ and}$$

$$\overline{\Delta t}_a = -\frac{1}{2}(\vartheta_0 + \bar{\vartheta}_{x=l}),$$

we obtain

$$\overline{Nu} = \frac{1}{2}\,Pe\,\frac{d}{l}\,\frac{1-\bar{\theta}_{x=l}}{1+\bar{\theta}_{x=l}}. \tag{6-32}$$

Substituting $\bar{\theta}_{x=l}$ from (6-25) into (6-32), we obtain

$$\overline{Nu} = \frac{1}{2}\,Pe\,\frac{d}{l}\,\frac{1-8\sum_{n=0}^{\infty}\frac{B_n}{\varepsilon_n^2}\exp\left(-2\varepsilon_n^2\frac{1}{Pe}\frac{l}{d}\right)}{1+8\sum_{n=0}^{\infty}\frac{B_n}{\varepsilon_n^2}\exp\left(-2\varepsilon_n^2\frac{1}{Pe}\frac{l}{d}\right)}. \tag{6-32a}$$

For large reduced lengths, where the fluid temperature at the exit is close to the wall temperature so that $\bar{\theta}_{x=l}\approx 0$, the $\overline{Nu}$ number approaches the following limit, as (6-32) shows:

$$\overline{Nu}_{\infty} = \frac{1}{2}\,Pe\,\frac{d}{l}, \tag{6-33}$$

which in the given case is no longer constant, but varies in inverse proportion to the reduced length. We note that Eq. (6-33) can be obtained directly from the heat balance.

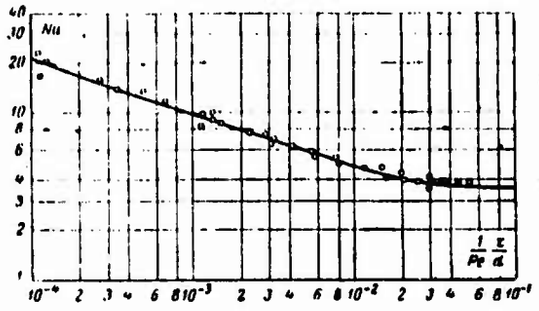

Fig. 6-3. Comparison of theoretical results and experimental data. Solid line) Graetz-Nusselt solution; circles) experiments of Ya. M. Rubinshteyn.

The results ofthe theoretical computation are well confirmed by experiment when the experimental conditions correspond to the assumptions used in solving the problem. Figure 6-6 compares the theoretical relationship (6-26) with experimental data of Ya.M. Rubinshteyn, obtained by the diffusion-analogy method [9]. These experiments are characteristic in that they were a practical realization of all the basic assumptions underlying the theoretical calculation. As the figure shows, within the limits of experimental accuracy, the empirical data are in good agreement with the results of the theoretical calculation.

In making practical application of the theoretical equations, we must remember the restrictions formulated at the beginning of this section (Assumptions 1-7). Later we shall consider problems in which some of these restrictions are removed.

6-2. HEAT EXCHANGE IN A FLAT TUBE WITH CONSTANT WALL TEMPERATURE

While retaining all the conditions and restrictions of the preceding problem, let us change the system geometry alone. Let the liquid flow in a flat tube, i.e., between two infinite plates separated by a distance $h = 2r_0$.[3]

We locate the origin at the center plane of the tube. The x axis is directed along the flow, and the y axis perpendicular to hhe wall. the values $x < 0$ correspond to the damping segment, within which the temperature field is uniform. Values $x \geq 0$ correspond to the heat-exchange segment; at the entrance to this segment, the fluid temperature is constant over a section; the wall temperature in this segment is constant over the surface.

With allowance for the restrictions formulated at the beginning of the preceding section (Assumptions 1-7), we write the energy equation for the problem in the form

$$w_x \frac{\partial t}{\partial x} = a \frac{\partial^2 t}{\partial y^2}.$$

Since the flow is stabilized, then according to (5-11)

$$w_x = \frac{3}{2} \bar{w} \left(1 - \frac{y^2}{r_0^2}\right),$$

where y is the distance from the tube axis to the point under consideration.

We substitute the expression for w_x into the energy equation. After conversion to dimensionless form, we obtain

$$\frac{\partial^2 \theta}{\partial Y^2} = (1 - Y^2) \frac{\partial \theta}{\partial X}, \qquad (6\text{-}34)$$

where

$$\theta = \frac{t - t_0}{t_0 - t_0}; \; Y = \frac{y}{r_0}; \; X = \frac{8}{3} \frac{1}{\mathrm{Pe}} \frac{x}{h}; \; \mathrm{Pe} = \frac{\bar{w} h}{a}.$$

The boundary conditions are written as

[3] /137

TABLE 6-3

Eigenfunctions in Problem of Heat Exchange in Flat Tube at t_s = const

Y	ψ_0	ψ_1	ψ_2	ψ_3	ψ_4	ψ_5
0,00	1,000000	1,000000	1,000000	1,000000	1,000000	1,000000
0,05	0,996469	0,960101	0,885460	0,775528	0,634685	0,468544
0,10	0,985918	0,843772	0,568534	0,203664	—0,193675	—0,560642
0,15	0,968474	0,660700	0,122495	—0,459406	—0,882896	—1,000849
0,20	0,944313	0,426158	—0,351258	—0,921270	—0,941399	—0,398588
0,25	0,913809	0,158833	—0,748049	—0,985885	—0,337119	0,615439
0,30	0,877224	—0,120471	—0,984308	—0,634258	0,501492	1,016112
0,35	0,835000	—0,391132	—1,015180	—0,021446	1,007459	0,424512
0,40	0,787600	—0,634506	—0,841406	0,601586	0,863177	—0,573740
0,45	0,735584	—0,835425	—0,504825	0,997970	0,181310	—1,057742
0,50	0,679303	—0,983217	—0,074980	1,035010	—0,612118	—0,627170
0,55	0,619481	—1,072154	0,368669	0,719609	—1,068827	0,323114
0,60	0,556603	—1,101348	0,753970	0,174334	—0,971307	1,036029
0,65	0,491205	—1,074172	1,028753	—0,424459	—0,406126	1,022915
0,70	0,423798	—0,997324	1,166876	—0,914201	0,340922	0,350528
0,75	0,354860	—0,879678	1,167602	—1,192769	0,963222	—0,532402
0,80	0,284819	—0,731087	1,049901	—1,232895	1,270307	—1,165137
0,85	0,214048	—0,561247	0,844080	—1,068439	1,231402	—1,329442
0,90	0,142850	—0,378731	0,583116	—0,765623	0,928494	—1,071980
0,95	0,071454	—0,190228	0,295444	—0,393116	0,485424	—0,573428
1,00	0,000000	0,000000	0,000000	0,000000	0,000000	0,000000

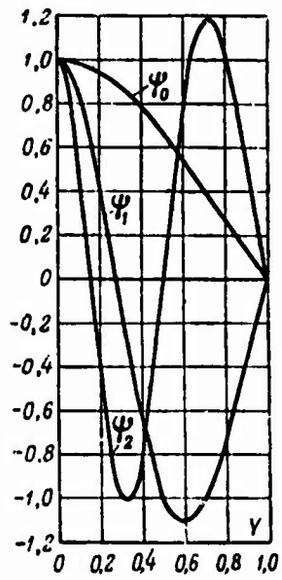

Fig. 6-7. Function $\psi_n(Y)$ for heat exchange in a flat tube at t_s = const.

$$\left.\begin{aligned} &\text{for } X=0 \text{ and } -1<Y<1 \quad \theta=1;\\ &\text{for } X\geqslant 0 \text{ and } Y=0 \quad \frac{\partial\theta}{\partial Y}=0;\\ &\text{for } X\geqslant 0 \text{ and } Y=\pm 1 \quad \theta=0. \end{aligned}\right\} \qquad (6\text{-}35)$$

1. As in the case of a round tube, we solve this problem by separation of variables. To do this, we represent θ as

$$\theta(X, Y)=\varphi(X)\psi(Y).$$

Substituting this expression into (6-34) and separating the variables, we find that (6-34) corresponds to two ordinary differential equations:

$$\frac{\partial\varphi}{\partial X}+\varepsilon^2\varphi=0,$$

$$\frac{d^2\psi}{dY^2}+\varepsilon^2(1-Y^2)\psi=0,$$

where ε^2 is an unknown constant.

The integral of the first equation is

$$\varphi=Ae^{-\varepsilon^2 X},$$

where A is a second unknown constant.

The solution of the second equation can be represented as the following series:

$$\psi(Y)=\sum_{n=0}^{\infty} b_{2n}Y^{2n}. \qquad (6\text{-}36)$$

Substituting this expression into the second equation, we obtain recursion relationships for the coefficients b_{2n}:

$$b_0=1^* \qquad (n=0);$$

$$b_2=-\frac{b_0}{2}\varepsilon^2 \qquad (n=1);$$

$$b_{2n}=\frac{\varepsilon^2}{2n(2n-1)}(b_{2n-4}-b_{2n-2}) \quad (n\geqslant 2).$$

Satisfying the condition at the wall, i.e., the third boundary condition of (6-35), we obtain

$$\sum_{n=0}^{\infty} b_{2n}=0.$$

From this we can find the eigenvalues ε_n ($n=0, 1, 2 \ldots$) of the problem; to each eigenvalue there corresponds an eigenfunction $\psi(Y, \varepsilon_n)=\psi_n(Y)$. Tables 6-3 and 6-4 show the values of $\psi_n(Y)$ and ε_n according to published data [6]. The first three eigenfunctions are shown in Fig. 6-7.

As was shown in [7], for sufficiently large ε_n, the follow-

*/137

ing relationship holds:

$$\varepsilon_n = 4n + \frac{5}{3} \quad (n = 0, 1, 2 \ldots),$$

which can be used in practice when $n \geq 3$.

Thus the general solution of the problem will have the form

$$\theta = \sum_{n=0}^{\infty} A_n \psi_n(Y) \exp\left(-\frac{8}{3} \varepsilon_n^2 \frac{1}{\mathrm{Pe}} \frac{x}{h}\right). \qquad (6\text{-}37)$$

The coefficients A_n of the series are found from the boundary condition at the entrance section, (6-35):

$$\theta(0, Y) = \sum_{n=0}^{\infty} A_n \psi_n(Y) = 1.$$

Using arguments completely analogous to those of §6-1, and the condition for orthogonality of the eigenfunctions, which in this case will have the form

$$\int_{-1}^{+1} \psi_n \psi_m (1 - Y^2)\, dY = 0,$$

we obtain an expression for the coefficients of Series (6-37):

$$A_n = \frac{\int_{-1}^{+1} \theta(0, Y) \psi_n(Y)(1 - Y^2)\, dY}{\int_{-1}^{+1} \psi_n^2(Y)(1 - Y^2)\, dY}. \qquad (6\text{-}38)$$

TABLE 6-4

Eigenvalues and Constants in Problem of Heat Exchange in Flat Tube for t_s = const

n	ε_n	ε_n^2	A_n	B_n
0	1,6815953	2,8277628	+1,2008303	0,85808650
1	5,6698573	32,147282	—0,2991606	0,56946270
2	9,6682395	93,474913	+0,16082646	0,47606545
3	13,667661	186,80496	—0,10743664	0,42397375
4	17,667374	312,13610	+0,07964607	0,389108655
5	21,667205	469,46777	—0,06277565	0,36346500
6	25,667096	658,79982	+0,05151921	0,34347545
7	29,667021	880,13214	—0,04351073	0,32726570
8	33,666966	1133,4646	+0,03754180	0,31373925
9	37,666924	1418,7972	—0,03293327	0,30220410

It can be shown that for θ (0, Y) = 1,[4]

$$A_n = -\frac{2}{\varepsilon_n \left(\frac{\partial \psi}{\partial \varepsilon}\right)_{\varepsilon=\varepsilon_n,\ Y=1}}. \qquad (6\text{-}38a)$$

Calculating the derivatives with the aid of (6-36), we can use (6-38a) to find the values of A_n (Table 6-4).

We determine the mean mass temperature of the fluid:

$$\bar{t} = \frac{1}{r_0 \bar{w}} \int_0^{r_0} t w_x \, dy.$$

Taking (5-11) into account and reducing the expression for t to dimensionless form, we obtain

$$\bar{\theta} = \frac{\bar{t} - t_c}{t_0 - t_c} = \frac{3}{2} \int_0^1 \theta (1 - Y^2) \, dY. \qquad (6\text{-}39)$$

Substituting in the value of θ from (6-37), we obtain

$$\bar{\theta} = \frac{3}{2} \sum_{n=0}^{\infty} A_n \exp\left(-\frac{8}{3} \varepsilon_n^2 \frac{1}{\mathrm{Pe}} \frac{x}{h}\right) \int_0^1 \psi_n(Y)(1 - Y^2) \, dY.$$

Integrating the differential equation for ψ and allowing for the second boundary condition of (6-35), we find

$$\int_0^1 \psi_n(Y)(1 - Y^2) \, dY = -\frac{1}{\varepsilon_n^2} \left(\frac{d\psi_n}{dY}\right)_{Y=1}.$$

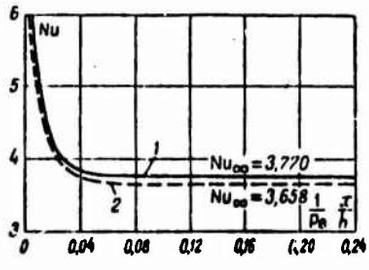

Fig. 6-8. Variation in Nu along tube length. 1) Flat tube; 2) round tube (in this case h corresponds to d).

Thus the final expression for $\bar{\theta}$ can be written as

$$\bar{\theta} = 3 \sum_{n=0}^{\infty} \frac{B_n}{\varepsilon_n^2} \exp\left(-\frac{8}{3} \varepsilon_n^2 \frac{1}{\mathrm{Pe}} \frac{x}{h}\right), \qquad (6\text{-}40)$$

where

$$B_n = -\frac{1}{2} A_n \left(\frac{d\psi_n}{d\bar{r}}\right)_{\bar{r}=1}.$$

Table 6-4 shows the values of B_n.

Relationship (6-40) is illustrated in Fig. 6-3, which also gives the curve for a round tube. The flat-tube curve is not as steep as the one for the round tube. The reason is that the ratio of perimeter to tube cross-sectional area is smaller in the first case than in the second; thus the fluid is cooled more slowly in the flat tube than in the round.

Let us determine the local Nu number, referring the heat-transfer coefficient to the local temperature difference $t_s - \bar{t}$. Then

$$\mathrm{Nu} = \frac{\alpha h}{\lambda} = -\frac{2}{\bar{\theta}} \left(\frac{\partial \theta}{\partial \bar{r}}\right)_{\bar{r}=1}.$$

Substituting the value of θ from (6-37) and $\bar{\theta}$ from (6-40) into this expression, we obtain

$$\mathrm{Nu} = \frac{4 \sum_{n=0}^{\infty} B_n \exp\left(-\frac{8}{3} \varepsilon_n^2 \frac{1}{\mathrm{Pe}} \frac{x}{h}\right)}{3 \sum_{n=0}^{\infty} \frac{B_n}{\varepsilon_n^2} \exp\left(-\frac{8}{3} \varepsilon_n^2 \frac{1}{\mathrm{Pe}} \frac{x}{h}\right)}. \qquad (6\text{-}41)$$

Letting $\frac{1}{\mathrm{Pe}} \frac{x}{h}$ go to infinity, we find the limiting Nusselt number:

$$\mathrm{Nu}_\infty = \frac{4}{3} \varepsilon_0^2 = 3{,}770. \qquad (6\text{-}42)$$

If we find the length of the thermal initial segment from the condition $\mathrm{Nu}_{x=l_{n.т}} = 1{,}01\,\mathrm{Nu}_\infty$, the value will be

$$\frac{l_{n.т}}{h} = 0{,}055\,\mathrm{Pe}.$$

Relationship (6-41) is shown in Fig. 6-8. This figure also shows the corresponding curve for a round tube. The two curves are quite close. Thus for a flat tube Nu_∞ is 3% greater than for a round tube. The lengths of the thermal initial segments are also nearly the same.

Let us determine the mean integral heat-transfer coefficient, or the corresponding mean Nusselt number:

$$\overline{\mathrm{Nu}} = \frac{\bar{\alpha} h}{\lambda} = \frac{1}{l} \int_0^l \mathrm{Nu}\, dx.$$

Carrying out calculations similar to those for a round tube (see §6-1), we obtain

$$\overline{\mathrm{Nu}} = -\frac{1}{2}\,\mathrm{Pe}\,\frac{h}{l}\,\ln\bar{\theta}_{x=l},$$

or

$$\overline{\mathrm{Nu}} = -\frac{1}{2}\,\mathrm{Pe}\,\frac{h}{l}\,\ln\left[3\sum_{n=0}^{\infty}\frac{B_n}{\varepsilon_n^2}\exp\left(-\frac{8}{3}\,\varepsilon_n^2\,\frac{1}{\mathrm{Pe}}\,\frac{l}{h}\right)\right]. \qquad (6\text{-}43)$$

2. We can also construct another (approximate) solution for the heat-exchange problem in a flat tube. For flow with a velocity profile that is uniform over a section (bar flow) the energy equation will be similar in representation to the heat-conduction equation, and the problem of heat exchange in a flat tube reduces to the problem of unsteady heat conduction in an infinite plate at t_s = const. As we know, the eigenfunctions of this problem have the form $\cos\left[(2m+1)\frac{\pi Y}{2}\right]$, where the m are integers from 0 to ∞. On the basis of this result, we can represent the eigenfunctions ψ_n of (6-34) as the following series in cosines, as was proposed in [15]:

$$\psi_n = \sum_{m=0}^{\infty} b_{nm}\cos\left[(2m+1)\frac{\pi}{2}Y\right].$$

By an appropriate choice of series coefficients, we can allow for the change in velocity over a section, i.e., for the presence of the function Y^2 in (6-34).

Then the general solution of the problem will have the form

$$\theta = \sum_{n=0}^{\infty}\left[\sum_{m=0}^{\infty} b_{nm}\cos\frac{(2m+1)\pi Y}{2}\right]\exp(-\varepsilon_n^2 X). \qquad (6\text{-}44)$$

We keep only five terms of the series, i.e., the of m and n will vary from 0 to 4. Substituting (6-44) into (6-34), after regrouping of the terms we have

$$(1-Y^2)\left[b_{n_0}\cos\frac{\pi Y}{2}+b_{n_1}\cos\frac{3\pi Y}{2}+\ldots+b_{n_4}\cos\frac{9\pi Y}{2}\right]-\left[\left(\frac{\pi}{2\varepsilon_n}\right)^2\times\right.$$
$$\left.\times\, b_{n_0}\cos\frac{\pi Y}{2}+\left(\frac{3\pi}{2\varepsilon_n}\right)^2 b_{n_1}\cos\frac{3\pi Y}{2}+\ldots+\left(\frac{9\pi}{2\varepsilon_n}\right)^2 b_{n_4}\cos\frac{9\pi Y}{2}\right]=0. \qquad (6\text{-}45)$$

We separately multiply Eq. (6-45) and $\cos\frac{\pi Y}{2}, \cos\frac{3\pi Y}{2}, \ldots, \cos\frac{9\pi Y}{2}$, and in each case integrate the equation with respect to Y from 0 to 1. Performing this operation for each harmonic of the cosine, we obtain the following system of five equations:

$$\left.\begin{aligned}
&\left(-\frac{\pi^2}{3}-1+\frac{\pi^4}{8\varepsilon_n^2}\right)b_{n0}-\frac{3}{4}b_{n1}+\frac{5}{36}b_{n2}-\frac{7}{144}b_{n3}+\frac{9}{400}b_{n4}=0;\\
&-\frac{3}{4}b_{n0}+\left(-\frac{\pi^2}{3}-\frac{1}{9}+\frac{9\pi^4}{8\varepsilon^2}\right)b_{n1}-\frac{15}{16}b_{n2}+\frac{21}{100}b_{n3}-\frac{1}{12}b_{n4}=0;\\
&\frac{5}{36}b_{n0}-\frac{15}{16}b_{n1}+\left(-\frac{\pi^2}{3}-\frac{1}{25}+\frac{25\pi^4}{8\varepsilon_n^2}\right)b_{n2}-\frac{35}{36}b_{n3}+\frac{45}{196}b_{n4}=0;\\
&-\frac{7}{144}b_{n0}+\frac{21}{100}b_{n1}-\frac{35}{36}b_{n2}+\left(-\frac{\pi^2}{3}-\frac{1}{49}+\frac{49\pi^4}{8\varepsilon_n^2}\right)b_{n3}-\frac{63}{64}b_{n4}=0;\\
&\frac{9}{400}b_{n0}-\frac{1}{12}b_{n1}+\frac{45}{196}b_{n2}-\frac{63}{64}b_{n3}+\left(-\frac{\pi^2}{3}-\frac{1}{81}+\frac{81\pi^4}{8\varepsilon_n^2}\right)b_{n4}=0.
\end{aligned}\right\} \qquad (6\text{-}46)$$

TABLE 6-5

Values of Constants in Eq. (6-47) (Problem of Heat Exchange in a Flat Tube with t_s = const)

n	ε_n^2	b_{n0}	$\frac{b_{n1}}{b_{n0}}$	$\frac{b_{n2}}{b_{n0}}$	$\frac{b_{n3}}{b_{n0}}$	$\frac{b_{n4}}{b_{n0}}$
0	2,82776	1,17776	0,0211834	−0,00113696	$0,207037\cdot10^{-4}$	$-0,586707\cdot10^{-4}$
1	32,1475	0,0579815	−5,37195	−0,838871	0,0230768	−0,0193795
2	93,4792	0,0165696	−4,00649	9,45808	3,31526	0,101483
3	187,388	0,0070883	−3,59673	7,94700	−12,0113	−7,12402
4	414,761	0,0138607	−3,32432	6,61879	−11,0745	13,7624

Since these are homogeneous equations, b_{nm} can be nonzero only if the determinant for their coefficients equals zero and, consequently, the ε_n^2 are the roots of the coefficient determinant. Table 6-5 shows values of ε_n^2, determined by computer. They are in good agreement with the values obtained for ε_n^2 by another method (see Table 6-4), with the exception of ε_4^2. The discrepancy in ε_4^2 is explained by the fact that only a five-term approximation was used in the computations.

Since the ε_n^2 are known, we can now determine the values of b_{nm}. It turns out that System (6-46) cannot be solved so as to determine all the values b_{nm}. By dividing each equation of System (6-46) by b_{n0} and solving any four of the five equations, however, we can find the ratios b_{n1}/b_{n0}, b_{n2}/b_{n0}, etc.; the values of b_{n0} will still be unknown. The solution of (6-44) can now be written as

$$\theta=\sum_{n=0}^{4}b_{n0}\left[\cos\frac{\pi Y}{2}+\sum_{m=1}^{4}\frac{b_{nm}}{b_{n0}}\cos\frac{(2m+1)\pi Y}{2}\right]\exp(-\varepsilon_n^2 X), \qquad (6\text{-}47)$$

where the $\frac{b_{nm}}{b_{n0}}$ are unknown.

To determine the b_{n0}, we use the boundary condition at the entrance ($\theta=1$ for $X=0$),; this leads to the equation

$$1 = \sum_{n=0}^{4} b_{n0}\left[\cos\frac{\pi Y}{2} + \sum_{m=1}^{4}\frac{b_{nm}}{b_{n0}}\cos\frac{2m+1}{2}\pi Y\right].$$

Multiplying this equation separately by each of the values $\cos\left[(2m+1)\times\frac{\pi Y}{2}\right]$ and integrating them with respect to Y from 0 to 1, we obtain a system of five equations:

$$\sum_{n=0}^{4} b_{n0} = \frac{4}{\pi};$$

$$\sum_{n=0}^{4}\left(\frac{b_{nm}}{b_{n0}}\right)b_{n0} = (-1)^m\frac{4}{(2m+1)\pi};\quad m = 1, 2, 3, 4.$$

Solving this system, we find the b_{n0}. The numerical values of the constants occurring in (6-47) are given in Table 6-5. By using (6-47), it is not difficult to compute all the other heat-exchange characteristics, including the Nusselt number.

6-3. HEAT EXCHANGE IN THE THERMAL INITIAL SEGMENTS OF ROUND AND FLAT TUBES WITH CONSTANT WALL TEMPERATURE (APPROXIMATE SOLUTION)

As we have already noted, for fluids with Pr >> 1, the reduced length of a tube in actual equipment will usually be less than the reduced length of the thermal initial segment. For this case it is possible to obtain an approximate solution to the problem of heat exchange in round and flat tubes in finite form, as has been done by Leveque [16].[5] All the restrictions 1-7 (see §6-1) are retained

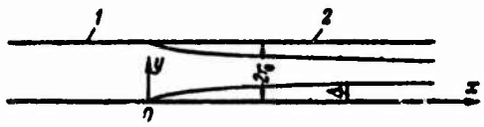

Fig. 6-9. Solution of the Leveque problem. 1) Damping segment; 2) heated segment; Δ) width of thermal boundary layer.

in solution of this problem, and still another is added: the width Δ of the thermal boundary layer appearing at the wall is assumed to be small as compared with the diameter of the round tube or the width of the flat tube (Fig. 6-9). In other words, the temperature in the flow core is assumed to be constant along the radius and length, and equal to the fluid temperature at the entrance to the heated segment. This condition is clearly satisfied only for small values of reduced length (smaller than the reduced length of the thermal initial segment).

The energy equation for this problem is easily found from (6-1), letting $w_r = w_e = 0$ and $\frac{\partial^2 t}{\partial x^2} = \frac{\partial^2 t}{\partial \varphi^2} = 0$ in accordance with the conditions

dopted. If, in addition, we replace the coordinate r by the coordinate $y = r_0 - r$ (i.e., the coordinate measured from the wall), we then obtain

$$w_x \frac{\partial t}{\partial x} = a \frac{1}{r_0 - y} \cdot \frac{\partial}{\partial y}\left[(r_0 - y)\frac{\partial t}{\partial y}\right].$$

Since $\Delta \ll r_0$, then within the thermal boundary layer $(0 \leqslant y \leqslant \Delta)$ the quantity y in the energy equation can be neglected as compared with r_0. Then this equation will look like this:

$$w_x \frac{\partial t}{\partial x} = a \frac{\partial^2 t}{\partial y^2}.$$

This equation will be exact for heat exchange in a flat tube (the wall radius of curvature $r_0 \to \infty$); it will be approximate for heat exchange in a round tube, since we have replaced the cylindrical boundary layer by a flat layer, which is permissible when the layer is thin.

The velocity distribution in a round tube is described by the equation

$$w_x = 2\bar{w}\left(1 - \frac{r^2}{r_0^2}\right) = 8\bar{w}\left(\frac{y}{d} - \frac{y^2}{d^2}\right),$$

and in a flat tube by the equation

$$w_x = 6\bar{w}\left(\frac{y}{h} - \frac{y^2}{h^2}\right),$$

where $d = 2r_0$ is the round-tube diameter and $h = 2r_0$ is the flat-tube width.

For values $y \ll r_0$, we can neglect the quadratic terms in the expressions for w_x as compared with the linear terms, i.e., we can assume that the velocity distribution in the thermal boundary layer is represented by a straight line tangent at the wall to the Poiesuille parabola. We can then let

$$w_x = Ay,$$

in the energy equation, where $A = (dw_x/dy)_{y=0}$ is the velocity gradient at the wall; for a round tube, $A = 8\bar{w}/d$, and for a flat tube $A = 6\bar{w}/h$.

As a result, the energy equation takes the form

$$Ay \frac{\partial t}{\partial x} = a \frac{\partial^2 t}{\partial y^2}. \qquad (6\text{-}48)$$

The assumption that the thermal boundary layer is thin permits us to formulate the boundary conditions in a form convenient for integration:

$$\left.\begin{aligned} &\text{for } x \geqslant 0 \text{ and } y = \infty \quad t = t_0^*; \\ &\text{for } x \geqslant 0 \text{ and } y = 0 \quad t = t_c, \end{aligned}\right\} \qquad (6\text{-}49)$$

where t_0 is the fluid temperature at the entrance to the heated segment; t_s is the wall temperature.

Equation (6-48) can be solved exactly for boundary conditions (6-49).

We introduce the new independent variable

$$\eta=\left(\frac{A}{9ax}\right)^{1/3}y$$

We now find the expressions for the derivatives:

$$\frac{\partial t}{\partial y}=\frac{dt}{d\eta}\frac{\partial\eta}{\partial y}=\left(\frac{A}{9ax}\right)^{1/3}\frac{dt}{d\eta};$$

$$\frac{\partial^2 t}{\partial y^2}=\frac{d}{d\eta}\left(\frac{\partial t}{\partial y}\right)\frac{\partial\eta}{\partial y}=\left(\frac{A}{9ax}\right)^{2/3}\frac{d^2t}{d\eta^2};$$

$$\frac{\partial t}{\partial x}=\frac{dt}{d\eta}\frac{\partial\eta}{\partial x}=-\frac{1}{3}\left(\frac{A}{9ax}\right)^{1/3}\frac{y}{x}\frac{dt}{d\eta}.$$

Substituting the last two expressions for the derivatives into (6-48), we see that this equation reduces to the ordinary differential equation

$$\frac{d^2t}{d\eta^2}+3\eta^2\frac{dt}{d\eta}=0. \qquad (6\text{-}50)$$

Boundary conditions (6-49) take the form

$$\left.\begin{array}{l}\text{for } \eta=\infty\ t=t_0;\\ \text{for } \eta=0\ \ t=t_c.\end{array}\right\} \qquad (6\text{-}51)$$

Integrating (6-50), we obtain

$$\frac{dt}{d\eta}=c_1e^{-\eta^3}$$

and

$$t=c_1\int_0^\eta e^{-\eta^3}d\eta+c_2.$$

TABLE 6-6

Values of Dimensionless Temperature As a Function of η According to Eq. (6-52)

η	$\frac{t-t_c}{t_0-t_c}$	η	$\frac{t-t_c}{t_0-t_c}$	η	$\frac{t-t_c}{t_0-t_c}$
0,0	0	0,70	0,7227	1,40	0,9897
0,05	0,0560	0,75	0,7610	1,45	0,9928
0,10	0,1120	0,80	0,7962	1,50	0,9951
0,15	0,1680	0,85	0,8281	1,55	0,9968
0,20	0,2235	0,90	0,8568	1,60	0,9979
0,25	0,2788	0,95	0,8821	1,65	0,9987
0,30	0,3337	1,00	0,9043	1,70	0,9991
0,35	0,3878	1,05	0,9234	1,75	0,9994
0,40	0,4409	1,10	0,9395	1,80	0,9997
0,45	0,4927	1,15	0,9530	1,85	0,9998
0,50	0,5430	1,20	0,9641	1,90	0,9999
0,55	0,5915	1,25	0,9730	1,95	0,9999
0,60	0,6377	1,30	0,9801	2,00	1,0000
0,65	0,6816	1,35	0,9856		

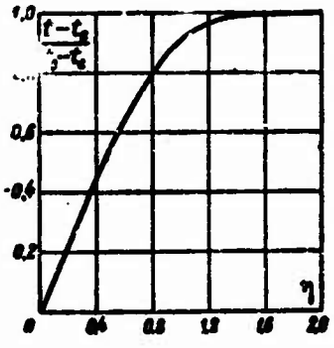

Fig. 6-10. Dimensionless temperature as a function of η.

The constants of integration are found from boundary conditions (6-51). The second condition yields $c_2 = t_s$, and the first condition gives

$$c_1 = \frac{t_0 - t_s}{\int_0^\infty e^{-\eta^3} d\eta}.$$

Thus the equation for the temperature distribution has the form

$$\frac{t - t_s}{t_0 - t_s} = \frac{\int_0^\eta e^{-\eta^3} d\eta}{\int_0^\infty e^{-\eta^3} d\eta}. \qquad (6\text{-}52)$$

The denominator of (6-52) is a gamma function, whose values have been tabulated:

$$\int_0^\infty e^{-\eta^3} d\eta = \Gamma\left(\frac{4}{3}\right) = 0{,}8930.$$

Table 6-6 shows the values of the dimensionless temperature, computed from Eq. (6-52). Figure 6-10 shows a graph of this function.

Let us now determine the local heat-transfer coefficient, referred to the difference between the wall temperature and the temperature of the fluid at the entrance to the heated segment. This is a convenient method for determining α in this case, since when $\frac{1}{Pe} \cdot \frac{x}{d}$ is small, the mean mass temperature of the fluid varies little with the length,

$$\alpha_0 = \frac{q_0}{t_0 - t_s} = -\frac{\lambda}{t_0 - t_s}\left(\frac{\partial t}{\partial y}\right)_{y=0}.$$

Using the relationships obtained previously, we find

$$\left(\frac{\partial t}{\partial y}\right)_{y=0} = \left(\frac{A}{9ax}\right)^{1/3}\left(\frac{dt}{d\eta}\right)_{\eta=0} = \left(\frac{A}{9ax}\right)^{1/3}\frac{t_0 - t_s}{0{,}893}.$$

Consequently,

$$\alpha_0 = \frac{\lambda}{0{,}893}\left(\frac{A}{9ax}\right)^{1/3}. \qquad (6\text{-}53)$$

The mean heat-transfer coefficient is

$$\bar{\alpha}_0 = \frac{1}{l}\int_0^l \alpha_0 dx = \frac{3}{2}\cdot\frac{\lambda}{0{,}893}\left(\frac{A}{9al}\right)^{1/3}. \qquad (6\text{-}54)$$

Substituting the value $A = \frac{8\bar{w}}{d}$, into (6-53) and (6-54), we obtain expressions for the local and mean Nusselt numbers in the initial

segment of a round tube:

$$\mathrm{Nu}_0=\frac{\alpha_0 d}{\lambda}=1{,}077\left(\mathrm{Pe}\frac{d}{x}\right)^{1/3}, \qquad (6\text{-}55)$$

$$\overline{\mathrm{Nu}}_0=\frac{\bar{\alpha}_0 d}{\lambda}=1{,}615\left(\mathrm{Pe}\frac{d}{l}\right)^{1/3}, \qquad (6\text{-}56)$$

where $\mathrm{Pe}=\frac{\bar{w}d}{a}$.

Substituting the value $A=\frac{6\bar{w}}{h}$ into (6-53) and (6-54), we obtain analogous expressions for a flat tube:

$$\mathrm{Nu}_0=\frac{\alpha_0 h}{\lambda}=0{,}978\left(\mathrm{Pe}\frac{h}{x}\right)^{1/3}, \qquad (6\text{-}57)$$

$$\overline{\mathrm{Nu}}_0=\frac{\bar{\alpha}_0 h}{\lambda}=1{,}467\left(\mathrm{Pe}\frac{h}{l}\right)^{1/3}, \qquad (6\text{-}58)$$

where $\mathrm{Pe}=\frac{\bar{w}h}{a}$.

To compare the approximate solutions obtained with the exact solutions of the same problems (see §§6-1 and 6-2), in (6-55) and (6-57) we must go from $\mathrm{Nu}_0=\frac{q_c d}{\lambda(t_c-t_0)}$ (for a round tube) to $\mathrm{Nu}=\frac{q_c d}{\lambda(t_c-\bar{t})}$, where $\bar{t}$ is the mean mass temperature of the fluid in the given section. Here Nu and Nu_0 are connected by the relationship

$$\mathrm{Nu}=\mathrm{Nu}_0\frac{t_0-t_c}{\bar{t}-t_c}.$$

The value of $\bar{t}$ is easily found from the heat-balance equation. For a round tube we have

$$\frac{d\bar{t}}{dx}=-\frac{2\pi r_0\lambda\left(\frac{\partial t}{\partial y}\right)_{y=0}}{\pi r_0^2\rho c_p\bar{w}}=-\frac{4(t_0-t_c)}{0{,}893}\cdot\frac{1}{\mathrm{Pe}}\left(\frac{A}{9ax}\right)^{1/3}.$$

Integrating this expression from 0 to x and substituting $A = 8\bar{w}/d$ into it, we obtain

$$\frac{\bar{t}-t_c}{t_0-t_c}=1-6{,}46\left(\frac{1}{\mathrm{Pe}}\cdot\frac{x}{d}\right)^{2/3}.$$

Thus if the heat-transfer coefficient is referred to the local temperature head $\left(\alpha=\frac{q_c}{t_c-\bar{t}}\right)$, then (6-55) will take the form

$$\mathrm{Nu}=\frac{\alpha d}{\lambda}=\frac{1{,}077\left(\frac{1}{\mathrm{Pe}}\cdot\frac{x}{d}\right)^{-1/3}}{1-6{,}46\left(\frac{1}{\mathrm{Pe}}\cdot\frac{x}{d}\right)^{2/3}}. \qquad (6\text{-}55a)$$

It is not difficult to obtain an analogous equation for a flat tube.

In Fig. 6-11, Eqs. (6-55) and (6-55a) are compared with the exact solution (6-26) for a round tube.

For values $\frac{1}{\mathrm{Pe}}\cdot\frac{x}{d}<0{,}0005$, Eq. (6-55a) [which should also be compared directly with (6-26)] gives values of Nu that are no more than 8-10% above those found with the exact solution. When $\frac{1}{\mathrm{Pe}}\cdot\frac{x}{d}>0{,}0005$

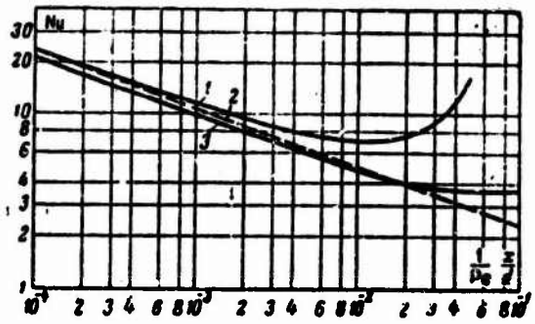

Fig. 6-11. The Nu number as a function of $\frac{1}{Pe}\cdot\frac{x}{d}$ for a round tube. 1) Eq. (6-55a); 2) Eq. (6-55); 3) exact solution (6-26).

the difference between (6-55a) and (6-26) increases, since as the reduced length becomes greater, the thermal boundary layer becomes thicker, and becomes commensurate with the tube diameter. The Leveque solution then ceases to apply.

Thus Eq. (6-55a) can be used with an error not exceeding 8-10% only when $\frac{1}{Pe}\cdot\frac{x}{d}<0{,}0005$. In this region, the difference between the initial $(t_s - t_0)$ and local $(t_s - \bar{t})$ temperature heads is insignificant, and thus the values obtained for Nu from (6-55a) and (6-55) almost agree.

Equation (6-55) is in better agreement with the exact solution over a wider range of $\frac{1}{Pe}\cdot\frac{x}{d}$; this does not mean, however, that it is more accurate or that it is applicable over a broader region. The error in determination of the heat flow with (6-55) and (6-55a) will naturally be the same for any $\frac{1}{Pe}\cdot\frac{x}{d}$

The fairly good agreement between the curves for (6-55) and (6-26) in the $\frac{1}{Pe}\cdot\frac{x}{d}<0{,}01$ region indicates that an equation of the type (6-55) can be used for interpolation in approximate representation of the exact solution (6-26). The equation

$$Nu=\frac{\alpha d}{\lambda}=1{,}03\left(\frac{1}{Pe}\frac{x}{d}\right)^{-\frac{1}{3}} \qquad (6\text{-}59)$$

can be used as such an interpolation formula, in particular; with an error of roughly $\pm 3\%$, it describes the exact solution in the region of values $\frac{1}{Pe}\cdot\frac{x}{d}\leq 0{,}01$ and is in good agreement with the experimental data (see §7-5).

The corresponding interpolation equation for the mean integral heat-transfer coefficient has the form

$$\overline{Nu}=\frac{\bar{\alpha} d}{\lambda}=1{,}55\left(\frac{1}{Pe}\frac{x}{d}\right)^{-1/3} \qquad (6\text{-}60)$$

and will be valid with the same accuracy for values $\frac{1}{\mathrm{Pe}}\cdot\frac{l}{d}\leqslant 0{,}05$.

The heat-transfer coefficients in (6-59) and (6-60) should naturally refer to the local and mean logarithmic temperature heads, respectively; only when $\frac{1}{\mathrm{Pe}}\cdot\frac{x}{d}<0{,}0005$ can they be replaced by the initial value.

We note that the lengths of tubes employed in heat exchangers usually satisfy the inequality $\frac{1}{\mathrm{Pe}}\cdot\frac{l}{d}\leqslant 0{,}05$, and even $\frac{1}{\mathrm{Pe}}\cdot\frac{l}{d}\leqslant 0{,}01$, provided the heat-transport medium is a viscous fluid possessing a fairly high value of Pr.

6-4. HEAT EXCHANGE IN A FLAT TUBE WITH ONE WALL HEAT-INSULATED AND CONSTANT TEMPERATURE AT THE OTHER WALL

We shall consider heat exchange in a flat tube for which the temperature of one wall is held constant; the other wall is heat-insulated. All other conditions are the same as in §6-2.

We locate the origin at the tube wall through which heat exchange takes place and, as usual, direct the x axis along the flow and the y axis along the normal to the wall.

Remembering that the velocity distribution is represented by the equation

$$\frac{w_x}{\bar{w}}=6(Y-Y^2),$$

we can represent the mathematical expectation for the heat-exchange process under these conditions as

$$\frac{\partial^2\theta}{\partial Y^2}=6(Y-Y^2)\frac{\partial\theta}{\partial X}; \tag{6-61}$$

$$\left.\begin{aligned}&\text{for } X=0 \text{ and } 0<Y<1\ \theta=1;\\ &\text{for } X\geqslant 0 \text{ and } Y=0 \quad \theta=0;\\ &\text{for } X\geqslant 0 \text{ and } Y=1 \quad \frac{\partial\theta}{\partial Y}=0.\end{aligned}\right\} \tag{6-62}$$

Here

$$\theta=\frac{t-t_c}{t_0-t_c};\ X=\frac{1}{\mathrm{Pe}}\cdot\frac{x}{h};\ Y=\frac{y}{h};\ \mathrm{Pe}=\frac{\bar{w}h}{a}.$$

The solution of this problem is fully analogous to the solution given in §6-2; thus we at once give the final results.

The fluid temperature at an arbitrary point in the flow is

$$\frac{t-t_c}{t_0-t_c}=\sum_{n=0}^{\infty}A_n\psi_n(Y)\exp\left(-\frac{1}{6}\varepsilon_n^2\frac{1}{\mathrm{Pe}}\cdot\frac{x}{h}\right). \tag{6-63}$$

The mean mass temperature of the fluid is

$$\bar{\theta}=\frac{\bar{t}-t_c}{t_0-t_c}=6\sum_{n=0}^{\infty}\frac{B_n}{\varepsilon_n^2}\exp\left(-\frac{1}{6}\varepsilon_n^2\frac{1}{\mathrm{Pe}}\cdot\frac{x}{h}\right). \tag{6-64}$$

TABLE 6-7

Eigenvalues and Constants in Problem of Heat Exchange in Flat Tube with Constant Temperature in One Wall and Heat Insulation at the Other

n	ε_n	ε_n^2	A_n	B_n
0	3,618667	14,5822	2,176	2,176545
1	11,89723	141,541	1,427	1,427232
2	19,92414	396,971	1,20	1,193603
3	27,93835	780,551	—	1,063792
4	35,94734	1292,21	—	0,9768908
5	43,95364	1931,92	—	0,9129374
6	51,95837	2699,67	—	0,8630460
7	59,96211	3595,45	—	0,8225616
8	67,96519	4619,27	—	0,7887606
9	75,96784	5771,11	—	0,7599269

TABLE 6-8

Values of Eigenfunctions $\psi_n(Y)$ in Problem of Heat Exchange in Flat Tube with Constant Temperature at One Wall and Thermal Insulation at the Other

Y	ψ_0	ψ_1	ψ_2	Y	ψ_0	ψ_1	ψ_2
0	0,0000	0,0000	0,0000	0,6	0,5079	—0,0125	—0,1320
0,1	0,1001	+0,0989	+0,0969	0,7	0,5419	—0,1378	—0,0230
0,2	0,1983	+0,1838	+0,1564	0,8	0,5636	—0,2244	—0,1074
0,3	0,2920	+0,2273	+0,1219	0,9	0,5723	—0,2625	—0,1779
0,4	0,3768	+0,2053	—0,0045	1,0	0,5736	—0,2686	—0,1896
0,5	0,4484	+0,1162	—0,1252				

where $B_n = A_n \left(\frac{d\psi_n}{dY}\right)_{Y=0}$.

The local Nu number, referred to the local temperature difference $t_s - \bar{t}$ is

$$\mathrm{Nu} = \frac{\alpha h}{\lambda} = \frac{\sum_{n=1}^{\infty} B_n \exp\left(-\frac{1}{6}\varepsilon_n^2 \frac{1}{\mathrm{Pe}} \cdot \frac{x}{h}\right)}{6\sum_{n=1}^{\infty} \frac{B_n}{\varepsilon_n^2} \exp\left(-\frac{1}{6}\varepsilon_n^2 \frac{1}{\mathrm{Pe}} \cdot \frac{x}{h}\right)}. \qquad (6\text{-}65)$$

The limiting Nusselt number is

$$\mathrm{Nu}_\infty = \frac{\varepsilon_0^2}{6} = 2{,}430. \qquad (6\text{-}66)$$

The length of the thermal initial segment is

$$\frac{l_{0.1}}{h} \approx 0{,}21\,\mathrm{Pe}. \qquad (6\text{-}67)$$

The eigenvalues ε_n and constants A_n and B_n are given in Table 6-7, and the eigenfunctions $\psi_n(Y)$ for $n = 0$, 1, and 2 in Table 6-8; the data is taken from [18].

For the problem under consideration, the limiting value of Nu_∞ is roughly 35% less than for the problem of heat exchange through both walls of the tube (in this latter case, $\mathrm{Nu}_\infty = 3.77$). The reduction in Nu_∞ is natural, since with one-sided cooling, heat exchange takes place through a fluid layer with thickness 2 times greater than for two-sided cooling. For the same reason, the length of the thermal initial segment is significantly greater for one-sided cooling than for two-sided.

The mean integral Nusselt number will obviously equal

$$\overline{\mathrm{Nu}} = \frac{\bar{\alpha} h}{\lambda} = -\mathrm{Pe}\,\frac{h}{l}\ln\bar{\theta}_{x=l}, \qquad (6\text{-}68)$$

where $\bar{\theta}_{x=l}$ is found from Eq. (6-64).

6-5. HEAT EXCHANGE IN A ROUND TUBE WITH ARBITRARY, IN PARTICULAR LINEAR, VARIATION IN WALL TEMPERATURE

Let the wall temperature of a round tube vary arbitrarily with the length, i.e., $t_s(x)$ is a specified function of x. All remaining conditions remain the same as for the problem of heat exchange with t_s = const (see §6-1).

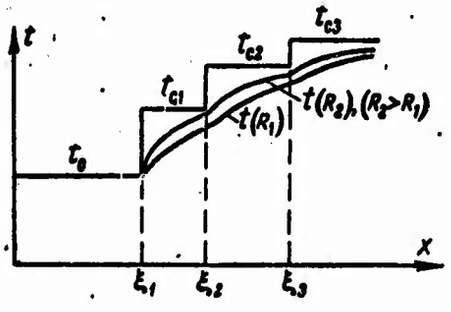

Fig. 6-12. Problem of heat exchange in a round tube with arbitrary variation in wall temperature.

Since the energy equation (6-2) is linear, the solution of the heat-exchange problem for t_s = const can be generalized to the case $t_s(x)$ by the method of superposition [7].

Solution (6-12a) for t_s = const can be represented in the form

$$t-t_0=(t_c-t_0)\left[1-\sum_{n=0}^{\infty}A_n\psi_n(R)\exp(-\varepsilon_n^2X)\right]. \qquad (6\text{-}69)$$

Here, as in §6-1, $X=\frac{2}{Pe}\cdot\frac{x}{d}$, $R=r/r_0$.

The temperature difference $t-t_0$ can be treated as a change in fluid temperature caused by a "source of thermal disturbance" in the form of an abrupt change in wall temperature from t_0 to t_s. This "source" is situated at the origin, i.e., at $X=0$.

If the source is located at the point with coordinate $X=\xi$ (Fig. 6-12), then in place of the preceding equation we must write:

$$t-t_0=(t_c-t_0)\left\{1-\right.$$

$$\left.-\sum_{n=0}^{\infty}A_n\psi_n(R)\exp[-\varepsilon_n^2(X-\xi)]\right\}.$$

When there are several such "disturbance sources," i.e., when there is a stepwise change in wall temperature (Fig. 6-12): $t_{c1}, t_{c2}, \ldots, t_{cm}$ $(i=1, 2, 3, \ldots, m)$, the total variation in fluid temperature can be represented as the sum of the changes produced by the action of each "source":

$$t-t_0=\sum_{i=1}^{m}\Delta t_{ci}\left\{1-\sum_{n=0}^{\infty}A_n\psi_n(R)\exp[-\varepsilon_n^2(X-\xi_i)]\right\},$$

where $\Delta t_{ci}=t_{ci}-t_{c(i-1)}$ is the wall-temperature variation at the point with coordinate ξ_i.

For a continuous wall-temperature variation, going from the sum to the integral, we obtain

$$t-t_0=\int_0^X\left\{1-\sum_{n=0}^{\infty}A_n\psi_n(R)\exp[-\varepsilon_n^2(X-\xi)]\right\}\frac{dt_c}{d\xi}d\xi. \qquad (6\text{-}70)$$

Thus, if we know the solution for $t_s=\text{const}$,

$$\theta(X, R)=\sum_{n=0}^{\infty}A_n\psi_n(R)\exp(-\varepsilon_n^2X),$$

then the solution for an arbitrary continuous wall-tempperature change will look like this:

$$t-t_0=\int_0^X[1-\theta(X-\xi, R)]t'_c(\xi)\,d\xi. \qquad (6\text{-}70a)$$

Let us consider the case of a linear change in wall temperature, i.e.

$$t_c(x)=t_0+kx, \text{ or } t_c(x)=t_0+KX,$$

where k and $K=\frac{k}{2}Ped$ are constants.

Th n $t_s' = K$, and in accordance with (6-70),

$$t-t_0=K\int_0^X\left\{1-\sum_{n=0}^{\infty}A_n\psi_n(R)\exp[-\varepsilon_n^2(X-\xi)]\right\}d\xi.$$

Integrating, we obtain the final equation for the temperature field:

$$t-t_0=KX-K\sum_{n=0}^{\infty}A_n\psi_n(R)\frac{1}{\varepsilon_n^2}[1-\exp(-\varepsilon_n^2X)]. \qquad (6\text{-}71)$$

The mean mass temperature of the fluid is

$$\bar{t}-t_0=4\int_0^1(t-t_0)(1-R^2)R\,dR=4KX\int_0^1(1-R^2)R\,dR-$$

$$-4K\sum_{n=0}^{\infty}A_n\frac{1}{\varepsilon_n^2}[1-\exp(-\varepsilon_n^2X)]\int_0^1\psi_n(R)(1-R^2)R\,dR.$$

Taking (6-17) into account, we obtain

$$\bar{t}-t_0=KX+8K\sum_{n=0}^{\infty}\frac{B_n}{\varepsilon_n^4}[\exp(-\varepsilon_n^2X)-1], \qquad (6\text{-}72)$$

where $B_n=-\frac{1}{2}A_n\left(\frac{d\psi_n}{dR}\right)_{R=1}$.

The eigenvalues ε_n and the constants A_n and B_n, as well as the eigenfunctions $\psi_n(R)$ in these equations are the same as for the problem of heat exchange with t_s = const (see §6-1). They are given in Tables 6-1 and 6-2.

The series $\sum_{n=0}^{\infty}\frac{B_n}{\varepsilon_n^4}$ converges rapidly to a value of 11/768. Thus Eq. (6-72) can be written in the form

$$\bar{t}-t_0=K\left[X-\frac{11}{96}+8\sum_{n=0}^{\infty}\frac{B_n}{\varepsilon_n^4}\exp(-\varepsilon_n^2X)\right]. \qquad (6\text{-}72a)$$

The local temperature head is

$$t_0-\bar{t}=K\left[\frac{11}{96}-8\sum_{n=0}^{\infty}\frac{B_n}{\varepsilon_n^4}\exp(-\varepsilon_n^2X)\right].$$

The heat-flow density at the wall is

$$q_0=\lambda\left(\frac{\partial t}{\partial r}\right)_{r=r_0}=\frac{\lambda}{r_0}\left(\frac{\partial t}{\partial R}\right)_{R=1}$$

Substituting the value of t from (6-71) into this expression, we obtain

$$q_c = 2K\frac{\lambda}{r_0}\sum_{n=0}^{\infty}\frac{B_n}{\varepsilon_n^2}\left[1-\exp\left(-\varepsilon_n^2 X\right)\right]. \qquad (6\text{-}73)$$

When $X \to \infty$, as we see from (6-72) and (6-73),

$$\frac{d\bar{t}}{dX} = K$$

and

$$q_c = 2K\frac{\lambda}{r_0}\sum_{n=0}^{\infty}\frac{B_n}{\varepsilon_n^2} = \text{const}.$$

In addition, it follows from the heat-balance equation that

$$\frac{d\bar{t}}{dX} = 4\frac{q_c r_0}{\lambda}.$$

Substituting in the values of $\overline{dt}/dX$ and q_s from the preceding relationships, we have

$$\sum_{n=0}^{\infty}\frac{B_n}{\varepsilon_n^2} = \frac{1}{8}.$$

Thus Eq. (6-73) can be represented as

$$q_c = 2K\frac{\lambda}{r_0}\left[\frac{1}{8}-\sum_{n=0}^{\infty}\frac{B_n}{\varepsilon_n^2}\exp\left(-\varepsilon_n^2 X\right)\right]. \qquad (6\text{-}73a)$$

There now is no difficulty in determining the local Nusselt number:

$$\mathrm{Nu} = \frac{q_c d}{\lambda(t_c-\bar{t})} = \frac{1-8\sum_{n=0}^{\infty}\frac{B_n}{\varepsilon_n^2}\exp\left(-2\varepsilon_n^2\frac{1}{\mathrm{Pe}}\cdot\frac{x}{d}\right)}{\frac{11}{48}-16\sum_{n=0}^{\infty}\frac{B_n}{\varepsilon_n^4}\exp\left(-2\varepsilon_n^2\frac{1}{\mathrm{Pe}}\cdot\frac{x}{d}\right)}. \qquad (6\text{-}74)$$

Figure 6-13 shows the variation in t_s, $\bar{t}$, and Nu as a function of X.

When $X \to \infty$, the series in (6-71)-(6-74), which contain exponential functions, vanish. Thus beginning at a certain value of X, the temperature of the fluid at any point will vary linearly with the length, together with $\bar{t}$, while q_s, $t_s - \bar{t}$, and Nu take on constant values. The limiting value of Nu will equal

$$\mathrm{Nu}_\infty = \frac{48}{11} = 4{,}36. \qquad (6\text{-}75)$$

In this case, the thermal initial segment will be longer than when t_s = const.

Thus, in the problem of heat exchange with linear variation in wall temperature, just as when there is a constant wall tempera-

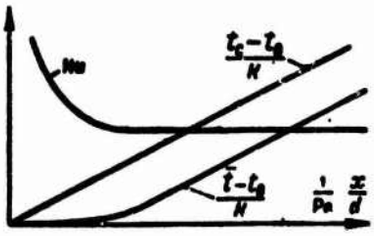

Fig. 6-13. Variation in $\frac{t_c-t_0}{K}$, $\frac{\bar{t}-t_0}{K}$ and Nu as function of $\frac{1}{Pe}\cdot\frac{x}{d}$.

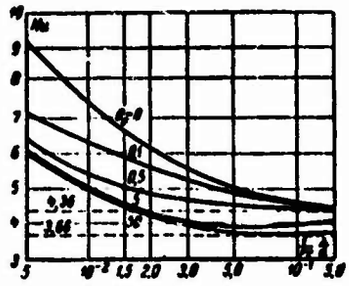

Fig. 6-14. The Nu number in round tube for linear variation in t_s and various values of θ_0.

ture, we find stabilization of the heat-exchange process. Here the same temperature profile will form in the region with incipient thermal stabilization as when a constant heat-flow density is specified at the wall. Thus Nu_∞ will have the same value as for the heat-exchange problem with q_s = const (see §8-1).

We have considered the problem of heat exchange with dt_s/dx = = const just for the special case in which there is no wall-temperature jump at $x = 0$ (i.e., $t_s = t_0$). If there is a jump in t_s at $x = 0$, then the problem can be solved by the same method. Grigull and Tratz [8a] recently determined the heat transfer for this case by a numerical method. Their results are shown in Fig. 6-14. Here the quantity

$$\theta_0=\frac{(t_c-t_0)_0}{(t_c-t_{R=0})_\infty}$$

was used as a parameter, i.e., the ratio of the wall-temperature jump at $x = 0$ to the difference between the wall temperature and the temperature on the tube axis in the region of stabilized heat exchange. The latter is easily found from Eq. (8-5) (see §8-1) in conjunction with the heat-balance equation

$$(t_c-t_{R=0})_\infty=\frac{3}{16}\frac{dt_c}{dX}.$$

As we see from Fig. 6-14, when $0<\theta_0\leq 1$, Nu decreases monotonically, while when $\theta_0>1$, it passes through a minimum, in either case approaching a limit of 4.36. As θ_0 increases, the thermal initial segment becomes longer. When $\theta_0\to\infty$, this problem degenerates to the problem of heat exchange with t_s = const, and Nu approaches $Nu_\infty=3{,}66$.

6-6. SOME GENERAL LAWS GOVERNING STABILIZATION OF HEAT EXCHANGE WITH WALL-TEMPERATURE VARIATION ALONG TUBE LENGTH

The method considered in the preceding section can be used to esamine the distribution of heat transfer along the length

of a tube for a specified variation in wall temperature. The results of such a determination show, in particular, whether self-similar or stabilized heat exchange sets in for a specified distribution $t_s(x)$. It is useful to investigate the question of self-similar-regime inception for the Nusselt number when t_s varies along the length in more general form, as was done recently by V.D. Vilenskiy [19]. Let us analyze the case of stabilized flow of a fluid with constant physical properties in a straigth tube of arbitrary cross section. The heat flow along the axis owing to heat conduction is assumed to be small as compared with the heat flow caused by convection. It is also assumed that there are no internal heat sources, and that the influence of dissipation is negligible.

Under these assumptions, the temperature field in the fluid flow is described by the equation

$$W_x(Y, Z)\frac{\partial\vartheta}{\partial X}=\frac{\partial^2\vartheta}{\partial Y^2}+\frac{\partial^2\vartheta}{\partial Z^2}, \qquad (6\text{-}76)$$

where

$$W_x=\frac{w_x}{\bar{w}};\ \vartheta=\frac{t-t_0}{t_0};\ X=\frac{4}{\mathrm{Pe}}\cdot\frac{x}{d_e};\ \mathrm{Pe}=\frac{\bar{w}d_e}{a};\ Y=\frac{y}{d_e/2};\ Z=\frac{z}{d_e/2};$$

y and z are the coordinates in the tube cross-sectional plane; $d_e = 4f/s$ is the equivalent diameter; f and s are the cross-sectional area and perimeter of this section; t_0 is the temperature of the fluid at the entrance, i.e., at $X = 0$.

The boundary conditions are written as

$$\vartheta_{X=0}=0, \qquad (6\text{-}77)$$

$$\vartheta_{\substack{Y=Y_c\\Z=Z_c}}=\varphi(X)^*. \qquad (6\text{-}78)$$

We assume that the function $\varphi(X)$ describing the wall-temperature distribution along the tube length exceeds zero when $0 < X < \infty$, and that it is continuous together with its derivatives.

To analyze heat exchange far from the tube entrance, it is necessary to consider the temperature field in the fluid flow when $X \to \infty$.

It was shown in [19], that if the function $\varphi(X)$ possesses the property that the limits

$$\lim_{X\to\infty}\frac{1}{\chi_n}\cdot\frac{d\chi_n}{dX}=K_n^{**}$$

exist, where the function χ_n is determined by the relationships

$$\chi_0=\varphi;$$
$$\cdots\cdots\cdots\cdots$$
$$\chi_n=\frac{d\chi_{n-1}}{dX}-K_{n-1}\chi_{n-1},$$

while $K_n > -\mu_1$, where μ_1 is the first eigenvalue of the problem

$$\left.\begin{aligned} \nabla^2\eta(Y, Z)+\mu W_z\eta(Y, Z)=0;\\ \eta(Y_c, Z_c)=0. \end{aligned}\right\} \tag{6-79}$$

then when $X \to \infty$ θ can be represented as the asymptotic series

$$\theta \approx \sum_{n=0}^{\infty} V_n(Y, Z)\chi_n(X), \tag{6-80}$$

where the functions V_n are solutions of the problems

$$\left.\begin{aligned} \nabla^2 V_0 - K_0 W_z V_0 = 0;\\ V_0(Y_c, Z_c)=1;\\ \cdots\cdots\cdots\cdots\cdots\\ \nabla^2 V_n - K_n W_z V_n = W_z V_{n-1};\\ V_n(Y_c, Z_c)=0. \end{aligned}\right\} \tag{6-81}$$

If for some $n=n_1$ $\frac{1}{\chi_{n1}}\cdot\frac{d\chi_{n1}}{dX}=K_{n1}$, then Series (6-80) breaks off at the n_1-th term and the difference between the exact solution of (6-76) and its asymptotic representation at $X \to \infty$ (6-80) will approach zero as $\exp(-\mu_1 X)$.

If

$$\lim_{X\to\infty}\frac{1}{\varphi}\cdot\frac{d\varphi}{dX}=K_0<-\mu_1,$$

or

$$\frac{1}{\varphi}\cdot\frac{d\varphi}{dX}\to-\infty \quad \text{as} \quad X\to\infty,$$

then for $X \to \infty$,

$$\theta \sim -\eta_1\left(\int_s \frac{\partial\eta_1}{\partial n}\,ds\right)\exp(-\mu_1 X)\int_0^X \varphi\exp(\mu_1\xi)\,d\xi, \tag{6-82}$$

where η_1 is the first normalized eigenfunction of Problem (6-79), while $\partial/\partial\vec{n}$ is the derivative with repsect to the normal n to the tube surface, directed toward the fluid.

It follows from (6-80) and (6-82) that if when $X \to \infty$, the logarithmic derivative of φ with respect to X has a finite limit or approaches $-\infty$, then the temperature field in the fluid flow admits of asymptotic representation as the product of a function of Y and Z and a function of X. In this case, there will be stabilization of the temperature field in the fluid flow, completely analogous to the stabilization (regularization) of the temperature field in a solid during unsteady heat conduction. Here the temperature gradient in the fluid flow at the tube wall and the difference between the wall temperature and the mean mass temperature of the fluid will become proportional to the same function of X, indicating that heat exchange has been stabilized.

If when $X \to \infty$ $\frac{1}{\varphi} \cdot \frac{d\varphi}{dX} \to +\infty$, then Θ cannot be represented as the product of a function of Y and Z and a function of X, i.e., the temperature field and, accordingly, the heat exchange are not stabilized.

The value of the Nusselt number in the region of stabilized heat exchange, $Nu_\infty = \frac{q_c d_э}{\lambda (t_c - \bar{t})}$ can be obtained on the basis of (6-80) and (6-82).

If the parameter $K_0 > -\mu_1$ (except for $K_0 = 0$), then Nu_∞ is determined by the first term of Series (6-80), i.e., essentially by the function V_0. The expression for Nu_∞ will have the form

$$Nu_\infty(Y_c, Z_c) = -2 \frac{\left(\frac{\partial V_0}{\partial N}\right)_{\substack{Y=Y_c \\ Z=Z_c}}}{1 - \frac{1}{F}\int_F V_0 W_0 \, dF}, \qquad (6\text{-}83)$$

where $N = \frac{n}{d_э/2}$ is the dimensionless normal to the wall, directed toward the fluid; $F = 4f/d_э^2$ is the dimensionless cross-sectional area. It is clear from (6-83) that here Nu_∞ depends on the tube geometry, the parameter K_0, and the coordinates of the perimeter point under consideration.

If $K_0 = 0$, then $V_0 = 1$. In this case, Nu_∞ is determined by the second term of Series (6-80):

$$Nu_\infty(Y_c, Z_c) = 2 \frac{\left(\frac{\partial V_1}{\partial N}\right)_{\substack{Y=Y_c \\ Z=Z_c}}}{\frac{1}{F}\int_F V_1 W_0 \, dF}. \qquad (6\text{-}84)$$

Thus when $K_0 = 0$, Nu_∞ is determined by the parameter $K_1 = \lim_{X \to \infty} \frac{\varphi''}{\varphi'}$.

If $K_0 < -\mu_1$, then Nu_∞ is described by the expression

$$Nu_\infty(Y_c Z_c) = -2\mu_1 \frac{\left(\frac{\partial \eta_1}{\partial N}\right)_{\substack{Y=Y_c \\ Z=Z_c}}}{\frac{1}{F}\int_S \frac{\partial \eta_1}{\partial N} \, dS}, \qquad (6\text{-}85)$$

where $S = \frac{s}{d_э/2}$ is the dimensionless perimeter of the section.

In this case, consequently, Nu_∞ does not depend at all on the law governing the variation in wall temperature, but is determined solely by the tube geometry and the coordinates of the perimeter point considered. In other words, when $K_0 < -\mu_1$ Nu_∞ will have the same value as if the wall temperature were constant.

We note that K_1 can take on negative or zero values. When $-\mu_1 < K_1 < 0$, Expression (6-84) goes over to (6-83); in this case, we should replace V_0 by V_1. If $K_1 \leq \mu_1$, then Nu_∞ is determined by (6-85).

To illustrate the foregoing general results, let us compute the limiting Nusselt numbers for laminar flow of a fluid in a round tube.

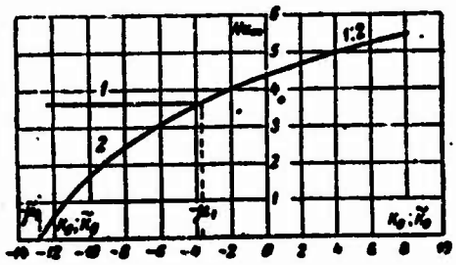

Fig. 6-15. The Nu_∞ number in a round tube for variations in t_s (curve 1) and q_s (curve 2) with length.

If $K_0 > -\mu_1$ (but $K_0 \neq 0$), , then to calculate Nu_∞ we must determine the function V_0. The latter is a solution of the equation

$$\frac{1}{R}\cdot\frac{d}{dR}\left(R\frac{dV_0}{dR}\right)-2K_0(1-R^2)V_0=0 \qquad (6\text{-}86)$$

Here the boundary conditions are

$$V_0(1)=1,\ \left(\frac{\partial V_0}{\partial R}\right)_{R=0}=0,$$

where $R = r/r_0$.

The solution of (6-86) has been investigated elsewhere [20, 21]. Using the results of these studies, we can represent V_0 as

$$\text{for } K_0>0 \quad V_0=\frac{P(R,\ K_0)}{P(1,\ K_0)};$$

$$\text{for } -\mu_1<K_0<0 \quad V_0=\frac{p(R,\ K_0)}{p(1,\ K_0)},$$

where $P(R, K_0)$ and $p(R, K_0)$ are Poiseuille functions. In [20, 21], they were represented as power series. Substituting these expressions into (6-83), we obtain expressions for Nu_∞ as a function of the parameter K_0 for $K_0>0$ and $-\mu_1<K_0<0$. .

If $K_0 = 0$, then, as we have already mentioned, Nu_∞ is determined by the parameter K_1. When $\mu_1<K<0$, the results obtained

with the aid of (6-83) are valid for Nu_∞. When $K_1 = 0$, Nu_∞ is found from (6-84). The function V_1 in this equation is a solution of the problem

$$\frac{1}{R}\frac{d}{dR}\left(R\frac{dV_1}{dR}\right)=2(1-R^2);$$

$$V_1(1)=0;\ \left(\frac{dV_1}{dR}\right)_{R=0}=0.$$

From this we have

$$V_1=\frac{1}{2}R^2\left(1-\frac{1}{4}R^2\right)-\frac{3}{8},$$

and $Nu_\infty = 4.36$.

The computational results are illustrated in Fig. 6-15 (Curve 1). As the figure shows, the minimum value of Nu_∞ corresponds to a wall temperature that is constant along the length of the tube. When $K_0 > -\mu_1$, Nu_∞ rises as the parameter K_0 increases.

Manuscript Page No.

Footnotes

95 [1]This last assumption is well confirmed in most cases. The problem of heat exchange with allowance for energy dissipation is considered in Chapter 15.

99 [2]The first coefficient b_0 of the series is arbitrarily taken equal to unity, since it can be removed from the summation sign in (6-10) and combined with the still indefinite constant A in Expression (6-5) for θ.

112 [3]This problem has been solved by a numerical method [10, 11]. An analytic solution using the Ritz method was first obtained by Leybenson [12], and refined in [3]. A solution based on power-series expansion of the function representing the temperature distribution over the flow section has been given by May'yamov [13], as well as in [14, 6].

114 *As in the case of a round tube, the coefficient b_0 is arbitrarily taken to equal unity.

115 [4]See the analogous proof in §6-1.

120 [5]The same solution was published quite a bit later in [17].

121 *In solving the heat problem, we can eliminate the opposite wall in our imagination, and assume that a medium with constant temperature equaling the entrance temperature t_0

extends to infinity.

133 *The subscript "s" is used with the tube-wall coordinates.

133 **Only the case of real K is considered.

Manuscript Page No.	Transliterated Symbols
95	с = s = stenka = wall
108	н.т = n.t = nachal'nyy termicheskiy = thermal initial
110	л = l = logarifmicheskiy = logarithmic
133	э = e = ekvivalentnyy = equivalent

Chapter 7

HEAT EXCHANGE AND RESISTANCE IN FLAT AND ROUND TUBES WITH VARIABLE FLUID PHYSICAL PROPERTIES AND BOUNDARY CONDITIONS OF THE FIRST KIND

7-1. PRELIMINARY REMARKS

Since the physical properties of a fluid depend on temperature, they vary in time and along the coordinates in accordance with the temperature variation. When the temperature differences in the flow are small or the physical properties depend little on temperature, these variations will not be great. Under such conditions, results obtained under the assumption of constant physical properties will be valid. If there are significant temperature differences in the flow, the variation in physical properties with temperature will have a significant influence on the velocity and temperature fields. Thus, for example, owing to the dependence of the viscosity coefficient on temperature, the velocity profile will not be parabolic for viscous flow of a liquid in a round tube. The variation in velocity profile entails a corresponding change in the temperature profile. Here, naturally, the heat transfer and friction resistance will change as compared with their values for constant physical properties.

Since the velocity and temperature fields are interrelated when the physical properties are variable, such problems require joint integration of the equations of motion and energy. As we have already noted, this involves considerable difficulties, associated with the nonlinearity of the initial equations. For this reason, theoretical calculations for flows and heat exchange with variable physical properties are carried out chiefly by approximate methods, and encompass a relatively small group of problems. Experiment plays a significant role in study of these questions.

For liquids under ordinary conditions, the dynamic viscosity varies most sharply with the temperature (see, for example, Table 3-1). Thus for a viscous flow of a liquid, we often consider only the variation in the viscosity alone, assuming that the remaining physical properties are constant.

The motion problem for a fluid with temperature-dependent viscosity was first formulated by L.S. Leybenson between 1922 and 1924 [1, 2]. He obtained an approximate solution to this problem on the assumption that the fluid temperature and viscosity are constant over sections and vary only along the tube length. This specific formulation of the problem is of interest in determination

of hydraulic resistance for motion of a hot fluid (petroleum, for example) in long pipelines. Here the intensity of heat exchange between fluid and wall is negligible, and the assumption of constant cross-section temperature is satisfied in approximation.

When a fluid moves under conditions of fairly intense heat exchange (in heat exchangers, for example), there is a very sharp radial variation in the temperature and, consequently, the viscosity, with relatively little lengthwise variation. Thus the solution of L.S. Leybenson is unsuitable for determination of hydraulic resistance in heat exchangers and similar devices.

Attempts have been made to consider flow with variable viscosity for a problem resembling the Graetz problem, with constant wall temperature [3, 4, 5, 6]. In these studies, the simplified equation of motion (with no inertial terms) is solved on the assumption that the temperature distribution in the flow remains the same as for constant viscosity. Using a linear relationship to approximate the velocity profile found by this method in the region of the thermal boundary layer, Jamagata [6] has calculated the local heat-transfer coefficient for the front part of the thermal initial segment (i.e., near the tube entrance). It is understandable that the results obtained in these studies should be treated as a first rough approximation.

In §§7-2 and 7-3, we present our approximate solutions for problems of fluid motion and heat exchange in flat and round tubes with allowance for the relationship between the viscosity coefficient and the temperature [7, 8]. These solutions are valid for the thermal initial segment in viscous flow (i.e., when there is no natural convection). In addition, in §7-4, we consider an approximate solution of the problem with allowance for variable viscosity, obtained by Yang Van Tszu [9] for the entire flow region in a round tube. In §§7-5 and 7-6, we give results of experimental investigations.

7-2. THEORETICAL DETERMINATION OF HEAT EXCHANGE AND RESISTANCE IN THERMAL INITIAL SEGMENT OF FLAT TUBE

1. Let us consider motion of a liquid and heat exchange in the thermal initial segment of a flat tube. Here we shall allow for the relationship between the viscosity coefficient and the temperature, assuming that the remaining physical properties are constant. Naturally, the assumption that the density, which depends little on temperature for most liquids, is constant eliminates the influence of free convection from consideration.

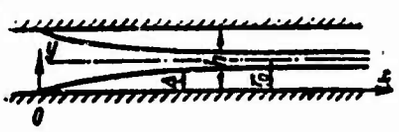

Fig. 7-1. Flow diagram for flat tube.

We assume that the velocity profile is fully developed (parabolic) in the tube entrance section. We also assume that the fluid temperature at the entrance is uniformly distributed over the section, while the wall temperature is constant over the surface.

We can isolate two regions in the thermal initial segment of the tube: a thermal boundary layer of thickness Δ, and the

core, which is not involved in heat exchange (Fig. 7-1). For subsequent simplification of the equations, we make the basic assumption that the thickness Δ of the thermal boundary layer is substantially less than the tube width h. This means that we restrict the problem to the region of small reduced lengths. We note, incidentally, that reduced lengths are usually small for motion of viscous fluids.

We neglect the heat transferred along the axis by heat conduction as compared with the convective transfer. For simplicity, we shall also neglect the heat of friction, although it is not difficult to make allowance for this quantity, as we shall show later.

It is convenient to use an equation of the type (3-4) to express the relationship between the viscosity coefficient and the temperature; it permits good approximation to almost any experimental curve for the viscosity coefficient.

As formulated, the problem corresponds to the following equation system:

$$w_x\frac{\partial t}{\partial x}+w_y\frac{\partial t}{\partial y}=a\frac{\partial^2 t}{\partial y^2}; \tag{7-1}$$

$$\rho\left(w_x\frac{\partial w_x}{\partial x}+w_y\frac{\partial w_x}{\partial y}\right)=-\frac{\partial p}{\partial x}+\frac{\partial}{\partial x}\left(\mu\frac{\partial w_x}{\partial x}\right)+\frac{\partial}{\partial y}\left(\mu\frac{\partial w_x}{\partial y}\right)+$$
$$+\frac{\partial\mu}{\partial x}\cdot\frac{\partial w_x}{\partial x}+\frac{\partial\mu}{\partial y}\cdot\frac{\partial w_y}{\partial x}; \tag{7-2}$$

$$\frac{\partial w_x}{\partial x}+\frac{\partial w_y}{\partial y}=0; \tag{7-3}$$

$$\frac{1}{\mu}=a_0+a_1t+a_2t^2+\ldots+a_mt^m, \tag{7-4}$$

where $a_0, a_1, a_2, \ldots, a_m$ are constants depending on the type of fluid and the temperature interval.

System (7-1)-(7-4) contains no equations for the projection of the velocity on the y axis. The proposed method for solving the problem makes it possible to do without this equation, provided we do not investigate the pressure distribution over the tube cross section.

The variation in velocity along the tube axis can be neglected, so that the next-to-last term in (7-2) can be dropped.

To solve the problem we must simplify (7-1) and (7-2) substantially. To do this, we replace the convective terms in (7-1) by their values averaged over the thickness of the thermal boundary layer. Since $\Delta \ll h$, this approximate way of allowing for the convective terms should not substantially influence the final results.

Thus in place of (7-1) we use the equation

$$a\frac{\partial^2 t}{\partial y^2}=\frac{1}{\Delta}\int_0^{\Delta}\left(w_x\frac{\partial t}{\partial x}+w_y\frac{\partial t}{\partial y}\right)dy. \tag{7-5}$$

If the motion were isothermal, w_y and $\partial w_x/\partial x$ in (7-2) would equal

zero, and p would not depend on y. These conditions are not satisfied for nonisothermal flow, when μ is a variable. We can state, however, that here w_y and $\partial w_x/\partial x$ will be small as compared with w_x and $\partial w_x/\partial y$. Thus we need only make approximate allowance for terms containing w_y and $\partial w_x/\partial x$; in (7-2) we use their values averaged over the tube width $h = 2r_0$. This can also be done with $\partial p/\partial x$. Thus in place of (7-2) we use the equation

$$\frac{\partial}{\partial y}\left(\mu\frac{\partial w_x}{\partial y}\right)=\frac{1}{r_0}\int_0^{r_0}\left[\frac{\partial p}{\partial x}+\rho\left(w_x\frac{\partial w_x}{\partial x}+w_y\frac{\partial w_x}{\partial y}\right)-\right.$$
$$\left.-\frac{\partial}{\partial x}\left(\mu\frac{\partial w_x}{\partial x}\right)-\frac{\partial\mu}{\partial y}\cdot\frac{\partial w_y}{\partial x}\right]dy. \qquad (7\text{-}6)$$

This way of making approximate allowance for the inertial terms in the equations of motion was proposed, insofar as we know, by N.A. Slezkin, and later utilized by S.M. Targ [2].

The boundary conditions for our problem have the form

$$\left.\begin{array}{l}\text{for } x\geqslant 0 \text{ and } y=0 \quad t=t_c,\ w_x=w_y=0;\\ \text{for } x\geqslant 0 \text{ and } r_0\geqslant y\geqslant\Delta \quad t=t_0,\ \dfrac{\partial t}{\partial y}=0;\\ \text{for } x\geqslant 0 \text{ and } y=r_0 \quad \dfrac{\partial w_x}{\partial y}=0.\end{array}\right\} \qquad (7\text{-}7)$$

We introduce the following dimensionless quantities for convenience:

$$\Theta=\frac{t-t_0}{t_c-t_0},\ W_x=\frac{w_x}{\bar{w}},\ W_y=\frac{w_y}{\bar{w}},\ \mathrm{Pe}=\frac{\bar{w}2r_0}{a},\ \mathrm{Re}_0=\frac{\bar{w}2r_0\rho}{\mu_0};\ X=\frac{x}{r_0},$$
$$Y=\frac{y}{r_0} \text{ and } k=\frac{\Delta}{r_0},$$

and write (7-3)-(7-6) in the dimensionless form

$$\frac{\partial^2\Theta}{\partial Y^2}=B(X), \qquad (7\text{-}8)$$

$$\frac{\partial}{\partial Y}\left(\frac{\mu}{\mu_c}\cdot\frac{\partial W_x}{\partial Y}\right)=A(X), \qquad (7\text{-}9)$$

$$\frac{\partial W_x}{\partial X}+\frac{\partial W_y}{\partial Y}=0, \qquad (7\text{-}10)$$

$$\frac{\mu_c}{\mu}=1+a'_1\Theta+a'_2\Theta^2+\ldots+a'_m\Theta^m, \qquad (7\text{-}11)$$

where

$$B(X)=\frac{1}{2}\cdot\frac{\mathrm{Pe}}{k}\int_0^k\left(W_x\frac{\partial\Theta}{\partial X}+W_y\frac{\partial\Theta}{\partial Y}\right)\partial Y; \qquad (7\text{-}12)$$

$$A(X)=\int_0^1\left[\frac{\partial}{\partial X}\left(\frac{r_0}{\bar{w}}\cdot\frac{p}{\mu_c}\right)+\frac{1}{2}\mathrm{Re}_0\left(W_x\frac{\partial W_x}{\partial X}+W_y\frac{\partial W_x}{\partial Y}\right)-\right.$$
$$\left.-\frac{\partial}{\partial X}\left(\frac{\mu}{\mu_c}\cdot\frac{\partial W_x}{\partial X}\right)-\frac{\partial}{\partial Y}\left(\frac{\mu}{\mu_c}\cdot\frac{\partial W_y}{\partial X}\right)\right]dY. \qquad (7\text{-}13)$$

The boundary conditions will be

$$\text{for } X \geqslant 0 \text{ and } Y = 0 \quad \Theta = 0,\ W_x = W_y = 0; \tag{7-14a}$$

$$\text{for } X \geqslant 0 \text{ and } 1 \geqslant Y \geqslant k \quad \Theta = 1,\ \frac{\partial \Theta}{\partial Y} = 0; \tag{7-14b}$$

$$\text{for } X \geqslant 0 \text{ and } Y = 1 \quad \frac{\partial W_x}{\partial Y} = 0. \tag{7-14c}$$

2. Let us determine the temperature and velocity distributions. Integrating (7-8) with respect to Y and using the second boundary condition of (7-14b), we obtain

$$\frac{\partial \Theta}{\partial Y} = B(X)(Y - k).$$

Again integrating with respect to Y and taking into account the first boundary conditions of (7-14a) and (7-14b), we determine $B(X)$ and the dimensionless temperature:

$$B(X) = -\frac{2}{k^2}, \tag{7-15}$$

$$\Theta = \frac{2Y}{k} - \frac{Y^2}{k^2}. \tag{7-16}$$

Substituting Θ into (7-11), we find

$$\frac{\mu_s}{\mu} = b_0 + b_1\frac{Y}{k} + b_2\left(\frac{Y}{k}\right)^2 + \ldots + b_n\left(\frac{Y}{k}\right)^n = \sum_{i=0}^{n=2m} b_i\left(\frac{Y}{k}\right)^i, \tag{7-17}$$

where the b_i are new constants; $b_0 = 1$.

Integrating (7-9) with respect to Y and taking (7-14c) into account, we obtain

$$\frac{\partial W_x}{\partial Y} = A(X)\frac{\mu_s}{\mu}(Y - 1). \tag{7-18}$$

The solution of (7-18) will be different for the thermal boundary layer and for the flow core, which is not involved in heat exchange.

For the thermal boundary layer, i.e., for $Y \leq k$, when μ_s/μ is described by (7-17):

$$\frac{\partial W_x}{\partial Y} = A(X)\sum_{i=0}^{n}\frac{b_i}{k^i}(Y^{i+1} - Y^i).$$

Integrating this equation with respect to Y and considering that when $Y = 0$, $W_x = 0$, we obtain an equation for W_x when $Y \leq k$:

$$W_x = A(X)\sum_{i=0}^{n}\frac{b_i}{k^i}\left(\frac{Y^{i+2}}{i+2} - \frac{Y^{i+1}}{i+1}\right). \tag{7-19}$$

We have the following expressions for W_x when $Y = k$

$$W_{xk} = A(X)\sum_{i=0}^{n} b_i\left(\frac{k^2}{i+2} - \frac{k}{i+1}\right). \tag{7-20}$$

For the flow core, i.e., when $Y \geqslant k$, $\mu = \mu_0 = \text{const}$. Here integration of (7-18) yields

$$W_x = A(X)\frac{\mu_0}{\mu_0}\left(\frac{Y^2}{2} - Y\right) + c.$$

Determining c from the condition $W_x = W_{xk}$ for $Y = k$ we obtain an equation for W_x for $Y > k$:

$$W_x = A(X)\frac{\mu_0}{\mu_0}\left[\frac{1}{2}(Y^2 - k^2) - (Y - k)\right] + A(X)\sum_{l=0}^{n} b_l\left(\frac{k^2}{l+2} - \frac{k}{l+1}\right). \quad (7\text{-}21)$$

The function $A(X)$ is found from the condition requiring that the flowrate be constant:

$$\int_0^k w_x\,dy + \int_k^{r_0} w_x\,dy = \overline{w}r_0,$$

or, in dimensionless form,

$$\int_0^k W_x\,dY + \int_k^1 W_x\,dY = 1. \quad (7\text{-}22)$$

We evaluate the first integral using (7-19), and the second using (7-21); this yields

$$(X) = -\frac{1}{P_0 + P_1 k + P_2 k^2 + P_3 k^3} = -\frac{1}{R}, \quad (7\text{-}23)$$

where

$$\left.\begin{aligned} P_0 &= \frac{1}{3}\frac{\mu_0}{\mu_0};\\ P_1 &= -\frac{\mu_0}{\mu_0} + \sum_{l=0}^{n}\frac{b_l}{l+1};\\ P_2 &= \frac{\mu_0}{\mu_0} - 2\sum_{l=0}^{n}\frac{b_l}{l+2};\\ P_3 &= -\frac{1}{3}\cdot\frac{\mu_0}{\mu_0} + \sum_{l=0}^{n}\frac{b_l}{l+3}. \end{aligned}\right\} \quad (7\text{-}24)$$

For brevity, we henceforth let

$$R = P_0 + P_1 k + P_2 k^2 + P_3 k^3. \quad (7\text{-}25)$$

Substituting the value of $A(X)$ into (7-19) and (7-21), we obtain the final equations for the distribution of velocity W_x:

for $Y < k$

$$W_x = \frac{1}{R}\sum_{l=0}^{n}\frac{b_l}{k^l}\left(\frac{Y^{l+1}}{l+1} - \frac{Y^{l+2}}{l+2}\right); \quad (7\text{-}26)$$

for $Y \geqslant k$

$$W_x = \frac{1}{R}\left\{\frac{\mu_c}{\mu_0}\left[(Y-k)-\frac{1}{2}(Y^2-k^2)\right]+\sum_{i=0}^{n} b_i\left(\frac{k}{i+1}-\frac{k^2}{i+2}\right)\right\}. \qquad (7\text{-}27)$$

When $\mu=\mu_c=\mu_0=\text{const}$, Eqs. (7-26) and (7-27) go over to the familiar equation

$$W_x = 3\left(Y-\frac{Y^2}{2}\right),$$

which describes the velocity distribution in a flat tube with stabilized isothermal fluid motion. The same result is obtained if we let $k = 0$ in (7-27). Thus Eq. (7-27) satisfies the specified velocity distribution at the entrance.

The transverse velocity component W_y is found from (7-10) when we allow for the fact that $W_y = 0$ at $Y = 0$:

$$W_y = -\int_0^Y \frac{\partial W_x}{\partial X}\,dY.$$

Using (7-26), we calculate the derivative

$$\frac{\partial W_x}{\partial X} = -\sum_{i=0}^{n} b_i\left(\frac{Y^{i+1}}{i+1}-\frac{Y^{i+2}}{i+2}\right)\frac{iR+T}{k^{i+3}R^i}\cdot\frac{dk}{dX}, \qquad (7\text{-}28)$$

where

$$T = P_1 k + 2P_2 k^2 + 3P_3 k^3.$$

Substituting (7-28) into the expression for W_y, after integration we obtain

$$W_y = \frac{dk}{dX}\sum_{i=0}^{n}\frac{b_i}{k^{i+3}}\cdot\frac{iR+T}{R^i}\left[\frac{Y^{i+2}}{(i+1)(i+2)}-\frac{Y^{i+3}}{(i+2)(i+3)}\right]. \qquad (7\text{-}29)$$

It follows from (7-29) that $W_y = 0$ for isothermal flow.

The equations for the temperature and velocity distributions still contain the unknown k, which is a function of X.

3. We determine the thickness of the thermal boundary layer and compute the heat transfer and friction resistance. To do this, we use (7-12) to determine the way in which k depends on X. Substituting $B(X)$ from (7-15) into this equation, we obtain

$$-\frac{2}{k^2} = \frac{\mathrm{Pe}}{2k}\int_0^k\left(W_x\frac{\partial\theta}{\partial X}+W_y\frac{\partial\theta}{\partial Y}\right)dY. \qquad (7\text{-}30)$$

We evaluate the integrals in (7-30):

$$\int_0^k W_x\frac{\partial\theta}{\partial X}\,dY = \frac{2}{R}\cdot\frac{dk}{dX}\sum_{i=0}^{n}\frac{b_i}{k^i}\int_0^k\left(\frac{Y^{i+1}}{i+1}-\frac{Y^{i+2}}{i+2}\right)\left(\frac{Y^2}{k^2}-\frac{Y}{k^2}\right)dY =$$

$$= \frac{2}{R}\cdot\frac{dk}{dX}\left[k^2\sum_{i=0}^{n}\frac{b_i}{(i+2)(i+4)(i+5)} - k\sum_{i=0}^{n}\frac{b_i}{(i+1)(i+3)(i+4)}\right];$$

$$\int_0^k W_y\frac{\partial\Theta}{\partial Y}\,dY = \frac{2}{R^2}\cdot\frac{dk}{dX}\sum_{i=0}^{n}\frac{b_i(iR+T)}{k^{i+1}(i+2)}\int_0^k\left(\frac{Y^{i+2}}{i+1} - \frac{Y^{i+3}}{i+3}\right)\times$$

$$\times\left(\frac{1}{k} - \frac{Y}{k^2}\right)dY = \frac{2}{R^2}\cdot\frac{dk}{dX}\sum_{i=0}^{n}b_i(iR+T)\left[\frac{k}{(i+1)(i+2)(i+3)(i+4)} - \right.$$

$$\left. - \frac{k^2}{(i+2)(i+3)(i+4)(i+5)}\right].$$

Substituting the values of the integrals into (7-30), after certain manipulations we find

$$\left[\left(2-\frac{T}{R}\right)\sum_{i=0}^{n}\frac{b_i}{(i+1)(i+2)(i+3)(i+4)} - \right.$$

$$\left. -\left(3-\frac{T}{R}\right)k\sum_{i=0}^{n}\frac{b_i}{(i+2)(i+3)(i+4)(i+5)}\right]\frac{k^2}{R}\,dk = \frac{2}{\mathrm{Pe}}\,dX.$$

Integrating this equation from 0 to k and 0 to X, respectively, we obtain an equation representing the dimensionless thickness k of the thermal boundary layer as a function of X/Pe:

$$\int_0^k\left[Б_1\left(2-\frac{T}{R}\right) - Б_2\left(3-\frac{T}{R}\right)k\right]\frac{k^2}{2R}\,dk = \frac{X}{\mathrm{Pe}}, \qquad (7\text{-}31)$$

where

$$Б_1 = \sum_{i=0}^{n}\frac{b_i}{(i+1)(i+2)(i+3)(i+4)}; \qquad (7\text{-}32)$$

$$Б_2 = \sum_{i=0}^{n}\frac{b_i}{(i+2)(i+3)(i+4)(i+5)}. \qquad (7\text{-}33)$$

The left side of the equation cannot be integrated analytically, and numerical integration methods must be used to determine the way in which k depends on X/Pe.

Having determined the relationship between k and X/Pe, we can use (7-16) to determine the temperature field, and (7-26), (7-27), and (7-29) to determine the velocity field; it is also simple to calculate the heat transfer, since the Nusselt number is uniquely determined by k.

The local heat-transfer coefficient, referred to the initial temperature difference, is

$$\alpha = -\frac{\lambda}{t_0 - t_0}\left(\frac{\partial t}{\partial y}\right)_{y=0},$$

or in dimensionless form,

$$\mathrm{Nu}=\frac{\alpha h}{\lambda}=2\left(\frac{\partial\theta}{\partial Y}\right)_{Y=0}.$$

Determining the derivative from (7-16), we find

$$\mathrm{Nu}=\frac{4}{k}. \qquad (7\text{-}34)$$

The mean Nusselt number over the length is

$$\overline{\mathrm{Nu}}=\frac{\bar{\alpha}h}{\lambda}=\frac{1}{X}\int_0^X \mathrm{Nu}\,dX. \qquad (7\text{-}35)$$

If the fluid viscosity is independent of the temperature, then (7-31) can be integrated analytically. Here (7-31) takes the form

$$\int_0^k\left(\frac{1}{4}-\frac{3k}{40}\right)k^3\,dk=\frac{2}{\mathrm{Pe}}X,$$

which yields

$$\frac{k^4}{12}-\frac{3k^5}{160}=\frac{2}{\mathrm{Pe}}X.$$

On the basis of (7-34), after replacing X by $2x/h$, we obtain

$$\mathrm{Nu}^3=\frac{4}{3}\,\mathrm{Pe}\,\frac{h}{x}\left(1-\frac{0{,}9}{\mathrm{Nu}}\right). \qquad (7\text{-}36)$$

For small k, we can neglect $\frac{0.9}{\mathrm{Nu}}=\frac{0{,}9k}{4}$ as compared with unity; then

$$\mathrm{Nu}=1{,}1\left(\mathrm{Pe}\,\frac{h}{x}\right)^{1/3} \qquad (7\text{-}37)$$

and

$$\overline{\mathrm{Nu}}=1{,}65\left(\mathrm{Pe}\,\frac{h}{x}\right)^{1/3}. \qquad (7\text{-}38)$$

These relationships agree with the Leceque equations (6-57) and (6-58) with the difference that the coefficients in the Leveque equations are 11% less than the values computed by us. This difference is apparently explained by the different degrees of approximation in volved in the basic assumptions used in our solution and the Leveque solution.

Let us calculate the local friction-resistance coefficient. For constant density, this will be determined by (4-17) or, after introduction of the equivalent diameter, by (5-3):

$$\xi=\frac{8\sigma_c}{\rho\bar{w}^2}.$$

The tangential stress at the wall is $\sigma_c=\mu_c\left(\frac{\partial w_x}{\partial y}\right)_{y=0}$; with allowance for (7-26), it can be represented as

$$\sigma_c=\frac{2\mu_c\bar{w}}{hR}.$$

Consequently,

$$\xi = \frac{16}{Re_0} \frac{1}{R}, \qquad (7\text{-}39)$$

where

$$Re_0 = \frac{\bar{w} d_0 \rho}{\mu_0}.$$

Equation (7-39) represents the relationship between the local friction-resistance ξ and the thickness k of the thermal boundary layer. First determining the relationship between k and X/Pe, we can use (7-31) to determine ξ as a function of X/Pe.

The mean friction-resistance coefficient for the tube segment between 0 and X equals

$$\bar{\xi} = \frac{1}{X} \int_0^X \xi \, dX. \qquad (7\text{-}40)$$

If we let $\mu = \mu_0 = \mu_c = \text{const}$ in (7-39), we obtain Eq. (5-12) for the resistance coefficient with isothermal flow in a flat tube.

The resistance coefficients ξ and $\bar{\xi}$ found here only allow for energy losses to friction. In determining the pressure drop along the tube length, in addition to friction we must also consider the change in flow kinetic energy caused by the variation in the velocity profile with the length. This is not difficult to do, since the velocity distribution is known.

Let us illustrate the computational method with a specific example.

4. *Sample calculation.* Grade MK oil moves in a flat tube. The oil temperature at the entrance is $t_0 = 150°C$; the wall temperature is $t_c = 38°C$. The relationship $\mu = f(t)$ between the oil viscosity and the temperature is specified as an experimental curve.

TABLE 7-1

t, °C	1) μ, $\frac{N \cdot cek}{m^2}$	$\frac{\mu_0}{\mu}$	$\theta = \frac{t - t_c}{t_0 - t_c}$	$\frac{Y}{k} = 1 - \sqrt{1-\theta}$
150	$5.96 \cdot 10^{-3}$	58	1.00	1.0
95	$23.25 \cdot 10^{-3}$	14.2	0.51	0.3
38	$329.6 \cdot 10^{-3}$	1.0	0.00	0.0

1) μ, $N \cdot s/m^2$.

a) Taking a polynomial of degree two as (7-17), we determine the coefficients b_0, b_1, and b_2. To do this, we take three values of μ on the curve $\mu = f(t)$: the values at temperatures t_0, t_s, and some intermediate temperature t', for example, $t' = 95°C$. For these values of t, we determine μ_s/μ, θ, and Y/k [from Eq. (7-16)]. Table 7-1

shows the results of the calculations.

The solution of the equations (7-17) set up for the three selected points yields: $b_0=1$, $b_1=39{,}2$ and $b_2=17{,}8$.

b) We find the coefficients of Polynomial (7-25). Using (7-24), we obtain $P_0=19{,}3$; $P_1=-31{,}46$; $P_2=22{,}0$ and $P_3=-5{,}6$.

By (7-32) and (7-33), the coefficients B_1 and B_2 will have the following values: $B_1=0{,}419$; $B_2=0{,}139$.

c) Evaluating the integral on the left side of (7-31), for arbitrarily selected values of k, we determine the values of the group $\frac{1}{Pe}\cdot\frac{x}{h}$, corresponding to the selected values of k. For these same values of k, we use (7-16), (7-26), and (7-27) to determine the temperature and velocity profiles, and employ (7-34) and (7-39) to determine Nu and ξRe_s. Table 7-2 shows the results of calculations for Nu and ξRe_s in condensed form. Using the relationships found for Nu and ξRe_s as functions of $\frac{1}{Pe}\cdot\frac{x}{h}$, we calculate $\overline{Nu}$ and $\overline{\xi Re_s}$ (Table 7-3).

TABLE 7-2

k	$\frac{1}{Pe}\cdot\frac{x}{h}\cdot 10^3$	Nu	ξRe_s	k	$\frac{1}{Pe}\cdot\frac{x}{h}\cdot 10^3$	Nu	ξRe_s
0	0	∞	0,829	0,10	4,30	40	0,978
0.01	0,005	400	0,842	0,20	37,8	20	1,154
0.02	0,032	200	0,856	0,50	929	8	1,906
0.05	0,54	80	0,922	1,00	11 932	4	3,780

TABLE 7-3

$\frac{1}{Pe}\cdot\frac{x}{h}\cdot 10^3$	$\overline{Nu}$	$\overline{\xi Re_s}$
0,1	207	0,86
1,0	97,0	0,90
10	45,3	0,97
100	21,7	1,17
1 000	10,9	1,61
10 000	5,78	2,79

Let us look at the results of the theoretical calculation and compare them with experimental data. Figure 7-2 shows the distribution of temperature and velocity over the section of a flat tube for various values of the reduced length. The curves for θ show that as $\frac{1}{Pe}\cdot\frac{x}{h}$ increases, the width of the thermal boundary layer increases considerably more slowly. Curve 1 for W_x corresponds to isothermal flow, and also gives the velocity distribution at the tube entrance.

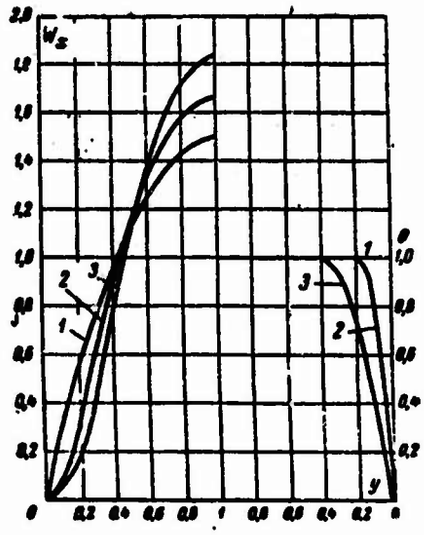

Fig. 7-2. Distribution of W_x and θ over section of flat tube for various values of $\frac{1}{Pe}\cdot\frac{x}{h}$. Grade MK oil flowing at $t_0 = 150°C$ and $t_c = 38°C$; $\mu_c/\mu_0 = 58$. 1 — $h=0$; $\frac{1}{Pe}\cdot\frac{x}{h}=0$; 2 — $h=0.2$; $\frac{1}{Pe}\cdot\frac{x}{h}=37.8\cdot10^{-4}$; 3 — $h=0.5$; $\frac{1}{Pe}\cdot\frac{x}{h}=929\cdot10^{-4}$.

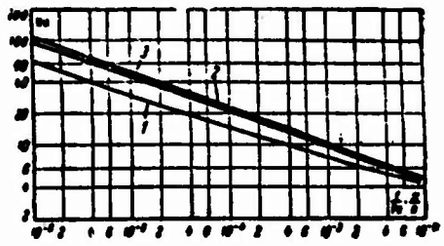

Fig. 7-3. The Nu number as a function of $\frac{1}{Pe}\cdot\frac{x}{h}$ for the data of the theoretical calculation. 1) $\frac{\mu_c}{\mu_0}=58$; 2) $\frac{\mu_c}{\mu_0}=1$; 3) Leveque equation for flat tube.

It is clear from the graph that the variation in viscosity with temperature has a significant influence on the velocity profile. Thus, for example, with cooling of the fluid $\left(\mu_c/\mu_0 = 58 \text{ and } \frac{1}{Pe}\frac{x}{h} \approx 0.001\right)$, the velocity is less by roughly a factor of 5 at a distance $Y = 0.1$ from the wall than for isothermal flow, while the velocity on the axis is roughly 25% greater. Conversely, with heating of the fluid, the velocity at the wall will be greater, and the velocity at the core smaller than the velocity for isothermal flow. This type of velocity variation accounts for the influence of variable viscosity on the heat exchange and hydraulic resistance.

Figure 7-3 shows the local Nu number as a function of $\frac{1}{Pe}\cdot\frac{x}{h}$ for grade MK oil at $\mu_s/\mu_0 = 58$ (see the example). It also gives curves for Eq. (7-36) with $\mu_s/\mu_0 = 1$ and for the Leveque equation (6-57). The last two curves are nearly parallel. As we have noted earlier, the difference in the Nu values calculated from these equations amounts to about 10%. The curve for $\mu_s/\mu_0 = 58$ first runs parallel to the other two curves (for $\frac{1}{Pe}\cdot\frac{x}{h} < 10^{-3}$); its slope then gradually decreases as the thickness of the thermal boundary layer increases (at $\frac{1}{Pe}\cdot\frac{x}{h} \approx 0{,}01$, k is close to unity). Figure 7-4 shows $\overline{Nu}$ as a function of Pe h/x for transformer oil and grade MK oil for various values of μ_s/μ_0. For comparison, the graph shows curves for $\mu_s/\mu_0 = 1$, plotted from (7-38) and the Leveque equation (6-58). The data shown in Figs. 7-3 and 7-3 indicate that the relationship between μ and t has a substantial influence on heat transfer. Thus when μ_s/μ_0 changes roughly from 0.2 to 1000, all other conditions being equal there is a reduction by a factor of 3 in the heat transfer. With cooling of the fluid, heat transfer will always be less under these conditions than for heating, since at the same value of Pe h/x, the velocity near the wall will be greater for heating than for cooling.

Figure 7-5 compares results of a theoretical determination of heat exchange in a flat tube with experimental data. Since there are no such experimental data available for comparison purposes, the data of E.A. Krasnoshchekov and the author [12] are given; they apply to heat exchange in a tube of rectangular cross section with side ratio $b/h \approx 5$ and relative length $l/h = 226$. The physical properties at $t = (1/2)(t_0 + t_s)$ were selected for the determination of $\overline{Nu}$ and Pe h/l from the experimental data. The latter correspond to fairly small values of Pe h/l, where the width of the thermal boundary layer is commensurate with $h/2$ and the theory is inexact. It is for this reason, most likely, as well as differences in geometry, that the experimental points lay 13-15% below the theoretical curves.

Figure 7-6 shows the results of a theoretical friction-resistance determination for grades TM and MK oils moving in a flat tube, for various values of μ_s/μ_0. The axis of ordinates shows the ratio of the mean friction-resistance coefficient in nonisothermal flow to the friction-resistance coefficient $\xi_{i.s}$ for isothermal flow. The latter is computed on the assumption that the fluid temperature everywhere equals the wall temperature. It follows from (7-39) and (7-40) that for the same value of Re_s,

$$\frac{\xi}{\xi_{i.s}} = \frac{1}{3}\cdot\frac{1}{X}\int_0^X \frac{1}{R}\,dX,$$

where

$$\xi_{u.c} = \frac{48}{Re_c},$$

$$Re_c = \frac{\bar{w} h \rho}{\mu_s}.$$

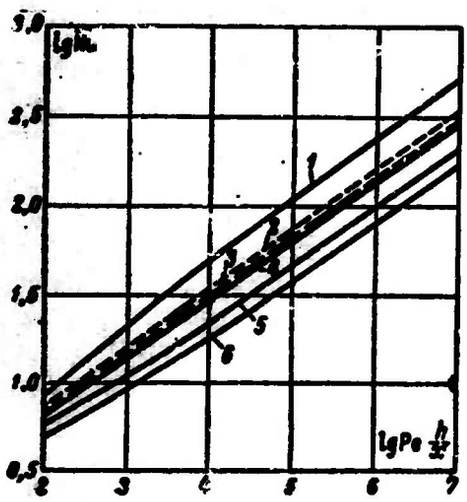

Fig. 7-4. The $\overline{Nu}$ number as a function of Pe h/x for various values of μ_s/μ_0 from theoretical data.

a Кривая	b Масло	t_0	t_c	$\frac{\mu_s}{\mu_0}$
1	ТМ	30	95	0,18
2	c По (7-38)			1
3	d По Левеку			1
4	ТМ	40	10	4,0
5	МК	180	30	58
6	МК	180	8	1 050

a) Curve; b) oil; c) buy (7-38); d) after Leveque.

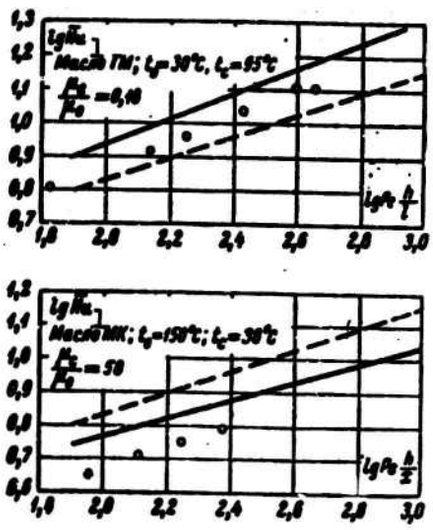

Fig. 7-5. $\overline{Nu}$ as a function of Pe h/x from theoretical data (solid lines), Leveque equation (dashed lines), and experimental data (circles). 1) Oil.

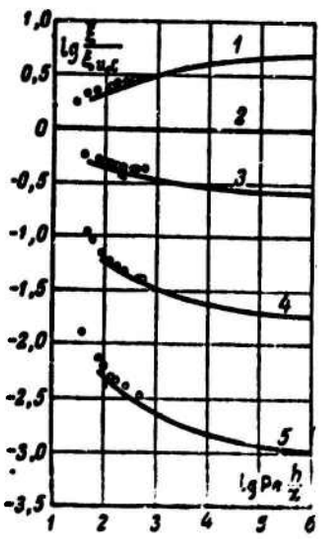

Fig. 7-6. Ratio $\bar{\xi}/\xi_{1.s}$ as a function of Pe h/x according to theoretical data (solid lines) and experimental dat (circles). 1) Grade TM oil, $\frac{\mu_s}{\mu_0} = 0,18$; 2) $\mu_s/\mu_0 = 1$; 3) grade TM oil, $\mu_s/\mu_0 = 4$; 4) grade MK oil, $\mu_s/\mu_0 = 58$; 5) grade MK oil, $\mu_s/\mu_0 = 1.050$.

The horizontal line 2 corresponds to isothermal flow at a fluid temperature $t = t_s$. Curves 1, 3, 4, and 5, which correspond to flow with heat exchange, show that the relationship between μ and t has a great influence on the resistance factor. In the final analysis, $\bar{\xi}$ also depends on Pe h/x owing to the variation in viscosity with temperature. At $\mathrm{Pe}\frac{h}{x}\to\infty$ or $x\to 0$, the coefficient $\bar{\xi}=\xi_{\mu.c}\frac{\mu_s}{\mu_c}=\xi_{\mu_0}$, i.e., it equals the resistance coefficient in isothermal flow, computed from the entrance temperature. When Pe h/x is small, $\bar{\xi}$ will approach $\xi_{1.s}$. Thus, $\bar{\xi}$ will always lie between $\xi_{1.s}$ and ξ_{10}, and it may vary widely for the same Reynolds number at the entrance.

The theoretical curves of Fig. 7-6 coincide with experimental data obtained for grades TM and MK oils flowing in a rectangular tube with a side ratio $b/h \approx 5$ [22]. As the graph shows, the experimental data are in quite satisfactory agreement with the theoretical results. Under the least favorable conditions (small Pe h/x), the experimental points do not deviate by more than 10-12% from the theoretical curves.

7-3. THEORETICAL DETERMINATION OF HEAT EXCHANGE AND RESISTANCE IN THERMAL ENTRANCE SEGMENT OF ROUND TUBE

1. All the conditions and assumptions formulated in the preceding section for flow in a flat tube are retained in this problem.

For flow of a fluid with variable viscosity in a round tube, the initial equation system will have the form

$$a\frac{1}{r}\cdot\frac{\partial}{\partial r}\left(r\frac{\partial t}{\partial r}\right)=w_x\frac{\partial t}{\partial x}+w_r\frac{\partial t}{\partial r}-\frac{\mu}{\rho c_p}\left(\frac{\partial w_x}{\partial r}\right)^2; \qquad (7\text{-}41)$$

$$\frac{1}{r}\cdot\frac{\partial}{\partial r}\left(r\mu\frac{\partial w_x}{\partial r}\right)=\frac{\partial p}{\partial x}+\rho\left(w_x\frac{\partial w_x}{\partial x}+w_r\frac{\partial w_x}{\partial r}\right)-\frac{\partial}{\partial x}\left(\mu\frac{\partial w_x}{\partial x}\right)-\frac{\partial\mu}{\partial r}\cdot\frac{\partial w_r}{\partial x}; \qquad (7\text{-}42)$$

$$\frac{\partial w_x}{\partial x}+\frac{1}{r}\cdot\frac{\partial}{\partial r}(rw_r)=0; \qquad (7\text{-}43)$$

$$\frac{1}{\mu}=c_0+a_1t+a_2t^2+\ldots+a_nt^n. \qquad (7\text{-}4)$$

In contrast to the preceding problem, here we allow for the heat of friction in the energy equation to illustrate the generality of the method.

As in the preceding section, we replace the exact equations (7-41) and (7-42) by approximate relationships in which the right sides are averaged over the thickness of the thermal boundary layer and the tube radius, respectively. Moreover, we replace the coordinate r by the coordinate $y = r_0 - r$, measured from the wall (r_0 is the tube radius), and $w_y = -w_r$.

After the approximate equations have been reduced to dimensionless form, following certain manipulations we obtain the equation system

$$\frac{1}{1-Y}\cdot\frac{\partial}{\partial Y}\left[(1-Y)\frac{\partial\theta}{\partial Y}\right]=B(X); \tag{7-44}$$

$$\frac{1}{1-Y}\cdot\frac{\partial}{\partial Y}\left[(1-Y)\frac{\mu}{\mu_c}\cdot\frac{\partial W_x}{\partial Y}\right]=A(X); \tag{7-45}$$

$$\frac{\partial W_x}{\partial X}+\frac{1}{1-Y}\cdot\frac{\partial}{\partial Y}[(1-Y)W_y]=0; \tag{7-46}$$

$$\frac{\mu_c}{\mu}=1+a'_1\theta+a'_2\theta^2+\ldots+a'_m\theta^m. \tag{7-47}$$

Here we let

$$B(X)=\frac{\mathrm{Pe}}{2\xi}\int_0^k\left[\left(W_x\frac{\partial\theta}{\partial X}+W_y\frac{\partial\theta}{\partial Y}\right)+\varkappa\frac{\mu}{\mu_c}\left(\frac{\partial W_x}{\partial Y}\right)^2\right]dY; \tag{7-48}$$

$A(X)$ is a certain function of X, which shall be defined below;

$$\theta=\frac{t-t_c}{t_0-t_c},\quad W_x=\frac{w_x}{\bar{w}},\quad W_y=\frac{w_y}{\bar{w}},\quad \mathrm{Pe}=\frac{\bar{w}2r_0}{a},$$

$$\varkappa=\frac{\bar{w}\mu_c}{\rho c_p(t_0-t_c)r_0},\quad X=\frac{x}{r_0},\quad Y=\frac{y}{r_0}\ \text{and}\ k=\frac{\Delta}{r_0}.$$

The boundary conditions will be the same as for the problem of heat exchange in a flat tube. They are determined by equation system (7-14a)-(7-14c).

2. We compute the temperature and velocity distributions. Integrating (7-44) with respect to Y, and taking the second boundary condition of (7-14b) into account, we obtain

$$\frac{\partial\theta}{\partial Y}=B(X)\left[\frac{Y-k}{1-Y}-\frac{Y^2-k^2}{2(1-Y)}\right].$$

or

$$\frac{\partial\theta}{\partial Y}=\frac{B(X)}{2}\left[\frac{(1-k)^2}{1-Y}-(1-Y)\right]. \tag{7-49}$$

Again integrating (7-49) with respect to Y and taking into account the first boundary condition of (7-14a), we obtain

$$\theta=\frac{B(X)}{2}\left[-(1-k)^2\ln(1-Y)-\left(Y-\frac{Y^2}{2}\right)\right].$$

Using the first boundary condition of (7-14b), we find an expression for $B(X)$ and the final equation for θ:

$$B(X)=-\frac{2}{(1-k)^2\ln(1-k)+\left(k-\frac{k^2}{2}\right)}; \tag{7-50}$$

$$\theta=\frac{(1-k)^2\ln(1-Y)+\left(Y-\frac{Y^2}{2}\right)}{(1-k)^2\ln(1-k)+\left(k-\frac{k^2}{2}\right)}. \qquad (7\text{-}51)$$

Since the thickness of the thermal boundary layer is assumed to be small as compared with the tube radius, in calculating the thickness, and in determining the viscosity variation over the boundary-layer thickness in (7-44), we can neglect Y as compared with unity (i.e., the curvature of the tube surface). In such case, in place of (7-50) and (7-51) we obtain the equations

$$B(X)=-\frac{2}{k^2}, \qquad (7\text{-}50a)$$

$$\theta=2\frac{Y}{k}-\frac{Y^2}{k^2}, \qquad (7\text{-}51a)$$

which coincide with the corresponding flat-tube equations.

Substituting the value of θ from (7-51a) into (7-47), we obtain

$$\frac{\mu_s}{\mu}=\sum_{i=0}^{i=2n} b_i\left(\frac{Y}{k}\right)^i, \qquad (7\text{-}52)$$

where the b_i are new constants; $b_0 = 1$.

Integrating (7-45) with respect to Y and noting that $\left(\frac{\partial W_x}{\partial Y}\right)_{Y=1}=0$, we find

$$\frac{\partial W_x}{\partial Y}=\frac{1}{2}A(X)\frac{\mu_s}{\mu}(Y-1). \qquad (7\text{-}53)$$

Integrating (7-53) for $Y \leq k$ [in this case, μ_s/μ is described by Eq. (7-52)] and $Y \geq k$ (here $\mu = \mu_0 = \text{const}$), we obtain the following equations for W_x:

for $Y \leq k$

$$W_x=\frac{1}{2}A(X)\sum_{i=0}^{n}\frac{b_i}{k^i}\left(\frac{Y^{i+2}}{i+2}-\frac{Y^{i+1}}{i+1}\right); \qquad (7\text{-}54)$$

for $Y = k$

$$W_{x,\,Y=k}=\frac{1}{2}A(X)\sum_{i=0}^{n}b_i\left(\frac{k^2}{i+2}-\frac{k}{i+1}\right); \qquad (7\text{-}55)$$

for $Y \geq k$

$$W_x=\frac{1}{2}A(X)\left\{\frac{\mu_s}{\mu_0}\left[\frac{1}{2}(Y^2-k^2)-(Y-k)\right]+\sum_{i=0}^{n}b_i\left(\frac{k^2}{i+2}-\frac{k}{i+1}\right)\right\}. \qquad (7\text{-}56)$$

The function $A(X)$ is determined from the condition requiring that the flowrate be constant:

$$\int_0^{r_0-\Delta} 2\pi r w_x\,dr + \int_{r_0-\Delta}^{r_0} 2\pi r w_x\,dr = \pi r_0^2 \bar{w}.$$

Going from the coordinate r to the coordinate y, after this equation has been reduced to dimensionless form we obtain

$$\int_0^k W_x(1-Y)\,dY + \int_k^1 W_x(1-Y)\,dY = \frac{1}{2}.$$

Using (7-54) to evaluate the first integral and (7-56) for the second, and performing certain manipulations, we find

$$A(X) = -\frac{2}{P_0 + P_1 k + P_2 k^2 + P_3 k^3 + P_4 k^4} = -\frac{2}{R}, \qquad (7\text{-}57)$$

where

$$\left.\begin{aligned} P_0 &= \frac{1}{4}\cdot\frac{\mu_r}{\mu_0},\\ P_1 &= -\frac{\mu_r}{\mu_0} + \sum_{i=0}^{n}\frac{b_i}{i+1},\\ P_2 &= \frac{3}{2}\cdot\frac{\mu_r}{\mu_0} - 3\sum_{i=0}^{n}\frac{b_i}{i+2},\\ P_3 &= -\frac{\mu_r}{\mu_0} + 3\sum_{i=0}^{n}\frac{b_i}{i+3},\\ P_4 &= \frac{1}{4}\cdot\frac{\mu_r}{\mu_0} - \sum_{i=0}^{n}\frac{b_i}{i+4}. \end{aligned}\right\} \qquad (7\text{-}58)$$

$$R = P_0 + P_1 k + P_2 k^2 + P_3 k^3 + P_4 k^4. \qquad (7\text{-}59)$$

Substituting $A(X)$ from (7-57) into (7-54) and (7-56), we obtain the final equations for W_x:

for $Y \leqslant k$

$$W_x = \frac{1}{R}\sum_{i=0}^{n}\frac{b_i}{k^i}\left(\frac{Y^{i+1}}{i+1} - \frac{Y^{i+2}}{i+2}\right); \qquad (7\text{-}60)$$

for $Y \geqslant k$

$$W_x = \frac{1}{R}\left\{\frac{\mu_r}{\mu_0}\left[(Y-k) - \frac{1}{2}(Y^2-k^2)\right] + \sum_{i=0}^{n} b_i\left(\frac{k}{i+1} - \frac{k^2}{i+2}\right)\right\}. \qquad (7\text{-}61)$$

For isothermal flow, (7-60) and (7-61) yield the familiar parabolic velocity distribution:

$$W_x = 2Y(2-Y),$$

or

$$\frac{w_x}{w} = 2\left(1 - \frac{r^2}{r_0^2}\right).$$

We determine W_y from the continuity equation (7-46). Within the thermal boundary layer we neglect Y as compared with unity; this yields

$$W_y = -\int_0^Y \frac{\partial W_x}{\partial X} dY.$$

Substituting in W_x from (7-60) and integrating, we obtain

$$W_y = \frac{dk}{dX} \sum_{i=0}^{n} \frac{b_i}{k^{i+1}} \cdot \frac{iR+T}{R^2} \left[\frac{Y^{i+2}}{(i+1)(i+2)} - \frac{Y^{i+3}}{(i+2)(i+3)} \right]. \qquad (7\text{-}62)$$

where

$$T = P_1 k + 2P_2 k^2 + 3P_3 k^3 + 4P_4 k^4.$$

3. We find the thickness of the thermal boundary layer and compute the heat transfer and friction resistance. The relationship between k and X is determined from (7-48). Substituting $B(X)$ from (7-50a) into this equation, we have

$$-\frac{2}{k^2} = \frac{Pe}{2k} \int_0^k \left[\left(W_x \frac{\partial \Theta}{\partial X} + W_y \frac{\partial \Theta}{\partial Y} \right) + \varepsilon \frac{\mu}{\mu_0} \left(\frac{\partial W_x}{\partial Y} \right)^2 \right] dY. \qquad (7\text{-}63)$$

Using the equations for W_x, W_y, and Θ, we evaluate the integrals:

$$\int_0^k W_x \frac{\partial \Theta}{\partial X} dY = \frac{2}{R} \cdot \frac{dk}{dX} \left[k^2 \sum_{i=0}^{n} \frac{b_i}{(i+2)(i+4)(i+5)} - \right.$$

$$\left. - k \sum_{i=0}^{n} \frac{b_i}{(i+1)(i+3)(i+4)} \right];$$

$$\int_0^k W_y \frac{\partial \Theta}{\partial Y} dY = \frac{2}{R^2} \cdot \frac{dk}{3X} \sum_{i=0}^{n} b_i (iR+T) \left[\frac{k}{(i+1)(i+2)(i+3)(i+4)} - \right.$$

$$\left. - \frac{k^2}{(i+2)(i+3)(i+4)(i+5)} \right];$$

$$\int_0^k \varepsilon \frac{\mu}{\mu_0} \left(\frac{\partial W_x}{\partial Y} \right)^2 dY = \varepsilon \frac{1}{R^2} \left(k \sum_{i=0}^{n} \frac{b_i}{i+1} - 2k^2 \sum_{i=0}^{n} \frac{b_i}{i+2} + k^3 \sum_{i=0}^{n} \frac{b_i}{i+3} \right).$$

Substituting the values of the integrals into (7-63) and integrating from 0 to k and from 0 to X, respectively, we finally obtain

$$\int_0^k \frac{B_1\left(2-\frac{T}{R}\right)-B_2 k\left(3-\frac{T}{R}\right)\frac{k^2}{2R}}{1+\frac{1}{2}\pi_1\frac{k^2}{R^2}(D_1-2D_2k+D_3k^2)}\,dk=\frac{X}{\mathrm{Pe}}, \qquad (7\text{-}64)$$

where

$$\left.\begin{aligned} B_1&=\sum_{i=0}^{n}\frac{b_i}{(i+1)(i+2)(i+3)(i+4)};\\ B_2&=\sum_{i=0}^{n}\frac{b_i}{(i+2)(i+3)(i+4)(i+5)}; \end{aligned}\right\} \qquad (7\text{-}65)$$

$$\pi_1=\frac{1}{2}\mathrm{Pe}\,\pi=\frac{\bar{w}^2\rho_c}{\lambda(t_0-t_c)}; \qquad (7\text{-}66)$$

$$D_1=\sum_{i=0}^{n}\frac{b_i}{i+1};\quad D_2=\sum_{i=0}^{n}\frac{b_i}{i+2};\quad D_3=\sum_{i=0}^{n}\frac{b_i}{i+3}. \qquad (7\text{-}67)$$

Equation (7-64) establishes the relationship between the dimensionless thickness k of the thermal boundary layer and X/Pe. The second term in the denominator of the integrand allows for the heat of friction. The integral on the left side of the equation must be evaluated numerically.

The only structural difference between (7-64) and the corresponding equation for a flat tube lies in the term allowing for the heat of friction. It should be noted, however, that the functions T and R differ in the equations for the round and flat tubes.

Evaluation of the influence of the heat of friction shows that in many cases it can be neglected. Thus, for the conditions of the example given in the preceding section (flow of grade MK oil at $\mu_s/\mu_0 = 58$), the term allowing for the heat of friction amounts to only 0.7% of the denominator.

Referring the local heat-transfer coefficient to the initial temperature difference $t_s - t_0$, we obtain the following expression for the Nusselt number:

$$\mathrm{Nu}=\frac{\alpha d}{\lambda}=2\left(\frac{\partial\Theta}{\partial Y}\right)_{Y=0},$$

where $d = 2r_0$.

Substituting in Θ from (7-51), we find

$$\mathrm{Nu}=\frac{4}{1+\frac{2(1-k)^3}{2k-k^2}\ln(1-k)}. \qquad (7\text{-}68)$$

If we replace (7-51) by (7-51a) (i.e., we neglect the curvature of the tube surface), then

$$\mathrm{Nu}=\frac{4}{k}, \qquad (7\text{-}68a)$$

which coincides with the corresponding flat-tube equation.

For constant viscosity, (7-64) takes the form

$$\int_0^k \frac{\left(\frac{1}{12}-\frac{k}{40}\right)k^3}{1+8a_1\left(k^2-k^3+\frac{1}{3}k^4\right)}\,dk=d\left(\frac{1}{Pe}\cdot\frac{x}{d}\right). \qquad (7\text{-}69)$$

Integrating this equation and neglecting the heat of friction, we obtain

$$\frac{k^3}{36}\left(1-\frac{9}{40}k\right)=\frac{1}{Pe}\cdot\frac{x}{d}. \qquad (7\text{-}70)$$

Solving (7-68) and (7-70) simultaneously, we can find the relationship $Nu=f\left(\frac{1}{Pe}\cdot\frac{x}{d}\right)$ for the constant-viscosity case.

If we use (7-68a) rather than (7-68), i.e., if we neglect the curvature of the tube surface, then for μ = const we have

$$Nu^3=\frac{16}{9}Pe\frac{d}{x}\left(1-\frac{0.9}{Nu}\right). \qquad (7\text{-}71)$$

For large values of Pe d/x, where k is small and Nu large, (7-71) will take the form

$$Nu=1.21\left(Pe\frac{d}{x}\right)^{1/3}. \qquad (7\text{-}72)$$

This coincides with the Leveque equation for a round tube, with the sole difference that the constant coefficient in (7-72) is 11% larger than in the Leveque equation (6-55).

Using Eq. (7-60) for W_x, as in the previously considered flat-tube case, it is not difficult to obtain an expression for the local friction-resistance coefficient:

$$\xi=\frac{16}{Re_c}\cdot\frac{1}{R}, \qquad (7\text{-}73)$$

where $Re_c=\frac{\bar{w}d\rho}{\mu_c}$.

For isothermal flow, R = 1/4 and (7-73) goes over to the familiar formula (5-10) for the resistance coefficient of a round tube.

4. Let us look at the results of the theoretical computation and compare them with experimental data. Figure 7-7 shows the temperature distribution over the cross section of a round tube for various values of k [the solid lines correspond to Eq. (7-51a), and the dashed lines to Eq. (7-51)]. When k = 1, the computational results agree for both equations. When k = 0.5, the dashed curve is somewhat lower. As k diminishes, the distance between the curves is reduced, and at k = 0.2 and 0.1 they nearly coincide. For very small k (about 0.01 or less), the dashed curve should run somewhat above the solid curve. Thus tube curvature has relatively little influence on the temperature field.

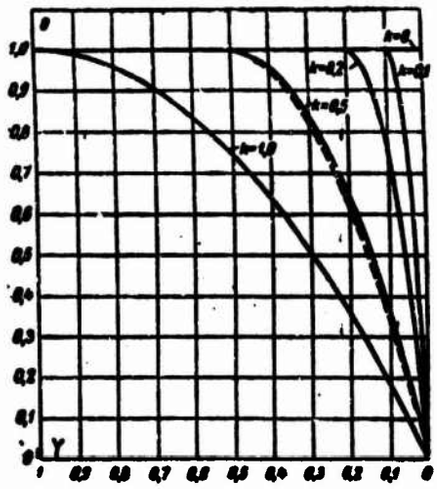

Fig. 7-7. Temperature distribution over section of round tube for various values of $k = \Delta/r_0$. Dashed line) With allowance for tube curvature; solid lines) no such allowance.

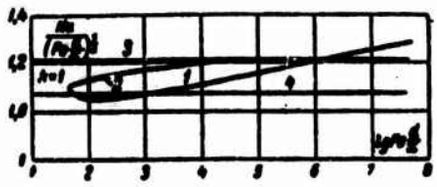

Fig. 7-8. Comparison of different formulas for Nu at μ = const. 1) Calculations by (7-68) and (7-70); $2-\mathrm{Nu}=\frac{17}{9}\mathrm{Pe}\frac{d}{x}\left(1-\frac{0.8}{\mathrm{Nu}}\right)$; $3-\mathrm{Nu}=1{,}21\left(\mathrm{Pe}\frac{d}{x}\right)^{1/3}$; $4-\mathrm{Nu}=1{,}077\left(\mathrm{Pe}\frac{d}{x}\right)^{1/3}$ Leveque formula.

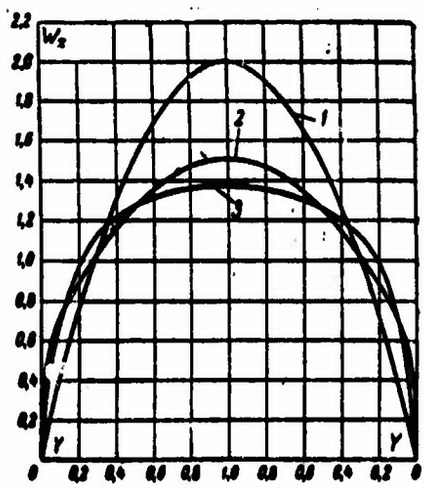

Fig. 7-9. Velocity profiles in round tube for heating of fluid (flow of grade MC oil at t_0 = 40°C, t_s = 98°C and μ_s/μ_0 = 0.0784). 1) $k = 0$, isothermal flow; 2) $k = 0{,}1$; $\mathrm{Pe}\frac{d}{x} = 11{,}4\cdot 10^3$; 3 — $k = 0{,}5$; $\mathrm{Pe}\frac{d}{x} = 280$.

Figure 7-8 compares the different equations for the local Nu number at constant viscosity. Equation (7-72) and Leveque equation (6-55) are represented by the horizontal lines 3 and 4 in the selected coordinates. As we have already noted, the difference between them does not exceed 11%. The curves corresponding to the other equations lie between curves 3 and 4 for the most part.

Figures 7-9 and 7-10 show the velocity profiles for heating and cooling of the fluid. For heating, as compared withthe velocity for isothermal flow, the velocity is higher near the wall and lower at the center of the tube. Thus the velocity profile becomes more rounded. For cooling, the reverse effect is observed, and the velocity of profile takes on a characteristic elongated shape. It is interesting to note that for the same values of k and μ_s/μ_0, the velocity variation at the axis is sharper for a round tube than for a flat one (compare Figs. 7-2 and 7-10).

Figure 7-11 shows theoretically computed curves for the local Nu numbers as a function of Pe d/x or a flow of grade MC oil. Curve 1 corresponds to oil heating at $\mu_s/\mu_0 = 0.78$; curve 2, constructed from Eqs. (7-68) and (7-70) refers to the case in which $\mu_s/\mu_0 = 1$; curve 3 corresponds to cooling of the oil with $\mu_s/\mu_0 = 58$. The fluid velocity at the wall is higher for heating and lower for cooling than the isothermal-flow value; thus curve 1 is above, and curve 3 below curve 2. As the graph shows, as μ_s/μ_0 varies from 0.078 to 58, heat transfer is reduced by roughly a factor of 3.

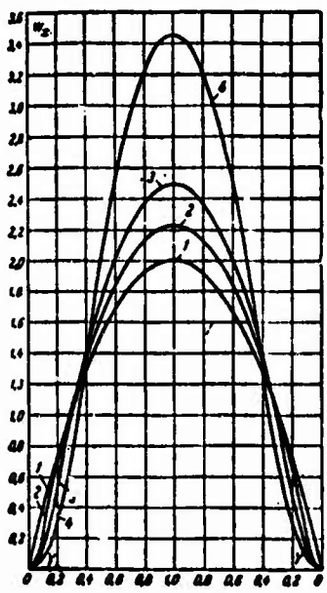

Fig. 7-10. Velocity profiles in round tube for cooling of fluid (flow of grade MC oil at $t_0 = 100°C$, $t_s = 20°C$, and $\mu_s/\mu_0 = 58$).
1) $k = 0$, isothermal flow; 2— $k = 0,1$; $\mathrm{Pe}\frac{d}{x} = 136 \cdot 10^3$; 3— $k = 0,2$; $\mathrm{Pe}\frac{d}{x} = 10,9 \cdot 10^3$; 4— $k = 0,5$; $\mathrm{Pe}\frac{d}{x} = 241$.

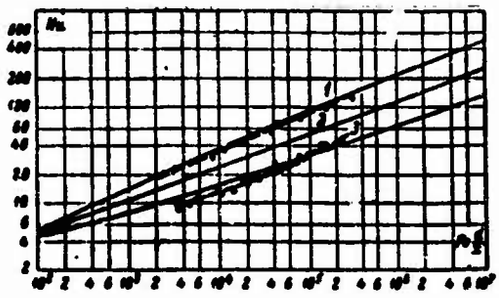

Fig. 7-11. Heat transfer in a round tube according to theoretical data (solid lines) and experiment (dashed lines with circles).

$1 - \frac{\mu_c}{\mu_0} = 0{,}078;\ 2 - \frac{\mu_c}{\mu_0} = 1;\ 3 - \frac{\mu_c}{\mu_0} = 58.$

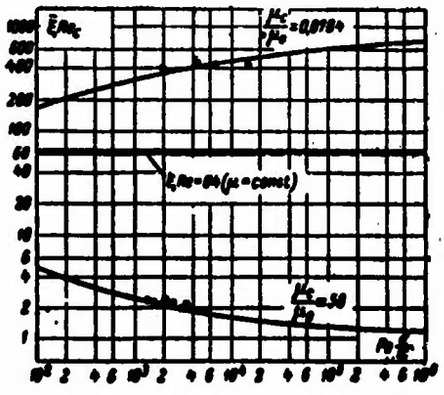

Fig. 7-12. Relationship $\xi Re_s = f\left(Pe\frac{d}{x}\right)$ for round tube according to theoretical data (solid lines) and experiment (circles).

Figure 7-11 also gives experimental data [13] for heat transfer in a round tube during flow of grade MC oil; the data were obtained under the same conditions as the theoretical curves 1 and 3. As we can see, the experimental data are in satisfactory agreement with calculation. It is only for the case of fluid cooling at Pe d/x > > $7 \cdot 10^4$ that the experimental curve is somewhat steeper. This is caused by the influence of the hydrodynamic initial segment, which in these experiments formed part of the heat-exchange segment.

Figure 7-12 shows the results of a theoretical determination of the mean friction-resistance coefficient. The horizontal line corresponds to isothermal flow ($\xi Re = 64$), the upper curve to flow of grade MC oil with heating ($\mu_s/\mu_0 = 0.078$), at the lower curve to cooling ($\mu_s/\mu_0 = 58$). The experimental data [22] plotted on the same graph are in good agreement with the theoretical results.

/-4. THEO ETICAL DETERMINATION OF HEAT EXCHANGE AND RESISTANCE FOR A ROUND TUBE

1. In contrast to the preceding section, we shall consider flow and heat exchange along the entire tube length, and not just in the thermal initial segment. As before, we shall assume that the fluid viscosity depends on the temperature, while the other physical properties are constant. The velocity profile at the entrance is taken to be parabolic, the temperature distribution at the entrance uniform, and the wall temperature constant. Following [9] in the analysis, we assume that the temperature differences in the flow are not too large. This permits us first to assume a linear relationship between $1/\mu$ and t and, second, to assume that the radial velocity component is small as compared with the axial component.[1]

Letting $w_r = 0$, we obtain $\partial w_x/\partial x = 0$ from the equation of continuity. Using these assumptions and neglecting the heat of friction, we reduce (7-41) and (7-42) to the form

$$a\frac{1}{r}\cdot\frac{\partial}{\partial r}\left(r\frac{\partial t}{\partial r}\right)=w_x\frac{\partial t}{\partial x}, \tag{7-74}$$

$$\frac{1}{r}\cdot\frac{\partial}{\partial r}\left(\mu r\frac{\partial w_x}{\partial r}\right)=\frac{dp}{dx}, \tag{7-75}$$

where p is a function of x alone.

Integrating (7-75) twice with respect to r, we find

$$w_x=-\frac{1}{2}\cdot\frac{dp}{dx}\int_r^{r_0}\frac{r}{\mu}dr. \tag{7-76}$$

Substituting w_x into the expression for the mean velocity over the section,

$$\bar{w}=\frac{2}{r_0^2}\int_0^{r_0}w_x r\,dr,$$

we represent the pressure gradient as follows:

$$\frac{dp}{dx}=-\frac{\bar{w}r_0^2}{\int_0^{r_0}\left(r\int_r^{r_0}\frac{r}{\mu}dr\right)dr}. \tag{7-77}$$

Substituting this expression into (7-76), we obtain

$$\frac{w_x}{\bar{w}}=\frac{r_0^2}{2}\cdot\frac{\int_r^{r_0}\frac{r}{\mu}dr}{\int_0^{r_0}\left(r\int_r^{r_0}\frac{r}{\mu}dr\right)dr}. \tag{7-78}$$

Using (7-78) and going over to dimensionless independent variables (in (7-74), we write the last equation as

[1]/177

$$\frac{\int_0^Y \frac{(1-Y)}{\mu}\,dY}{8\int_0^1 (1-Y)\left[\int_0^Y \frac{(1-Y)}{\mu}\,dY\right]dY}\,\frac{\partial t}{\partial X}=\frac{1}{1-Y}\cdot\frac{\partial}{\partial Y}\left[(1-Y)\frac{\partial t}{\partial Y}\right], \qquad (7\text{-}79)$$

where $X=\frac{1}{Pe}\cdot\frac{x}{d}$; $Pe=\frac{\bar{w}d}{a}$; $Y=\frac{y}{r_0}=1-\frac{r}{r_0}$.

We introduce the dimensionless temperature $\theta=\frac{t-t_0}{t_0-t_0}$ and use the following equation to represent the relationship between viscosity and temperature:

$$\frac{\mu_c}{\mu}=1+\gamma\theta, \qquad (7\text{-}80)$$

where γ is a constant parameter.

Letting $\theta = 1$ in (7-80), we find

$$\gamma=\frac{\mu_c}{\mu_0}-1,$$

where μ_s and μ_0 are the values of the viscosity coefficient for the wall temperature and the fluid temperature at the entrance. For cooling of the fluid, $\mu_c/\mu_0>1$ and $\gamma>0$; for heating, $\mu_c/\mu_0<1$ and $\gamma<0$.

Substituting μ from (7-80) into (7-79) and going over to the dimensionless temperature, we obtain

$$\frac{\int_0^Y (1-Y)(1+\gamma\theta)\,dY}{8\int_0^1 (1-Y)\left[\int_0^Y (1-Y)(1+\gamma\theta)\,dY\right]dY}\,\frac{\partial\theta}{\partial X}=$$
$$=\frac{1}{1-Y}\cdot\frac{\partial}{\partial Y}\left[(1-Y)\frac{\partial\theta}{\partial Y}\right]. \qquad (7\text{-}81)$$

This equation must be solved under the following boundary conditions.

for $X=0$ and $0<Y\leq 1$ $\theta=1$;
for $X\geqslant 0$ and $Y=0$ $\theta=0$.

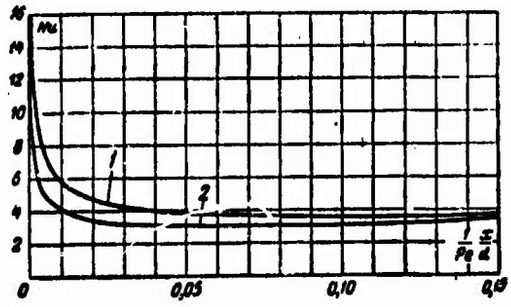

Fig. 7-13. The Nu number in a round tube as a function of $\frac{1}{Pe}\cdot\frac{x}{d}$.

1 — $\frac{\mu_c}{\mu_0}=0.1$; 2 — $\frac{\mu_c}{\mu_0}=10$.

We seek separate solutions of (7-81) for the thermal initial segment and the region of stabilized heat exchange; we then join these solutions. In first approximation, both the first and second solutions are obtained by means of the Karman-Pohlhausen integral method. The solution found is substituted into the initial differential equation, which is then transformed into an ordinary linear second-order differential equation in θ. Solution of the latter gives the final expression for the temperature profile. The temperature profile found by this method is in significantly better agreement with the exact solution (for constant viscosity) than the arbitrarily chosen profile (first approximation for θ) in the usual integral method. Knowing the temperature profile, it is not difficult to compute the Nusselt number, velocity profile, and resistance coefficient. [2]

TABLE 7-4

The Nu Number for a Round Tube as a Function of $\frac{1}{Pe}\cdot\frac{x}{d}$ for Various Values of μ_s/μ_0 When t_s = const

$\frac{1}{Pe}\cdot\frac{x}{d}$	Nu	$\frac{1}{Pe}\cdot\frac{x}{d}$	Nu	$\frac{1}{Pe}\cdot\frac{x}{d}$	Nu
$\frac{\mu_s}{\mu_0}=0,1$		$\frac{\mu_s}{\mu_0}=0,4$		$\frac{\mu_s}{\mu_0}=0,7$	
0,00075	16,004	0,0005	15,470	0,0004	15,194
0,0047	7,685	0,0038	7,370	0,00335	7,172
0,0130	5,317	0,0117	5,118	0,0110	4,973
0,0247	4,447	0,0234	4,320	0,0227	4,217
0,0500	3,912	0,0500	3,829	0,0500	3,760
0,0750	3,829	0,0750	3,781	0,0750	3,739
0,1000	3,781	0,1000	3,752	0,1000	3,725
0,1250	3,752	0,1250	3,734	0,1250	3,717
0,1500	3,734	0,1500	3,722	0,1500	3,711
$\frac{\mu_s}{\mu_0}=4$		$\frac{\mu_s}{\mu_0}=7$		$\frac{\mu_s}{\mu_0}=10$	
0,0002	14,427	0,0002	14,274	0,0002	14,203
0,00235	6,563	0,0022	6,440	0,00215	6,382
0,0091	4,425	0,00875	4,294	0,00855	4,231
0,0208	3,737	0,02045	3,600	0,0203	3,531
0,0500	3,353	0,0500	3,200	0,0500	3,115
0,0750	3,432	0,0750	3,284	0,0750	3,193
0,1000	3,500	0,1000	3,368	0,1000	3,276
0,1250	3,555	0,1250	3,445	0,1250	3,360
0,1500	3,598	0,1500	3,511	0,1500	3,438

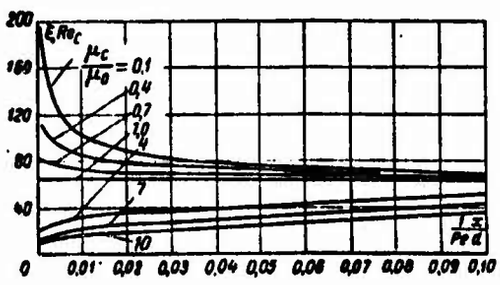

Fig. 7-14. Values of ξRe_s for a round tube as a function of $\frac{1}{Pe}\cdot\frac{x}{d}$ for various values of μ_c/μ_0.

[2]/177

Numerical calculations were carried out by digital computer for values of μ_s/μ_0 from 10 to 0.1. Some results of these calculations are shown in Table 7-4 and Figs. 7-13 and 7-14.

The relationship between $Nu = \alpha d/\lambda^*$ and X is shown in Fig. 7-13 for $\mu_s/\mu_0 = 0.1$ and 10; the curves indicate that the change in viscosity with temperature has a stronger influence on heat exchange in the thermal initial segment than in the thermal-stabilization region. It is also interesting to note that at $\mu_s/\mu_0 > 1$, Nu passes through a minimum as X increases, while it decreases monotonically when $\mu_s/\mu_0 < 1$. This results from the joint action of two factors, the reduction in heat transfer in the thermal initial segment, which occurs for all values of μ_s/μ_0, and the increase (for $\mu_s/\mu_0 > 1$) or decrease (for $\mu_s/\mu_0 < 1$) in heat transfer resulting from the change in velocity near the wall with tube length caused by the variation in viscosity.

Thus when the physical properties of the fluid, in particular the viscosity, are variable, Nu will vary along the length in the thermal-stabilization region as well, although far less strongly than in the thermal initial segment. Naturally, when $X \to \infty$, Nu approaches its limit, $Nu_\infty = 3.66$. This constant value is attained only a certain distance away from the entrance, where the temperature differences in the flow become sufficiently small. It is understood that this difference by no means correspond to the length of the thermal initial segment.

When the physical properties of the fluid are constant (see Chapter 6), the length of the thermal initial segment is defined as the distance from the entrance beginning at which Nu takes on a constant value. It is quite obvious that with variable fluid physical properties, this definition is unsuitable. For this more general case, by the length of the thermal initial segment we should mean the distance from the entrance beginning with which the temperature field and, consequently, the Nusselt number cease to depend on the initial temperature distribution (i.e., the distribution at $X = 0$).

As we might expect, the friction-resistance coefficient $\xi = \frac{\delta p_c}{\frac{\rho \bar{w}^2}{2}}$ (Fig. 7-14) depends not only on $Re_c = \frac{\bar{w} d \rho}{\mu_c}$, but also on X and μ_s/μ_0. For the limiting cases, i.e., when $\frac{\mu_s}{\mu_c} \to 1$ or $X \to \infty$, the quantity ξRe_s approaches a constant value corresponding to isothermal flow ($\xi Re = 64$).

2. The results given here and in the preceding sections hold only for liquids. For a gas flowing at high temperature heads, we must consider not only the way in which μ depends on T, but also the dependences of ρ, λ, and c_p on T. Some heat-exchange and friction calculations have been published for air under cooling conditions far from the tube entrance with $T_s = \text{const}$ [10]. They show

*/178

hat if λ in the expression for Nu_∞ is selected for the mean mass temperature $\bar{T}$, then as $T_s/\bar{T}$ decreases from 1 to 0.25, Nu_∞ will rise when the physical properties are variable. This increase is not great, however, not exceeding 6% of the Nu_∞ value for constant physical properties. The resistance coefficient under these conditions varies as a function of $T_s/\bar{T}$ in roughly the same way as when q_s = = const (see §9-4).

Worse-Schmidt and Leppert [11] have made a more detailed investigation of heat exchange and resistance in a round tube for a flow of a gas with variable physical properties. The system of equations of motion, energy, and continuity, describing the boundary layer in approximation, were solved numerically by finite differences. The calculations were carried out for air with allowance for the way in which ρ, c_p, μ and λ depend on T as well as the relationship between ρ and p, in accordance with (3-5), (3-7), (3-9), and (3-10) for values $n_c=0{,}12$; $n_\mu=0{,}67$ and $n_\lambda=0{,}71$, Pr = 0.72 (for the gas temperature at the entrance). The flow parameters were so chosen that the influence of energy dissipation, work of gas expansion, and free convection would be negligible. The parabolic velocity profile and the uniform temperature distribution ($T = T_0$) were specified at the tube entrance, while a constant temperature ($T = T_s$) was given at the wall.

The calculations were carried out for $T_c/T_0=0{,}5$; 1; 2 and 5. They show that the variable physical parameters have relatively little influence on heat transfer, and quite significant influence on the resistance. A somewhat unexpected type of variation in Nu as a function of T_s/T_0 was also found. For small values of the reduced length $\left(\frac{1}{Pe}\cdot\frac{x}{d}<10^{-3}\right)$, Nu increases, while at still higher values it decreases as T_s/T_0 becomes larger. For all values of X, the resistance coefficient increases as T_s/T_0 increases. These features are associated with the way in which the longitudinal and transverse velocity components and physical properties are distributed over the tube cross sections at different distances from the entrance. The variation in Nu and ξ as a function of T_s/T_0 is observed chiefly within the thermal initial segment, whose length is roughly the same as for constant physical properties. For $x>l_{n.т}$, these relationships degenerate rapidly, and Nu and ξ approach the corresponding values for constant physical properties. The reason is that at the fairly low gas flowrates corresponding to laminar flow, with large temperature differences at the entrance, the mean mass temperature of the gas varies rapidly along the length, and $T_c/T \to 1$. The distance from the entrance at which $T_s/\bar{T}$ takes on a value close to unity will roughly coincide with the length of the thermal initial segment.

For the local Nu number and local resistance coefficient ξ, interpolation equations describing the computational results to which +3% have been proposed [11].

For $0{,}5 < \frac{T_c}{T_0} < 2$ and $X > 0{,}0005$

$$\mathrm{Nu} = 3{,}66\,[1 - \exp(-27X)] + aX^{-1/3}\exp(-bX), \qquad (7\text{-}82)$$

where

$$a = 0{,}905 + 0{,}123\frac{T_0}{T_0};$$

$$b = 16{,}2 + 3{,}90\frac{T_c}{T_0};$$

$$\mathrm{Nu} = \frac{q_0 d}{(T_c - \bar{T})\lambda_m};\quad X = \frac{1}{\mathrm{Pe}}\cdot\frac{x}{d};\quad \mathrm{Pe} = \frac{\bar{w}_0 d}{a_0};$$

Here $\bar{T}$ is the mean mass temperature in the given section (found from the mean mass enthalpy for this section); λ_{zh} is the thermal-conductivity coefficient of the gas at $\bar{T}$; $\bar{w}_0$ is the mean gas velocity over the section at the entrance (i.e., for $x = 0$); a_0 is the coefficient of thermal diffusivity for the entrance temperature T_0.

For $0{,}5 < \frac{T_0}{\bar{T}} < 3$ and $X > 0{,}0005$

$$\xi\mathrm{Re} = A\left(\frac{T_0}{\bar{T}}\right)^m, \qquad (7\text{-}82a)$$

where

$$A = 64 \text{ and } m = 0{,}81 \text{ for } 0{,}5 < \frac{T_0}{\bar{T}} < 1;$$

$$A = 64 \text{ and } m = 1{,}0 \text{ for } 1 < \frac{T_0}{\bar{T}} < 1{,}5;$$

$$A = 62 \text{ and } m = 1{,}1 \text{ for } 1{,}5 < \frac{T_0}{\bar{T}} < 3;$$

$$\xi = \frac{8\sigma_0}{\overline{\rho w}\,\bar{w}};\quad \mathrm{Re} = \frac{\overline{\rho w} d}{\mu_m};$$

here $\overline{\rho w}$ is the mean mass gas velocity; $\bar{w}$ is the mean gas velocity in the given section; μ_{zh} is the dynamic viscosity coefficient of the gas at $\bar{T}$.

Equation (7-82a) has also been confirmed for helium and carbon dioxide (for $T_c/T > 1$) with the difference that for CO_2, when $1{,}2 < \frac{T_0}{\bar{T}} \leq 2$ $A = 62$ and $m = 1{,}25$.

Equations (7-82) and (7-82a) are valid for T_s = const, values

of $Pe_x = \frac{\bar{w}_0 x}{a_0} > 500$ and negligible influence of free convection. The last condition will be satisfied if $\frac{g\beta_0 t^2 d^3}{\nu_0 \rho w} < 20$.

7-5. RESULTS OF EXPERIMENTAL INVESTIGATIONS INTO HEAT TRANSFER

Several investigators have carried out experiments on heat transfer with viscous flow of a fluid in tubes [11, 13-19]. The mean heat transfer in tubes of various diameters and lengths was measured in the earlier studies [16, 17, 18]. The measurement method was imperfect, so that the measurement results occasionally contained significant errors. The empirical formulas for mean heat transfer based on these measurements either neglect or make improper allowance for the influence of several factors. Thus, for example, the formulas of Kraussold [16] and Boehm [18], often recommended

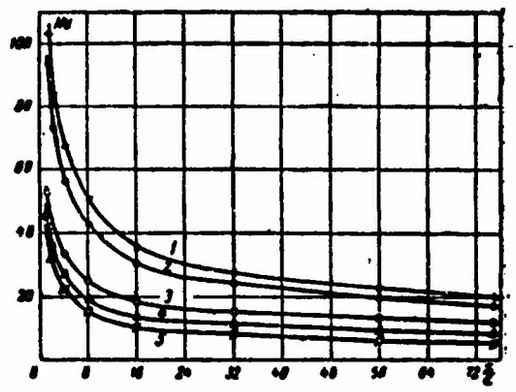

Fig. 7-15. Number Nu = $f(x/d)$ for various values of μ_s/μ_{zh} with constant Pe.

$1 - \frac{\mu_c}{\mu_{zh}} = 0{,}09 - 0{,}1$; $2 - \frac{\mu_c}{\mu_{zh}} = 0{,}31 - 0{,}36$; $3 - \frac{\mu_c}{\mu_{zh}} = 5{,}8 - 7{,}2$;
$4 - \frac{\mu_c}{\mu_{zh}} = 20 - 30$; $5 - \frac{\mu_c}{\mu_{zh}} = 250 - 680$.

in the literature, do not properly allow for the influence of Pe and the ratio of tube length to diameter, and totally neglect the influence of the relationship between viscosity and temperature.

Measurements of local heat transfer have been carried out by the author together with Ye.A. Krasnoshchekov and L.D. Nol'de [13, 14, 15]. The heat transfer was studied for viscous flow of grade MC oil in a round tube; the physical properties of the oil were first determined experimentally. The oil was supplied to the tube from a stilling chamber through a nozzle of smooth configuration; there was a mixing device at the tube outlet. The local values of heat-flow density were found from the temperature drops in the thick wall of the tube, which was externally heated or cooled. The temperature of the outside tube surface was held constant, while the temperature of the inside surface varied along the length

in accordance with the nature of the change in the heat-transfer coefficient. The experiments encompass the following ranges: Re betweeen 44 and 2100, Pr between 130 and 3900, and μ_s/μ_{zh} between 0.07 and 1500.

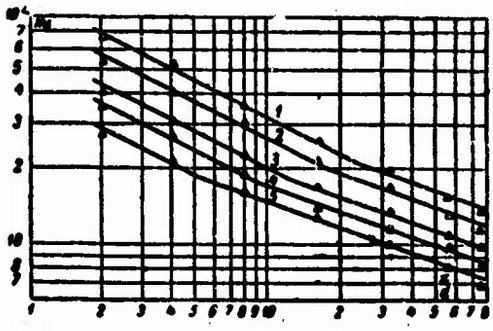

Fig. 7-16. Number Nu = $f(x/d)$ for various values of Pe at μ_s/μ_{zh} = = 13-30.

1—Pe = $10 \cdot 10^3$; 2—Pe = $6 \cdot 10^3$; 3—Pe = $3 \cdot 10^3$; 4—Pe = = $2{,}3 \cdot 10^3$; 5—Pe = $1{,}5 \cdot 10^3$.

Figures 7-15 and 7-16 show the change in local Nusselt number along tube length for certain characteristic experiments. Near the tube entrance, Nu is proportional to $(x/d)^{-1/2}$, while a certain distance from the entrance it is proportional to $(x/d)^{-1/3}$. When we consider that the velocity was distributed nearly uniformly over the entrance section, this type of variation in heat transfer near the entrance can be explained by the simultaneous development of velocity and temperature profiles with the length. Velocity-profile development terminates at the end of the hydrodynamic initial segment, and the −1/2 power law becomes a −1/3 law. The latter corresponds to the relationship usually observed for the thermal initial segment with stabilized flow.

Heat exchange with simultaneous development of velocity and temperature profiles along the tube length is considered in Chapter 12. Here, therefore, we shall only give measurement results for values of x/d exceeding the length of the hydrodynamic initial segment. These results will clearly be valid for the entire thermal initial segment as well if the entrance velocity is parabolically distributed.

Looking at Figs. 7-15 and 7-16, we also see that when Pe is constant, heat transfer drops as μ_s/μ_{zh} increases (Fig. 7-15), while when μ_s/μ_{zh} stays the same, heat transfer rises with increasing Pe (Fig. 7-16). Here $Nu \sim Pe^{1/3}$ sufficiently far from the entrance. Thus in complete agreement with theory, Nu is proportional to $\left(\frac{1}{Pe} \cdot \frac{x}{d}\right)^{-1/3}$ in the thermal initial segment for flow that is being stabilized.

To account for the influence of the variable viscosity, the experimental data was represented as

$$\frac{Nu}{Nu_0} = \varphi\left(\frac{\mu_c}{\mu_w}\right),$$

where Nu is the experimentally determined Nusselt number; Nu_0 is the Nusselt number (for the same value of $\frac{1}{Pe}\cdot\frac{x}{d}$) calculated on the assumption of constant fluid physical properties; μ_s and μ_{zh} are the dynamic viscosity coefficients at wall temperature and at the mean mass temperature of the fluid in the given section. We can use (6-59), which is valid $\frac{1}{Pe}\cdot\frac{x}{d}\leqslant 0{,}01$ as the simplest relationship for Nu_0.

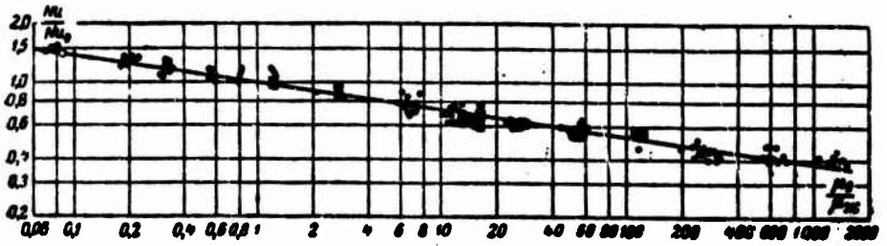

Fig. 7-17. Ratio Nu/Nu_0 as function of μ_s/μ_{zh} with developed velocity profile at entrance.

This treatment of the experimental data shown in Fig. 7-17 leads to the following interpolation equation for local heat transfer in the thermal initial segment of a round tube:

$$Nu = 1{,}03\left(\frac{1}{Pe}\cdot\frac{x}{d}\right)^{-1/3}\left(\frac{\mu_c}{\mu_w}\right)^{-0{,}14}, \qquad (7\text{-}83)$$

The heat-transfer coefficient in (7-83) refers to the local temperature head $t_s - \bar{t}$. The fluid physical properties entering into Nu and Pe are chosen for a temperature $t = \frac{1}{2}(t_c + \bar{t})$.

Equation (7-83) is valid in the region of values $\frac{1}{Pe}\cdot\frac{x}{d} < 0{,}01$ and $0{,}07 < \frac{\mu_c}{\mu_w} < 1500$ both when the wall temperature is constant and when it varies along the length (if the variation is fairly small).

We integrate (7-83) over the length, assuming that μ_s/μ_{zh} is constant, since the mean mass temperature $\bar{t}$ varies little along the length. As a result, we obtain an equation for the mean Nusselt number over the length:

$$\overline{Nu} = 1{,}55\left(\frac{1}{Pe}\cdot\frac{l}{d}\right)^{-1/3}\left(\frac{\mu_c}{\mu_w}\right)^{-0{,}14}. \qquad (7\text{-}84)$$

In (7-84), the mean heat-transfer coefficient refers to the mean logarithmic temperature head (since $\bar{t}$ varies little with the length, so that the temperature head can ordinarily be replaced by the arithmetic mean). In the expressions for $\overline{Nu}$ and Pe, the physical properties of the fluid and the value of μ_{zh} are selected for a temperature $t = \bar{t}_c - \frac{1}{2}\overline{\Delta t}_n$. Equation (7-84) can be used for values $\frac{1}{Pe}\cdot\frac{x}{d} \leqslant 0{,}05$.

Equation (7-84) differs from the familiar formula of Sieder and Tate [17] only in a constant coefficient (1.5 rather than 1.86). Thus this formula gives values of heat-transfer coefficients that are 20% too high, which is not surprising, since it is based on experimental data that deviate by as much as 100% from the average curve.

The ratio $(\mu_s/\mu_{zh})^{-0.14}$ can validly be used to allow for the influence of variable viscosity in (7-83) and (7-84) for liquids (petroleum products, water, etc.) whose dynamic viscosity coefficient decreases in roughly the same way with temperature as for the liquids employed in the experiments. Naturally, this way of allowing for variable viscosity is not suited to gases whose viscosities increase with temperature.

To conclude, we note that (7-83) and (7-84) refer to the case of viscous flow of a fluid, where free convection does not have a substantial influence on forced flow and, consequently, on heat transfer. This condition is satisfied in approximation if $Gr \cdot Pr < 8 \cdot 10^5$, where $Gr = \frac{g\beta \Delta t d^3}{\nu^2}$; $\Delta t = |t_c - t_0|$; t_0 is the fluid temperature at the tube entrance; and the physical properties in the Gr·Pr expression are selected for a temperature of $t = (t_0 + t_s)/2$.

7-6. RESULTS OF EXPERIMENTAL INVESTIGATIONS INTO HYDRAULIC RESISTANCE

It was shown in the preceding sections of this chapter that the relationships between viscosity and temperature has a significant influence on the velocity profile and the resistance coefficient. Thus the relationships obtained for isothermal flow cannot be used directly in calculating the hydraulic resistance when there is heat exchange.

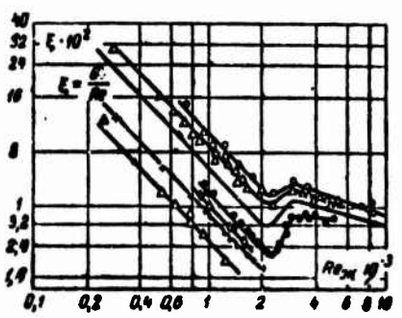

Fig. 7-18. Relationship between $\bar{\xi}$ and $Re_{zh} = \bar{w}d\rho/\mu_{zh}$ for nonisothermal flow of viscous fluids according to data of Kivel, MacAdams, et al.

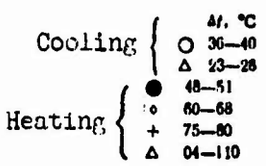

The first experimental investigations into hydraulic resistance with nonisothermal flow of water and air were carried out by M.A. Mikheyev [20, 21] and by several American authors for flow of oils [17]. The data obtained in these studies (some of them are shown in Fig. 7-18) cover a fairly narrow region of variation in physical properties, chiefly viscosity. In this connection, together with Ye. A. Krasnoshchekov, we performed new measurements of hydraulic resistance for nonisothermal flow of oils [22]. The experiments were carried out for grade MC oil in a round tube and grade MK oil and transformer oil in a tube of rectangular cross section.

The round tube had a relative length $l/d=88$; the rectangular tube had a side ratio of $b/h=5.2$ for the cross section, and a relative length $l/h=227$. In neither case was there a damping segment, and the oil entered the experimental segments through nozzles of smooth configuration. The static pressure in the experimental segments was measured near the oil entrance and exit, and for the round tube, at the center as well.

The mean resistance coefficient is found from the experiment by means of the relationship

$$\bar{\xi}=\left(\frac{2\Delta p}{\rho_0 w_0^2}-k\right)\frac{d}{l}, \qquad (7\text{-}85)$$

where Δp is the difference in static pressures for a segment of length l (measuring from the entrance); w_0 and ρ_0 are the fluid velocity and density at the tube entrance; d is the diameter or equivalent diameter of the tube; k is a correction for the hydrodynamic initial segment (based on the data for isothermal flow).

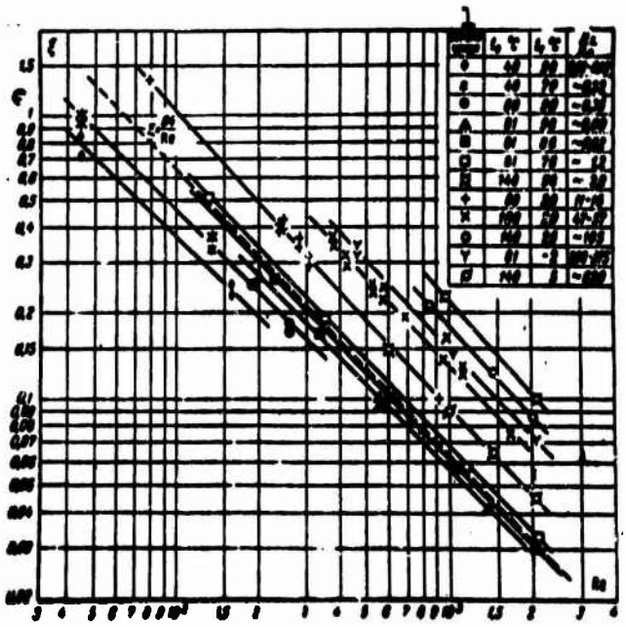

Fig. 7-19. Relationship between $\bar{\xi}$ and Re for a round tube with various temperature regimes. 1) Symbols.

The method used in computing $\bar{\xi}$ for introducing the correction to the hydrodynamic initial segment is valid, strictly speaking, only for isothermal flow.* Its application to nonisothermal flow is in great measure arbitrary, and the coefficient $\bar{\xi}$ found on the basis of experimental data and (7-85) makes allowance not only for the friction resistance, but also for the rearrangement of the velocity profile in the stabilized-flow region. Processing of the experimental data has shown, however, that when such a correction is introduced the relationship for the resistance coefficient is simpler and more general.

Relationship (7-85) is valid provided the length of the tube segment $l > l_{n.r.}$, where $l_{n.r}$ is the length of the hydrodynamic initial segment. This condition was ordinarily satisfied in our experiments (the few experiments in which $l < l_{n.g}$ were disregarded).

Figures 7-19 and 7-20 show $\bar{\xi}$ as a function of Re for round and rectangular tubes. The individual lines on the graphs correspond to specific temperature regimes, each of which is characterized by roughly identical values of t_0, the fluid temperature at the entrance, and t_s, the wall temperature. Thus the ratio μ_s/μ_0 is roughly constant for each regime. The dashed lines pertain to isothermal flow ($\mu_s/\mu_0 = 1$). The lines corresponding to fluid heating are located below, and the lines corresponding to fluid cooling above the dashed lines. It is clear from the graphs that for identical Re, the resistance coefficient will be greater the greater μ_s/μ_0.

It is noteworthy that the lines for di ferent regimes have different slopes in logarithmic coordinates. This is understandable if we consider the results of the theoretical determination of hydraulic resistance for variable viscosity (see §§7-2, 7-3, and 7-4). When $\mu_c/\mu_0 = 1$, the product $\bar{\xi}\mathrm{Re} = \mathrm{const}$, so that the lines for isothermal flow have a slope $n = -1$. For $\mu_c/\mu_0 \neq 1$, the product $\bar{\xi}\mathrm{Re}$ depends not only on μ_s/μ_0, but on Pe d/l as well. Here if $\mu_c/\mu_0 < 1$ (fluid heating), then $\bar{\xi}\mathrm{Re}$ rises as $\mathrm{Pe}\frac{d}{l}$ increases; if $\mu_c/\mu_0 > 1$ (fluid cooling), then $\bar{\xi}\mathrm{Re}$ decreases as $\mathrm{Pe}\frac{d}{l}$ increases. Thus the lines for fluid heating will have slope $n > -1$, while for fluid cooling, $n < -1$. The product $\bar{\xi}\mathrm{Re}$ varies more as a function Pe d/l the more μ_s/μ_0 departs from 1. Accordingly, the slopes of the lines in Figs. 7-19 and 7-20 will depart more from -1 the more μ_s/μ_0 differs from 1.[5]

Analysis of the experimental data indicates that the influence of variable viscosity on the resistance coefficient is roughly the same for tubes differing in shape of cross section, and it can be taken into account by the parameters μ_s/μ_0 and Pe d_e/l. This leads to the following interpolation formula for the mean resistance coefficient for viscous nonisothermal flow:

$$\frac{\bar{\xi}}{\xi_0} = \left(\frac{\mu_r}{\mu_0}\right)^n, \qquad (7\text{-}86)$$

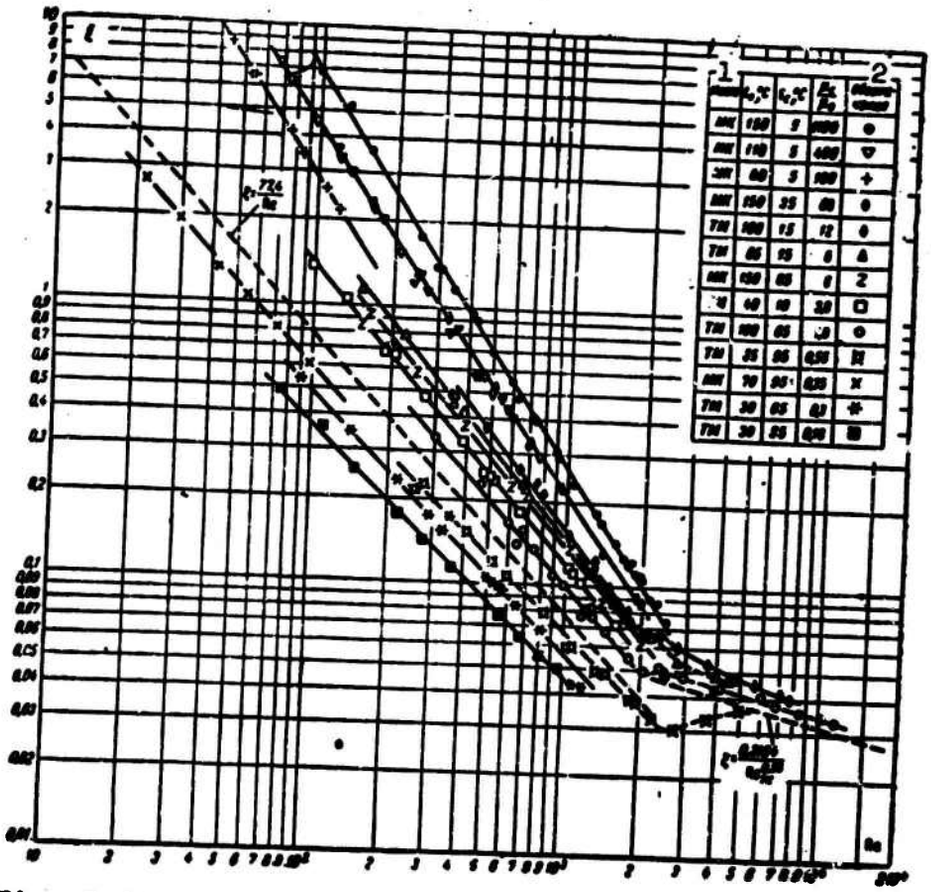

Fig. 7-20. Relationship between $\bar{\xi}$ and Re for tube of rectangular cross section for various temperature regimes. 1) Oil; 2) symbols.

where $\xi_0 = 64\varphi/Re$ is the resistance coefficient for isothermal flow, computed for the fluid temperature at the tube entrance. The constant φ depends on the shape of the tube cross section, and is determined from the data given in §§5-2, 5-3, and 5-4.

TABLE 7-5

Values of Exponent n in Eq. (7-86)

$Pe\frac{d_0}{l}$	μ_c/μ_0				
	0,1	1	10	100	1 000
60	0,776	0,673	0,583	0,505	0,44
100	0,667	0,578	0,502	0,435	0,37
1 000	0,334	0,290	0,251	0,218	0,18
10 000	0,246	0,213	0,185	0,160	0,139
30 000	0,220	0,191	0,165	0,144	0,125

The equation

$$n = C\left(Pe\frac{d_0}{l}\right)^m\left(\frac{\mu_c}{\mu_0}\right)^{-0,\ldots} \qquad (7\text{-}87)$$

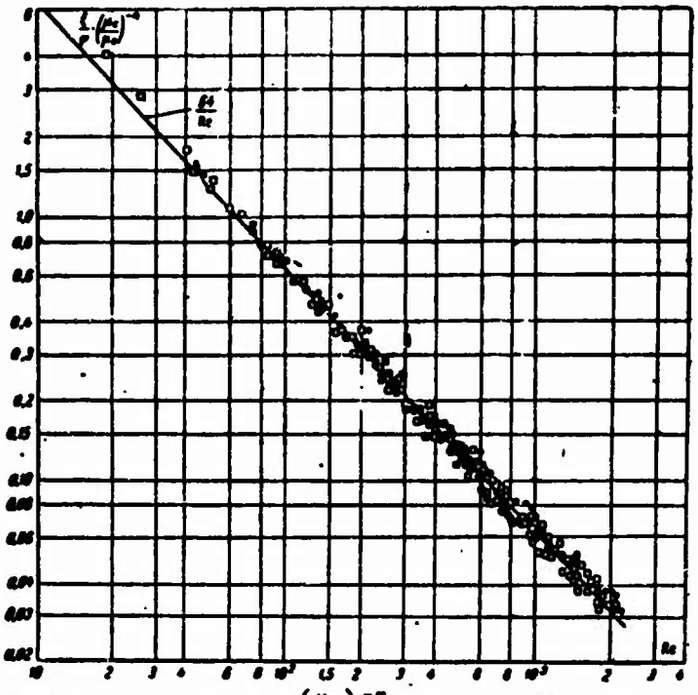

Fig. 7-21. The group $\bar{\varepsilon}\left(\frac{\mu_c}{\mu_0}\right)^{-n}$ has a function of Re for round and rectangular tubes.

1 Форма канала	2 Направление теплового потока	$\mathrm{Pe}\frac{d}{l}$	μ_c/μ_0	Обозначения 3
4 Круглая	5 Охлаждение	870—28 500	1,2—635	○
	6 Нагревание	930—15 000	0,09—0,830	●
7 Прямоугольная	5 Охлаждение	90—1 800	180—1 200	□
	6 Нагревание	75—1 250	0,165—0,550	■

1) Channel shape; 2) direction of heat flow; 3) symbols; 4) round; 5) cooling; 6) heating; 7) rectangular.

was selected for the exponent n, where C and m are constants;

$$\text{for } \mathrm{Pe}\frac{d_0}{l} < 1500 \quad C = 2{,}30; \quad m = -0{,}3;$$

$$\text{for } \mathrm{Pe}\frac{d_0}{l} > 1500 \quad C = 0{,}535; \quad m = -0{,}1.$$

The Re and Pe numbers in (7-86) and (7-87) are computed from the equivalent diameter and values of the physical properties at the temperature of the fluid at the entrance. Table 7-5 shows values of n calculated from (7-87).

Figure 7-21 shows results obtained by generalizing the experimental data on the basis of (7-86). As we can see, for the vast majority of experimental points (more than 95%) the deviation from the curve corresponding to (7-86) does not exceed 12%.

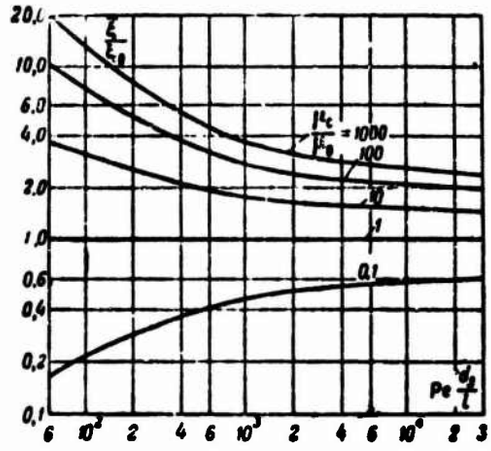

Fig. 7-22. Ratio $\bar{\xi}/\xi_0$ as function of μ_s/μ_0 and Pe d_e/l on basis of Eq. (7-86).

Equation (7-86) is valid for liquids in the region of values $Re<2\,300$; $0{,}08<\mu_c/\mu_0<1\,200$; $60<Pe\,\frac{d_e}{l}<3\cdot10^4$ and, naturally, when free convection has no influence (see §7-5).

Figure 7-22 shows the ratio $\bar{\xi}/\xi_0$ calculated from (7-86); it clearly demonstrates that $\bar{\xi}$ varies substantially not only with changes in μ_s/μ_0, but also in Pe d_e/l; the influence of μ_s/μ_0 drops as Pe d_e/l increases.

Equations of type (7-86), but with constant n, have been proposed before. Thus, according to the data of [17], $n = 0.25$, while according to [21], $n = 0.33$. In the last case, moreover, the ratio Pr_s/Pr_{zh} is used in place of μ_s/μ_0; for most fluids under ordinary conditions, this r tio deviates only slightly from μ_s/μ_{zh}.[6] As Table 7-5 shows, the exponent n varies widely (from 0.776 to 0.125). It is thus clear that these relationships are more special in nature, and correspond to narrow ranges of variation in Pe d_e/l and μ_s/μ_0.

Manuscript Page No.

Footnotes

163 [1]In this case, w_r is nonzero only as a result of deformation of the velocity profile along the length owing to the dependence of viscosity on temperature.

165 [2]For more details, see [9].

165 The heat-transfer coefficient α is referred to the local temperature difference $t_s - \bar{t}$.

167 [3]That is, neglecting molecular transfer of heat and momentum in the axial direction, as well as all forces acting radially. This means that the radial velocities are assumed to be small as compared with the axial velocities.

174 [4]With nonisothermal fluid flow, where the viscosity and other physical properties do not remain constant, the actual concept of the length of the hydrodynamic initial segment requires refinement. In the general case, it is desirable to take as the length of the initial segment the distance from the tube entrance at which the boundary layer developing at the walls fills the entire tube cross section and the influence of the initial velocity distribution vanishes. It follows from this definition that the velocity profile and resistance coefficient will remain constant beyond the initial segment for isothermal motion, while there may be a variation along the length for nonisothermal motion. In the latter case, full stabilization of the velocity profile can set in only after there has been full equalization of the temperature over the flow cross section.

174 [5]The slopes of the lines in Fig. 7-19 vary within narrower limits than in Fig. 7-20. The reason is that the experiments with the round tube correspond to higher values of Pe d/l, where $\bar{\xi}$Re depends little on Pe d/l.

177 [6]The values of μ_0 and μ_{zh} also differ negligibly, since the fluid temperature varies little along the length in the thermal initial segment.

Manuscript Page No.	Transliterated Symbols
142	c = s = stenka = wall
151	и.с = i.s = isotermicheskiye soprotivleniye = isothermal resistance
167	н.т = n.t = nachal'nyy termicheskiy = initial thermal
168	ж = zh = zhidkost' = fluid
171	л = l = logarifmicheskiy = logarithmic

174 н.г = n.g = nachal'nyy gidrodinamicheskiy = initial hydrodynamic

174 э = e = ekvivalentnyy = equivalent

Chapter 8

HEAT EXCHANGE IN ROUND AND FLAT TUBES WITH CONSTANT PHYSICAL PROPERTIES OF THE FLUID AND BOUNDARY CONDITIONS OF THE SECOND KIND

8-1. HEAT EXCHANGE IN A ROUND TUBE WITH CONSTANT HEAT-FLOW DENSITY AT THE WALL

We first assume the following conditions:

1) the flow and heat-exchange processes are steady;

2) the physical properties of the fluid are constant;

3) the velocity profile is parabolic over the entire length of the heat-exchange segment;

4) the temperature at the entrance to the heat-exchange segment is constant over the cross section;

5) a constant heat-flow density is maintained at the inside surface of the tube walls;

6) there are no internal heat sources in the flow, while the heat of friction is negligibly small;

7) the variation in heat-flow density owing to axial heat conduction is slight, and can be neglected.

Conditions 5, 6, and 7 show that the mean mass temperature of the fluid varies linearly along the length of the tube. In fact, from the heat-balance equation we have

$$\bar{t}=t_0+\frac{2q_c x}{\rho c_p \bar{w} r_0},$$

or, in dimensionless form,

$$\bar{\theta}=\frac{\bar{t}-t_0}{\frac{q_c d}{\lambda}}=\frac{4}{\mathrm{Pe}}\cdot\frac{x}{d}, \qquad (8\text{-}1)$$

where $\mathrm{Pe}=\bar{w}d/a$; t_0 is the constant for mean mass temperature of the fluid at the entrance.

Thus the mean mass temperature of the fluid is given in this

case while the wall temperature and heat-transfer coefficient must be determined.

The problem formulated corresponds to an energy equation analogous to (6-2), except that the dimensionless temperature is defined differently in this equation:

$$\frac{\partial^2\theta}{\partial R^2}+\frac{1}{R}\cdot\frac{\partial\theta}{\partial R}=(1-R^2)\frac{\partial\theta}{\partial X}. \qquad (8\text{-}2)$$

The boundary conditions are

$$\theta(0, R)=0;\ \left(\frac{\partial\theta}{\partial R}\right)_{R=0}=0 \text{ and } \left(\frac{\partial\theta}{\partial R}\right)_{R=1}=\frac{1}{2}. \qquad (8\text{-}3)$$

Here

$$\theta=\frac{t-t_0}{\frac{q_c d}{\lambda}},\ R=\frac{r}{r_0},\ X=\frac{2}{\mathrm{Pe}}\cdot\frac{x}{d}.$$

1. We first consider the solution of this problem for the region far from the tube entrance, where the influence of the specified temperature distribution in the entrance section becomes unimportant [1]. We can assume that here the excess-temperature field $t-\bar{t}$ (or $\theta-\bar{\theta}$) will be selfsimilar with respect to the X coordinate. Thus the solution is representable as

$$\theta=AX+f(R), \qquad (8\text{-}4)$$

where A is a constant and $f(R)$ is an unknown function.

Substitution of the expression for θ into (8-2) yields

$$\frac{d}{dR}\left(R\frac{df}{dR}\right)=A(1-R^2)R.$$

Integrating this equation from 0 to R and considering that $f'(0) = 0$, we have

$$\frac{df}{dR}=\frac{A}{R}\int_0^R(1-R^2)R\,dR=A\left(\frac{R}{2}-\frac{R^3}{4}\right).$$

Using the third boundary condition of (8-3), we find $A = 2$.

A second integration yields

$$f(R)=\frac{R^2}{2}-\frac{R^4}{8}+C,$$

where C is a constant of integration.

Substituting the expression for $f(R)$ into (8-4), we obtain

$$\theta=2X+\frac{R^2}{2}-\frac{R^4}{8}+C.$$

Evaluating the mean mass temperature by means of the equation

$$\bar{\theta}=4\int_0^1\theta(1-R^2)R\,dR$$

and comparing the result with (8-1), we find $C = -7/48$.

Thus the temperature field far from the tube entrance is described by the equation

$$\theta=\frac{t-t_0}{\frac{q_c d}{\lambda}}=\frac{4}{Pe}\frac{x}{d}+\frac{1}{2}R^2-\frac{1}{8}R^4-\frac{7}{48}. \qquad (8\text{-}5)$$

The wall temperature is

$$\theta_c=\theta_{R=1}=\frac{4}{Pe}\cdot\frac{x}{d}+\frac{11}{48}, \qquad (8\text{-}6)$$

while the limiting Nusselt number is

$$Nu_\infty=\frac{q_c d}{(t_c-\bar{t})\lambda}=(\theta_c-\bar{\theta})^{-1}=\frac{48}{11}\approx 4{,}36. \qquad (8\text{-}7)$$

The results obtained correspond to a region, far from the tube entrance, characterized by identical radial temperature distributions in different tube cross sections, a linear variation in temperature with length, and a constant value of Nu. Expression (8-5) is thus a particular solution of differential equation (8-2) for the region of stabilized heat exchange.

2. We now turn to a study of heat exchange in the initial tube segment [2, 3]. To do this, we must find a general solution of (8-2) that will satisfy both the boundary condition at the wall and the boundary condition at the tube entrance section.

In (8-2) and (8-3) we go from the temperature θ to the temperature

$$\theta_1=\theta-\theta_*,$$

where θ_* is the known particular solution of (8-2) for the region of stabilized heat exchange:

$$\theta_*=2X+\frac{1}{2}R^2-\frac{1}{8}R^4-\frac{7}{48}.$$

Then the mathematical description of the process will take the form

$$\frac{\partial^2\theta_1}{\partial R^2}+\frac{1}{R}\cdot\frac{\partial\theta_1}{\partial R}=(1-R^2)\frac{\partial\theta_1}{\partial X}; \qquad (8\text{-}8)$$

$$\left.\begin{aligned}&\theta_1(0,\ R)=-\left(\frac{1}{2}R^2-\frac{1}{8}R^4-\frac{7}{48}\right);\\&\left(\frac{\partial\theta_1}{\partial R}\right)_{R=0}=0;\ \left(\frac{\partial\theta_1}{\partial R}\right)_{R=1}=0.\end{aligned}\right\} \qquad (8\text{-}9)$$

A solution can be constructed for this problem with homogeneous boundary condition at the wall in analogy to the solution of the problem considered in §6-1.

The particular solution for θ_1 can be represented as

$$\theta_1 = \psi(R)\varphi(X) = A\psi(R)\exp(-\varepsilon^2 X),$$

where A and ε are unknown constants, and $\psi(R)$ is an unknown function.

Substituting this expression into (8-8) and going from the variable R to the variable εR, we obtain

$$\frac{\partial^2\psi}{d(\varepsilon R)^2} + \frac{1}{\varepsilon R}\cdot\frac{d\psi}{d(\varepsilon R)} + \left[1 - \frac{(\varepsilon R)^2}{\varepsilon^2}\right]\psi = 0.$$

Representing $\psi(\varepsilon R)$ as a power series

$$\psi(\varepsilon R) = \sum_{n=0}^{\infty} b_{2n}(\varepsilon R)^{2n},$$

we determine the series coefficients from the preceding equation. The relationships for the coefficients b_{2n} $(n=0, 1, 2\ldots)$ prove to be the same as the relationships found earlier for the coefficients b_{2n} in the problem of heat exchange at t_s = const (see §6-1).

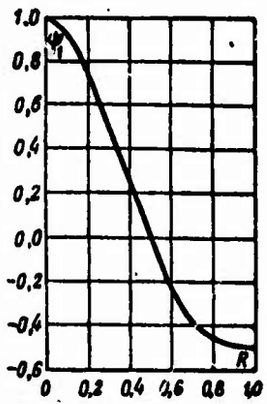

Fig. 8-1. Function $\psi_1(R)$ in problem of heat exchange in round tube with q_s = const.

Satisfying the condition $(\partial\theta/\partial R)_{R=1}=0$, or, what is the same, $[\psi'(\varepsilon R)]_{R=1}=0$, we obtain

$$\sum_{n=0}^{\infty} 2nb_{2n}\varepsilon^{2n-1} = 0\,!$$

This equation has an infinity of roots (eigenvalues) ε_i $(i = 1, 2, 3\ldots)$. The first seven of them, found by computer [2] are shown in Table 8-1. The limiting values of ε_i, corresponding to

large i, equal $\varepsilon_i = 4i + \frac{4}{3}$.

The eigenvalues $\varepsilon_i (i = 1, 2, 3 \ldots)$ correspond to the eigenfunctions $\psi(\varepsilon_i R, \varepsilon_i) = \psi_i(R)$. Figure 8-1 shows the graph for the first of these, $\psi_1(R)$.

Thus the general solution has the form

$$\theta_1 = \sum_{i=1}^{\infty} A_i \psi_i(R) \exp(-\varepsilon_i^2 X). \qquad (8\text{-}10)$$

The coefficients A_i can be computed from the known distribution of θ_1 at the entrance on the basis of the orthogonality property of the eigenfunctions,

$$A_i = \frac{\int_0^1 \theta_1(0, R)\, \psi_i(R)\, R(1 - R^2)\, dR}{\int_0^1 \psi_i^2(R)\, R(1 - R^2)\, dR}.$$

The ultimate equation for the temperature field can be written as

$$\theta = \frac{t - t_0}{\frac{q_c d}{\lambda}} = \frac{4}{\mathrm{Pe}} \cdot \frac{x}{d} + \frac{1}{2} R^2 - \frac{1}{8} R^4 - \frac{7}{48} +$$

$$+ \sum_{i=1}^{\infty} A_i \psi_i(R) \exp\left(-2\varepsilon_i^2 \frac{1}{\mathrm{Pe}} \cdot \frac{x}{d}\right). \qquad (8\text{-}11)$$

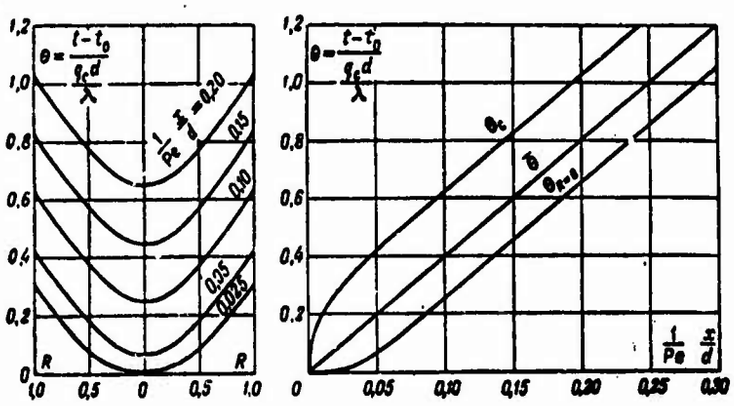

Fig. 8-2. Temperature distribution in fluid flow along radius and along tube length with q_s = const.

TABLE 8-1

Values of Constants for Problem of Heat Exchange in Round Tube with q_s = const

i	ε_i^2	$\psi_i(1)$	A_i
1	25,6796	—0,492517	0,201741
2	83,8618	0,395508	—0,087555
3	174,167	—0,345872	0,052797
4	296,536	0,314047	—0,0366402
5	450,947	—0,291252	0,0275178
6	637,387	0,273808	—0,0217415
7	855,850	—0,259852	0,0177985

Figure 8-2 shows a graph of this relationship.

The wall temperature is

$$\theta_c = \frac{t_c - t_0}{\frac{q_c d}{\lambda}} = \frac{4}{Pe}\cdot\frac{x}{d} + \frac{11}{48} + \sum_{i=1}^{\infty} A_i \psi_i(1) \exp\left(-2\varepsilon_i^2 \frac{1}{Pe}\cdot\frac{x}{d}\right). \qquad (8\text{-}12)$$

The values of A_i and $\psi_i(1)$ are given in Table 8-1.

The Nusselt number, found from the relationship

$$Nu = \frac{q_c d}{(t_c - \bar{t})\lambda} = (\theta_c - \bar{\theta})^{-1},$$

will equal

$$Nu = \frac{1}{\frac{11}{48} + \sum_{i=1}^{\infty} A_i \psi_i(1) \exp\left(-2\varepsilon_i^2 \frac{1}{Pe}\cdot\frac{x}{d}\right)}. \qquad (8\text{-}13)$$

Figure 8-3 shows the relationship between Nu and $\frac{1}{Pe}\cdot\frac{x}{d}$

For sufficiently large values of the reduced length, the sum of the terms of the series in (8-11), (8-12), and (8-13) approaches zero, and the equations go over to the relationships found previously for the region of stabilized heat exchange.

Determining the length of the thermal initial segment from the condition $Nu_{x=l_{n.t}} = 1{,}01 Nu_\infty$, we obtain

$$\frac{l_{n.t}}{d} = 0{,}07\,Pe.$$

Thus for the heat-exchange problem, when q_s = const the values

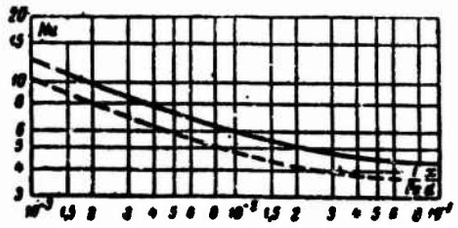

Fig. 8-3. Variation in Nu along length of round tube with q_s = const (solid line) and t_s = const (dashed line).

of $Nu_\infty = 4{,}36$ and $\bar{l}_{н.т}/d$ prove larger than for the problem with t_s = const (see §6-1).

For small reduced lengths, it is inconvenient to use (8-13) in practical computations, since many terms of the series must be computed. For small X, it is far more convenient to use the approximate solution for the problem of heat exchange in the initial segment q_s = const [3]. This solution, similar to the Leveque solution for t_s = const (see §6-3) leads to the following equation for the local Nusselt number:

$$Nu = 1{,}301\left(\frac{1}{Pe}\cdot\frac{x}{d}\right)^{-\frac{1}{3}}. \qquad (8\text{-}14)$$

According to data of another approximate calculation (see §12-4), the coefficient in (8-14) equals 1.31 rather than 1.301. Equation (8-14) can be used for values of $\frac{1}{Pe}\cdot\frac{x}{d} < 0{,}001$.

For values of $\frac{1}{Pe}\cdot\frac{x}{d} > 0{,}001$, the following interpolation equation is valid:

$$Nu = 4{,}364 + \frac{0{,}2633}{\left(\frac{1}{Pe}\cdot\frac{x}{d}\right)^{0{,}506}\exp\left(41\frac{1}{Pe}\cdot\frac{x}{d}\right)}^{2}, \qquad (8\text{-}14a)$$

which describes the results of calculations carried out with high accuracy by a numerical method, with no more than 0.5% deviation.

The following interpolation equation can be used for almost the entire region of the thermal initial segment (for $\frac{1}{Pe}\cdot\frac{x}{d} < 0{,}037$)

$$Nu = 1{,}31\left(\frac{1}{Pe}\cdot\frac{x}{d}\right)^{-\frac{1}{3}}\left(1+2\frac{1}{Pe}\cdot\frac{x}{d}\right), \qquad (8\text{-}15)$$

which yields an error not exceeding $\pm 4\%$. For $\frac{1}{Pe}\cdot\frac{x}{d} > 0{,}037$ we can take $Nu \approx Nu_\infty = 4{,}36$ with an error of about 5%.

8-2. HEAT EXCHANGE IN A FLAT PIPE WITH CONSTANT HEAT-FLOW DENSITY THAT IS THE SAME FOR BOTH WALLS

Let us look at the problem of heat exchange for a fluid flowing between parallel plates; the heat-flow density is maintained constant and identical for both plates. In all other respects, the problem is analogous to the one considered in the preceding section.

In this case, the mean mass temperature of the fluid will also be given by the equation

$$\bar{t} = t_0 + \frac{q_c x}{\rho c_p \bar{w} r_0},$$

or, in dimensionless form,

$$\bar{\theta} = \frac{\bar{t} - t_0}{\frac{q_c h}{\lambda}} = \frac{2}{\mathrm{Pe}} \cdot \frac{x}{h}. \qquad (8\text{-}16)$$

where $h = 2r_0$ is the distance between the plates; $\mathrm{Pe} = \bar{w}h/a$ is the Peclet number.

The wall temperature and heat-transfer coefficient must be determined.

For fluid flowing in a flat tube, the temperature field is described by the following equation, with allowance for Conditions 1, 2, 3, 6, and 7 (see §8-1):

$$\frac{\partial^2 \theta}{\partial Y^2} = \frac{3}{8}(1 - Y^2)\frac{\partial \theta}{\partial X}. \qquad (8\text{-}17)$$

The boundary conditions for constant fluid temperature at the entrance and constant heat-flow density at the walls is written as

$$\theta(0, Y) = 0; \left(\frac{\partial \theta}{\partial Y}\right)_{Y=0} = 0 \text{ and } \left(\frac{\partial \theta}{\partial Y}\right)_{Y=1} = \frac{1}{2}. \qquad (8\text{-}18)$$

Here

$$\theta = \frac{t - t_0}{\frac{q_c h}{\lambda}}, \quad X = \frac{1}{\mathrm{Pe}} \frac{x}{h} \text{ and } Y = \frac{y}{r_0} = \frac{2y}{h}.$$

The asymptotic (particular) solution of (8-17), satisfying the second and third boundary conditions of (8-18) and valid in the region of stabilized heat exchange, has the form[3]

$$\theta_* = \frac{t_* - t_0}{\frac{q_c h}{\lambda}} = \frac{2}{\mathrm{Pe}} \cdot \frac{x}{h} + \frac{3}{8} Y^2 - \frac{1}{16} Y^4 - \frac{39}{560}. \qquad (8\text{-}19)$$

To obtain a general solution of the problem that will also satisfy the boundary condition at the entrance, in (8-17) and (8-18) we go from θ to $\theta_1 = \theta - \theta_*$. Then in place of (8-17) and (8-18), we obtain the following equation and boundary conditions:

[3] /209

$$\frac{\partial^2\theta_1}{\partial Y^2}=\frac{3}{8}(1-Y^2)\frac{\partial\theta_1}{\partial X}; \tag{8-20}$$

$$\theta_1(0, Y)=-\left(\frac{3}{8}Y^2-\frac{1}{16}Y^4-\frac{29}{280}\right); \tag{8-21}$$

$$\left(\frac{\partial\theta_1}{\partial Y}\right)_{Y=0}=0;\ \left(\frac{\partial\theta_1}{\partial Y}\right)_{Y=1}=0. \tag{8-22}$$

TABLE 8-2

Values of Constants in Problem of Heat Exchange in Flat Tube for q_s = const

i	ε_i	ε_i^2	$\psi_i(1)$	A_i
1	4,28722	18,3803	−1,26970	0,087512
2	8,30372	68,9518	1,4022	−0,025662
3	12,3114	151,5706	−1,4911	0,01253

The general solution of the problem formulated, found in [4] by the usual method of separation of variables,[4] has the form

$$\theta_1=\sum_{i=1}^{\infty}A_i\psi_i(Y)\exp\left(-\frac{8}{3}\varepsilon_i^2X\right), \tag{8-23}$$

where ε_i and $\psi_i(Y)$ are the eigenvalues and eigenfunctions of the equation

$$\psi''+\varepsilon^2(1-Y^2)\psi=0 \tag{8-24}$$

under the boundary conditions

$$\psi'(0)=0 \text{ and } \psi'(1)=0.$$

Substituting $\psi(Y)$ as the power series

$$\psi(Y)=\sum_{n=0}^{\infty}b_{2n}Y^{2n} \tag{8-25}$$

into (8-24), we see that the relationships for the coefficients b_{2n} ($n=0, 1, 2\ldots$) are identical to the relationships obtained earlier for the coefficients of the same series in the problem of heat exchange for t_s = const (see §6-2).

The expression for $\psi(Y)$ satisfies the condition $\psi'(0) = 0$. Expression (8-25) satisfies the condition $\psi'(1) = 0$ for eigenvalues ε_i($i=1, 2, 3\ldots$), that are roots of the equation

$$\sum_{n=0}^{\infty}2nb_{2n}=0,$$

where $b_0=1$, $b_1=-\frac{\varepsilon^2}{2}$, etc.

[4]/210

The first three values of ε_i are given in Table 8-2.

The coefficients A_i in Series (8-23) are found from the relationship

$$A_i = \frac{\int_0^1 \theta_i(0, Y)\,\psi_i(Y)(1-Y^2)\,dY}{\int_0^1 \psi_i^2(Y)(1-Y^2)\,dY}.$$

With the aid of the Graetz method (see §6-1), the expression for the A_i can be reduced to a form more convenient for computation:

$$A_i = \frac{1}{\varepsilon_i \left(\frac{\partial^2 \psi(Y)}{\partial \varepsilon \partial Y}\right)_{\varepsilon=\varepsilon_i,\, Y=1}}. \qquad (8\text{-}26)$$

From (8-19) and (8-23) we obtain the final equation for the temperature field:

$$\theta = \frac{2}{Pe}\cdot\frac{x}{h} + \frac{3}{8}Y^2 - \frac{1}{16}Y^4 - \frac{39}{560} + \sum_{i=1}^{\infty} A_i \psi_i(Y) \exp\left(-\frac{8}{3}\varepsilon_i^2 \frac{1}{Pe}\cdot\frac{x}{h}\right). \qquad (8\text{-}27)$$

The wall temperature is

$$\theta_c = \frac{t_c - t_0}{\frac{q_c h}{\lambda}} = \frac{2}{Pe}\cdot\frac{x}{h} + \frac{17}{70} + \sum_{i=1}^{\infty} A_i \psi_i(1) \exp\left(-\frac{8}{3}\varepsilon_i^2 \frac{1}{Pe}\cdot\frac{x}{h}\right). \qquad (8\text{-}28)$$

The local Nusselt number is

$$Nu = \frac{q_c h}{(t_c - \bar{t})\lambda} = (\theta_c - \bar{\theta})^{-1}.$$

Taking (8-16) and (8-28) into account, we find

$$Nu = \frac{1}{\frac{17}{70} + \sum_{i=1}^{\infty} A_i \psi_i(1) \exp\left(-\frac{8}{3}\varepsilon_i^2 \frac{1}{Pe}\cdot\frac{x}{h}\right)}. \qquad (8\text{-}29)$$

The values of the constants ε_i, A_i and $\psi_i(1)$ are given for $i = 1$, 2, and 3 in Table 8-2. For $i > 3$, the values of the constants can be found from the following equations:

$$\varepsilon_i = 4i + \frac{1}{3},$$

$$A_i = (-1)^{i+1} \cdot 1{,}2363\,\varepsilon_i^{-\frac{11}{6}},$$

$$\varphi_1(1)=(-1)^1\cdot 0{,}97103\varepsilon_i^{\frac{1}{3}},$$

obtained with the aid of the asymptotic solution for large ε_i [4].

The limiting Nusselt number is

$$Nu_\infty=\frac{70}{17}\approx 4.12. \qquad (8\text{-}30)$$

The length of the thermal initial segment found, as usual, from the condition $Nu_{x=l_{n.t}}=1{,}01Nu_\infty$, is

$$\frac{l_{n.t}}{h}=0{,}079\,Pe. \qquad (8\text{-}31)$$

8-3. HEAT EXCHANGE IN A FLAT TUBE WHEN THE HEAT-FLOW DENSITY IS CONSTANT BUT DIFFERENT FOR EACH WALL

The sole difference between this problem and the preceding is that the heat-flow densities are not the same at the walls of the flat tube (nonsymmetric boundary conditions). Let the heat-flow density be q_{s1} at one of the walls and q_{s2} at the other; $q_{c1}\neq q_{c2}$.

We find the mean mass temperature of the fluid from the heat-balance equation:

$$\bar{\theta}=\frac{\bar{t}-t_0}{\frac{(q_{c1}+q_{c2})h}{2\lambda}}=\frac{2}{Pe}\cdot\frac{x}{h}. \qquad (8\text{-}32)$$

If we introduce the dimensionless temperature

$$\theta=\frac{t-t_0}{\frac{(q_{c1}+q_{c2})h}{2\lambda}},$$

then the nonsymmetric boundary conditions at the walls are written as

$$\left(\frac{\partial\theta}{\partial Y}\right)_{Y=1}=\frac{q_{c1}}{q_{c1}+q_{c2}};\quad \left(\frac{\partial\theta}{\partial Y}\right)_{Y=-1}=-\frac{q_{c2}}{q_{c1}+q_{c2}}. \qquad (8\text{-}33)$$

Under boundary conditions (8-33), the asymptotic solution of (8-17) for the region of stabilized heat exchange will have the following form:

$$\theta_*=\frac{(t_0-t_0)2\lambda}{(q_{c1}+q_{c2})h}=\frac{2}{Pe}\cdot\frac{x}{h}+\frac{3}{8}Y^2-$$
$$-\frac{1}{16}Y^4-\frac{39}{560}+\frac{q_{c1}-q_{c2}}{2(q_{c1}+q_{c2})}Y. \qquad (8\text{-}34)$$

When $q_{c1}=q_{c2}$, Eq. (8-34) goes over to (8-19).

A general solution of the problem has been obtained in [5]; it satisfies not only the conditions (8-33) at the wall, but also the condition $\theta(0, Y) = 0$ at the entrance.

As in the preceding sections, we introduce the dimensionless temperature $\theta - \theta_*$. This new independent variable is conveniently

represented as the sum of two functions:

$$\theta-\theta_0=\theta_1(X, Y)+\frac{q_{c1}-q_{c2}}{2(q_{c1}+q_{c2})}\theta_2(X, Y). \qquad (8\text{-}35)$$

It is not difficult to see that the problem now splits into two problems.

To determine the function $\theta_1(X, Y)$ we have the equation

$$\frac{\partial^2\theta_1}{\partial Y^2}=\frac{3}{5}(1-Y^2)\frac{\partial\theta_1}{\partial X} \qquad (8\text{-}36)$$

and the boundary conditions

$$\left.\begin{aligned}&\theta_1(0, Y)=-\left(\frac{3}{5}Y^2-\frac{1}{16}Y^4-\frac{29}{560}\right);\\&\left(\frac{\partial\theta_1}{\partial Y}\right)_{Y=1}=0;\ \left(\frac{\partial\theta_1}{\partial Y}\right)_{Y=-1}=0;\end{aligned}\right\} \qquad (8\text{-}37)$$

for the function $\theta_2(X, Y)$ we have the equation

$$\frac{\partial^2\theta_2}{\partial Y^2}=\frac{3}{5}(1-Y^2)\frac{\partial\theta_2}{\partial X} \qquad (8\text{-}38)$$

and the boundary conditions

$$\theta_2(0, Y)=-Y;\ \left(\frac{\partial\theta_2}{\partial Y}\right)_{Y=1}=0;\ \left(\frac{\partial\theta_2}{\partial Y}\right)_{Y=-1}=0. \qquad (8\text{-}39)$$

TABLE 8-3

Values of Constants in Heat-Exchange Problem for Flat Tube with Nonsymmetric Heating ($q_{c1}\neq q_{c2}$)

i	μ_i	μ_i^2	D_i	$G_i(1)$
0	2,263106	5,121649	−1,33817	0,49629
1	6,29768	39,6606	0,54548	−0,21214
2	10,3077	106,249	−0,35889	0,14036
3	14,3141	204,893	0,2710	−0,1065

The even function θ_1 is a solution of the symmetric problem ($q_{s1}=q_{s2}$) which was obtained in the preceding section:

$$\theta_1=\sum_{i=1}^{\infty}A_i\psi_i(Y)\exp\left(-\frac{8}{3}\mu_i^2X\right). \qquad (8\text{-}23)$$

Similarly, for the odd function θ_2 we obtain the solution

$$\theta_2=\sum_{i=0}^{\infty}D_iG_i(Y)\exp\left(-\frac{8}{3}\mu_i^2X\right), \qquad (8\text{-}40)$$

where

$$D_i=\frac{2}{\omega_i\left(\frac{\partial G(Y)}{\partial\omega\partial Y}\right)_{\omega=\omega_i,\ Y=1}};$$

$$G(Y)=\sum_{n=1}^{\infty}a_nY^n,\ (n=1,\ 3,\ 5\ldots);$$

$$a_1=1,\ a_3=-\frac{\omega^2}{6},$$

$$a_n=\frac{\omega^2}{n(n-1)}(a_{n-4}-a_{n-2});$$

here the ω_i are roots of the equation $\sum_{n=1}^{\infty}na_n=0(n=1,\ 3,\ 5\ldots)$.

The first four values of ω_i are given in Table 8-3 together with the corresponding values of D_i and $G_i(1)$. The following equations are valid for $i > 3$:

$$\omega_i=4i+\frac{7}{3};$$

$$D_i=(-1)^{i+1}\cdot 2{,}4727\omega_i^{-\frac{5}{6}};$$

$$G_i(1)=(-1)^i\cdot 0{,}97103\omega_i^{-\frac{5}{6}}.$$

Thus on the basis of (8-35) we can use the expressions found for θ_*, θ_1, and θ_2 to determine the temperature at any point in the flow:

$$\theta=\frac{t-t_0}{(q_{c1}+q_{c2})\frac{h}{2\lambda}}=\theta_*(X,\ Y)+$$

$$+\theta_1(X,\ Y)+\frac{q_{c1}-q_{c2}}{2(q_{c1}+q_{c2})}\theta_2(X,\ Y). \qquad (8\text{-}35a)$$

Substituting the values of θ_*, θ_1, and θ_2 from (8-34), (8-23), and (8-40) into this equation and letting $Y = 1$, we obtain an expressionfor the temperature of the first wall (at which the heat-flow density equals q_{s1}):

$$\frac{t_{c1}-t_0}{(q_{c1}+q_{c2})\frac{h}{2\lambda}}=\frac{2}{\mathrm{Pe}}\cdot\frac{x}{h}+\frac{17}{70}+$$

$$+\sum_{i=1}^{\infty}A_i\psi_i(1)\exp\left(-\frac{8}{3}\varepsilon_i^2X\right)+\frac{q_{c1}-q_{c2}}{2(q_{c1}+q_{c2})}\times$$

$$\times\left[1+\sum_{i=0}^{\infty}D_iG_i(1)\exp\left(-\frac{8}{3}\omega_i^2X\right)\right]. \qquad (8\text{-}41)$$

Subtracting (8-32) from (8-41), we can obtain the difference between the temperature of the first wall and the mean mass temperature of the fluid in a given section, as well as the Nusselt number for the first wall. Multiplying this difference by $(q_{s1} + q_{s2})/2$ and dividing it by q_{s1}, we finally obtain

$$\frac{1}{\mathrm{Nu}_1}=\frac{t_{c1}-\bar{t}}{\frac{q_{c1}h}{\lambda}}=\frac{17}{140}\left(1+\frac{q_{c2}}{q_{c1}}\right)+\frac{1}{2}\left(1+\frac{q_{c2}}{q_{c1}}\right)\times$$

$$\times\sum_{i=1}^{\infty}A_i\varphi_i(1)\exp\left(-\frac{8}{3}\varepsilon_i^2\frac{1}{\mathrm{Pe}}\cdot\frac{x}{h}\right)+\frac{1}{4}\left(1-\frac{q_{c2}}{q_{c1}}\right)\times$$

$$\times\left[1+\sum_{i=0}^{\infty}D_iG_i(1)\exp\left(-\frac{8}{3}\omega_i^2\frac{1}{\mathrm{Pe}}\cdot\frac{x}{h}\right)\right]. \qquad (8\text{-}42)$$

Similar expressions are obtained for Nu_2 and t_{s2} (second wall) simply by replacing the subscript "s1" by "s2" and *vice versa* in (8-42). When $q_{s2} = q_{s1}$, Eq. (8-42) goes over to (8-29).

Figure 8-4 shows the change in the dimensionless temperature difference $\frac{(t_{c1}-\bar{t})\lambda}{q_{c1}h}$ (the reciprocal of Nu_1) along the tube length. The curves for the various values of q_{s2}/q_{s1} correspond to the following conditions: $q_{c2}/q_{c1}=-1$: the heat supplied to the first wall equals the heat taken from the second wall (here $\bar{t}$ remains constant along the tube length); $q_{c2}/q_{c1}=0$: the second wall is heat-insulated, i.e., heat is neither delivered nor removed through it; $q_{c2}/q_{c1}=1$: heat is identically supplied (or removed) through both walls; $q_{c2}/q_{c1}=2$: the heat supplied to the second wall is 2 times that supplied through the first.

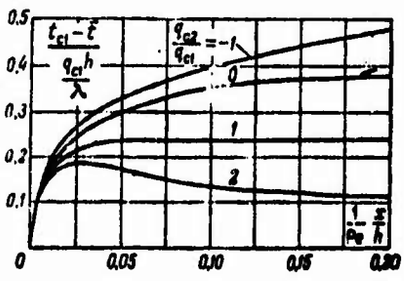

Fig. 8-4. Variation in $\frac{(t_{c1}-\bar{t})\lambda}{q_{c1}h}=\frac{1}{\mathrm{Nu}_1}$ along tube length.

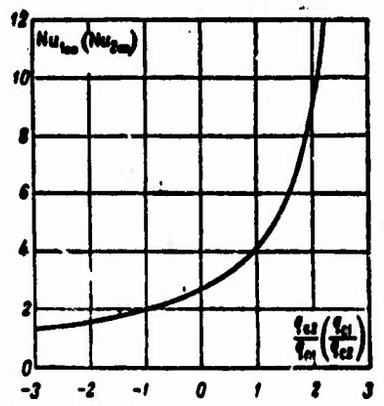

Fig. 8-5. Numbers $\mathrm{Nu}_{1\infty}$ and $\mathrm{Nu}_{2\infty}$ as functions of q_{s2}/q_{s1}.

When $X=\frac{1}{\mathrm{Pe}}\cdot\frac{x}{h}\to\infty$, the series on the right side of (8-42)

approach zero, and we arrive at the following expressions for the limiting Nusselt numbers:

$$\left.\begin{aligned} \mathrm{Nu}_{1\infty} &= \frac{70}{26-9\left(\frac{q_{c2}}{q_{c1}}\right)}, \\ \mathrm{Nu}_{2\infty} &= \frac{70}{26-9\left(\frac{q_{c1}}{q_{c2}}\right)}. \end{aligned}\right\} \qquad (8\text{-}43)$$

These relationships are shown in Fig. 8-5. Thus both Nu_∞ and the length of the thermal initial segment depends on the relationship between the specified values of heat-flow density at the walls. For symmetric heating ($q_{s2} = q_{s1}$), as we can see from Fig. 8-4, the thermal initial segment will have minimum length.

8-4. HEAT EXCHANGE IN A ROUND TUBE WHEN THE HEAT-FLOW DENSITY VARIES ARBITRARILY AT THE WALL WITH THE LENGTH

1. The problem of heat exchange in a round tube with q_s = const (see §8-1) can be generalized to the case of arbitrary variation in q_s with tube length, as was done in §6-5 for heat exchange with t_s = = const. This problem has been considered elsewhere [2, 6].

When q_s = const, the solution for the wall temperature of a round tube has the form

$$t_c - t_0 = \frac{q_c d}{\lambda}\left[\frac{4}{\mathrm{Pe}}\cdot\frac{x}{d} + \frac{11}{48} + \sum_{i=1}^{\infty} A_i \psi_i(1) \exp\left(-2\varepsilon_i^2 \frac{1}{\mathrm{Pe}}\cdot\frac{x}{d}\right)\right]. \qquad (8\text{-}12)$$

Now let the heat-flow density q_s be a specified function of x. The $q_s(x)$ curve can be represented as the result of summation of unit disturbances dq_s (Fig. 8-6). If a finite unit disturbance Δq_s takes place at a point with coordinate ξ, and this disturbance remains unchanged when $x \geq \xi$, then the wall temperature occasioned by this disturbance will equal, in accordance with (8-12):

$$t_c - t_0 = \Delta q_c \frac{d}{\lambda}\left[\frac{4}{\mathrm{Pe}}\cdot\frac{x-\xi}{d} + \frac{11}{48} + \right.$$
$$\left. + \sum_{i=1}^{\infty} A_i \psi_i(1) \exp\left(-2\varepsilon_i^2 \frac{1}{\mathrm{Pe}}\cdot\frac{x-\xi}{d}\right)\right]. \qquad (8\text{-}44)$$

If a series of unit disturbances takes place, since the energy equation is linear in the temperature, we can represent the solution for the wall temperature as a sum of expression of the type (8-44); replacing Δq_s by the differential dq_s and going over from this sum to the integral [the right side of (8-44) is integrated by parts], which corresponds to continuous variation in q_s with the length, we obtain an expression for the wall temperature in this case:

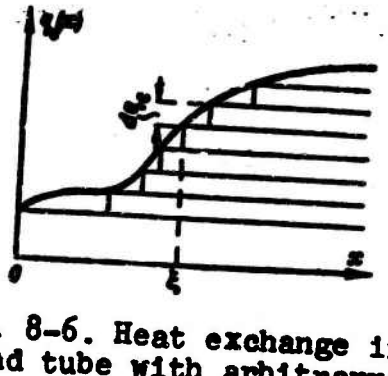

Fig. 8-6. Heat exchange in a round tube with arbitrary variation in heat-flow density at the wall.

$$t_c - t_0 = \frac{1}{\lambda}\int_0^x \left[\frac{4}{Pe} - \sum_{i=1}^{\infty}\frac{2\varepsilon_i^2 A_i \psi_i(1)}{Pe} \times \right.$$
$$\left. \times \exp\left(-2\varepsilon_i^2 \frac{1}{Pe}\cdot\frac{x-\xi}{d}\right)\right] q_0(\xi)\, d\xi. \qquad (8\text{-}45)$$

Introducing the dimensionless quantities

$$\frac{q_0}{\bar{q}_0} = \varphi(\tilde{x}),\ \tilde{x} = \frac{x}{l},$$

where q_s and $\bar{q}_s$ are the local and length-averaged values of heat-flow density at the wall, l is the length of the heated segment, and letting $N_i = -2\varepsilon_i^2 A_i \psi_i(1)$, we write (8-45) in the form

$$\theta_0 = \frac{t_c - t_0}{\frac{\bar{q}_0 d}{\lambda}} = \frac{1}{Pe}\cdot\frac{l}{d} \times$$
$$\times \int_0^{\tilde{x}} \left\{4 + \sum_{i=1}^{\infty} N_i \exp\left[-2\varepsilon_i^2 \frac{1}{Pe}\cdot\frac{l}{d}(\tilde{x}-\tilde{\xi})\right]\right\} \varphi(\tilde{\xi})\, d\tilde{\xi}. \qquad (8\text{-}46)$$

From the heat-balance equation for the tube segment of length x, we find an expresson for the mean mass temperature of the fluid:

$$\bar{\theta} = \frac{\bar{t} - t_0}{\frac{\bar{q}_0 d}{\lambda}} = \frac{4}{Pe}\cdot\frac{l}{d}\int_0^{\tilde{x}} \varphi(\tilde{\xi})\, d\tilde{\xi}. \qquad (8\text{-}47)$$

Since by definition the Nusselt number equals

$$Nu = \frac{\alpha d}{\lambda} = \frac{q_c d}{(t_c - \bar{t})\lambda} = \frac{\varphi(\tilde{x})}{\theta_c - \bar{\theta}},$$

on the basis of (8-46) and (8-47) we obtain

$$Nu = \frac{\varphi(\tilde{x})}{\frac{1}{Pe}\cdot\frac{l}{d}\int_0^{\tilde{x}} \left\{\sum_{i=1}^{\infty} N_i \exp\left[-2\varepsilon_i^2 \frac{1}{Pe}\cdot\frac{l}{d}(\tilde{x}-\tilde{\xi})\right]\right\} \varphi(\tilde{\xi})\, d\tilde{\xi}}, \qquad (8\text{-}48)$$

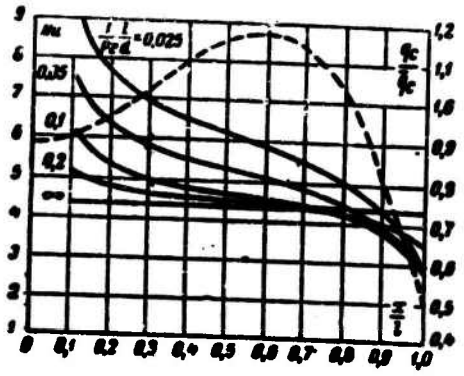

Fig. 8-7. Distribution of heat-flow density (dashed line) and Nu (solid lines) along tube length.

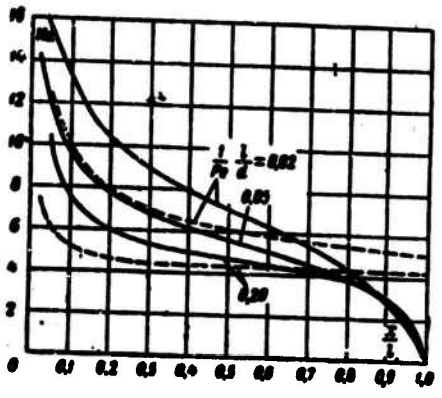

Fig. 8-8. Number Nu as function of x/l for $q_s \sim \sin(\pi x/l)$ (solid lines) and $q_s = \text{const}$ (dashed line).

To evaluate the integral in (8-48), we assume that within the limits $0 \leq \tilde{x} \leq 1$, the function $\varphi(\tilde{x})$ is continuous and differentiable together with its derivatives, so that it can be expanded into Maclaurin series:

$$\frac{q_0}{q_c} = \varphi(\tilde{x}) = b_0 + b_1\tilde{x} + b_2\tilde{x}^2 + \ldots + b_m\tilde{x}^m = \sum_{j=0}^{m} b_j\tilde{x}^j, \qquad (8\text{-}49)$$

where m can take on values between 0 and ∞.

Substituting Series (8-49) into (8-48) and evaluating the integral in the denominator term-by-term, we finally obtain

$$\mathrm{Nu} = \frac{1}{\frac{11}{48} + \frac{1}{\varphi(\tilde{x})}\sum_{i=1}^{\infty} A_i\psi_i(1)\left[b_0\exp(-k_i\tilde{x}) + \sum_{j=1}^{m} j b_j P_{j-1}(\tilde{x})\right]}, \qquad (8\text{-}50)$$

where $k_i = 2\mu_i^2 \frac{1}{\mathrm{Pe}} \frac{l}{d}$; $P_0(\tilde{x}) = \frac{1-\exp(-k_i\tilde{x})}{k_i}$; $P_j(\tilde{x}) = \frac{\tilde{x}^j - jP_{j-1}(\tilde{x})}{k_i}$.

If $m = 0$, then $\varphi(\tilde{x}) = b_0 = 1$ and (8-50) goes over to (8-13) for q_s = const.

As an example[5] we consider a specific distribution of heat-flow density over the length, in the form of the following polynomial

$$\frac{q_0}{q_0} = \varphi(\tilde{x}) = 0{,}885 - 0{,}127\tilde{x} + 2{,}967\tilde{x}^2 - 3{,}269\tilde{x}^3. \qquad (8\text{-}51)$$

This relationship is represented by the dashed line in Fig. 8-7.

Substituting the values of the coefficients b_0, b_1, b_2 ... b_3 from (8-51) into (8-50) and performing the appropriate computations, we obtain a family of curves (the solid lines in Fig. 8-7), whose parameter is the number $\frac{1}{Pe}\cdot\frac{l}{d}$. For $\frac{1}{Pe}\cdot\frac{l}{d}\to\infty$, the coefficient $k_i\to\infty$, and the exponential term and the function $P_j(\tilde{x})$ in (8-50) approach zero, so that Nu approaches $Nu_\infty = \frac{48}{11} = 4{,}36$. This result is explained by the fact that in a very long tube the per-unit variation in q_s is small.

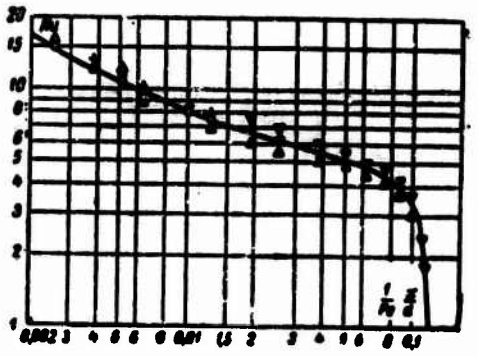

Fig. 8-9. Number $Nu = f\left(\frac{1}{Pe}\frac{x}{d}\right)$ for $q_s \sim \sin(\pi x/l)$ and $\frac{1}{Pe}\cdot\frac{l}{d} = 0{,}12$. Solid line) Theoretical computation; points) solution using hydraulic integrator.

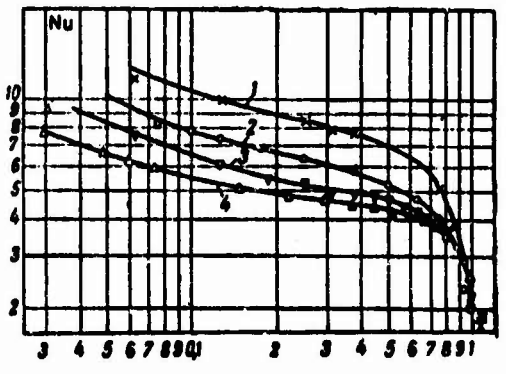

Fig. 8-10. Number Nu = $f(x/l)$ with truncated-sinusoid variation of q_s. 1 – $\frac{1}{Pe}\cdot\frac{l}{d} = 0{,}02$; 2 – $\frac{1}{Pe}\cdot\frac{l}{d} = 0{,}06$; 3 – $\frac{1}{Pe}\cdot\frac{l}{d} = 0{,}1$; 4 – $\frac{1}{Pe}\cdot\frac{l}{d} = 0{,}18$ (solution obtained with hydraulic integrator).

This way of determining the heat exchange can be used for various laws governing the variation in q_s with length. In addition, a method has been proposed [7, 8] for determining heat exchange in round and flat tubes (in the latter case, for one- and two-sided heating) where the heat-flow density varies in accordance with a sinusoid and a sinusoid truncated at the ends. These cases are of particular interest in nuclear-reactor engineering, since these are roughly the laws governing the heat-flow distribution along the axes of the fuel elements.

Figure 8-8 shows the variation in the local Nu number along the tube length with a sinusoidally distributed heat-flow density [$q_s \sim \sin(\pi x/l)$]; the curves were found by the method of [7]. For comparison, this figure also gives the corresponding relationships for q_s = const. When q_s is distributed sinusoidally, Nu is higher in the thermal initial segment than when q_s = const. At the end of the tube, Nu drops off rapidly, approaching zero. When the reduced length is sufficiently great, Nu remains nearly constant and equal to 4.36 at the center tube segment; this segment will obviously be longer the greater $\frac{1}{Pe}\cdot\frac{l}{d}$.

As in certain other cases of convective heat exchange, to solve problems involving heat exchange with arbitrary variation in q_s or t_s with the length, we can successfully employ analog computers, in particular hydraulic integrators. Figure 8-9 compares the results of a hydraulic-integrator solution to the problem of heat exchange in a round pipe with sinusoidal variation in q_s with length and the results of a theoretical calculation by the method of [7]. The good agreement of these results confirms that hydraulic integrators can be used for such computations.

Figure 8-10 shows the results of a hydraulic-integrator solution of the heat-exchange problem for a round tube when there is a truncated-sinusoid variation in q_s:

$$q_s \sim \sin \pi \frac{x+0.11}{1.21}.$$

Each curve of Fig. 8-10 corresponds to a specific value of $\frac{1}{Pe}\cdot\frac{l}{d}$. The curves are the same in nature as for a sinusoidal variation in q_s, but when $x = l$, Nu is finite.[6]

2. In a previously cited study (see §6-6), V.D. Vilenskiy has investigated the influence of the way in which q_s varies along the tube length on the onset of selfsimilar heat exchange and on the limiting Nusselt number in fairly general form. The analysis was carried out for flow in a tube of arbitrary cross section under the same conditions as in §6-6, with the sole difference that in place of the distribution $t_s(x)$, the distribution $q_s(x)$ of heat-flow density at the wall was specified. In this case,

[6] /210

the temperature field in the fluid flow is described by (6-76) with condition (6-77) at the entrance and the following condition at the wall:

$$Q_c = -\left(\frac{\partial \vartheta}{\partial N}\right)_{\substack{Y=Y_c \\ Z=Z_c}} = \psi(X). \tag{8-52}$$

Here $Q_c = q_c d_э / \lambda t_0$; $\psi(X)$ is a specified function characterizing the length distribution of q_s; the remaining notation is the same as in §6-6. We assume that the function $\psi(X)$ exceeds zero (for $0 < X < \infty$), and that it is continuous together with its derivatives. For the case under consideration, it has been shown that if ψ possesses the property such that the limits

$$\lim_{X \to \infty} \frac{1}{\tilde{\chi}_n} \cdot \frac{d\tilde{\chi}_n}{dX} = \tilde{K}_n$$

exist, where the functions $\tilde{\chi}$ are described by the relationships

$$\begin{aligned} &\tilde{\chi}_0 = \psi; \\ &\cdots\cdots\cdots\cdots \\ &\tilde{\chi}_n = \frac{d\tilde{\chi}_{n-1}}{dX} - \tilde{K}_{n-1}\tilde{\chi}_{n-1}, \end{aligned}$$

and $\tilde{K}_n > -\tilde{\mu}_1$, where $\tilde{\mu}_1 \neq 0$ is the first eigenvalue of the problem

$$\begin{aligned} &\nabla^2 \tilde{\eta}(Y, Z) + \tilde{\mu} W_x \tilde{\eta}(Y, Z) = 0, \\ &\left(\frac{\partial \tilde{\eta}}{\partial N}\right)_{\substack{Y=Y_c \\ Z=Z_c}} = 0, \end{aligned} \tag{8-53}$$

then when $X \to \infty$, θ can be represented as the asymptotic series

$$\theta \sim \frac{S}{F} \int_0^X \psi(\xi)\, d\xi + \sum_{n=0}^{\infty} \tilde{V}_n(Y, Z)\, \tilde{\chi}_n(X), \tag{8-54}$$

where the $\tilde{V}_n$ are solutions of the problems

$$\left.\begin{aligned} &\nabla^2 \tilde{V}_0 - \tilde{K}_0 W_x \tilde{V}_0 = \frac{S}{F} W_x; \\ &-\left(\frac{\partial \tilde{V}_0}{\partial N}\right)_{\substack{Y=Y_c \\ Z=Z_c}} = 1; \\ &\cdots\cdots\cdots\cdots \\ &\nabla^2 \tilde{V}_n - \tilde{K}_n W_x \tilde{V}_n = W_x \tilde{V}_{n-1}; \\ &\left(\frac{\partial \tilde{V}_n}{\partial N}\right)_{\substack{Y=Y_c \\ Z=Z_c}} = 0. \end{aligned}\right\} \tag{8-55}$$

When $\tilde{K}_0 = 0$, the corresponding function of $\tilde{V}_n$ is determined only to within a constant. The constant is found from the condition

$$\int_F W_x \tilde{V}_n \, dF = 0.$$

In exact analogy to the case in which the wall temperature is specified, Series (8-54) terminates if, for a certain $n = n_1$, $\frac{1}{\tilde{q}} \cdot \frac{d\tilde{q}}{dX} = \tilde{K}_n$; here the difference between the exact solution and its asymptotic representation approaches zero, since $\exp(-\tilde{\mu}_1 X)$.

If

$$\lim_{X \to \infty} \frac{1}{\psi} \cdot \frac{d\psi}{dX} = \tilde{K}_0 < \tilde{\mu}_1,$$

or

$$\frac{1}{\psi} \cdot \frac{d\psi}{dX} \to -\infty \quad \text{as} \quad X \to \infty,$$

then for $X \to \infty$,

$$\theta \sim \frac{S}{F} \int_0^X \psi(\xi) \, d\xi + \tilde{\eta}_1 \left(\int_S \tilde{\eta}_1 \, dS \right) \exp(-\tilde{\mu}_1 X) \int_0^X \psi(\xi) \exp(\tilde{\mu}_1 \xi) \, d\xi, \qquad (8\text{-}56)$$

where η_1 is the first normalized eigenfunction of (8-53).

It follows from (8-54) and (8-56) that when the heat-flow density is specified at the tube wall, stabilization of the temperature field in the fluid flow and, consequently, stabilization of the heat-transfer coefficient, will take place under the same conditions as when the wall temperature is specified (except that restrictions are imposed on the law governing the variation in heat-flow density at the wall) (see §6-6).

From (8-54) we find that when $-\tilde{\mu} < \tilde{K}_0 < +\infty$

$$\mathrm{Nu}_\infty(Y_c Z_c) = \frac{2}{(\tilde{V}_0)_{\substack{Y=Y_c \\ Z=Z_c}}}. \qquad (8\text{-}57)$$

Thus in the case under consideration, Nu_∞ is determined by the tube geometry, the coordinates of the perimeter point considered, and the value of the parameter K_0.

When $K_0 \leqslant -\tilde{\mu}_1$, $\mathrm{Nu}_\infty = 0$, which is not difficult to show, using Expression (8-56). Physically, the explanation is that in our case for large X the heat-flow density at the wall approaches zero more rapidly than does the difference between the wall temperature and the mean mass temperature of the fluid.

Figure 6-15 shows Nu_∞ as a function of the parameter K_0 for heat exchange in a round tube (curve 2). It is interesting to note that if K_0 and $K_0 \geqslant -\mu_1$, then when K_0 and K_0 have identical values (and also when $K_0 = K_0 = 0$ for $K_1 = 0$), the values of Nu_∞ will be identical, regardless of which varies, the wall temperature or the heat flow at the wall (see §6-6).

8-5. HEAT EXCHANGE IN A ROUND TUBE WHEN THE HEAT-FLOW DENSITY AT THE WALL VARIES ARBITRARILY OVER THE CIRCUMFERENCE

So far, we have studied heat-exchange problems under boundary conditions symmetric with respect to the axis (uniform distribution of t_s or q_s over the circumference). In this case, naturally, the temperature field will also be symmetric about the axis. Following [9], let us look at an elementary problem with asymmetric boundary conditions. Let the heat-flow density at the wall be constant over the length, but variable over the circumference. Eliminating the thermal initial segment from the analysis, we shall only consider the region of stabilized heat exchange. All other conditions are the same as in §8-1.

With allowance for these assumptions, the energy equation will take the form

$$a\left(\frac{\partial^2 t}{\partial r^2}+\frac{1}{r}\cdot\frac{\partial t}{\partial r}+\frac{1}{r^2}\cdot\frac{\partial^2 t}{\partial \varphi^2}\right)=2\bar{w}\left(1-\frac{r^2}{r_0^2}\right)\frac{\partial t}{\partial x}. \qquad (8\text{-}58)$$

Since the heat-flow density at the wall is constant with length, while the heat-exchange process is stabilized, at every point in the flow

$$\frac{\partial t}{\partial x}=\frac{d\bar{t}}{dx}=\text{const}.$$

1. Let the circle segment with angle 2β (Fig. 8-11a) be heated with constant q_s, and let the entire remaining tube surface be heat-insulated ($q_s = 0$). We then have from the heat-balance equation

$$\frac{d\bar{t}}{dx}=\frac{2r_0\beta q_0}{\pi r_0^2\rho c_p\bar{w}}.$$

We introduce the temperature

$$\vartheta(r,\varphi)=t(r,\varphi,x)-\bar{t}(x)$$

and the dimensionless radius $R = r/r_0$. Then with allowance for the relationships given abcve, Eq. (8-58) can be written as

$$\frac{\partial^2\vartheta}{\partial R^2}+\frac{1}{R}\cdot\frac{\partial\vartheta}{\partial R}+\frac{1}{R^2}\cdot\frac{\partial^2\vartheta}{\partial\varphi^2}=k(1-R^2), \qquad (8\text{-}59)$$

where

$$k=\frac{4r_0\beta q_0}{\pi\lambda}.$$

For the case shown in Fig. 8-11a, the boundary conditions will have the form

$$\left.\begin{aligned}&\text{for } -\beta<\varphi<\beta \quad \left(\frac{\partial\vartheta}{\partial R}\right)_{R=1}=\frac{q_0 r_0}{\lambda};\\ &\text{for } \beta<\varphi<2\pi-\beta \quad \left(\frac{\partial\vartheta}{\partial R}\right)_{R=1}=0.\end{aligned}\right\} \qquad (8\text{-}60)$$

To simplify the analysis, we represent ϑ as

$$\vartheta = F(R, \varphi) + k\left(\frac{R^2}{4} - \frac{R^4}{16}\right). \qquad (8\text{-}61)$$

Substituting (8-61) into (8-59) and (8-60), we see that the function $F(R, \varphi)$ must satisfy the Laplace equation

$$\frac{\partial^2 F}{\partial R^2} + \frac{1}{R}\cdot\frac{\partial F}{\partial R} + \frac{1}{R^2}\cdot\frac{\partial^2 F}{\partial \varphi^2} = 0 \qquad (8\text{-}62)$$

and the boundary conditions

$$\left.\begin{aligned}\left(\frac{\partial F}{\partial R}\right)_{R=1} &= \frac{q_c r_0}{\lambda}\left(1 - \frac{1}{\pi}\right) \text{ for } -\beta < \varphi < \beta;\\ \left(\frac{\partial F}{\partial R}\right)_{R=1} &= -\frac{q_c r_0}{\lambda}\cdot\frac{1}{\pi} \text{ for } \beta < \varphi < 2\pi - \beta.\end{aligned}\right\} \qquad (8\text{-}63)$$

Solving (8-62) by the usual method of separation of variables, we obtain

$$F = C_0 + \sum_{n=1}^{\infty} C_n R^n \cos n\varphi.$$

Using the boundary conditions, we have

$$C_n = \frac{2}{n^2\pi}\cdot\frac{q_c r_0}{\lambda}\sin n\beta, \quad n = 1, 2 \ldots$$

Thus for the case shown in Fig. 8-11a, the solution will have the form

$$\vartheta = k\left(\frac{R^2}{4} - \frac{R^4}{16}\right) + C_0 + \sum_{n=1}^{\infty}\frac{2q_c r_0}{n^2\pi\lambda}\sin n\beta R^n \cos n\varphi. \qquad (8\text{-}64)$$

The remaining unknown constant C_0 is found from the equation determining the mean mass temperature of the fluid:

$$\bar{t} = \frac{1}{\pi r_0^2 \bar{w}}\int_0^{2\pi} d\varphi \int_0^{r_0} t w_x r\, dr,$$

or

$$\int_0^{2\pi} d\varphi \int_0^1 \vartheta\,(1 - R^2)\, R\, dR = 0.$$

Substituting in ϑ from (8-64) and integrating, we find

$$C_0 = -\frac{14\beta q_c r_0}{48\pi\lambda}.$$

The expression for the difference between the wall temperature and the mean mass temperature of the fluid, $\vartheta_c(\varphi) = t_c - \bar{t}$, is found from (8-64) when we let $R = 1$:

$$\frac{\vartheta_c(\varphi)}{\frac{q_c 2r_0}{\lambda}} = \frac{11}{48}\frac{\beta}{\pi} + \sum_{n=1}^{\infty}\frac{1}{n^2\pi}\sin n\beta\cos n\varphi. \qquad (8\text{-}65)$$

This expression is the reciprocal of the local Nu_φ number. If we let $\beta = \pi$, which corresponds to a constant heat-flow density over the circumference, we obtain the usual value $Nu_\infty = 48/11 = 4.36$.

2. Let us now consider the wall-temperature distribution when a narrow circular segment with angle $\Delta\omega$ is heated; this segment is an angular distance $\varphi = \omega$ away from the origin (Fig. 8-11b). The heat-flow density at the surface of the circle segment is constant and equal to $q_s(\omega)$; the remaining tube surface is heat-insulated ($q_s = 0$). Here the expression for the wall-temperature increase $\delta\vartheta_s$ can be written on the basis of (8-65) by a simple change of coordinates:

$$\delta\vartheta_s(\varphi, \omega) = \frac{q_c(\omega)2r_0}{\lambda}\left[\frac{11}{48}\frac{\Delta\omega}{2\pi} + \sum_{n=1}^{\infty}\frac{1}{n^2\pi}\sin\left(\frac{n\Delta\omega}{2}\right)\cos n\left(\varphi - \omega - \frac{\Delta\omega}{2}\right)\right]. \qquad (8\text{-}66)$$

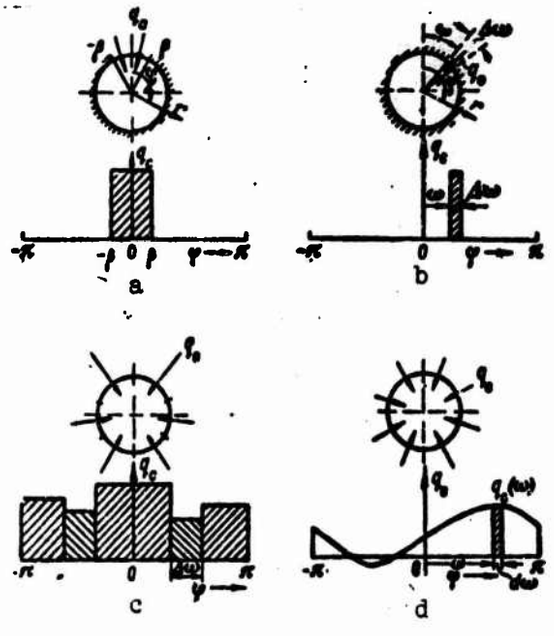

Fig. 8-11. The problem of heat exchange in a round tube when the heat-flow density at the wall varies over the circumference.

If there are several circle segments along the tube circumference, and constant heat-flow densities are maintained at each

circle segments, with the densities differing from segment to segment (Fig. 8-11c), since Eq. (8-58) is linear in the temperature, the solution for this case can be constructed as the sum of solutions of (8-66). Here the boundary conditions at the wall will also be satisfied. Thus for the case shown in Fig. 8-11c we have

$$\vartheta_c(\varphi)=\sum_{m=1}^{M}\frac{q_c(\omega_m)2r_0}{\lambda}\left[\frac{11}{48}\cdot\frac{\Delta\omega_m}{2\pi}+\sum_{n=1}^{\infty}\frac{1}{n^2\pi}\sin\left(\frac{n\Delta\omega_m}{2}\right)\cos n\left(\varphi-\omega_m-\frac{\Delta\omega_m}{2}\right)\right], \quad (8\text{-}67)$$

where $m = 1, 2, \ldots, M$; M is the number of segments.

Finally, for an arbitrary variationin the heat-flow density over the circumference (Fig. 8-11d), if we replace $\Delta\omega$ by the infinitesimal $d\omega$ and sum the elementary circle segments in (8-65) by integrating over the circumference, we obtain

$$\vartheta_c(\varphi)=\int_{\omega=0}^{2\pi}\frac{q_c(\omega)2r_0}{\lambda}\left[\frac{11}{48}+\sum_{n=1}^{\infty}\frac{\cos n(\varphi-\omega)}{n}\right]\frac{d\omega}{2\pi}. \quad (8\text{-}68)$$

The series in (8-68) converges to the finite expression

$$\sum_{n=1}^{\infty}\frac{\cos n(\varphi-\omega)}{n}=-\ln\left(2\sin\frac{\varphi-\omega}{2}\right).$$

Thus the general solution of the problem with arbitrary distribution of q_s over the circumference can be written as

$$\vartheta_c(\varphi)=\frac{2r_0}{\lambda}\int_0^{2\pi}q_c(\omega)\,G(\varphi,\omega)\frac{d\omega}{2\pi}, \quad (8\text{-}69)$$

where

$$G(\varphi,\omega)=\frac{11}{48}+\sum_{n=1}^{\infty}\frac{\cos n(\varphi-\omega)}{n}, \quad (8\text{-}70a)$$

or

$$G(\varphi,\omega)=\frac{11}{48}-\ln\left(2\sin\frac{\varphi-\omega}{2}\right). \quad (8\text{-}70b)$$

Knowing the distribution $q_s(\omega)$ of the heat-flow density over the circumference and evaluating the integral in (8-69), we can compute the wall-temperature distribution $\vartheta_c(\varphi)=t_c-\bar{t}$, and then $\mathrm{Nu}_m(\varphi)=q_c\cdot 2r_0/\vartheta_c\lambda$. Convenience dictates the choice of expressions for the function G to be used in the computations. For example, if the problem does not admit of analytic integration then, integrating numerically, we find it more convenient to use (8-70b).

3. Let us look at two examples.

a. Let q_s be constant over the circumference, i.e., $q_c(\omega)=$

$= q_{c_0} = \text{con}$. Here integration of (8-69) yields

$$\vartheta_c(\varphi) = \frac{q_{c_0} 2r_0}{\lambda} \cdot \frac{11}{48} = \text{const} \quad \text{and} \quad \text{Nu}_\infty(\varphi) = \frac{48}{11} = \text{const}.$$

b. Let q_c be cosinusoidally distributed, i.e.,

$$q_c(\varphi) = q_{c0}(1 + b\cos\omega).$$

Using (8-69) and (8-70a), we find the wall-temperature distribution over the circumference:

$$\vartheta_c(\varphi) = \frac{q_{c_0} 2r_0}{\lambda} \int_0^{2\pi} (1 + b\cos\omega) \left[\frac{11}{48} + \sum_{n=1}^{\infty} \frac{\cos n(\varphi - \omega)}{n}\right] \frac{d\omega}{2\pi}.$$

Integrating, we obtain

$$\vartheta_c(\varphi) = \frac{q_{c_0} 2r_0}{\lambda} \left(\frac{11}{48} + b\frac{\cos\varphi}{2}\right).$$

The distribution of the local Nu_∞ number over the circumference is

$$\text{Nu}_\infty(\varphi) = \frac{1 + b\cos\varphi}{\frac{11}{48} + b\frac{\cos\varphi}{2}}.$$

Figure 8-12 shows the results of this computation for $b = 1$. They show that Nu_∞ varies substantially over the circumference, and differs significantly from Nu_∞ when q_s = const, when the value is 4.36. At the point where $t_c = \bar{t}$, i.e. $\vartheta_c = 0$, $\text{Nu}_\infty \to \pm\infty$, when $t_s < \bar{t}$, it becomes negative. The local difference between the wall temperature and the mean fluid temperature ϑ_s also varies substantially over circumference. Thus when $\varphi = 0$, the local value of this difference is roughly 3 times the mean value over the circumference ($\bar{\vartheta}_s$). It is clear from the figure that significant errors will result if we determine $\vartheta_s(\varphi)$ as the quotient resulting from division of $q_s(\varphi)$ by the constant value $\alpha = 4.36\ \lambda/d$.

The same problem has been considered in [10], but with allowance for heat conduction in the wall. Naturally, as the thermal-conductivity coefficient and the wall thickness increase, the nonuniformity in temperature distribution over the circumference is smoothed. If the medium flowing in the tube is transparent to radiation, then heat exchange by radiation between wall elements at different temperatures will lead to the same effect.

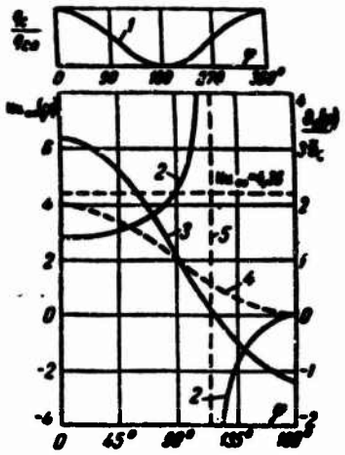

Fig. 8-12. Results of calculation for sinusoidal distribution of q_s over circumference. 1) $q_c = q_{c0}(1 + \cos\varphi)$; 2) $Nu_{c0}(\varphi)$; 3) $\frac{\delta_c(\varphi)}{\delta_c}$; 4) $\frac{\delta_c}{\delta_c}$ on the assumption that $q_c = q_c(\varphi)$, while $Nu_{c0} = 4{,}36$; 5) asymptote.

8-6. INFLUENCE OF RADIATION ON HEAT EXCHANGE IN FLAT TUBE

Under boundary conditions of the second kind, the temperature distribution at the inside surface of the tube wall will be nonuniform: the temperature can vary both along the length and the perimeter. If in this case the medium flowing in the tube is transparent to radiation, heat will be exchanged by radiation between surface segments at different temperatures. This leads to a reduction in the temperature differences between individual surface segments, i.e., there is a certain equalization of wall temperature, which in turn will usually promote improved heat transfer.

The treatment of heat exchange with joint transfer of energy by convection and by radiation is still not very advanced. We shall not consider such problems in detail. To form an idea as to the influence of radiation on convective heat exchange, we shall analyze an elementary case, flow of a diathermal medium in a flat tube far from the entrance [11]. The heat-flow densities are specified for each tube wall. The densities are constant over the surface, but do not equal one another ($q_{s1} \neq q_{s2}$).

If the medium is diathermal, the energy equation has the same form as for purely convective heat exchange, i.e., Eq. (8-17) is also valid here. Assuming that the condition $\frac{\partial\theta}{\partial X} = \frac{\partial\bar{\theta}}{\partial X} = \text{const}$ is also satisfied, let us determine this constant from (8-32), and substitute it into (8-17). As a result, the energy equation takes the form

$$\frac{\partial^2\theta}{\partial Y^2} = \frac{3}{4}(1 - Y^2), \qquad (8\text{-}71)$$

where

$$\theta = \frac{T2\lambda}{(q_{c1} + q_{c2})h}; \quad Y = \frac{y}{r_0} = \frac{2y}{h}; \quad X = \frac{1}{Pe}\cdot\frac{x}{h}; \quad Pe = \frac{\bar{w}h}{a}.$$

The radiation exerts its influence through the boundary conditions. Each surface element delivers heat to the fluid flow owing to convective heat exchange and to colder segments of the surface owing to radiative heat exchange. For simplicity, we shall formulate the boundary conditions in approximation, on the assumption that heat transfer by radiation takes place only in the plane of each cross section. This means that heat generated in the walls at a given section will be delivered to the flow in this section alone. This assumption will be closer to the facts the less the relative tube width h/l and the smaller the wall-temperature variation along the axis as compared with the mean temperatures. Thus we write the boundary conditions in the form

$$\left.\begin{aligned} q_{c_1} &= \lambda\left(\frac{\partial T}{\partial y}\right)_{y=r_0} + \varepsilon_{np}\sigma\left(T_{c1}^4 - T_{c2}^4\right); \\ q_{c_2} &= -\lambda\left(\frac{\partial T}{\partial y}\right)_{y=-r_0} + \varepsilon_{np}\sigma\left(T_{c2}^4 - T_{c1}^4\right), \end{aligned}\right\} \qquad (8\text{-}72)$$

where σ is the Stefan constant; ε_{pr} is the reduced emissivity;

$$\frac{1}{\varepsilon_{np}} = \frac{1}{\varepsilon_1} + \frac{1}{\varepsilon_2} - 1;$$

here ε_1 and ε_2 are the emissivities of the tube walls.

If the wall-temperature difference $(T_{s1} - T_{s2})$ is small as compared with T_{s1} and T_{s2}, we can then assume, in approximation, that

$$T_{c1}^4 - T_{c2}^4 = 4\overline{T}_c^3\left(T_{c_1} - T_{c_2}\right), \qquad (8\text{-}73)$$

where

$$\overline{T}_c = \frac{1}{2}\left(T_{c_1} + T_{c_2}\right).$$

Using (8-73) and reducing (8-72) to dimensionless form, we obtain

$$\left.\begin{aligned} \left(\frac{\partial\theta}{\partial Y}\right)_{Y=1} &= \frac{1}{1+\beta} - 2\Phi\left(\theta_{c_1} - \theta_{c_2}\right), \\ \left(\frac{\partial\theta}{\partial Y}\right)_{Y=-1} &= -\frac{\beta}{1+\beta} - 2\Phi\left(\theta_{c_1} - \theta_{c_2}\right), \end{aligned}\right\} \qquad (8\text{-}74)$$

where $\beta = \frac{q_{c_2}}{q_{c_1}}$ is the ratio of the heat-flow densities at the walls; $\Phi = \frac{\varepsilon_{np}\sigma\overline{T}_c^3 h}{\lambda}$ is a dimensionless parameter allowing for the influence of heat exchange by radiation.

We represent θ as

$$\theta = \theta_0 + AX + f(Y),$$

where θ_0 is the dimensionless temperature at the entrance; $A = 2$, as we can see from (8-32). Substituting this expression for θ into (8-71) and integrating the latter twice, we find

$$f(Y)=\frac{3}{8}\left(Y^3-\frac{Y^5}{6}\right)+c_1Y+c_2,$$

where c_1 and c_2 are constants of integration.

Thus

$$\theta=\theta_0+2X+\frac{3}{8}\left(Y^3-\frac{Y^5}{6}\right)+c_1Y+c_2. \qquad (8\text{-}75)$$

Using the first boundary condition of (8-74) and the condition $\theta=\theta_{c2}$ for $Y=-1$, we determine the constants. After they have been substituted into (8-75), we have

$$\theta-\theta_{c2}=\frac{3}{8}\left(Y^3-\frac{Y^5}{6}\right)-\frac{15}{48}+\left[\frac{1-\beta}{2(1+\beta)}-2\Phi(\theta_{c1}-\theta_{c2})\right](Y+1).$$

Letting $Y = 1$, we find

$$\theta_{c1}-\theta_{c2}=\frac{1-\beta}{(1+\beta)(1+4\Phi)}. \qquad (8\text{-}76)$$

Substituting this value into the preceding equation, we finally obtain

$$\theta-\theta_{c1}=\frac{3}{8}\left(Y^3-\frac{Y^5}{6}\right)+\left[\frac{1-\beta}{2(1+\beta)}-\frac{2\Phi(1-\beta)}{(1+\beta)(1+4\Phi)}\right]Y+$$
$$+\left[\frac{3\beta-13}{16(1+\beta)}+\frac{(1-\beta)(1+2\Phi)}{(1+\beta)(1+4\Phi)}\right]. \qquad (8\text{-}77)$$

The expression for $\theta - \theta_{s1}$ is easily found by subtracting (8-76) from (8-77).

There is no difficulty in computing the differences between the wall temperatures and the mean mass temperature of the fluid, and the limiting Nusselt numbers at each wall:

$$\theta_{ci}-\bar{\theta}=\frac{3}{4}\int_{-1}^{+1}(\theta_{ci}-\theta)(1-Y^2)\,dY,\ (i=1;\ 2);$$

$$\mathrm{Nu}_{i\infty}=\frac{q_{ci}h}{T_{ci}-\bar{T}}=\frac{2D_i}{(1+\beta)(\theta_{ci}-\bar{\theta})},$$

where $D_i=1$ when $i=1$ and $D_i=\beta$ when $i=2$.

Performing the computations, we obtain

$$\theta_{ci}-\bar{\theta}=\frac{26-9\beta}{35(1+\beta)}-\frac{(1-\beta)(2\Phi+C_i)}{(1+\beta)(1+4\Phi)}; \qquad (8\text{-}78)$$

$$\mathrm{Nu}_{i\infty}=\frac{2D_i}{\frac{26-9\beta}{35}-\frac{(1-\beta)(2\Phi+C_i)}{1+4\Phi}}, \qquad (8\text{-}79)$$

where $C_i=0$ when $i=1$ and $C_i=1$ when $i=2$.

When $\Phi = 0$, i.e., when there is no heat exchange by radiation, Eq. (8-79) reduces to (8-43).

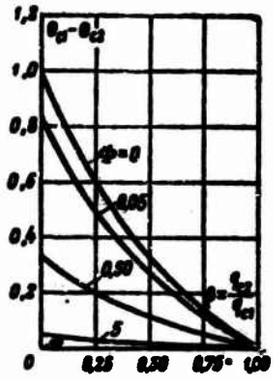

Fig. 8-13. Influence of radiation on dimensionless wall-temperature difference for flat tube.

Figure 8-13 shows the change in the dimensionless tube-wall temperature difference as a function of β for various values of the parameter Φ. As Φ increases, the influence of radiative heat exchange rises; this substantially reduces the wall-temperature difference. Thus when $\beta=0{,}25$ and $\Phi=0{,}5$, the wall-temperature difference decreases by a factor of 3 as compared with its value in the absence of radiative heat exchange.

Manuscript Page. No.

Footnotes

183 [1]If we seek a solution by applying the method of separation of variables directly to θ, rather than to $\theta_1=\theta-\theta_0$, then in satisfying the boundary condition $\left(\frac{\partial\theta}{\partial R}\right)_{R=1}=-\frac{1}{\varepsilon}$, we would have obtained a different relationship:

$$\varphi(X)\sum_{n=0}^{\infty}2nb_{2n}e^{2n-1}=-\frac{1}{2}.$$

In other words, the method of separation of variables is unsuitable for this case. Thus we see that it is necessary to isolate one particular solution (θ_0), since this eliminates the inhomogeneity from the last boundary condition of (8-3), and the solution for θ_1 can be found by separation of variables.

186 [2]See [8a] of the references for Chapter 6.

187 [3]This solution is found in analogy with the solution for a round tube (see §8-1).

188 [4]See the analogous solution for the case in which $t_{ж}$ = = const, §6-2.

197 [5]The example is taken from [6].

198 [6]The hydraulic-integrator calculations whose results are shown in Figs. 8-9 and 8-10 were carried out at the Moscow Power Institute by I.V. Kurayeva.

Manuscript Page No.	Transliterated Symbols
180	c = s = stenka = wall
185	н.т = n.t = nachal'nyy termicheskiy [uchastok] = initial thermal [segment]
199	$d_э$ = d_e = [equivalent diameter]
199	п = p = [not identified]
207	пр = pr = privedennyy = reduced

Chapter 9

HEAT EXCHANGE AND RESISTANCE IN ROUND TUBE WITH VARIABLE FLUID PHYSICAL PROPERTIES AND BOUNDARY CONDITIONS OF THE SECOND KIND

9-1. HEAT EXCHANGE AND RESISTANCE IN THERMAL INITIAL SEGMENT

1. We consider liquid flow and heat exchange in the thermal initial segment of a round tube; the viscosity coefficient is assumed to be temperature-dependent, while all other physical properties are taken to be constant. A similar problem was investigated in §7-3 for constant wall temperature. Proceeding in similar fashion, we can also solve this case without difficulty when the heat-flux density is constant at the wall; this was done in [1]. Since the remaining conditions and the solution method are the same as in §§7-2 and 7-3, we shall only give the initial equations and the computational results.

We introduce the following definitions for the dimensionless variables:

$$\theta=\frac{(t-t_0)\lambda}{q_c r_0};\quad W_x=\frac{w_x}{\bar{w}};\quad W_y=-\frac{w_y}{\bar{w}};\quad M=\frac{\mu}{\mu_0};$$

$$\mathrm{Pe}=\frac{\bar{w}d}{a};\quad X=\frac{x}{r_0};\quad Y=1-\frac{r}{r_0};\quad k=\frac{\Delta}{r_0}.$$

The definitions of the dimensioned variables are the same as in §§7-2 and 7-3.

If we neglect energy dissipation, the problem reduces to joint integration of an equation system that takes the following form with our notation:

$$\frac{1}{1-Y}\cdot\frac{\partial}{\partial Y}\left[(1-Y)\frac{\partial\theta}{\partial Y}\right]=B(X), \tag{9-1}$$

$$\frac{1}{1-Y}\cdot\frac{\partial}{\partial Y}\left[(1-Y)M\frac{\partial W_x}{\partial Y}\right]=A(X), \tag{9-2}$$

$$\frac{\partial W_x}{\partial X}+\frac{1}{1-Y}\cdot\frac{\partial}{\partial Y}[(1-Y)W_y]=0, \tag{9-3}$$

$$\frac{1}{M}=1+c_1\theta+c_2\theta^2+\ldots+c_m\theta^m, \tag{9-4}$$

where

$$B=\frac{\mathrm{Pe}}{2k}\int_0^k\left(W_x\frac{\partial\theta}{\partial X}+W_y\frac{\partial\theta}{\partial Y}\right)dY; \tag{9-5}$$

Here $A(X)$ is a certain function of X.

The solution of this system must satisfy the following boundary conditions:

$$\left.\begin{array}{l} \text{for } X>0 \text{ and } Y=0 \quad \dfrac{\partial\theta}{\partial Y}=-1,\ W_x=W_y=0; \\ \text{for } X>0 \text{ and } 1\geqslant Y>k \quad \theta=0,\ \dfrac{\partial\theta}{\partial Y}=0; \\ \text{for } X>0 \text{ and } Y=1 \quad \dfrac{\partial W_x}{\partial Y}=0. \end{array}\right\} \qquad (9\text{-}6)$$

Integrating (9-1) and using the temperature boundary conditions, we find

$$B(X)=\frac{2}{2k-k^2}, \qquad (9\text{-}7)$$

$$\theta=\frac{1}{k(2-k)}\left[-(1-k)^2\ln\frac{1-Y}{1-k}-Y\left(1-\frac{Y}{2}\right)+k\left(1-\frac{k}{2}\right)\right]. \qquad (9\text{-}8)$$

Since the thickness of the thermal boundary layer is substantially less than the tube radius, when $0<Y<k$, we can neglect k and Y as compared with unity. Here Expression (9-8) becomes simpler, taking the form

$$\theta\approx\frac{1}{2k}(Y-k)^2. \qquad (9\text{-}8a)$$

Substituting (9-8a) into (9-4), we determine the law governing the variation in viscosity over the thickness of the thermal boundary layer:

$$\frac{1}{M}=1+\frac{c_1}{2k}(Y-k)^2+\frac{c_2}{4k^2}(Y-k)^4+\ldots+\frac{c_m}{mk^m}(Y-k)^{2m}.$$

In most practical cases, the relationship between the viscosity and temperture will be described with sufficient accuracy by a second-degree trinomial. Thus we only keep the first three terms of the last equation. Then after certain manipulations we obtain

$$\frac{1}{M}=\left(1+\frac{c_1}{2}k+\frac{c_2}{4}k^2\right)-(c_1+c_2k)Y+\frac{1}{2}\left(\frac{c_1}{k}+3c_2\right)Y^2-\frac{c_2}{k}Y^3+\frac{c_2}{4k^2}Y^4. \qquad (9\text{-}9)$$

We integrate equation of motion (9-2) separately in the thermal boundary layer region where M is described by Eq. (9-9), and in the flow core, where M = 1; determining the function $A(X)$ from the condition requiring that the flowrate be constant, we obtain equations for the longidutinal velocity component:

for $Y\leqslant k$

$$W_x=\frac{1}{2R}\sum_{l=0}^{5}\frac{b_l}{l+1}Y^{l+1}; \qquad (9\text{-}10)$$

for $Y\geqslant k$

$$W_x=\frac{1}{2R}\left[\frac{1}{2}(Y^2-k^2)-(Y-k)+\sum_{l=0}^{5}\frac{b_l}{l+1}k^{l+1}\right], \qquad (9\text{-}11)$$

where

$$R=-\frac{1}{8}+\frac{1}{2}k-\frac{3}{4}k^2+\frac{1}{2}k^3-\frac{1}{8}k^4+\frac{1}{2}(1-k)^3\sum_{l=0}^{5}\frac{b_l}{l+1}k^{l+1}+$$

$$+\sum_{l=0}^{5}\frac{b_l}{l+1}\left(\frac{k^{l+2}}{l+2}-\frac{k^{l+3}}{l+3}\right);$$

$$b_0=-\left(1+\frac{c_1}{2}k+\frac{c_2}{4}k^2\right);$$

$$b_1=1+c_2+\left(\frac{c_1}{2}+c_3\right)k+\frac{c_2}{4}k^2;$$

$$b_2=-\left(c_2+\frac{3}{2}c_3\right)-\left(\frac{c_1}{2}+c_3\right)k;$$

$$b_3=\frac{3}{2}c_3+\left(\frac{c_1}{2}+c_3\right)\frac{1}{k};$$

$$b_4=-\left(\frac{c_2}{k}+\frac{c_3}{4k^2}\right);\quad b_5=\frac{c_3}{4k^2}.$$

For constant viscosity, Eqs. (9-10) and (9-11) yield a parabolic velocity distribution.

Using the continuity equation (9-3) and Eq. (9-11) for W_x, we obtain an expression for the transverse velocity component:

$$W_y=\frac{1}{2R}\cdot\frac{dk}{dX}\left[-\frac{1}{4}(c_1+c_2k)Y^2+\frac{1}{6}\left(\frac{c_1}{2}+c_2+\frac{c_3}{2}k\right)Y^3+\frac{1}{12}\left(\frac{c_1}{2k^2}-c_3\right)Y^4-\right.$$

$$\left.-\frac{1}{20}\left(\frac{c_1}{2k^2}+\frac{c_2}{k^2}\right)Y^5+\frac{1}{30}\left(\frac{c_2}{k^2}+\frac{c_3}{2k^2}\right)Y^6-\frac{c_3}{84k^2}Y^7\right]+$$

$$+\frac{1}{2R^2}\cdot\frac{dR}{dk}\cdot\frac{dk}{dX}\sum_{l=0}^{5}\frac{b_l}{(l+1)(l+2)}Y^{l+2}. \qquad (9\text{-}12)$$

When $\mu=\text{const}, c_1=c_2=0$, $R=-\frac{1}{8}$ and $W_y=0$.

The relationship between the thickness k of the thermal boundary layer and X is determined from (9-5). Substituting in the value of $B(X)$ from (9-7), as well as θ, W_x and W_y from (9-8a), (9-10), and (9-12), we have

$$\frac{1}{4}\int_0^k\left\{\frac{1}{2R}\left[\sum_{l=0}^{5}\frac{b_l}{(l+1)(l+2)}k^{l+2}-\frac{1}{k^2}\sum_{l=0}^{5}\frac{b_l}{(l+1)(l+4)}k^{l+4}\right]+\right.$$

$$+\frac{1}{R^2}\cdot\frac{dR}{dk}\left[\frac{1}{k}\sum_{l=0}^{5}\frac{b_l}{(l+1)(l+2)(l+4)}k^{l+4}-\sum_{l=0}^{5}\frac{b_l}{(l+1)(l+2)(l+3)}k^{l+3}\right]+$$

$$\left.+\frac{1}{R}\left(-\frac{7}{360}c_1k^3+\frac{1}{280}c_2k^4-\frac{3}{224}c_3k^5+\frac{11}{6048}c_3k^6\right)\right\}dk=\frac{X}{\mathrm{Pe}}. \qquad (9\text{-}13)$$

A numerical method is used to integrate (9-13).

For constant viscosity, $c_1=c_2=0$, $b_0=-1$, $b_1=1$, $R=-\frac{1}{8}$, and $dR/dk = 0$. In this case, (9-13) takes the form

$$\int_0^k \left(\frac{1}{4}k^2 - \frac{1}{15}k^3\right)dk = \frac{X}{Pe}.$$

As a result of integration we obtain

$$k^3\left(1 - \frac{k}{5}\right) = 24\frac{1}{Pe}\cdot\frac{x}{d}. \qquad (9\text{-}14)$$

After the relationship between k and $\frac{1}{Pe}\cdot\frac{x}{d}$ has been found, we can calculate the velocity and temperature profiles, as well as the wall temperature, heat-transfer coefficient, and resistance coefficient.

We obtain the expression for the dimensionless wall temperature from (9-8), letting $Y = 0$:

$$\theta_c = \frac{1}{k(2-k)}\left[(1-k)^2\ln(1-k) + k\left(1 - \frac{k}{2}\right)\right]. \qquad (9\text{-}15)$$

If we use approximate equation (9-8a), then

$$\theta_c = \frac{k}{2}. \qquad (9\text{-}15a)$$

Determining the local heat-transfer coefficient in the form

$$\alpha = \frac{q_c}{t_c - \bar{t}},$$

we obtain the following expression for Nu:

$$Nu = \frac{\alpha d}{\lambda} = \frac{2}{\theta_c - \bar{\theta}}. \qquad (9\text{-}16)$$

The dimensionless mean mass temperature of the liquid in the given section is

$$\bar{\theta} = 2\int_0^1 \theta W_x (1-Y)\,dY,$$

or, since when $k < Y < 1$, $\theta = 0$,

$$\bar{\theta} = 2\int_0^k \theta W_x (1-Y)\,dY.$$

If we now substitute in the value of θ from (9-8a) and W_x from (9-10), we obtain

$$\bar{\theta} = \frac{1}{K}\left[-\frac{1}{2k}\sum_{i=0}^{5}\frac{b_i}{(i+1)(i+5)}k^{i+5} + \frac{2k+1}{2k}\sum_{i=0}^{5}\frac{b_i}{(i+1)(i+4)}k^{i+4} - \right.$$
$$\left. - \frac{2+k}{2}\sum_{i=0}^{5}\frac{b_i}{(i+1)(i+3)}k^{i+3} + \frac{k}{2}\sum_{i=0}^{5}\frac{b_i}{(i+1)(i+2)}k^{i+2}\right]. \qquad (9\text{-}17)$$

The Nu number can be determined differently by representing α as $q_s/t_s - t_0$. Then using (9-15a), we find

$$\mathrm{Nu}=\frac{2}{\theta_c}=\frac{4}{k}. \qquad (9\text{-}16a)$$

TABLE 9-1

Comparison of Results of Theoretical Heat-Transfer Calculation with Experimental Data for Flow of BM-4 Oil in Tube 10 mm in Diameter at t_0 = 35.5°C and q_s = 20.8·10³ kW/m²

$\frac{1}{Pe}\cdot\frac{x}{d}$	k	t_c, °C	$\frac{\mu_c}{\mu_0}$	$Nu_{теор}$	$Nu_{опыт}$
4,55·10⁻⁴	0,04	53,0	0,371	98,3	93,3
1,14·10⁻³	0,10	79,3	0,131	38,8	37,9
1,15·10⁻³	0,20	123	0,0527	20,8	20,4

When the viscosity is constant, $\frac{1}{Pe}\cdot\frac{x}{d}$ is sufficiently small, and $k/5 \ll 1$ in (9-14), we have

$$\mathrm{Nu}=1{,}40\left(\frac{1}{Pe}\cdot\frac{x}{d}\right)^{-1/3}.$$

This is nearly the same as Eq. (8-14). The sole difference lies in the value of the constant, which is 8% greater here than in (8-14). We also note that in (8-14), Nu refers to the difference $t_s - \bar{t}$ rather than $t_s - t_0$. When $\frac{1}{Pe}\cdot\frac{x}{d}$ is small, however, this is of no great importance.

The local friction-resistance coefficient is

$$\xi=\frac{8\sigma_c}{\rho\bar{w}^2}=\frac{8\mu_c}{\rho\bar{w}^2}\left(\frac{\partial w_x}{\partial y}\right)_{y=0}=\frac{16}{Re_c}\left(\frac{\partial W_x}{\partial Y}\right)_{Y=0}.$$

Finding the derivative from (9-10), we finally obtain

$$\xi=\frac{8}{Re_c}\cdot\frac{b_0}{R}, \qquad (9\text{-}18)$$

where $Re_c=\bar{w}\rho d/\mu_c$.

For constant viscosity, Eq. (9-18) gives the usual value ξRe = 64.

The results of a theoretical determination of heat transfer using the foregoing method are compared in Table 9-1 with experimental data. For this table, $Nu_{опыт}$ was computed from (9-19). Comparison shows good agreement of the calculated and experimental values of Nu.

2. As we can see, it is a quite complicated matter to make a theoretical determination of heat exchange and hydraulic resistance with allowance for the relationship between viscosity and temperature. Each specific case requires a great deal of computational effort. In practice, therefore, if we do not need to know the detailed process characteristics (velocity field, temperature field, etc.), preference is given to the simplest possible empirical equations.

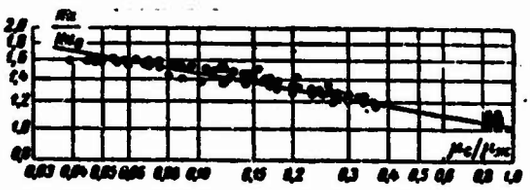

Fig. 9-1. Relationship between Nu/Nu_0 and μ_s/μ_{zh} for q_s = const, based on experimental data for type BM-4 oil (circles) and water (squares).

M.A. Mikheyev, S.S. Filimonov, and B.A. Khrustalev have measured heat transfer for viscous flow of water in round tubes [2]; Ma Tun-tsze has performed such measurements for viscous flow of type BM-4 oil [1]. In these experiments, the heat-flux density at the wall was held constant by passing an electric current directly through the tube wall, or by means of an external electric heater. In most cases, the liquid was introduced into the working segment through a nozzle of smooth outline so that the velocity and temperature profiles developed simultaneously along the tube length. Here stabilization of the velocity profile terminated a certain distance from the tube entrance, while, as a rule, the temperature profile did not become stabilized within the limits of the working segment (except for some of the water experiments).

Here we shall only consider experimental data pertaining to the flow region far from the entrance, at a distance exceeding the length of the hydrodynamic initial segment ($x \geq l_{n.g}$).[1] Figure 9-1 shows these experimental results in power treatment. The axis of ordinates shows the ratio of the local number $Nu = \frac{q_c d}{\lambda (t_c - \bar{t})}$ found experimentally to the value of Nu_0 computed from (8-15) on the assumption that the physical properties of the liquid remain constant. The axis of abscissas shows the ratio of the dynamic viscosity coefficients at the wall temperature t_s and the mean mass temperature $\bar{t}$ of the liquid. The curve of Fig. 9-1 corresponds to the equations

$$Nu = 1{,}31 \left(\frac{1}{Pe} \cdot \frac{x}{d}\right)^{-1/3} \left(1 + 2\frac{1}{Pe} \cdot \frac{x}{d}\right) \left(\frac{\mu_0}{\mu_w}\right)^{-1/6}, \qquad (9\text{-}19)$$

which, as we can see, is a quite good description of the experimental data. Approximate allowance is made for the dependence of

[1] /241

λ and a on the temperature by choosing the values of these parameters in the expressions for Nu, Nu_0, and Pe for a temperature $t=\frac{1}{2}(t_c+\bar{t})$.

Equation (9-19) is valid for heating of liquids (their viscosity decreases with temperature) with constant heat-flux density at the wall and, of course, with no influence of free convection. It covers the region of values of Re < 2300, $\frac{1}{Pe}\cdot\frac{x}{d}\leqslant 0{,}04$ and $0{,}04<\frac{\mu_c}{\mu_w}<1$.

Comparing Eq. (9-19) with (7-83) (for the case in which $t_s \approx$ const), we find that the influence of variable viscosity on heat exchange is roughly the same for q_s = const as for t_s = const. We can therefore assume that, first, Eq. (9-19) will be valid not only for heating, but also for cooling of the liquid (at least to values $\mu_s/\mu_{zh} \leq 10$) and, second, that the influence of the variable viscosity on heat exchange can be taken into account with the aid of the ratio $(\mu_c/\mu_w)^n$, where $n=0{,}14-0{,}16$ both when the heat-flux density at the wall is constant along the length and when it varies with the length.

3. In the study of Worse-Schmidt and Leppert, cited in §7-4, paragraph 2 (see [11] of the references for Chapter 7), a numerical method was used to solve the problem of heat exchange and resistance for air flowing with variable physical properties in the thermal initial segment of a round tube. The calculations were carried out both for constant wall temperature and with constant density of heat flux at the wall. All remaining conditions were the same in the two cases (see §7-4, paragraph 2).

The computational results show that the influence of variable physical properties on heat exchange and resistance for q_s = const is roughly the same as for t_s = const. For small values of the reduced length $\left(\frac{1}{Pe}\cdot\frac{x}{d}<10^{-2}\right)$, Nu increases slowly, while for high values it decreases slowly as q_s (or $T_s/\bar{T}$) increases. The friction resistance coefficient ξ increases as $T_s/\bar{T}$ increases for all values of X; the rise is far sharper than for Nu. The variation in Nu and ξ with q_s (or $T_s/\bar{T}$) is greater in the thermal initial segment than in the region of stabilized heat exchange. When the physical properties are variable, the thermal initial section is roughly as long as for constant properties.

When q_s = const, an interpolation equation was proposed in the above-cited study for the local Nu numbers; the equation describes the computational results to within ±3%:

$$\mathrm{Nu}=4{,}36[1-\exp(-34X)]+aX^{-1/3}\exp(-bX^m). \qquad (9\text{-}19a)$$

The values of the parameters a, b, and m depend on the parameter $Q_c=\frac{q_0 d}{\lambda_0 T_0}$:

for $0<Q_c\leq 20$ $a=1{,}21+0{,}0661Q_c^{0.4}$, $b=47{,}6+8{,}42\sqrt[3]{Q_c}$, $m=5/4$;

for $20<Q_c\leq 40$ $a=1{,}38+0{,}00429Q_c$, $b=20+3{,}82\sqrt[3]{Q_c}$, $m=1$.

Here λ_0 is the thermal-conductivity coefficient of a gas for an entrance temperature T_0. The remaining symbols, as well as the limits of applicability of (9-19a) are the same as for the case in which T_s = const (see §7-4, paragraph 2).[2]

When q_s = const, Eq. (7-82a) holds for the local resistance coefficient.

9-2. HEAT EXCHANGE AND RESISTANCE FAR FROM THE TUBE ENTRANCE. THEORETICAL-COMPUTATION METHOD

We shall investigate flow and heat exchange in a round tube at a distance from the entrance such that the velocity and temperature fields have become stabilized, i.e., where the fields have ceased to depend on the boundary conditions at the entrance section. Let the heat-flux density at the wall be constant along the length. In §7-1, this problem was solved on the assumption that the physical properties of the fluid remain constant. Here this restriction is removed: the fluid physical properties are treated as arbitrary functions of the temperature, but, as before, the fluid is assumed to be incompressible. The problem has been considered in this formulation by V.N. Popov and the present author [3].

We make the following assumptions:

1. The fluid velocity is not large, so that energy dissipation can be neglected.

2. The mass-force influence occasioned by the variable density is small as compared with the influence of the viscosity forces and the inertia.

3. The change in heat-flux density produced by heat conduction along the axis is small as compared with the variation along the radius.

4. The axial component of the mass velocity varies little along the tube axis, i.e., $\partial(\rho w_x)/\partial x\approx 0$. As a consequence of this assumption, we find that the radial velocity component equals zero (w_r = 0), while the pressure p is constant over a section.

With allowance for these assumptions, the energy equation and equation of motion will take the form

$$\rho w_x\frac{\partial h}{\partial x}=\frac{1}{r}\cdot\frac{\partial}{\partial r}(rq), \tag{9-20}$$

$$\frac{\partial}{\partial x}(p+\rho w_x^2)=\frac{1}{r}\cdot\frac{\partial}{\partial r}(r\sigma), \tag{9-21}$$

$$q = \lambda \frac{\partial T}{\partial r};$$

$$\sigma = -\mu \frac{\partial w_x}{\partial r};$$

Here h is the enthalpy, T the temperature, p the pressure, w_x the longitudinal velocity, component, q the heat-flux density, and σ the tangential stress.

To simplify the simultaneous solution of (9-20) and (9-21), we make two more assumptions. We assume that the derivatives with respect to x occurring on the left sides of (9-20) and (9-21) do not vary over a section, i.e.,

5. $\frac{\partial h}{\partial x} = f_1(x)$.

6. $\frac{\partial (p + \rho w_x^2)}{\partial x} = f_2(x)$.

When the heat-flux density at the wall is constant with length, assumption 5 should be sufficiently well satisfied. The same can be said of assumption 6, since for a gas flowing at moderate subsonic velocities, and even more certainly for a liquid, the pressure gradient produced by the longitudinal density variation $\partial(\rho w_x^2)/\partial x$, will be small as compared with the resultant pressure gradient dp/dx which, as we have already noted, does not change over a tube cross section. Nonetheless, by introducing assumptions 4, 5, and 6 we make the problem solution approximate.

On the basis of (9-20), (9-21), and assumptions 5 and 6 we can obtain equations for the distribution of heat-flux density, tangential stress, temperature, and mass velocity over a tube section, as well as expressions for the Nusselt number and the friction resistance coefficient.

Multiplying (9-20) by $r\,dr$, using assumption 5, and integrating over the radius between 0 and r_0, we have

$$\frac{dh}{dx} = \frac{2q_s}{\bar{\rho w} r_0}, \qquad (9\text{-}22)$$

where q_s is the heat-flux density at the wall; $\bar{\rho w}$ is the mean mass velocity of the fluid over a section, and r_0 is the tube radius.

Substituting (9-22) into (9-20) and integrating the latter between 0 and r, we obtain the distribution of heat-flux density over the radius:

$$\frac{q}{q_s} = \frac{2}{R} \int_0^R \frac{\rho w_x}{\bar{\rho w}} R\,dR, \qquad (9\text{-}23)$$

where $R = r/r_0$.

Since the pressure is constant over a tube section,

$$\frac{\partial h}{\partial r} = c_p \frac{\partial T}{\partial r}. \qquad (9\text{-}24)$$

We can use this relationship to represent the heat-flux density in the form

$$q=\frac{\lambda}{c_p}\cdot\frac{\partial h}{\partial r}. \qquad (9\text{-}25)$$

From (9-23) and (9-25) we find

$$\frac{\partial h}{\partial R}=q_c d\,\frac{c_p}{\lambda}\cdot\frac{1}{R}\int_0^R\frac{\rho w_x}{\rho w}R\,dR. \qquad (9\text{-}26)$$

Integrating (9-26) from R to 1, we obtain the enthalpy distribution over the radius:

$$h_c-h=q_c d\int_R^1\frac{\int_0^R\frac{\rho w_x}{\rho w}R\,dR}{\frac{\lambda}{c_p}R}dR, \qquad (9\text{-}27)$$

where h_s is the enthalpy at the wall.

We can now obtain the temperature distribution if in (9-26) we represent $\partial h/\partial R$ in terms of $\partial T/\partial R$ with the aid of (9-24) and integrate the resulting equation between R and 1:

$$T_c-T=\frac{q_c d}{\lambda_c}\int_R^1\frac{\int_0^R\frac{\rho w_x}{\rho w}R\,dR}{\frac{\lambda}{\lambda_c}R}dR, \qquad (9\text{-}28)$$

where T_s is the temperature at the tube wall; λ_s is the thermal-conductivity coefficient of the fluid at temperature T_s.

By definition, the heat-transfer coefficient equals

$$\alpha=\frac{q_c}{T_c-\bar{T}}=\frac{q_c\bar{c}_p}{h_c-\bar{h}}, \qquad (9\text{-}29)$$

where $\bar{T}$ and $\bar{h}$ are the mean mass temperatures and the enthalpy of the fluid;

$$\bar{c}_p=\frac{h_c-\bar{h}}{T_c-\bar{T}}=\frac{1}{T_c-\bar{T}}\int_{\bar{T}}^{T_c}c_p\,dT$$

is the mean integral value of heat capacity for the temperature-variation interval between T_s and $\bar{T}$.

In turn,

$$h_c-\bar{h}=2\int_0^1(h_c-h)\frac{\rho w_x}{\rho w}R\,dR. \qquad (9\text{-}30)$$

Multiplying (9-27) by $2\frac{\rho w_x}{\rho w}R\,dR$ and integrating with respect to

R between 0 and 1, we obtain

$$h_c - \bar{h} = 2q_c d \int_0^1 \frac{\rho w_x}{\rho w} R \left(\int_R^1 \frac{\int_0^R \frac{\rho w_x}{\rho w} R\, dR}{\frac{\lambda}{c_p} R} dR \right) dR.$$

The integral on the right side of this expression is evaluated by parts. Integrating, we obtain

$$h_c - \bar{h} = 2q_c d \int_0^1 \frac{\left(\int_0^R \frac{\rho w_x}{\rho w} R\, dR \right)^2}{\frac{\lambda}{c_p} R} dR. \qquad (9\text{-}31)$$

Using (9-29), on the basis of (9-31), we obtain an expression for the Nusselt number:

$$\frac{1}{\mathrm{Nu}_{c\infty}} = 2 \frac{c_{pc}}{\bar{c}_p} \int_0^1 \frac{\left(\int_0^R \frac{\rho w_x}{\rho w} R\, dR \right)^2}{\frac{\lambda}{\lambda_c} \cdot \frac{c_{pc}}{\bar{c}_p} R} dR, \qquad (9\text{-}32)$$

where $\mathrm{Nu}_{c\infty} = \alpha d/\lambda_c$ is the limiting Nusselt number, computed from the value of the thermal-conductivity coefficient at the wall temperature; c_{ps} is the fluid heat capacity at the wall temperature.

It is easy to see that when the physical properties of the fluid are constant, Eq. (9-32) reduces to the familiar Layon integral.

We now turn to equation of motion (9-21). Integrating this equation between 0 and r, making allowance for assumption 6, and eliminating $\frac{\partial}{\partial x}(p + \rho w_x^2)$ by means of the boundary condition at the wall, we obtain

$$\frac{\sigma}{\sigma_c} = R, \qquad (9\text{-}33)$$

where σ_s is the tangential stress at the wall.

Relationship (9-33) follows from assumption 6. Introduction of this assumption means that the actual radial distribution of tangential stress is replaced, in approximation, by a linear distribution.

Substituting the value $\sigma = -\mu \partial w_x/\partial r$ into (9-33) and integrating between R and 1, we find the velocity distribution:

$$w_x = \frac{\sigma_c r_0}{\mu_c} \int_R^1 \frac{\mu_c}{\mu} R\, dR. \qquad (9\text{-}34)$$

Multiplying this equation by ρ and dividing by

$$\overline{\rho w} = 2\int_0^1 \rho w_x R\, dR,$$

we obtain the mass-velocity distribution:

$$\frac{w_x}{w} = \frac{\frac{\rho}{\rho_c}\int_R^1 \frac{\mu_c}{\mu} R\, dR}{2\int_0^1 \frac{\rho}{\rho_c}\left(\int_R^1 \frac{\mu_c}{\mu} R\, dR\right) R\, dR}. \qquad (9\text{-}35)$$

The friction-resistance coefficient can be determined in the form

$$\xi_c = \frac{8\tau_c \rho_c}{(\rho w)^2}. \qquad (9\text{-}36)$$

Representing σ_s in terms of the velocity gradient at the wall and finding the latter from (9-35), on the basis of (9-36), we obtain an equation for the friction-resistance coefficient:

$$\xi_c = \frac{8}{\mathrm{Re}_c} \cdot \frac{1}{\int_0^1 \frac{\rho}{\rho_c}\left(\int_R^1 \frac{\mu_c}{\mu} R\, dR\right) R\, dR}, \qquad (9\text{-}37)$$

where $\mathrm{Re}_c = \overline{\rho w} d/\mu_c$ is the Reynolds number, calculated from the value of the dynamic-viscosity coefficient at the wall temperature.

When the physical properties of the fluid are constant, Eqs. (9-23), (9-32), (9-33), (9-35) and (9-37) take the familiar forms

$$\frac{q}{q_c} = 2R\left(1 - \frac{R^2}{2}\right), \qquad (9\text{-}23a)$$

$$T_c - T = \frac{q_c d}{8\lambda}(3 - 4R^2 + R^4), \qquad (9\text{-}28a)$$

$$\mathrm{Nu}_\infty = \frac{48}{11}, \qquad (9\text{-}32a)$$

$$\frac{\theta}{\theta_c} = R, \qquad (9\text{-}33a)$$

$$\frac{w_x}{w} = 2(1 - R^2), \qquad (9\text{-}35a)$$

$$\xi = \frac{64}{\mathrm{Re}}. \qquad (9\text{-}37a)$$

Equations (9-28), (9-32), (9-35) and (9-37) permit us to determine the heat transfer and friction resistance, and incidentally the temperature and velocity fields when the fluid physical properties (ρ, μ, λ, c_p) vary arbitrarily with the temperature.

As we can see from (9-32), (9-37) and (9-35) to determine

$Nu_{c\infty}$ and ξ_c, we must know the radial distribution of the fluid physical properties or of the temperature (since we assume that we know the way in which the physical properties depend on the temperature). Since the temperature distribution (with variable physical properties) is not known in advance, a successive-approximation method must be used.

The calculations are carried out as follows:

1) the values of T_s and $q_s d/\lambda_s$ are specified;

2) the temperature profile is calculated in first approximation on the assumption that the fluid physical properties are constant and equal to the values of the physical properties at the wall temperature; Eq. (9-28a) is used for the computations; the radial distributions of the fluid physical properties are determined, and Eqs. (9-35) and (9-28) are used for the initial determination of the mass-velocity profile and then for the second approximation to the temperature profile;

3) the mass-velocity profile and the third-approximation temperature profile are determined, and so on until the difference in the temperature distribution for the $(n + 1)$st and nth approximation becomes less than some specified amount within which the variation in fluid physical properties is negligible;

4) the distributionof fluid physical properties corresponding to the temperature profile found in the last approximation is used to evaluate the integrals in (9-32) and (9-37); we then determine

$$\frac{Nu_{c\infty}}{c_p} = \frac{q_c d}{\lambda_c (h_c - \bar{h})} \text{ and } \xi_c Re_c.$$

Since the values of $q_c d/\lambda_c$ and T_c are specified, it is easy to find the mean mass enthalpy $\bar{h}$ and the corresponding mean mass temperature $\bar{T}$. After this, we calculate the Nusselt number:

$$Nu_{c\infty} = \frac{q_c d}{\lambda_c (T_c - \bar{T})}.$$

After appropriate modification, this method of determining heat exchange with variable physical properties can be extended to the case of friction in flat and annular tubes.

In the succeeding sections, we shall give results of heat-exchange and friction-resistance calculations for flow of fluids, diatomic gases, and hydrogen and carbon dioxide in a condition of equilibrium dissociation for the supercritical region of the state parameters.

9-5. HEAT EXCHANGE AND RESISTANCE FAR FROM THE TUBE ENTRANCE FOR FLOW OF LIQUIDS

Heat-exchange and friction-resistance calculations have been carried out [3] for water at a wall temperature t_s between 0 and 300°C, transformer oil with t_s between 0 and 120°C, and type

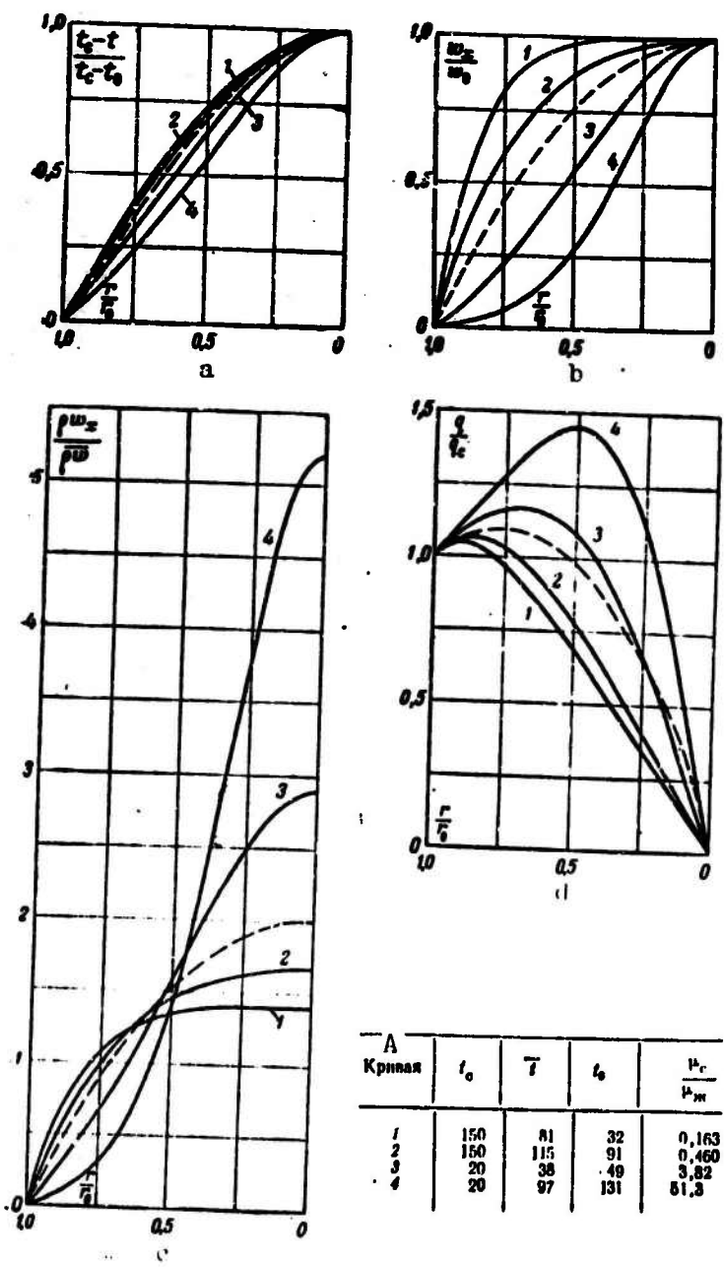

A Кривая	t_0	$\bar{T}$	t_s	$\frac{\mu_c}{\mu_{ж}}$
1	150	81	32	0,163
2	150	115	91	0,460
3	20	38	49	3,82
4	20	97	131	51,3

Fig. 9-2. Radial distributions of temperature (a) velocity (b), mass velocity (c), and heat-flux density (d) in tube with flow of type MC-20 oil; t_0 and w_0 are the values of t and w on the tube axis. The dashed line corresponds to constant physical properties. A) Curve.

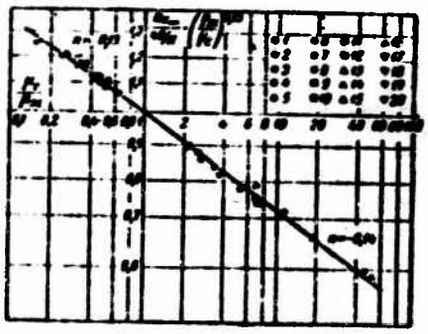

A Вода				B Масло трансформаторное	
1	t_c = 300° C	5	t_c = 70° C	9	t_c = 120° C
2	t_c = 250° C	6	t_c = 50° C	10	t_c = 80° C
3	t_c = 150° C	7	t_c = 5° C	11	t_c = 30° C
4	t_c = 100° C	8	t_c = 0° C	12	t_c = 0° C

C Масло МС-20 (переменны все физические свойства)		D Масло МС-20 (переменна лишь вязкость)	
13	t_c = 150° C	17	t_c = 150° C
14	t_c = 90° C	18	t_c = 90° C
15	t_c = 65° C	19	t_c = 65° C
16	t_c = 20° C	20	t_c = 20° C

Fig. 9-3. Results of heat-transfer calculations for water, transformer oil, and type MC-20 oil flowing in a round tube. The curve corresponds to the equation

$$Nu_{\infty} = \frac{48}{11}\left(\frac{\rho_r}{\rho_m}\right)^{0.25}\left(\frac{\mu_c}{\mu_m}\right)^{n}.$$

A) Water; B) transformer oil; C) type MC-20 oil (all physical properties variable); D) type MC-20 oil (only viscosity variable).

MC-20 oil with t_s between 20 and 150°C, with both heating and cooling of the liquids. The ratio of dynamic viscosity coefficients at the wall temperature and at the mean mass temperature μ_s/μ_{zh} of the liquid varied from 0.426 to 12.6 for water, from 0.356 to 18.5 for transformer oil, and from 0.163 to 51.3 for type MC-20 oil. The remaining physical parameters varied negligibly, as we can see from Table 9-2, which gives certain data for water. Nonetheless, allowance was made for the variation in all physical properties during the calculations.[3] Naturally, for liquids the relationship between μ and t has the greatest influence on heat exchange and resistance. Moderate variations in the otherphysical parameters may only have a slight influence. To check this, additional calculations were carried out for type MC-20 oil; only the viscosity-temperature relationship was considered. As the graphs given show, for Nu and ξ, variations in ρ, c_p, and λ have negligible influence on heat transfer and resistance during flow of oils.

TABLE 9-2

Some Calculated Data for Water

t_c, °C	$\bar{t}$, °C	t_0, °C*	$\frac{c_{pc}}{c_{p\bar{t}}}$	$\frac{\rho_c}{\rho_{\bar{t}}}$	$\frac{\lambda_c}{\lambda_{\bar{t}}}$	$\frac{\mu_c}{\mu_{\bar{t}}}$
300	132	26	1,34	0,764	0,787	0,426
0	193	295	0,941	1,17	0,826	12,6

*t_0 is the temperature on the tube axis.

Figure 9-2 illustrates the influence of the variable physical properties (viscosity, in the main) of type MC-20 oil on the radial distribution of temperature, velocity, mass velocity, and heat-flux density. As the curves show, the dependence of the viscosity on the temperature has the greatest influence on the velocity profile (or on the mass velocity, which is almost the same thing in this case). The velocity-profile variation entails a corresponding change in the distribution of heat-flux density, as follows from Eq. (9-23). For cooling of the liquid, the velocity near the wall decreases as compared with the isothermal case. This leads to a reduction in the convective transport of heat along the axis in this region, and to a corresponding increase in the density of the radial heat flux.[4] In heating of the liquid, the reverse effect is observed.

Figure 9-3 shows computed heat-transfer results for water and the oils as theoretical points. The following equation is a good generalization of the calculated data:

$$\mathrm{Nu}_\infty = \frac{48}{11}\left(\frac{\rho_c}{\rho_{\bar{t}}}\right)^{0,25}\left(\frac{\mu_c}{\mu_{\bar{t}}}\right)^n, \qquad (9\text{-}38)$$

where

$$\mathrm{Nu}_\infty = \frac{q_{wl}}{\lambda_r(t_c - \bar{t})};$$

Here λ_r is the thermal-conductivity coefficient at the temperature $t_r = \frac{1}{2}(t_c + \bar{t})$; ρ_s and μ_s are the values of ρ and μ at t_c; ρ_m and μ_m are the values of ρ and μ at the temperature $\bar{t}$.

The exponent has a value $n = -0.13$ for heating of the liquid and -0.14 for cooling. The coefficient 48/11 corresponds to the value of the Nusselt number for constant physical properties of the liquid. By introducing λ_r into Nu_∞, we allow for the influence of the variable thermal conductivity. For water, the correction $(\rho_c/\rho_m)^{0.25}$, which allows for the influence of density variability, reaches 7%, but does not exceed 1.5% for the oils. The maximum departure of the calculated points from Eq. (9-38) is 3% for water and 2.3% for the oils.

Comparison of (9-38) with the empirical equation (9-19) for heat transfer in the thermal initial segment shows that when q_s = = const, the influence of variable viscosity on heat exchange in the region in which thermal stabilization sets in is somewhat less than in the thermal initial segment (in the first case n = $= -0.13$, in the second case $n = -\frac{1}{6} \approx -0.166$).

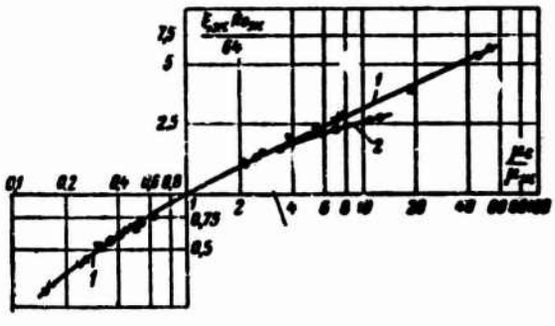

Fig. 9-4. Results of friction-resistance calculations for water and oils flowing in round tube. The curves correspond to Eq. (9-39) with the following values of the constants: 1 – A=1,36; n=0,38; 2 – A=38,8; n=0,616 (the symbols are the same as in Fig. 9-3).

Figure 9-4 shows the results of the friction-resistance calculations. They are well described by an equation of the form

$$\frac{\xi_m Re_m}{64} = 1 + A\left[\left(\frac{\mu_r}{\mu_m}\right)^n - 1\right]. \qquad (9\text{-}39)$$

In this equation

$$\xi_m = \frac{8\sigma_1 \rho_m}{(\rho w)^2}; \quad Re_m = \frac{\rho w d}{\mu_m}.$$

As we can see from Fig. 9-4, the calculated points for water

and the oils lie on the same curve for heating. With cooling the points representing water lie somewhat below the points for the oils. For oils in cooling and heating and for water in heating, the constants in (9-39) have the following values: $A = 1.38$ and $n = 0.38$. Here the maximum deviation of the calculated points from Eq. (9-39) does not exceed 3.5%. To within 1.5%, the computational results for water with cooling are also described by (9-39) with $A = 38.8$ and $n = 0.016$.

Equations (9-38) and (9-39) will obviously be valid not only for water, transformer oil, and type MC-20 oil, but for other liquids for which the nature of the relationship between the physical properties and the temperature is not too different from the corresponding relationships for the investigated liquids. It is understandable that the applicability of the equations is restricted by the limits of variation in the physical properties encompassed by the computation.

We also note that (9-38) and (9-39) only permit us to determine the local values of the limiting Nu_∞ and ξ numbers far from the tube entrance, where the velocity and temperature profiles are stabilized (i.e., where they cease to depend on the conditions at the entrance). Since these physical properties of the liquid vary with the length, Nu_∞ and ξ will also vary with the length.

9-4. HEAT EXCHANGE AND RESISTANCE FAR FROM THE TUBE ENTRANCE WITH FLOW OF DIATOMIC GASES

Heat-exchange and resistance calculations have been given in [3] for air and hydrogen both with heating and cooling of the gas. For heating, the calculations were carried out at $T_s = 1000°K$ for air and $T_s = 1000$ and $2000°K$ for hydrogen; for cooling, they were carried out at $T_s = 300°K$ for both gases.[5] For both air and hydrogen, the temperature factor $T_s/\bar{T}$ varied between 0.4 and 1.75.

The graphs of Fig. 9-5 illustrate the influence of the variable physical properties of air on the radial distributions of temperature, velocity, mass velocity, and heat-flux density in the tube. The particularly sharp redistribution of mass velocity over the tube section is striking. This is of course associated primarily with the dependence of the density on the temperature. In contrast to liquids, the mass-velocity profile (and the velocity profile to a lesser extent) is filled for cooling and elongated for heating of a gas. Since the mass velocity near the wall decreases when a gas is heated and increases during cooling as compared with an isothermal flow, there will be a corresponding increase or decrease in the heat-flux density near the wall.

Figure 9-6 gives calculated curves for heat transfer to hydrogen and air. The axis of ordinates shows the ratio of the Nusselt number for variable physical properties, with the thermal-conductivity coefficient taken for the gas temperature $\bar{T}$, to the Nusselt number for constant properties, 48/11; the axis of abscissas shows the temperature factor $T_s/\bar{T}$. It is clear from Fig. 9-6 that

[5] /242

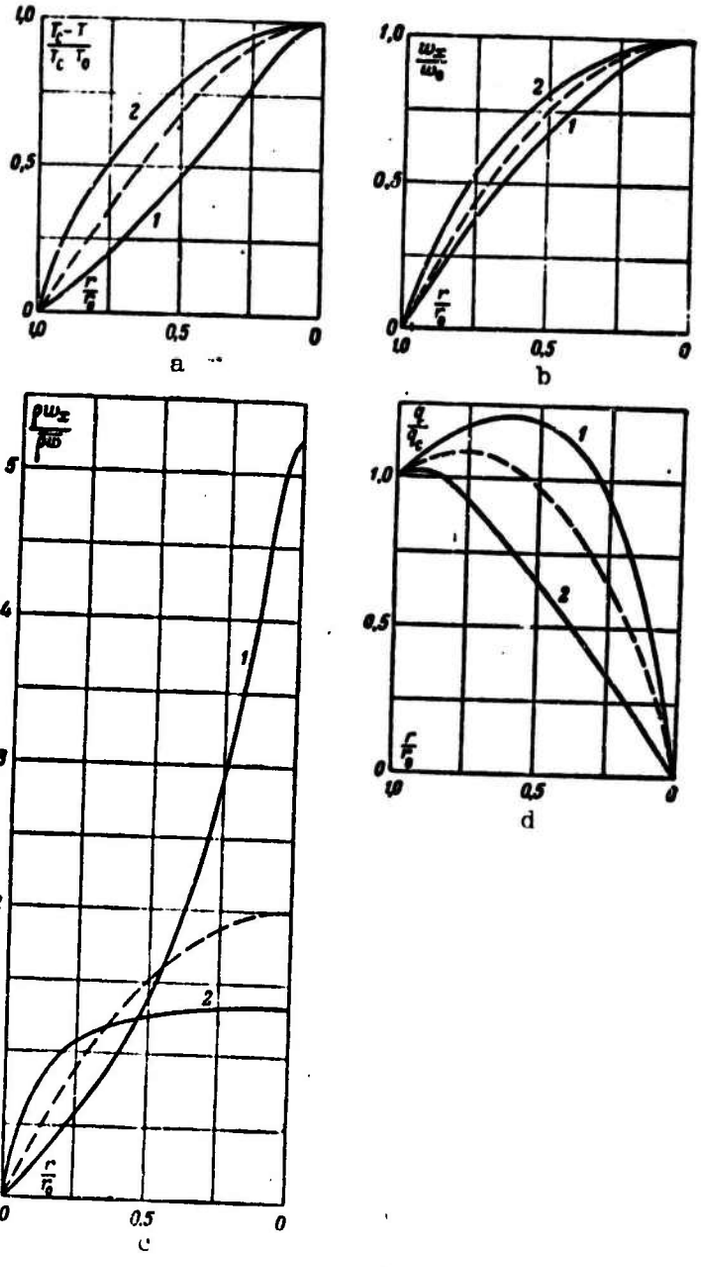

Fig. 9-5. Distributions of temperature (a), velocity (b), mass velocity (c), and heat-flux density (d) over tube cross section in flow of air. Dashed line) Constant physical properties.

$1 - T_0 = 1\,000°$ K; $T_0 = 226°$ K; $\frac{T_c}{T} = 1{,}72$; $2 - T_c = 300°$ K; $T_0 = 989°$ K; $\frac{T_c}{T} = 0{,}404$.

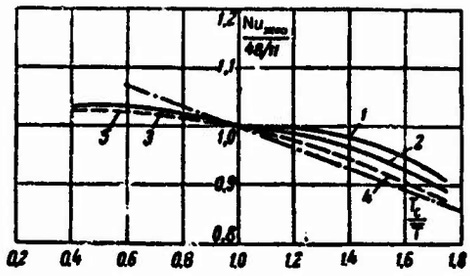

Fig.9-6. Results of heat-transfer calculations for air and hydrogen flowing in round tubes. Solid lines) Hydrogen; 1) T_s = 2000°K; 2) T_s = 1000°K; 3) T_s = 300°K; Dashed line) Air; 4) T_s = 1000°K; 5) T_s = 300°K; Dash-dot line) Deisler computations for air.

the calculated curves for air and hydrogen differ somewhat for identical values of T_s'. This difference is slight, however, and lies in the 1-2% range. It should also be noted that for hydrogen in the heating case, the curves corresponding to T_s = 2000 and 1000°K also diverge somewhat. Here too, the difference amounts to 1-2%.

TABLE 9-3

Values of Constants B and m in Eq. (9-40)

1 Газ, направление теплового потока	B	m
2 Водород при нагревании (T_c = = 1 000 и 2 000° К)	0,0065	5
3 Воздух при нагревании (T_c = = 1 000° К)	0,029	3
4 Водород и воздух при охлаждении (T_c = 300° К)	0,065	1

1) Gas, direction of heat flow; 2) hydrogen with heating (T_s = 1000 and 2000°K; 3) Air with heating (T_s = 1000°K); 4) hydrogen and air with cooling (T_s = 300°K).

The equation

$$\mathrm{Nu}_{ж\infty} = \frac{48}{11}\left\{1 + B\left[1 + \left(\frac{T_c}{\overline{T}}\right)^m\right]\right\} \qquad (9\text{-}40)$$

is a good description of the calculated heat-transfer data for air and hydrogen; here

$$\mathrm{Nu}_{ж\infty} = \frac{q_c d}{\lambda_ж (T_c - \overline{T})},$$

and λ_{zh} is the value of λ at the temperature $\overline{T}$.

Table 9-3 shows the values of the constants B and m in (9-40). Equation (9-40) describes the computational results with an error not exceeding 1%.

Figure 9-6 also shows the calculated relationship obtained by Deisler for air. The equation for this curve has been taken from [7]. The difference in the absolute values of Nu_{∞} obtained with our data and by Deisler's calculations is not great, but there is some difference in the nature of the relationship. It is difficult to account for this discrepancy, since we have not been able to obtain information about the Deisler computation method.

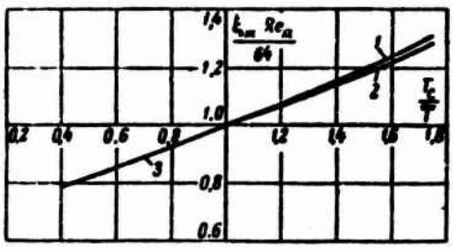

Fig. 9-7. Results of friction-resistance calculations for air and hydrogen flowing in round tube. 1) Hydrogen, T_s = 1000 and 2000°K; 2) air, T_s = 1000°K; 3) hydrogen and air, T_s = 300°K.

Figure 9-7 shows the results of friction-resistance computations for air and hydrogen. The relationship between the friction-resistance coefficient and the temperature factor turns out to be the same for heating of hydrogen with T_s = 1000 and 2000°K. The similar relationship for air at T_s = 1000°K differs only slightly (by roughly 2%). For cooling of hydrogen and air (at T_s = 300°K in both cases), the same relationship is obtained between ξ and $T_s/\bar{T}$.

The results of the calculation of friction resistance coefficients for air and hydrogen are described by an equation of the form

$$\frac{\xi_{\infty}\,\mathrm{Re}_{\infty}}{64} = 1 + C\left[\left(\frac{T_s}{\bar{T}}\right)^{k} - 1\right], \qquad (9\text{-}41)$$

where

$$\xi_{\infty} = \frac{\mathrm{Nu}_{\infty}\rho_{\infty}}{(\bar{\rho}\bar{w})^2}; \quad \mathrm{Re}_{\infty} = \frac{\bar{\rho}\bar{w}d}{\mu_{\infty}}.$$

When the gas is heated, C = 0.23 and k = 3/2; when it is cooled, C = 0.36 and k = 1.

It is interesting that as the temperature factor increases, the heat transfer decreases while the friction resistance increases. The drop in heat transfer is associated with the fact that the re-

duction in temperature gradient at the wall (see Fig. 9-5) is not compensated by a corresponding increase in the thermal-conductivity coefficient of the gas at the wall. The increased resistance is explained by the fact that the viscosity of the gas at the wall rises faster than the velocity gradient at the wall decreases.

As we have noted, the wall temperature has very little influence on the friction-resistance coefficient and the Nusselt number. Thus Eqs. (9-40) and (9-41) can be used for different wall temperatures (at least between 300 and 2000°K) over the 0.4 to 1.75 range of temperature-factor variation.

Unfortunately, there still have been no reliable and systematic measurements of heat transfer and resistance for laminar flow of gases in tubes. Certain experimental data published for gas heating [8] show that within experimental accuracy (±10%), Nu_∞ is independent of the temperature factor. This does not contradict the results of the theoretical computation. As we can see from Fig. 9-6, when $T_s/\overline{T}$ varies from 1 to 1.8, Nu changes by no more than 10%. Naturally, such a change in Nu is undetectable owing to the inadequate measurement accuracy. The same experimental data indicate that the resistance coefficient rises far more sharply as $T_s/\overline{T}$ increases than is predicted by theory. Thus when $T_s/\overline{T} = 1.8$, $\xi Re/64 = 2.2$ according to the experimental data, while theory yields $\xi Re/64 = 1.35$. It is apparent that the difference is associated with the approximate nature of the theory, which disregards the transverse velocity components. Calculations based on the theoretically derived equation (7-82a), which allows for the transverse velocity components, yield a value $\xi Re/64 = 1.85$, which is much closer to the experimental data. The definitive solution of the problem requires further development of the theory and more systematic measurements.

9-5. HEAT EXCHANGE AND RESISTANCE FAR FROM THE TUBE ENTRANCE WITH EQUILIBRIUM DISSOCIATION OF HYDROGEN

As sufficiently high temperatures, thermal dissociation takes place in diatomic and multiatomic gases. In this connection it is interesting to investigate the influence of dissociation on flow and heat-exchange processes. For simplicity, we shall henceforth assume that the dissociation rate far exceeds the rates of convection and diffusion transport of matter. In this case, there will be chemical equilibrium at each point in the flow, and the mixture composition will depend solely on the pressure and temperature at the given point. It is well known that if we have equilibrium dissociation, the flow and heat-exchange processes are described by equations of continuity, motion, and energy that have the same form as for a homogeneous gas.[6] Dissociation makes its influence felt only through the physical properties entering these equations. We take as these physical properties certain effective values of density, enthalpy, heat content, thermal conductivity, and viscosity that are calculated with allowance for the dissociation reaction. The boundary conditions for homogeneous equilibrium dissociation are the same as for heat exchange and motion of a homogeneous gas, provided the flow does not interact with the mater-

ial of the wall, as we shall henceforth assume.

Figure 9-8 shows the effective physical properties for equilibrium dissociation of hydrogen (reaction $H_2 \rightleftarrows 2H$) at pressures of 1, 10, and 100 atm and temperatures of from 2000 to 5000°K [9]. The degree of dissociation α characterizes the fraction of atomic hydrogen in the mixture for various T and p. The density ρ and dynamic viscosity μ change not only as a result of variation in temperature and pressure, but also in connection with the fact that the mixture composition varies together with T and p. In contrast to the situation for a homogeneous gas, the specific heat content and enthalpy of a dissociating gas include the heat of reaction. Here the contribution made to the heat capacity by the thermal effect of the reaction far exceeds the heat capacity of a mixture whose components do not interact. Thus the heat capacity of a dissociating gas is far greater than that of a mixture with no chemical reactions, and it varies sharply with the temperature and pressure (since the proportions of the atoms in the mixture vary with T and p). When there is dissociation, molecular transport of heat in the mixture occurs not only through heat conduction ($\vec{q}_{tp} = \lambda_{tp}$ grad T), but also through the heat transferred by diffusion ($\vec{q}_д = \sum_{i=1}^{N} h_i \vec{I}_i$, where h_i is the enthalpy of the ith mixture component, with allowance for the heat of formation; $\vec{I}_i$ is the mass flow of the ith component; N is the number of mixture components). For equilibrium dissociation, q_d can be represented as the Fourier law ($\vec{q}_д = -\lambda_д$ grad T). Thus the total heat-flux density $\vec{q} = \lambda$ grad T, where $\lambda = \lambda_{тп} + \lambda_д$ is the effective thermal-conductivity coefficient for the gas in equilibrium dissociation. Since λ_d may be several times λ_{tp} for certain values of T and p, for these same values of T and p, λ can exceed λ_{tp}; in such case, the pressure will also vary sharply with the temperature. As we can see from Fig. 9-8, the presence of dissociation leads to extremely varied changes in the physical properties as a function of temperature and pressure; the heat capacity and thermal conductivity vary particularly sharply with the temperature, and have pronounced peaks.

Thus the problem of heat exchange and resistance in equilibrium dissociation reduces to the analogous problem for a chemically homogeneous gas with strongly temperature-dependent physical properties. Thus the method discussed in §9-2 for determining heat exchange and resistance far from the tube entrance can also be used for equilibrium dissociation. This method has been used to determine heat transfer and resistance for hydrogen in equilibrium dissociation at 1, 10, and 100 atm and temperatures from 2000 to 5000°K [10]. For heating of the gas, the calculations were carried out at T_s = 3000, 4000, and 5000°K and a series of values of $\bar{T}$ between T_s and 2000°K, and for cooling for T_s = 2000, 3000, and 4000°K, and $\bar{T}$ between T_s and 5000°K.

Figure 9-9 illustrates the influence of the variable physical

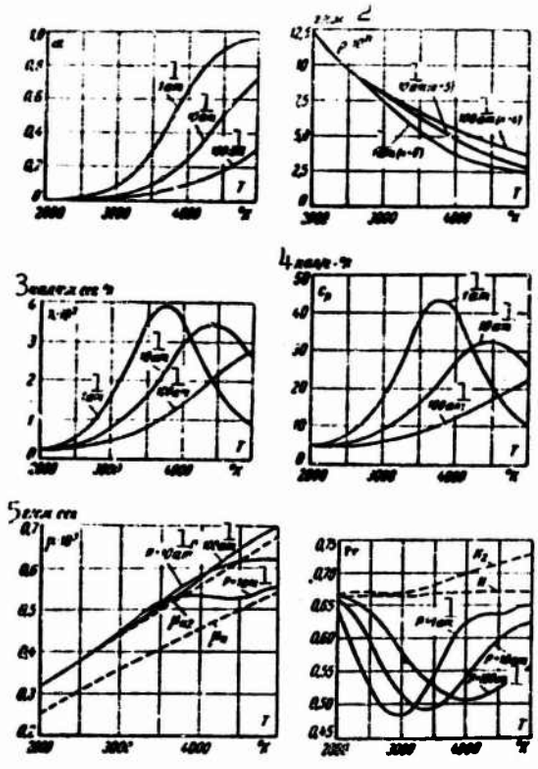

Fig. 9-8. Physical properties of hydrogen undergoing equilibrium dissociation. 1) atm; 2) g/cm; 3) cal/cm·s·°K; 4) cal/g·°K; 5) g/cm·s.

properties of hydrogen in equilibrium dissociation on the radial distribution of the dimensionless values of temperature, velocity, and mass velocity.[7] The figure also gives profiles of the variables for two computational points in heating and two points in cooling. For comparison, temperature and velocity profiles are also given for constant physical properties. It is clear from Fig. 9-9 that the variable physical properties exert the greatest influence on the temperature and mass-velocity profiles.

Figure 9-10 shows the results of heat-transfer calculations, as $Nu_{zh\infty} = \frac{q_r}{\lambda_w (T_c - \bar{T})}$ as a function of ρ_{zh}/ρ_s (the subscripts "zh" and "s" indicate physical parameters taken for $\bar{T}$ and T_s, respectively). The points for $\rho_w/\rho_c > 1$ refer to the case of gas heating, and those for $\rho_w/\rho_c < 1$ to the case of cooling. As we can see, with equilibrium dissociation of hydrogen, the variation in physical properties with temperature has a considerable influence on heat transfer. Thus with variable properties, $Nu_{zh\infty}$ may differ from Nu_∞ for constant properties (equaling 48/11) by a factor of 2.5. A still greater difference

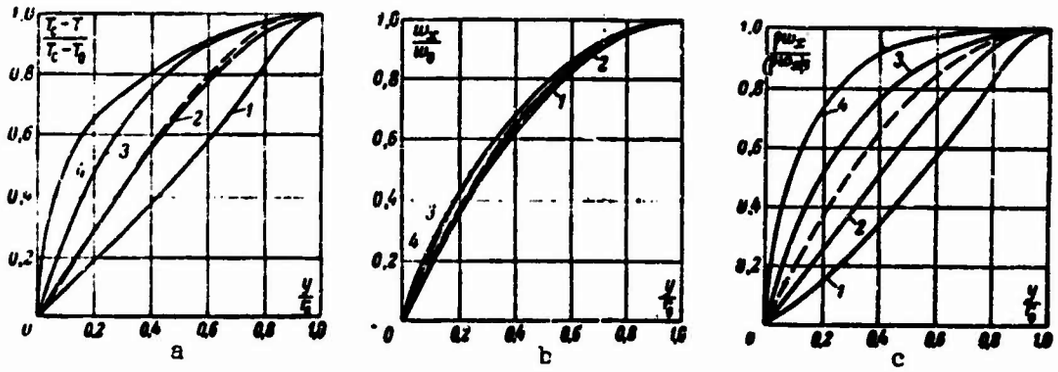

Кривая	a: p, atm	T_c, °K	$\bar{T}$, °K	T_0, °K
1	10	5 000	4 630	2 990
2	10	5 000	4 450	4 130
3	10	2 000	2 810	3 100
4	10	2 000	1 190	4 790

Fig. 9-9. Distributions of temperature (a), velocity (b), and mass velocity (c) over tube radius for flow of hydrogen in equilibrium dissociation. The dashed line represents constant physical properties. a) Curve; b) p, atm.

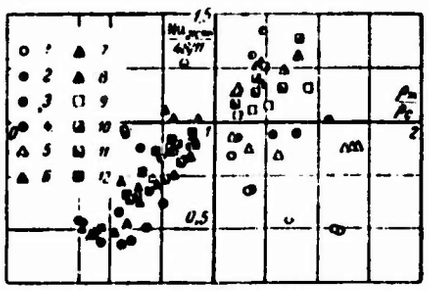

T_c, °K	a: p, atm 1	10	100
	b: Расчетные точки		
5 000	1	5	9
4 000	2	6	10
3 000	3	7	11
2 000	4	8	12

Fig. 9-10. Results of heat-transfer calculations for flow of hydrogen in equilibrium dissociation. a) p, atm; b) computational points.

is found for $\mathrm{Nu}_{c\infty} = \frac{q_c}{\lambda_c (T_c - \bar{T})}$ (up to a factor of 10).

If in (9-32), we go from $\mathrm{Nu}_{s\infty}$ to $\mathrm{Nu}_{zh\infty}$, replacing λ_s and c_{ps} by λ_{zh} and c_{pzh}, it is not difficult to see (remembering that for a dissociating gas, Pr varies little with the pressure and temperature) that the difference between the product $\mathrm{Nu}_{\infty} \frac{c_{p\mathrm{m}}}{c_p}$ and the corresponding value for constant physical properties (48/11) is caused basically by the temperature-dependence of the density and viscosity.

Thus $Nu_{\infty}\frac{c_{p\infty}}{\bar{c}_p}$ can be represented, in approximation, as a function of ρ_c/ρ_{∞} and μ_c/μ_{∞}. Analysis of the calculated data leads to the following interpolation equation, describing the computational results to within ±6%:

$$Nu_{\infty}=\frac{48}{11}\cdot\frac{\bar{c}_p}{c_{p\infty}}\left(\frac{\mu_c}{\mu_{\infty}}\right)^n\left(\frac{\rho_c}{\rho_{\infty}}\right)^m, \qquad (9\text{-}42)$$

where

$$n=\begin{cases}1{,}0 \text{ for } \frac{\mu_c}{\mu_{\infty}}<1;\\ 0{,}5 \text{ for } \frac{\mu_c}{\mu_{\infty}}>1;\end{cases}$$

$$m=\begin{cases}0{,}5 \text{ for } \frac{\rho_c}{\rho_{\infty}}<1;\\ 0{,}7 \text{ for } \frac{\rho_c}{\rho_{\infty}}>1;\end{cases}$$

$$\bar{c}_p=\frac{h_c-\bar{h}}{T_c-\bar{T}}=\frac{1}{T_c-\bar{T}}\int_{\bar{T}}^{T_c}c_p\,dT$$

is the mean integral heat capacity over the range of temperature variation from T_s to $\bar{T}$.

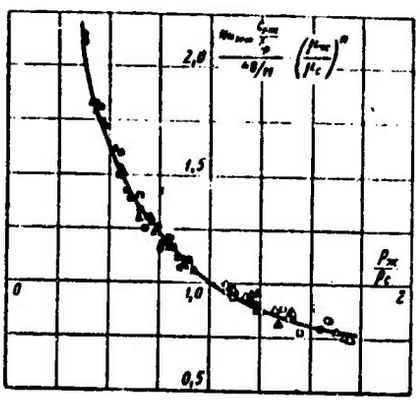

Fig. 9-11. Comparison of calculated heat-transfer data with Eq. (9-42) (solid curve).

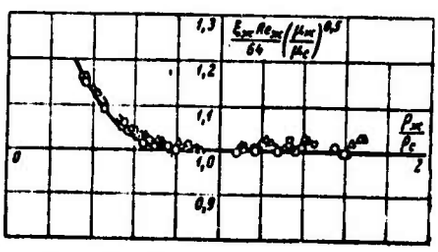

Fig. 9-12. Comparison of calculated resistance data with Eq. (9-43) (solid curve).

The parameters occurring in (9-42) were varied in the calculations over the following ranges: $0{,}38 \leqslant \frac{\bar{c}_p}{c_{pm}} \leqslant 1{,}5$; $0{,}53 \leqslant \frac{\mu_c}{\mu_m} \leqslant 1{,}3$ and $0{,}59 \leqslant \frac{\rho_c}{\rho_m} \leqslant 2{,}9$.

Figure 9-11 compares the calculated points with the interpolation equation (9-42).

The results of the friction-resistance calculations show that for variable physical properties, $\xi_{zh}\mathrm{Re}_{zh}$ differs from $\xi\mathrm{Re} = 64$ for constant properties by no more than 20%. This difference amounts to a factor of 4.5 for $\xi_s\mathrm{Re}_s$, however. As (9-37) shows, the change in $\xi_{zh}\mathrm{Re}_{zh}$ is caused by the fact that ρ and μ depend on T, so that the product can be represented as a function of the parameters ρ_s/ρ_{zh} and μ_s/μ_{zh}. To within $\pm 3\%$, the computational results are described by the interpolation equation

$$\xi_m \mathrm{Re}_m = 64 \left(\frac{\mu_c}{\mu_m}\right)^{0.5} \left[\varkappa \left(\frac{\rho_c}{\rho_m}\right)^3 + (1-\varkappa)\right], \qquad (9\text{-}43)$$

where

$$\xi_m = \frac{2\sigma_c \rho_m}{(\rho w)^2}; \quad \mathrm{Re}_m = \frac{\bar{\rho} w d}{\mu_m};$$

Here $\varkappa = 0$ when $\rho_c/\rho_m < 1$ and $\varkappa = 0{,}008$ when $\rho_c/\rho_m > 1$.

The ranges of variation for the parameters ρ_c/ρ_m and μ_c/μ_m are the same for (9-43) as for (9-42). Figure 9-12 compares the calculated points with interpolation equation (9-43).

9-6. HEAT EXCHANGE AND RESISTANCE IN THE SUPERCRITICAL REGION OF STATE PARAMETERS FOR MATTER

In the supercritical region of state parameters, the physical properties of matter (ρ, c_p, μ and λ) vary extremely sharply and differently with the temperature, and depend substantially on the pressure (see §3-4). Thus even for fairly small temperature differences in the flow, the change in physical properties will have a great influence on heat exchange and resistance.

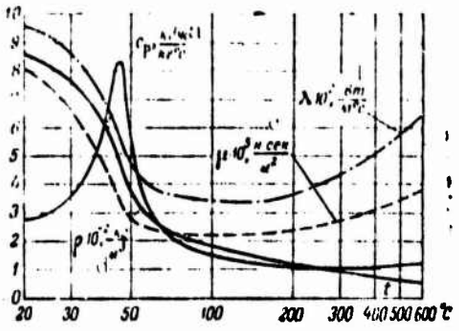

Fig. 9-13. Physical properties of carbon dioxide at p = 100 atm. a) kJ/kg·°C; b) W/m·°C; c) N·s/m²; d) kg/m³.

With supercritical state parameters for matter, theoretical calculations of heat exchange and friction far from the tube entrance (i.e., for the tube segment where the hydrodynamic and thermal boundary layers merge) can be carried out by the method considered in §9-2. V.N. Popov [11] has used this method to compute the heat transfer and resistance for carbon dioxide at a pressure of 100 atm[8] over the 20 to 600°C temperature range with

constant heat-flux density at the wall. For heating of CO_2, the calculations were carried out for t_c=600, 400, 360, 200, 100, 70, 50, and 45°C, and a series of values of $\bar{t}$ between t_s and 20°C; for cooling, t_c 20, 45, 50, 70, 100, 200, 300 and 400°C, with $\bar{t}$ ranging from t_s to 600°C.

Figure 9-13 shows the physical properties of carbon dioxide (ρ, c_p, λ, and μ) for p = 100 atm [12, 13, 14, 15]. The computational results show that in the supercritical region, the variable physical properties of carbon dioxide have a sharp influence on the temperature and mass-velocity profiles (Fig. 9-14), and less influence on the velocity profile. The heat transfer and friction resistance also vary sharply owing to the changes in the physical properties. Thus the ratio of $Nu_{zh\infty}$ for variable properties to $Nu_{\infty zh}$ = = 48/11 for constant property varies from 0.5 to 2.5, while the ratio of the corresponding resistance coefficients ξ_{zh} varies from 0.7 to 2 (Fig. 9-15).

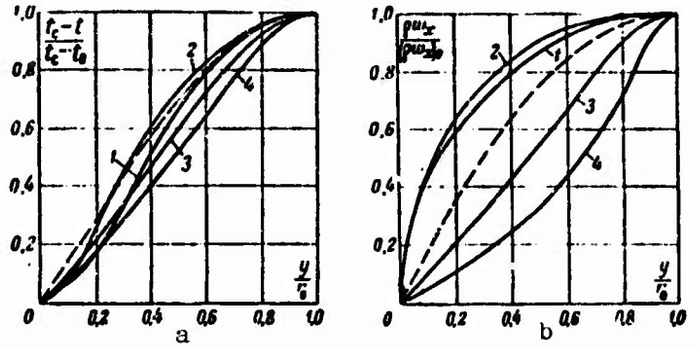

a' Кривая	t_c, °C	$t_{вх}$, °C	t_0, °C
1	20	86,7	196
2	20	187	336
3	600	405	287
4	600	319	106

Fig. 9-14. Radial distributions of temperature (a) and mass velocity (b) for carbon dioxide at p = 100 atm. Solid lines) Variable physical properties; dashed line) constant physical properties. a') Curve.

TABLE 9-4

Values of Constants in Eq. (9-44)

$\frac{c_{pc}}{\bar{c}_p}$	A	n	$\frac{\bar{\mu}}{\mu_c}$	B	k	$\frac{\rho_c}{\rho_w}$	C
$\leqslant 1$	0,80	0,25	$\leqslant 1$	3,2	0,25	$\leqslant 1$	0,69
>1	0,16	1,0	>1	0,9	2,0	>1	0,24

To within ±10% the results of the heat-transfer calculations are described by the interpolation equation

$$\mathrm{Nu}_{c\infty}=\frac{48}{11}\frac{\left\{B\left[\left(\frac{\bar{\mu}}{\mu_c}\right)^k-1\right]+1\right\}\left[C\left(\frac{\rho_c}{\rho_m}-1\right)+1\right]}{A\left[\left(\frac{c_{pc}}{\bar{c}_p}\right)^n-1\right]+1}, \qquad (9\text{-}44)$$

where

$$\mathrm{Nu}_{c\infty}=\frac{q_c d}{\lambda_c(t_c-\bar{t})};\quad \bar{\mu}=\frac{1}{t_c-\bar{t}}\int_{\bar{t}}^{t_c}\mu\,dt$$

is the mean integral value of the dynamic viscosity coefficient in the temperature range between $\bar{t}$ and t_s; A, B, C, n, and k are constants whose values are given in Table 9-4.

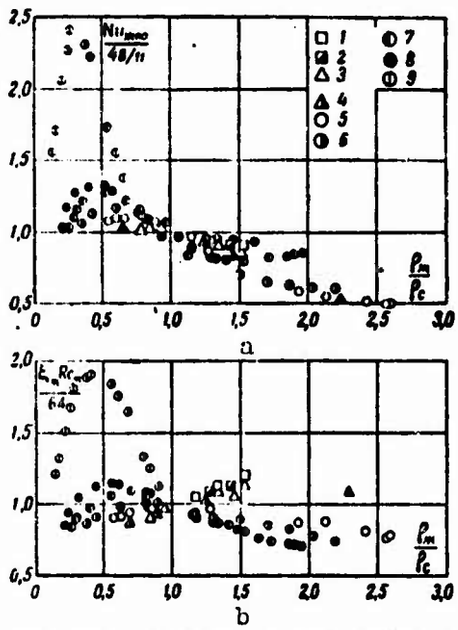

Fig. 9-15. Results of calculations for heat transfer (a) and friction resistance (b) for carbon dioxide at p = 100 atm. 1) t_s = = 600°C; 2) t_s = 400°C; 3) t_s = 300°C; 4) t_s = 200°C; 5) t_s = = 100°C; 6) t_s = 70°C; 7) t_s = 50°C; 8) t_s = 45°C; 9) t_s = 20°C.

The right side of (9-44) does not contain the thermal-conductivity coefficient λ. The reason is that, qualitatively speaking, μ and λ depend in the same way on the temperature, and this was taken into account in the choice of interpolation equation. Introduction of the mean integral parameters $\bar{c}_p$ and $\bar{\mu}$ was dictated by the nonmonotonic nature of the variation in heat content and viscosity with temperature. The relatively low accuracy of (9-44) is explained by the fact that for simplicity and convenience the parameters c_{pc}/c_{pm}, $\mu_c/\bar{\mu}$ and ρ_c/ρ_m were used to allow for the influence of the variable physical parameters on heat exchange; these parameters reflect the variation in physical properties only over the tempera-

ture range between t_s and $\bar{t}$. Moreover, the heat transfer is naturally influenced by the nature of the relationship between the physical properties and temperature over the entire range of variation from t_s to $t_{r=0}$. While for turbulent flow, the ratio $t_c - \bar{t}/t_c - t_{r=0}$ is close to unity, under our conditions, with laminar flow it varies from 0.35 to 0.8 [for constant physical properties, $(t_c - \bar{t}/t_c - t_{r=0} = \frac{11}{18} \approx 0{,}61)$]. Construction of a more exact interpolation equation at the expense of substantial complication is hardly worthwhile when we consider the approximate nature of the theoretical calculations themselves.

Analysis of the calculated friction-resistance data shows that if we substitute the mean integral value of dynamic viscosity into the expression for the Reynolds number, then with variable properties the product $\xi_{zh}\overline{Re}$ will differ little from the value of this product, equaling 64, for constant properties. For cooling of the fluid, the difference amounts to ±6%, and it does not exceed 10% for heating. Here, therefore, the approximate equation

$$\xi_{zh}\overline{Re} = 64 \qquad (9\text{-}45)$$

is valid, where

$$\overline{Re} = \frac{\bar{\rho} w d}{\bar{\mu}}.$$

In the supercritical region, the physical properties of the fluid depend on the temperature and pressure, while the latter vary along the length of the tube; thus the heat transfer and resistance will also vary with length. Using (9-44) and (9-45), we can calculate α (or t_s) and σ_s at each tube section.

Figure 9-16 gives a notion of the possible nature of the variation in heat-transfer coefficient along the length of the tube for carbon dioxide with supercritical parameters. It gives the results of an approximate heat-transfer determination with p = 77.3 atm for one special case.[10] Near the tube entrance, the heat-transfer coefficient drops rapidly, as must also be the case in the thermal initial segment. Since as we move away from the entrance, t_s and $\bar{t}$ increase ($t_s > \bar{t}$), then at a certain distance from the entrance, the heat capacity of the fluid for t_s will considerably exceed the heat capacity for $\bar{t}$. The difference in the values of c_p leads to a slower increase in t_s along the length than in $\bar{t}$ and, consequently, to a slower increase in α. After t_s exceeds the temperature t_{maks} corresponding to the point of maximum c_p, the pattern changes: t_s increases more rapidly than $\bar{t}$; thus α passes through a maximum and then decreases. When both t_s and $\bar{t}$ become considerably greater than t_{maks}, the heat capacities will differ little for t_s and $\bar{t}$, and the curves for different q_s will draw together, as we see from Fig. 9-16. As q_s increases,

the minimum and maximum points for the curves $\alpha = \alpha(x/d)$ shift toward the entrance, since t takes on a value approaching t_{maks} closer to the entrance. Naturally, the way in which α changes with the length is determined not only by the relationship between c_p and t, but also by the way in which the other physical parameters depend on the temperature. The data shown in Fig. 9-16 exemplify the great diversity of heat-exchange phenomena in the supercritical region.

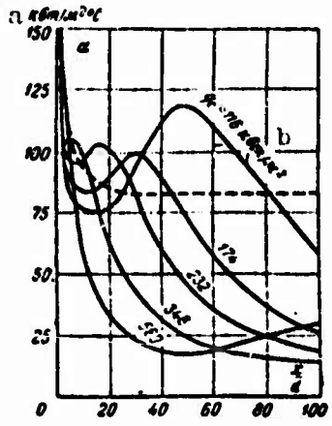

Fig. 9-16. Variation in α along tube length for carbon dioxide at p = 77.3 atm, t_{vkh} = 21°C, Re = 100, and various values of q_s (the dashed line represents constant physical properties). a) kW/m²·°C; b) q_s = 116 kW/m².

Manuscript Page No.

Footnotes

216 [1]The experimental data for the entire flow region, including the hydrodynamic initial segment, are given in §12.4.

218 [2]The same authors have performed similar computations for helium and carbon dioxide. The Nu number turned out to be 3-5% lower for He and 18% lower for CO_2 than for air [17].

220 [3]The physical properties of transformer oil and type MC-20 oil are taken from the data published in [4].

226 [4]In the general case, q varies as a function of r owing to the change in the surface through which the radial heat flow passes and to the variation in convective heat transfer along the axis, which is associated with the variation in velocity along the radius.

228 [5]All physical properties of air and c_p, h, ρ, λ up to 700°K and μ up to 1100°K for hydrogen were taken from [5]. The values of λ for hydrogen at T between 1200 and 2000°K were computed from the empirical equation proposed in [6], while for T between 700 and 1200°K, they were found by graphical interpolation. The values of μ for hydrogen at T = 1100-2000°K were calculated theoretically with the aid of the modified Buckingham potential.

232 [6]See, for example [9]. There is no need to solve the diffusion equation for equilibrium dissociation, since the gas composition at every point in the flow is determined completely in this case by the pressure and temperature at this point.

234 [7]The subscript 0 indicates the value of the corresponding parameter on the tube axis.

237 [8]The critical parameters for CO_2 are: $\rho_{кр}=75.3$ ат and $t_{кр}=31°C$.

239 [9]For practical calculations it is convenient if we first construct $M=\int_{t_a}^{t}\mu\,dt$ as a function of t (where t_a is a certain arbitrary constant temperature value) and find $\bar{\mu}$ from the relationship

$$\mu=\frac{M(t_0)-M(\bar{t})}{t_0-\bar{t}}.$$

240 [10]In [16], the calculations were performed by numerical integration of the energy equation on the assumption that the profile for the longitudinal mass-velocity component is parabolic over the entire length of the tube (which is far from actually being the case, as we have seen) and that the transverse velocity component equals zero.

Manuscript Page No.	Transliterated Symbols
211	c = s = stenka = wall
215	теор = teor = teoreticheskiy = theoretical
215	опыт = opyt = opytnyy = experimental
216	ж = zh = zhidkostnyy = liquid, fluid
216	н.г = n.g = nachal'nyy gidrodinamicheskiy = hydrodynamic initial

232 тп = tp = teploprovodnost' = thermal conductivity

232 д = d = diffusiya = diffusion

240 макс = maks = maksimal'nyy = maximum

241 вх = vkh = vkhod = entrance